Nouvelles cibles et nouveaux régimes thérapeutiques dans le traitement des infections à Mycobacterium abscessus

Clément Raynaud

THÈSE POUR OBTENIR LE GRADE DE DOCTEUR DE L'UNIVERSITÉ DE MONTPELLIER

En Microbiologie

École doctorale CBS2

Unité de recherche :
Institut de Recherche en Infectiologie de Montpellier
Equipe :
Pathogénie mycobactérienne et nouvelles cibles thérapeutiques

Nouvelles cibles et nouveaux régimes thérapeutiques dans le traitement des infections à *Mycobacterium abscessus*

Présentée par Clément Raynaud
Le 8 Décembre 2020

Sous la direction de Laurent Kremer

Devant le jury composé de

Pr Hélène Marchandin, Professeur, Université de Montpellier-CHU de Nîmes	**Présidente du jury**
Dr Fabienne Misguich, maître de conférence, Université de Versailles Saint-Quentin	**Rapporteur**
Pr Nicolas Veziris, Professeur, Sorbonne Universités	**Rapporteur**
Dr Stéphane Canaan, directeur de recherche CNRS, Laboratoire d'ingénierie des systèmes macromoléculaires	**Examinateur**
Dr Laurent Kremer, directeur de recherche INSERM, Institut de recherche en infectiologie de Montpellier	**Directeur de thèse**

UNIVERSITÉ DE MONTPELLIER

Remerciements

Je voudrais tout d'abord remercier les membres de mon jury,

Le professeur Nicolas Véziris et le Docteur Fabienne Misguich

D'avoir accepté d'être rapporteurs afin d'examiner mon manuscrit de thèse,

Le professeur Hélène Marchandin et le Docteur Stéphane Canaan

D'avoir accepté d'être examinateurs pour évaluer mon travail de thèse,

Mon directeur de thèse, **le Docteur Laurent Kremer**,

De m'avoir guidé et d'avoir su être patient tout au long de ces 3 années. Merci de m'avoir appris que, même quand les résultats ne sont pas là, le travail paye. Grâce à ses conseils et toutes ces discussions, j'ai pu développer mon esprit critique de chercheur.

Les membres de mon comité de thèse le **Pr Jean-Louis Herrmann et le Docteur Edouard Tuaillon**,

De m'avoir suivi pendant ces 3 ans, conseillé et soutenu autant que possible.

Les membres de l'équipe de recherche qui m'ont accompagné pendant cette période et pour qui j'exprime un profond respect.

Mes amis et collègues **Ana-Victoria Gutierrez**, **Matthias Richard et Matt D. Johansen**,

Un grand merci pour toute l'aide et le soutien et les techniques qu'ils m'ont apporté tout au long de mon apprentissage et pour tous les bons moments passés au laboratoire et en dehors.

Merci à toutes les personnes qui travaillent à l'IRIM et qui font de cet institut un cadre de travail exceptionnel,

Pascale Bouhours,

À qui j'adresse un grand merci et qui a toujours le petit mot qui motive.

Pour finir, je voudrais remercier ma famille, mes parents et mes proches, **Clothilde**, et tous les amis en dehors du laboratoire qui m'ont soutenu pendant ces 3 années de thèse.

Table des matières

Tables des figures

Abréviations

MNT: Mycobactéries non-tuberculeuses

LPS: Lipopolysaccharides

PIM: Phosphatidyl-*myo*-inositol

LM: Lipomannane

LAM: Lipoarabinomannane

NGM: N-glycolylmuramique

NAM: N-acétylmuramique

NAG: N-acétylglucosamine

AM: Acides mycoliques

ACP: Acyl Carrier Protein

TMM: Tréhalose MonoMycolate

DAT: DiAcyl Tréhalose

PAT: PolyAcyl Tréhalose

PDIM: Phthirocérol DiMycocérosate

SGL: SulfoGlycoLipides

TPP: Tréhalose PolyPhléate

ROS: Reactive Oxygen Species

GPL: GlycoPeptidoLipides

MmpL: Mycobacterial Membrane Protein Large

RND: Resistance-Nodulation-cell Division

TM: Transmembrane domain

MmpS: Mycobacterial Membrane Protein Small

MMDAG: Monomeromycolyl diacylglycérol

TDM: Tréhalose DiMycolate

GDND: Gycosyl Diacetylated Nonadecyl Diol

BDQ: Bédaquiline

CFZ: Clofazimine

MCL: Mycobactéries à croissance lente

MCR: Mycobactéries à croissance rapide

MAC: *Mycobacterium avium* complex

MABSC: *Mycobacterium abscessus* complex

TLR2: Toll-Like Receptor 2

IV: Intraveineuse

CFTR: Cystic Fibrosis Transmembrane Regulator

SNC: Système nerveux central

BPCO: Broncho-pneumopathies chroniques obstructives

VIH: Virus de l'Immunodéficience Humaine

AMK: Amikacine

IPM: Imipénème

CFX: Céfoxitine

TGC: Tigécycline

LZD: Linézolide

MOX: Moxifloxacine

STP: Streptomycine

KAN: Kanamycine

GEN: Gentamycine

CLR: Clarithromycine

AZR: Azithromycine

ERY: Erythromycine

IFN-γ: Interféron gamma

TNFα: Tumor Necrosis Factor alpha

MIN: Minocycline

TDZ: Tédizolide

RIF: Rifampicine

RFB: Rifabutine

VAN: Vancomycine

VER: Vérapamil

INH: Isoniazide

ETH: Ethionamide

TAC: Thiacétazone

EMB: Ethambutol

QRDR: Quinolone Resistance-Determining Regions

Eis: Enchanced intracellular survival

FICI: Fractional inhibitory concentration index

STZ: Sutézolide

CFU: Colony forming unit

CMI: Concentration minimale inhibitrice

INTRODUCTION

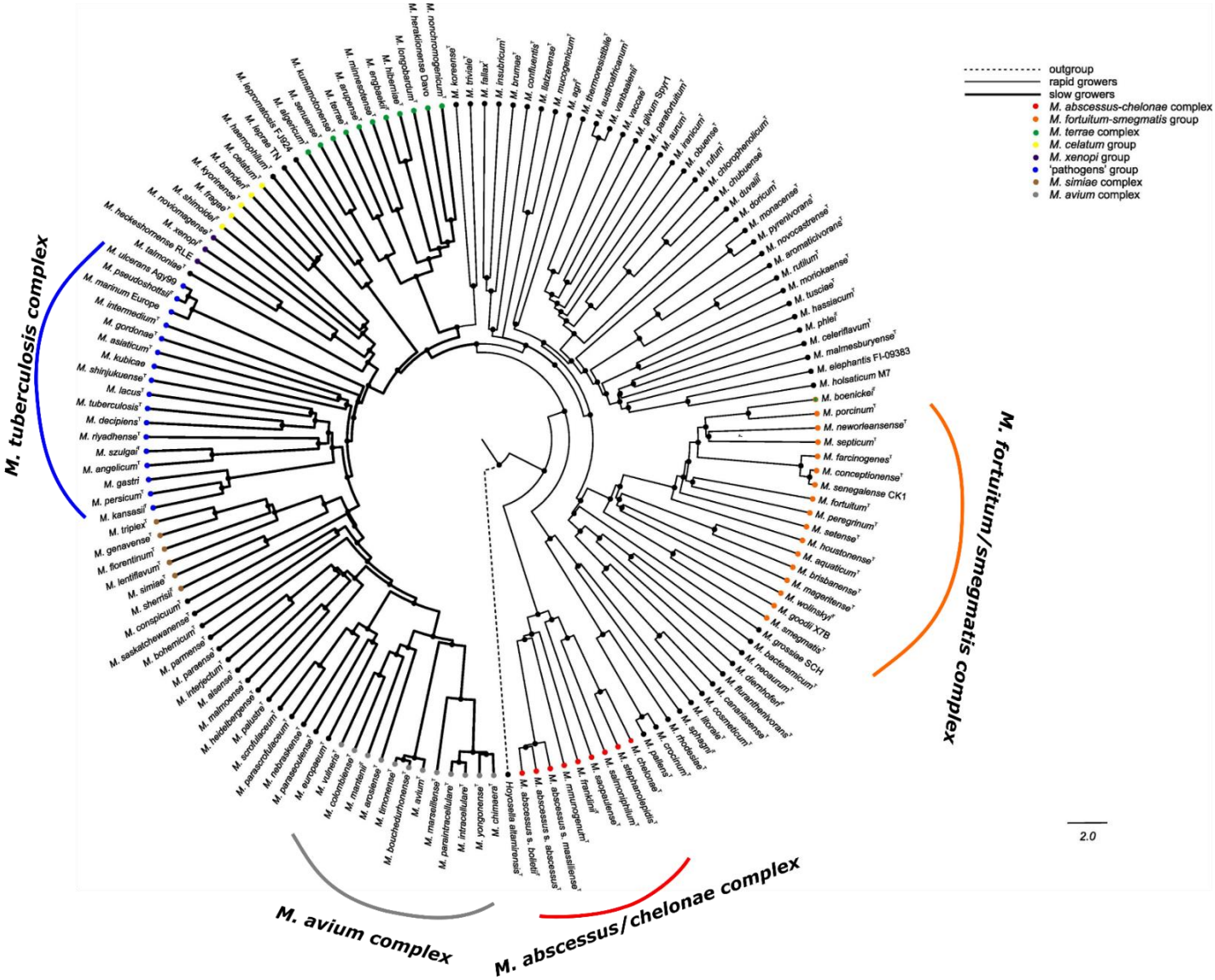

Figure 1. Arbre phylogénétique représentant le genre *Mycobacterium*.

Arbre phylogénétique construit grâce à un algorithme UPGMA, avec une matrice de distance de 10878 ANI-divergence scores. Echelle = 2 unités de différence dans la valeur ANI-divergence. Sont représentés en bleu le complexe *M. tuberculosis,* en gris le complexe *M. avium,* en orange le complexe *M. fortuitum* et en rouge le complexe *M. abscessus*. (Adapté de Tortoli et al, 2017)

I. *Les mycobactéries*

I.1. Présentation générale

Les mycobactéries sont des bactéries appartenant aux actinobactéries. Les bactéries de ce phylum sont originaires de l'environnement (sol ou eau) mais leur réservoir d'origine n'est pas clairement défini. On les retrouve également dans des organismes supérieurs car beaucoup d'entre elles produisent des molécules anti-microbiennes, ce qui assure leur survie. En effet, les actinomycètes, en particulier, sont des organismes à l'origine de la plupart des antibiotiques utilisés en routine à l'hôpital et permettent encore, à l'heure actuelle, la découverte de nouvelles molécules anti-microbiennes actives qui permettent d'alimenter les pipelines de développement de nouvelles molécules (Genilloud 2017). Les mycobactéries, elles, ne produisent rien de tel et sont connues pour leur capacité à infecter de nombreux organismes tels que oiseaux, poissons, mammifères etc. Elles appartiennent à l'ordre des actinomycétales, au sous-ordre des *corynebacterineae* et à la famille des *mycobacteriaceae* qui comprend plus de 200 espèces différentes (https://www.bacterio.net/genus/mycobacterium). La plupart des mycobactéries sont environnementales et non-pathogènes mais certaines sont responsables de diverses maladies telles que la tuberculose ou la lèpre par le biais d'espèces pathogènes strictes comme *Mycobacterium tuberculosis* ou *Mycobacterium leprae*, respectivement. D'autres sont des pathogènes opportunistes qui appartiennent généralement aux mycobactéries non tuberculeuses (MNT) auxquelles appartiennent *Mycobacterium avium* et *Mycobacterium abscessus* (Figure 1) (Medjahed et al. 2010).

I.2. Spécificités des mycobactéries

Les mycobactéries ne sont pas colorées par la technique de Gram mais par celle de Ziehl-Nielsen qui est une coloration acide rapide qui repose sur le même principe d'hydrophobicité de la membrane bactérienne. La première étape consiste en un lavage avec une solution acido-alcoolique puis une coloration avec de la fuchsine qui va alors être retenue par les bacilles. Ceci est dû à la composition de la membrane des mycobactéries qui est très riche en lipide (Vilchèze and Kremer 2017). Elles sont classées en deux groupes différents définis par la classification de Runyon. Celle-ci décrit différents groupes reposant sur des critères visuels et temporels : les mycobactéries à croissance rapide (qui forment une colonie en moins de 7 jours) et les mycobactéries à croissance lente qui sont sous-divisées en trois groupes :

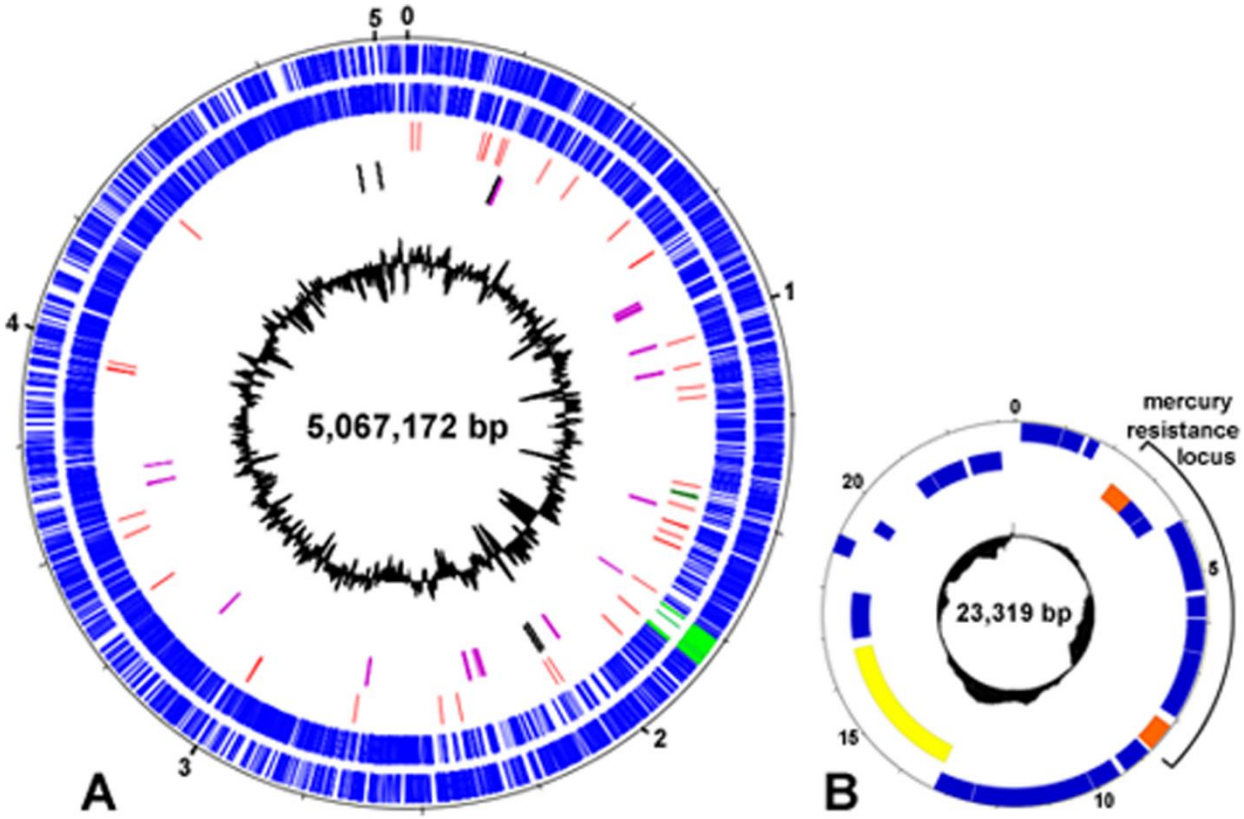

Figure 2. Le génome de *M. abscessus* CIP104536T.

(A) Représentation circulaire du génome. Le point de départ de numérotation correspond au codon d'initiation du gène *dnaA.* Les deux cercles extérieurs bleus montrent les gènes dans le sens transcrit et non transcrit. Le troisième cercle montre les tRNA en rouge et les rRNA en vert foncé. L'histogramme noir le plus à l'intérieur montre le GC%. L'échelle est en Mb.
(B) Représentation circulaire du plasmide de résistance au mercure de 23 kb de *M. abscessus,* il porte l'opéron de résistance au mercure entouré de deux gènes qui codent pour des recombinases ainsi que d'autre pour des relaxases/hélicases. (D'après Ripoll et al, 2007)

(1) les photochromogènes qui développent une pigmentation au contact de la lumière (*Mycobacterium marinum, Mycobacterium kansasii*) ;

(2) les scotochromogènes qui développent une pigmentation dans l'obscurité (*Mycobacterium xenopii, Mycobacterium gordonae*) ;

(3) les non-chromogènes qui ne présentent aucune pigmentation (*M. avium, Mycobacterium intracellulare*).

Le génome des mycobactéries est très spécifique car il est très riche en GC, le GC% de *M. tuberculosis* est de 65.5% et celui de *M. abscessus* est de 64%. Les variations interespèces de ce taux de GC dépendent principalement de l'environnement dans lequel une espèce a évolué (Foerstner et al. 2005). Il a également été montré que le taux de GC est plus élevé pour les gènes qui sont les plus conservés parmi une même espèce («core genome») (Bohlin et al. 2017). Concernant la taille du génome, elle varie considérablement puisque le plus petit est celui de *M. leprae* avec une taille de 3,27 Mb, qui correspond à son mode de vie uniquement intracellulaire, alors que le plus grand génome est celui de *Mycobacterium aquaticum* avec une taille de 7,9 Mb, une espèce proche de *Mycobacterium fortuitum*. Celui de *M. abscessus* est de 5 Mb (Figure 2) (Wee et al. 2017; Tortoli et al. 2017).

I.3. Les membranes bactériennes

I.3.1. Les parois des bactéries à Gram⁻ et Gram⁺

Les bactéries sont souvent classées selon leur type membranaire par la dénomination Gram⁺ ou Gram⁻ résultant de leur coloration. L'enveloppe des mycobactéries étant plus complexe, elles ne peuvent être classées selon ces règles.

Les bactéries à Gram⁻ possèdent une membrane plasmique surmontée d'une fine couche de peptidoglycane puis d'une paroi comprenant des lipopolysaccharides (LPS) qui sont des éléments indispensables à la virulence de ces bactéries (Beveridge 1999). Chez les bactéries à Gram⁺ la membrane plasmique est surmontée d'un épais peptidoglycane composé de plusieurs couches associées qui sont empilées les unes sur les autres, ce qui confère une certaine rigidité à cette membrane. Les bactéries à Gram⁺ ne possèdent pas de LPS mais d'autres facteurs de virulence enchâssés dans le peptidoglycane, tels que les acides téichoïques (Rohde 2019).

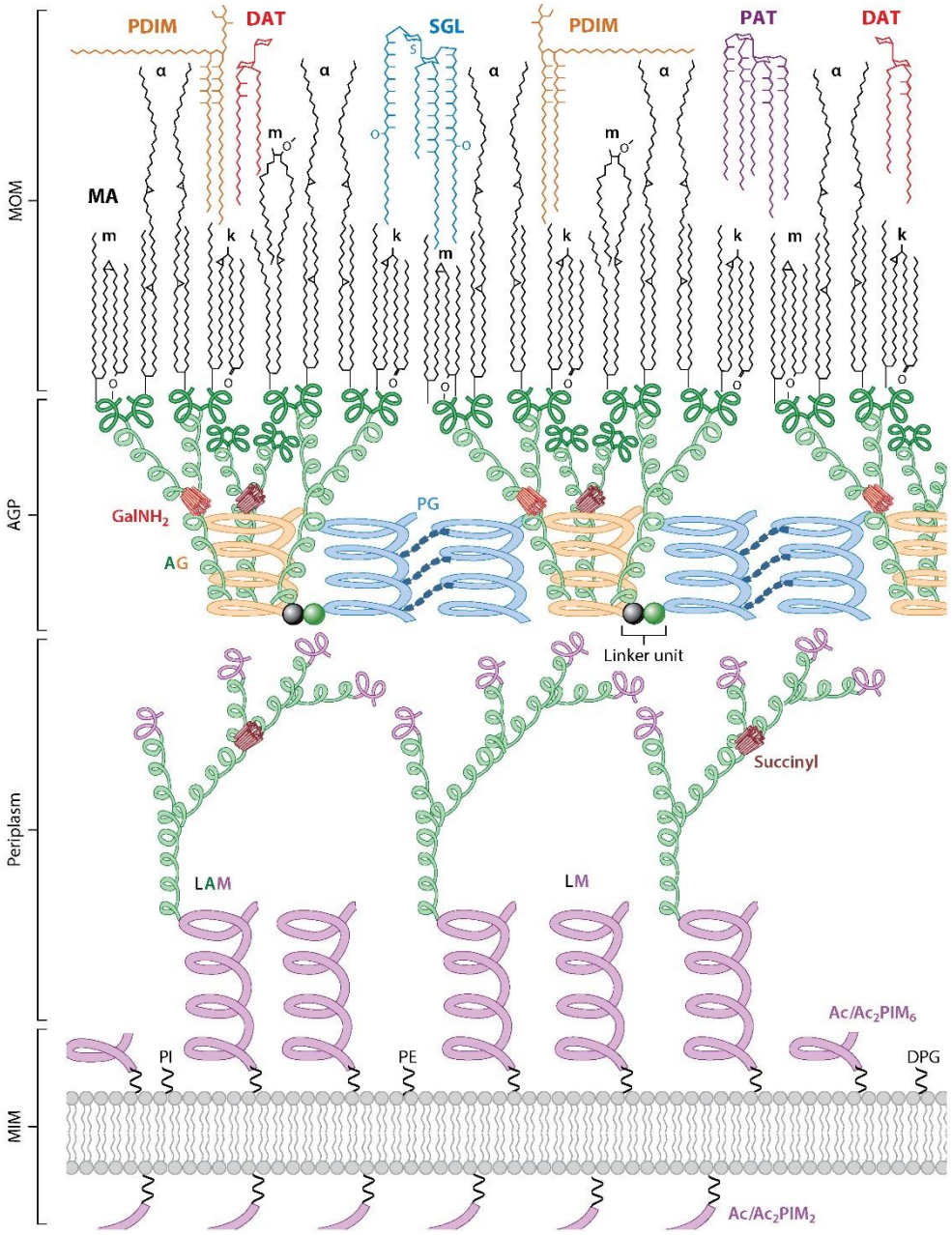

Figure 3. Modèle de la paroi de *M. tuberculosis*.

Modèle de la paroi mycobactérienne montrant les différentes couches retrouvées, la membrane plasmique avec ses PL (phospholipide), ses GL (glycolipide), ses LAM (lipoarabinomannane), ses PIM (phosphatidylmyoinositolmannoside). On retrouve ensuite une couche de peptidoglycane puis d'arabinogalactane (AGP) et enfin la mycomembrane avec ses acides mycoliques (α, k, m), TMM (tréhalose mono mycolates) et TDM (tréhalose di mycolates). On retrouve parfois une capsule composée de protéines, de LAM, de mannane et de glucane. (D'après Daffé et al, 2019)

I.3.2. La paroi mycobactérienne

La paroi mycobactérienne n'appartient ni aux Gram$^-$ ni aux Gram$^+$ même si classiquement elle est rapprochée du groupe Gram$^+$ car c'est une paroi très épaisse et très riche en lipides spécifiques.

I.3.2.1. La membrane plasmique

Une membrane plasmique composée d'une bicouche phospholipidique ainsi que de glycolipides insérés tels que les phosphadityl-*myo*-inositol mannosides (PIM), du lipomannane (LM) et enfin du lipoarabinomannane (LAM) qui, eux, traversent toute la paroi jusqu'à la surface de celle-ci. Un nombre important de protéines membranaires sont également présentes telles que des porines, les plus étudiées étant les protéines MspA chez *Mycobacterium smegmatis,* qui possèdent des homologues chez *M. abscessus* et permettent l'entrée de solutés de faible taille du périplasme vers le cytoplasme (Figure 3).

I.3.2.2. Peptidoglycane

Le peptidoglycane mycobactérien est composé d'unités glycosidiques reliées par des liaisons β 1-4 osidiques. Les principales différences avec le peptidoglycane retrouvé chez les Gram$^+$ est la présence de N-glycolylmuramique (NGM) en plus du N-acétylmuramique (NAM) et du N-acétylglucosamine (NAG), cette présence de N-glycosylation expliquerait la forte résistance physique du peptidoglycane mycobactérien (Mocé-llivina et al. 2004). Il est différent du peptidoglycane classique car il possède également des L,D-transpeptidases (en plus des D,D-transpeptidases). Un équilibre existe entre ces deux types de transpeptidases pour permettre de renouveler le peptidoglycane (Mainardi et al. 2002). Chez *M. tuberculosis* il a été montré qu'en phase stationnaire les L,D-transpeptidases sont les plus actives (Lavollay et al. 2008). En revanche chez *M. abscessus*, peu importe que la phase de croissance soit exponentielle ou stationnaire, il existe un équilibre entre D,D-transpeptidases et L,D-transpeptidases même si ces dernières sont légèrement plus actives (Lavollay et al. 2011). (Figure 3)

I.3.2.3. L'arabinogalactane

Une couche d'arabinogalactane, située au-dessus du peptidoglycane, est constituée d'un long polysaccharide composé d'une partie arabinane et d'une partie galactane, qui sont des polymères d'arabinose et de galactose, respectivement. L'arabinogalactane est lié covalemment au peptidoglycane par les molécules de D-galactofuranosyle *via* une molécule de L-rhamnose-phosphate. (Alderwick et al. 2015) (Figure 3)

I.3.2.4. La mycomembrane

Situé au-dessus de l'arabinogalactane, le feuillet interne de la mycomembrane qui représente la dernière structure solide de la paroi mycobactérienne. Elle est composée d'acides mycoliques (AM) qui sont spécifiques et uniques aux mycobactéries. Chez *M. tuberculosis,* les mycolates sont synthétisés par une voie métabolique complexe. Elle consiste en la synthèse et l'élongation d'une chaîne d'acide gras précurseur α et d'une chaîne acide méromycolique. Ces chaînes seront ensuite activées et condensées ensembles.

Cette voie métabolique possède deux systèmes « Fatty Acid Synthesis » (FASI et FASII), possédant 4 fonctions catalytiques : condensation, réduction, déshydratation et réduction. Ces systèmes de synthèse d'acides gras sont essentiels chez les mycobactéries (Zimhony et al. 2004).

Dans un premier temps , le système FasI, codé par le gène *fas*, possède 7 domaines différents les uns des autres et assure la synthèse des lipides à partir d'acétyl-CoA (Bloch and Vance 1977). Dans une première étape, le complexe Acyl-CoA Carboxylase 6 (ACCase 6) va intervenir pour synthétiser du malonyl-CoA, substrat de FasI, à partir d'acétyl-CoA. Ce complexe est formé de deux sous-unités : AccD6 (qui possède une fonction carboxyltransférase) et AccD3 (Kurth et al. 2009).

Dans un second temps, le système FasII, composé d'enzymes discrètes assure les 4 étapes suivantes : condensation, réduction, déshydratation et réduction. Toutes ces étapes constituent un cycle et à chaque fois que le cycle est complété, deux carbones sont ajoutés à la chaîne carbonée initiale, produite par FasI. Le malonyl-CoA synthétisé par FasI nécessite une activation

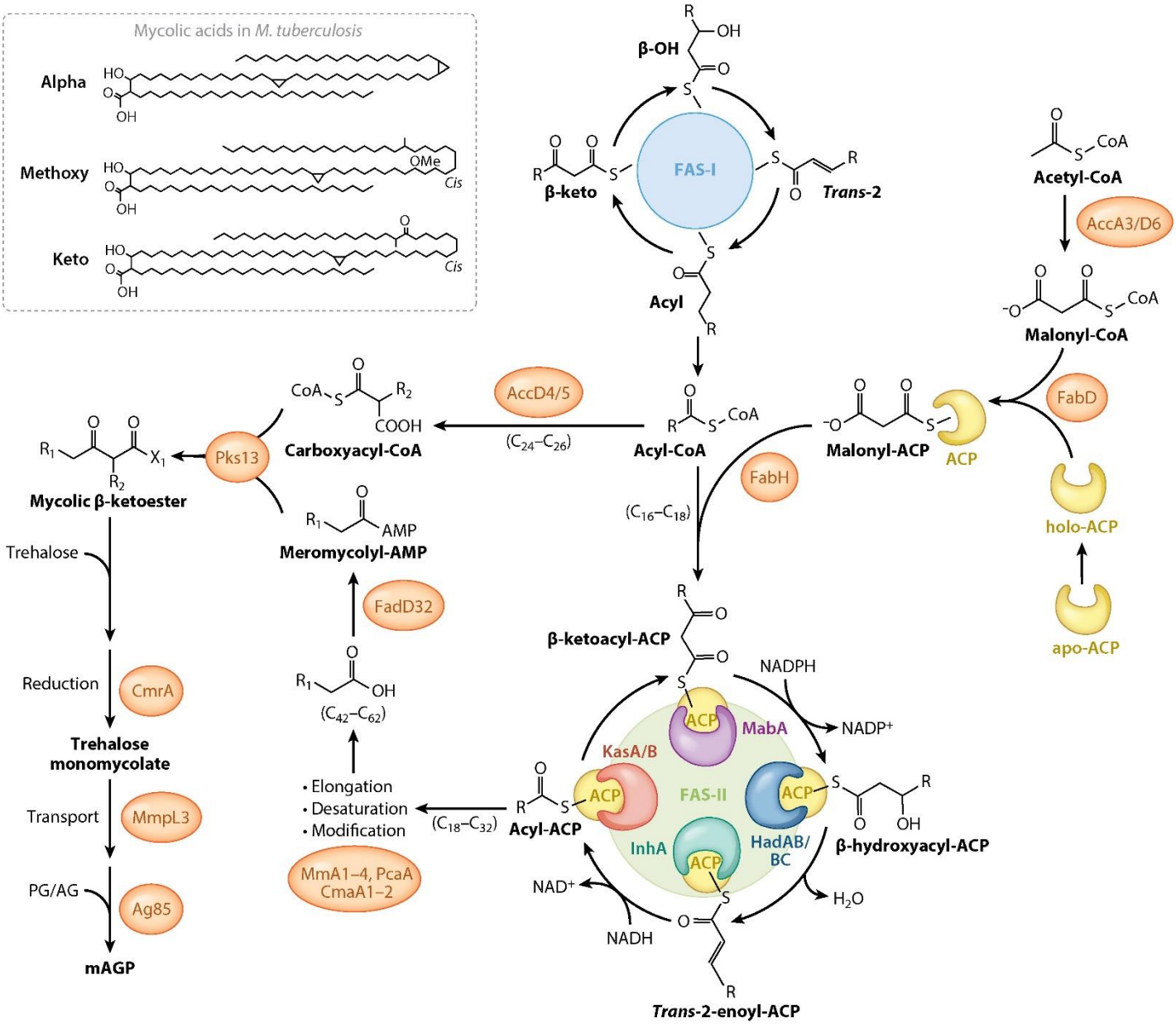

Figure 4. Schéma de la voie de biosynthèse et structure des principaux des acides mycoliques.

Les deux systèmes FasI et FasII impliqués dans l'élongation des chaînes carbonées constituant les AM sont représentés sur ce schéma ainsi que les enzymes permettant l'activation des substrats ainsi que la synthèse des TMM. (D'après Jankute et al. 2015)

pour pouvoir être pris en charge par FasII. Tout d'abord l'enzyme 4'PhosphoPantetheinyl Transférase (Ppt) va permettre d'activer une Acyl Carrier Protein (ACP) qui passe d'une forme apo-ACP à une forme holo-ACP (Zimhony et al. 2015). Ensuite l'enzyme FabD, une malonyl-CoA:ACP transacylase qui utilise du malonyl-CoA et de l'holo-ACP pour former du malonyl-ACP qui peut être directement utilisé par le système FasII (Kremer et al. 2001). Enfin, FabH, une β-cétoacyl-ACP synthase utilise préférentiellement l'acyl-CoA issue de FasI plutôt que l'acyl-ACP, et du malonyl-CoA pour produire du β-cétoacyl-ACP qui pourra être utilisé directement par le système FasII (Figure 4) (K. H. Choi et al. 2000).

L'élongation par FasII est une suite de 4 réactions enzymatiques. La première est médiée par les enzymes KasA et KasB qui vont permettre, par la réaction de condensation du malonyl-ACP en acyl-ACP, d'allonger la chaîne méromycolique de 2 carbones. Ces enzymes sont très proches et possèdent une forte homologie de séquence (66% d'identité). L'utilisation de malonyl-CoA marqué au ^{14}C a permis de montrer, chez *M. smegmatis*, que KasA utilise préférentiellement des lipides d'une taille d'environ 40 atomes de carbone tandis que KasB catalyse préférentiellement l'élongation des acides gras d'une taille d'environ 54 atomes de carbone. KasA aurait un rôle plus précoce alors que KasB n'agirait que lors des derniers cycles d'élongation (Slayden and Barry 2002). KasA est essentielle à la synthèse des AM contrairement à KasB (Bhatt et al. 2005). La seconde réaction est catalysée par MabA, une β-cétoacyl-ACP réductase NADPH dépendante, qui produit du β-hydroxyacyl-ACP à partir du produit issu de la condensation de KasA générant le β-cétoacyl-ACP (Marrakchi et al. 2002). La troisième réaction est catalysée par InhA, une 2-trans-enoyl-ACP réductase NADH dépendante qui utilise le produit de la déshydratation, le 2-trans-énoyl-ACP pour produire de l'acyl-ACP (Quémard et al. 1995). Les gènes *mabA et inhA* sont en opéron chez *M. tuberculosis* et *M. bovis* BCG mais possède une transcription indépendante chez *M. smegmatis* (Banerjee et al. 1998). L'inactivation chromosomique d'*inhA* chez *M. smegmatis* conduit à un arrêt du système FasII et une absence de synthèse des AM induisant la lyse du bacille. Les gènes *mabA et inhA* sont essentiels à la survie des mycobactéries (Parish et al. 2007; Vilchèze et al. 2000). Chez *M. tuberculosis*, la réaction de déshydratation du système FasII est réalisée par 3 déshydratases HadA, HadB et HadC qui sont encodées par les gènes *hadA (Rv0635)*, *hadB (Rv0636)* et *hadC (Rv0637)*, respectivement. Comme pour KasA et KasB, HadAB intervient dans les cycles précoces de l'élongation tandis que HadBC intervient dans les derniers cycles (Sacco et al. 2007; Brown et al. 2007). Une fois les chaînes α et méromycoliques synthétisées, elles vont être condensées ensembles en deux étapes distinctes : la carboxylation de la chaîne α puis la condensation des deux chaînes ensembles. La

première est médiée par les carboxylases AccA3 et AccA4 qui vont carboxyler l'acyl-CoA en carboxyacyl-CoA (Portevin et al. 2005; T. J. Oh et al. 2006). Ensuite, une fatty-acyl-AMP ligase (FadD32) va activer les longs acides gras pour produire de l'acyl-AMP (Trivedi et al. 2004). Enfin, cet acyl-AMP va être pris en charge par Pks13, une polykétide synthase. Cette enzyme nécessite une activation au préalable par une phosphopantéthéine transférase (PptT) qui va permettre l'ajout de P-Pant sur les deux domaines ACP de Pks13. Elle va catalyser la condensation des chaînes α et méromycoliques avec l'ajout d'une molécule de tréhalose pour générer de l'α-alkyl β-cétoacyl tréhalose (TMMk). Enfin, la dernière étape est la réduction du TMMk en Tréhalose MonoMycolate (TMM) par la *Corynebacterinae* mycolate réductase A, CmrA. Tous les gènes *accD4*, *fadD32k, pks13* codant pour ces enzymes impliquées dans la condensation mycolique sont retrouvés en opéron chez *M. tuberculosis*, ce qui appuie le fait que ces enzymes appartiennent au même système métabolique, FasII (Chalut et al. 2006; Gavalda et al. 2009; 2014; Lea-Smith et al. 2007). Ces TMM seront ensuite transportés par MmpL3, une protéine membranaire, présentée dans la sous-partie suivante « I.4 Mycobacterial membrane protein Large (MmpL) ». Ils seront ensuite soit donneurs pour la mycolylation de l'AG, soit convertis en Tréhalose di-mycolate (TDM) pour être enchâssés dans la mycomembrane (Figure 4) (Marrakchi et al. 2014).

Les acides mycoliques sont classés en 3 grands groupes : alpha, méthoxys et kétos, suivant leur composition en lipides et glycolipides complexes, et sont considérés comme des facteurs de virulence majeurs (Figure 4).

Intercalées entre ces acides mycoliques, sont présentes chez *M. tuberculosis*, d'autres lipides complexes tels que du DiAcyl Tréhalose (DAT), du PolyAcyl Tréhalose (PAT), du Phthirocérol DiMycocérosate (PDIM) et des SulfoGlycoLipides (SGL)(Abrahams and Besra 2018). Enfin les GlycoPeptidoLipides (GPL), qui sont transportés par MmpL4 à travers la membrane plasmique. Ils sont indispensables à la détermination du morphotype de la bactérie et sont considérés comme des facteurs de virulence. (Gutiérrez et al. 2018)

Sur la partie externe de la mycomembrane est parfois observé une couche peu organisée, la capsule, qui est composée de molécules libres telles que des protéines et de polysaccharides. Il a été montré que les principales molécules présentes dans la capsule des mycobactéries à croissance lente sont les polysaccharides alors que pour les mycobactéries à croissance rapide ce sont les protéines (Daffé and Marrakchi 2019).

I.4. Mycobacterial Membrane Protein Large (MmpL)

Les Mycobacterial Membrane Protein Large (MmpL) sont des protéines membranaires dont les fonctions sont très peu décrites. Elles sont spécifiques des mycobactéries, même si des orthologues existent chez d'autres familles bactériennes.

Ces protéines représentent une sous-classe de la superfamille de transporteurs RND (Resistance-Nodulation-cell Division) dont la taille est comprise entre 700 et 1300 résidus et qui comprennent en général 10 à 12 domaines transmembranaires (TM) avec des domaines C-terminal et N-terminal cytosoliques (Figure 5). Deux domaines périplasmiques sont souvent présents, le premier entre les TM 1 et TM 2 et le second entre les TM 7 et TM 8 (Yamaguchi et al. 2015). Leur rôle principal est l'efflux d'un large éventail de composés organiques, métaux lourds, lipides et antibiotiques (Nikaido 2010).

Concernant la topologie des MmpL, *Chim et al.* ont proposé un modèle pour lequel l'organisation est conservée parmi tous les MmpL. La structure proposée est constituée de 12 TM avec deux domaines périplasmiques entre les TM 1 et TM 2 ainsi qu'entre les TM 7 et TM 8, ce qui concorde avec les structures décrites pour les transporteurs RND. Cependant dans leur étude, ces deux domaines périplasmiques sont sensiblement plus petits que ceux retrouvés pour les RND. Grâce à la structure du deuxième domaine (D2), ils ont pu conclure que l'organisation de ce domaine était la même que pour les transporteurs RND. La dernière caractéristique qu'ils ont décrite concerne le domaine C-terminal pour lequel ils prédisent deux groupes différents parmi les MmpL, le deuxième (MmpL3/MmpL11) possèderait un domaine C-terminal étendu permettant l'amarrage de protéines accessoires requises pour leur fonction de transport de lipides (Figure 5) (Chim et al. 2015). *Carel et al.* ont localisé par microscopie à fluorescence MmpL3 aux pôles de la bactérie et ont montré que ce domaine C-terminal spécifique était nécessaire à la localisation polaire de la protéine chez *M. smegmatis* (Carel et al. 2014). Chez *M. abscessus*, les MmpL sont au nombre de 27, un nombre élevé par rapport à d'autres espèces telles que *M. tuberculosis* ou *M. leprae* qui n'en possède que 13 et 4, respectivement. Les gènes codant pour ces protéines (environ 3000 pb) sont souvent associés à des gènes *mmpS* (environ 500 pb) qui codent pour des protéines accessoires Mycobacterial membrane protein Small (MmpS), qui semblent être impliquées dans la stabilisation des MmpL pour permettre le transport de lipides. D'autres protéines accessoires sont en relation étroites avec les MmpL, un exemple est la protéine TtfA qui est associée à MmpL3 qui a été identifiée par Fay *et al* et dont

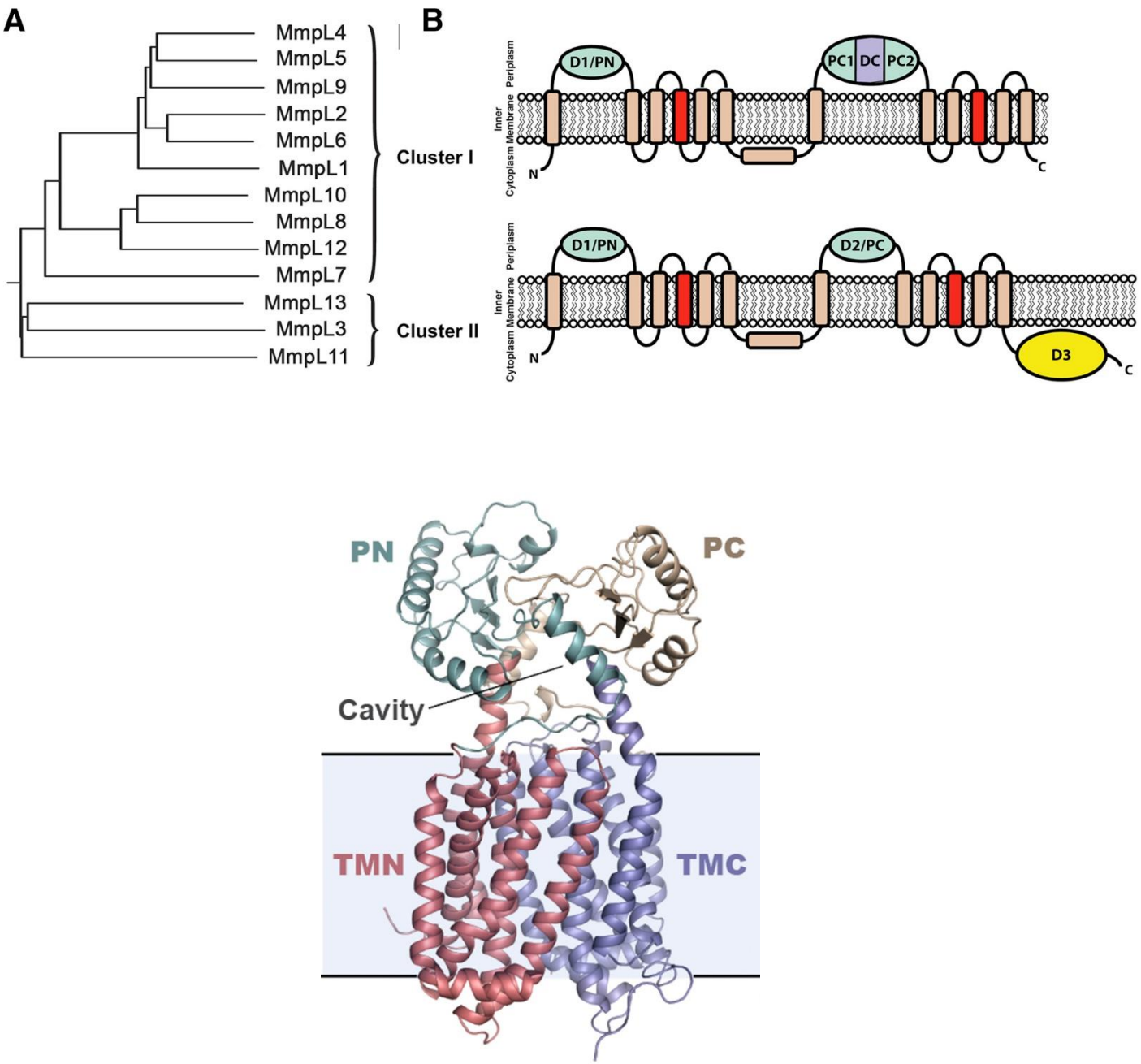

Figure 5. Topologie et structure des MmpL.

(A) Arbre phylogénétique montrant deux groupes distincts au sein de la famille MmpL. **(B)** Prédiction de la topologie des MmpL des groupes I et II basée sur celle des transporteurs RND. Les domaines porteurs (PC1, PC2, PC et DC) sont représentés en vert, le domaine D3 en jaune et les domaines transmembranaires en beige à l'exception des TM4 et TM10 centraux qui sont en rouge. Les TM6 et TM7 sont représentés parallèles à la membrane plasmique, comme observés dans la structure des transporteurs RND**. (C)** Représentation de la structure cristallographique de MmpL3 de *M. smegmatis*. Les domaines PN et PC s'entrelacent pour former une cavité annotée en gris, qui se connecte à trois ouvertures, un entonnoir au-dessus, une ouverture devant et une autre derrière. (Adapté de *Chim et al.* et *Zhang et al.*).

la structure a ensuite été résolue récemment mais sa fonction demeure encore inconnue (Fay et al. 2019; Ung et al. 2020).

La première MmpL impliquée dans le transport de lipide chez *M. tuberculosis* à avoir été décrite est MmpL7, qui assure le transport des PDIM (J. S. Cox et al. 1999; Camacho et al. 2001). Ensuite, la fonction de MmpL8 a été décrite dans le transport des SL (Converse et al. 2003) et enfin MmpL10 dans le transport du PAT (Belardinelli et al. 2014). MmpL11 semble être impliquée dans l'export de monoméromycolyl diacylglycérol (MMDAG) ainsi que des esters de mycolate chez *M. smegmatis*. La complémentation d'un mutant *mmpL11* chez *M. smegmatis* avec le gène *mmpL11* de *M. tuberculosis* restaure l'export de ces lipides, ce qui semble indiquer que le gène présent chez *M. tuberculosis* possède la même fonction (Pacheco et al. 2013).

La principale fonction des MmpL semblerait être le transport de lipides à travers la paroi et l'exemple le mieux décrit chez *M. abscessus* concerne l'export des GPL grâce au système MmpS4-MmpL4a/MmpL4b. Cet opéron est entouré par tous les gènes nécessaires à la synthèse et l'assemblage de ces GPL complexes. Ce locus de gènes est très conservé chez toutes les espèces mycobactériennes productrices de GPL telles que *M. abscessus*, *M. avium* ainsi que *M. smegmatis* (Figure 6). La délétion de *mmpL4b* dans une souche parentale de *M. abscessus* entraîne également l'apparition de la capacité à former des cordes et d'une virulence globalement accrue dans un modèle d'infection de zebrafish (Bernut et al. 2014). Cette étude a permis d'associer un rôle dans la virulence aux MmpL, ce qui avait déjà été montré chez *M. tuberculosis* avec l'étude de *Domenech et al.* consistant à inactiver 11 gènes *mmpL* dans la bactérie et observer leurs phénotypes dans un modèle souris. Globalement les mutants *mmpL4*, *mmpL7*, *mmpL8* et *mmpL11* présentaient une virulence atténuée dans la souris (Domenech et al. 2005). Ceci a été confirmé dans une autre étude dans laquelle différents MmpL ont été étudiés et pour lesquels les auteurs ont observé des difficultés de croissance dans les poumons des souris pour les mutants *mmpL4*, *mmpL5, mmpL7, mmpL8*, *mmpL10*, et *mmpL11* (Lamichhane et al. 2005).

Un autre exemple est celui de MmpL3 qui est impliquée dans le transport de mycolates sous forme de TMM chez *M. smegmatis et M. tuberculosis* (Varela et al. 2012). Ces TMM seront pris en charge par les mycolyltransférases du complexe Ag85 pour être, soit associés à l'AG, soit associés en TDM, lesquels seront par la suite insérés dans la membrane externe. MmpL3 est actuellement la seule MmpL décrite comme essentielle expliquant pourquoi ce locus est très conservé parmi les mycobactéries telles que *M. abscessus, M. tuberculosis, M. leprae, M. avium* et enfin *M. marinum* (Viljoen et al. 2017). Ces caractéristiques rendent MmpL3

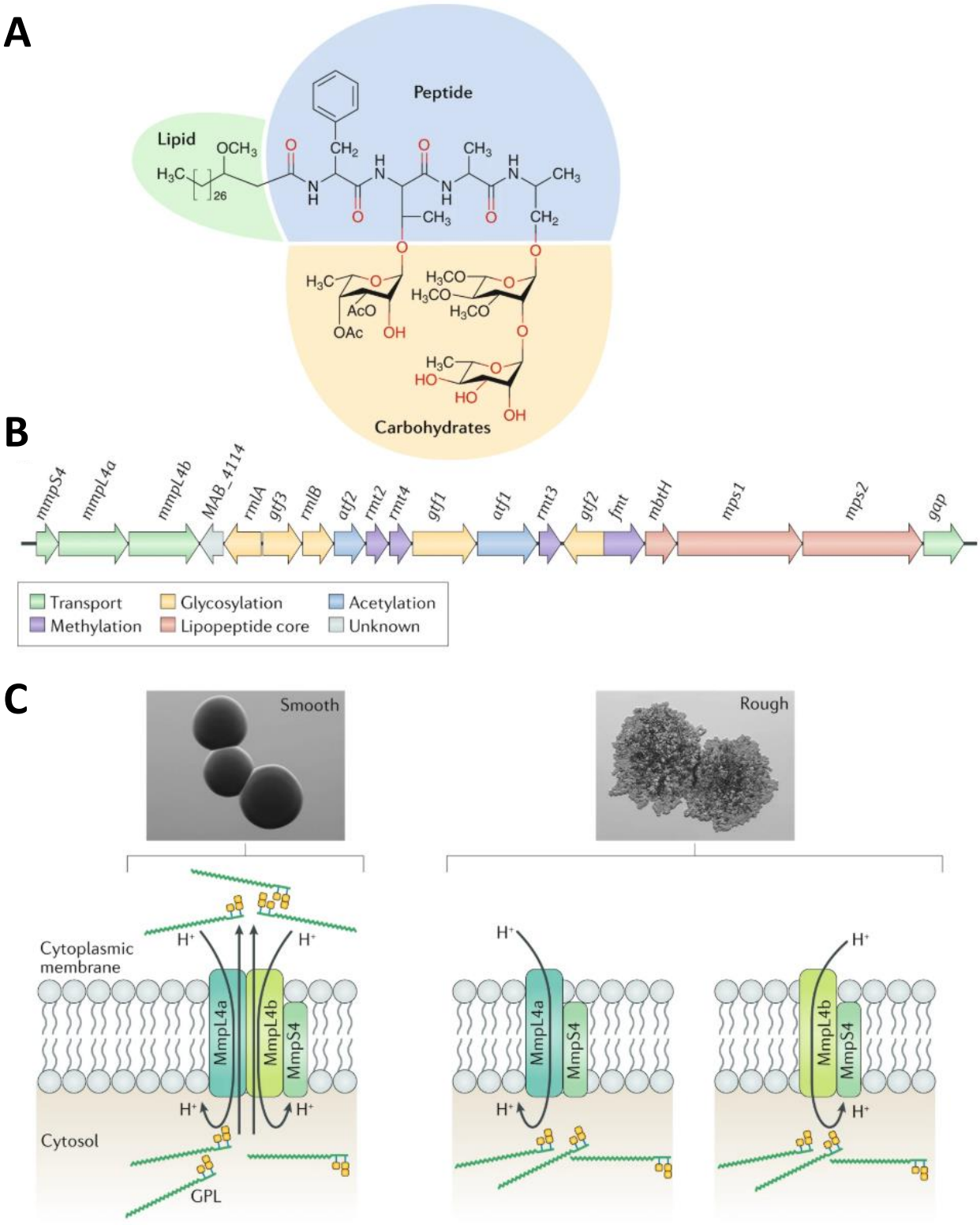

Figure 6. L'export des GPL à travers la membrane plasmique par MmpL4 est responsable du morphotype chez *M. abscessus.*

(A) Structure d'une molécule de GPL constitué de peptide, de lipide et de sucres. **(B)** Locus de synthèse/modification/transport des GPL. **(C)** Les GPL régulent l'hydrophobicité de la bactérie ainsi que sa capacité à former des biofilms. Chez *M. abscessus,* le morphotype S produit une large quantité de GPL tandis que la R n'en produit pas (ou peu). MmpL4a et MmpL4b transportent les GPL à travers la membrane plasmique et leur fonction est indispensable à la détermination d'un phénotype S ou R. (D'après Johansen et al, 2020)

très intéressante en tant de cible thérapeutique (Dupont et al. 2016; Kozikowski et al. 2017). Cet aspect thérapeutique sera abordé plus en détail dans la partie « III.9.4 Les inhibiteurs de MmpL3 ».

Chez *M.* tuberculosis, *mmpL8* est impliqué dans le transport des SL tandis que chez *M. abscessus* il est impliqué dans le transport d'un autre lipide, le Gycosyl Diacetylated Nonadecyl Diol (GDND), dont la fonction biologique reste inconnue. L'absence de ce lipide fait perdre à *M. abscessus* sa capacité de survie intracellulaire dans différents modèles d'infection tels que l'amibe, le macrophage ou encore chez le zebrafish ce qui montre aussi son implication dans la virulence (Dubois et al. 2018).

Deux autres MmpL, MmpL4 et MmpL5, qui sont impliquées dans l'export de sidérophores chez *M. tuberculosis,* peuvent expulser des substrats hors de la bactérie tels que des antibiotiques. MmpL5 est impliquée dans la résistance à la bédaquiline (BDQ) et à la clofazimine (CFZ) chez *M. tuberculosis* (Hartkoorn et al. 2014). Récemment *Richard et al.* ont montré que MmpL5 était impliquée dans la résistance à la BDQ et à la CFZ chez *M. abscessus via* un système de régulation TetR (Richard et al. 2019). Des mutants résistants au linézolide ont été séquencés afin d'identifier les mutations responsables dans cette résistance, et *mmpL10* fait partie des gènes mutés (Ye et al. 2019). Cette partie sur la fonction pompe à efflux des MmpL sera développée plus en détail dans les parties « IV.2.3.1 Efflux de la bédaquiline et la clofazimine » et « IV.2.3.2 Efflux du linézolide ».

I.5. Les mycobactéries à croissance lente (MCL)

Le groupe des MCL comprend surtout des mycobactéries pathogènes telles que *M. tuberculosis, M. leprae, M. avium* et *M. kansasii*. La principale caractéristique de ces bactéries est de mettre plus de 7 jours pour qu'une colonie soit visible sur milieu solide. Elles sont surtout responsables d'infections pulmonaires persistantes et sont très difficiles à éradiquer (Figure 7).

I.6. Les mycobactéries à croissance rapide (MCR)

Le groupe des MCR comprend majoritairement des bactéries environnementales souvent non-pathogènes telles que *M. smegmatis* mais certaines peuvent devenir des pathogènes opportunistes lorsque l'hôte possède un système immunitaire affaibli. Parmi celles-ci, les complexes *M. fortuitum* et *M. abscessus* sont les plus connus. Leur caractéristique principale est

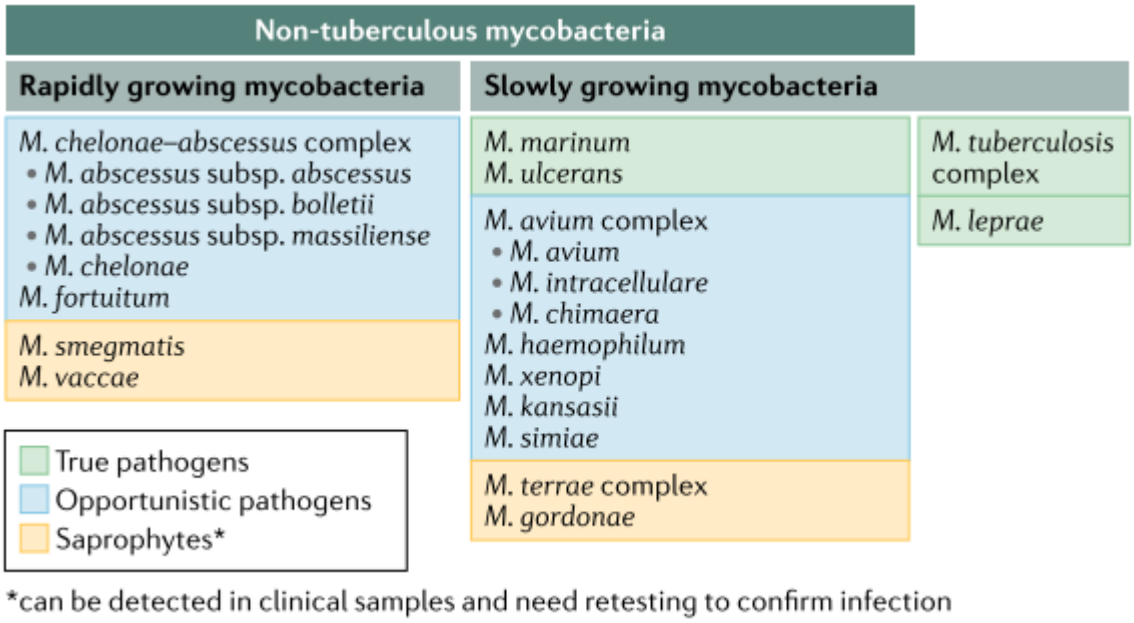

Figure 7. Représentation des mycobactéries notoires.

La classification des mycobactéries évolue sans cesse et a changé énormément ces dernières années du fait de la modernisation du séquençage à haut débit. Cette avancée technologique a permis la classification de beaucoup de mycobactéries pathogènes émergentes dont l'identification a été méconnue pendant longtemps. (D'après Johansen et al, 2019)

qu'il faut moins de 7 jours pour qu'une colonie soit visible sur milieu solide (Figure 7) (Howard and Byrd 2000).

I.7. Les mycobactéries non-tuberculeuses

Les MNT englobent les espèces ne présentant pas les caractéristiques cliniques classiques du bacille tuberculeux. Elles comprennent surtout des espèces environnementales non pathogènes mais beaucoup d'entre elles sont des pathogènes opportunistes. Ces pathogènes profitent souvent d'une pathologie sous-jacente au niveau pulmonaire, cutané, des muqueuses ou d'une défaillance au niveau du système immunitaire pour coloniser l'hôte (Won-Jung Koh 2016). De nos jours, elles occupent une place de plus en plus importante car les cas cliniques ne cessent d'augmenter. Les espèces les plus fréquentes appartiennent au complexe *M. avium* (MAC) ainsi qu'au complexe *M. abscessus* (MABSC) (Mougari et al. 2016). Plus récemment, de nouvelles espèces ont été identifiées en clinique et commencent à être caractérisées du point de vue de leur pathogénicité comme *M. fortuitum* ou *M. kansasii.* (Figure 7) (Johansen and Kremer 2020a; 2020b)

II. Le complexe *Mycobacterium abscessus*

II.1. Histoire et présentation du complexe

Les membres du MABSC étaient autrefois assimilés à *M. chelonae* au sein du complexe *M. fortuitum*. En 1992, *M. abscessus* est devenue une seule et même espèce et après de nombreuses hésitations sur la légitimité de l'intégration de *Mycobacterium bolletii* au sein du complexe, aujourd'hui le MABSC comprend 3 sous-espèces qui sont *M. abscessus subsp abscessus, M. abscessus subsp massiliense (M. massiliense) et M. abscessus subsp bolletii* (*M. bolletii)* (Figure 8) (Adekambi et al. 2017; Tortoli et al. 2016). Ces trois sous-espèces se différencient majoritairement par leurs différences au niveau de leur spectre de sensibilité aux antibiotiques et c'est pour cette raison qu'il est indispensable en clinique de déterminer la sous-espèce avant de décider d'un traitement (Benwill and Wallace 2014).

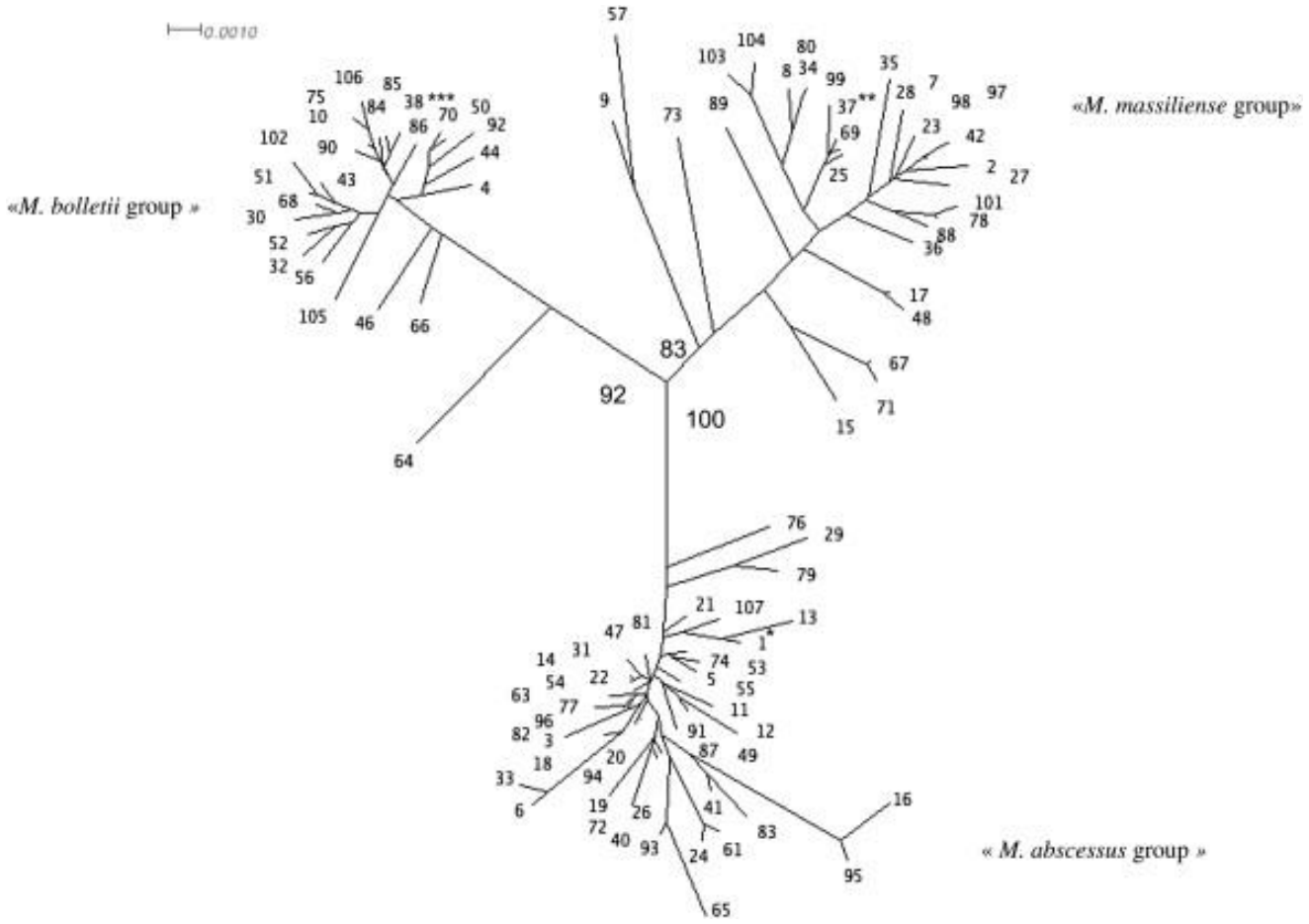

Figure 8. Arbre phylogénétique représentant le complexe *M. abscessus.*

Cet arbre a été construit par analyse MLST. Les locus pris en compte dans cette étude sont *argH, cya, glpK, gnd, murC, pta, purH*. **M. abscessus* CIP 104536^{T}; ***M. massiliense* CIP 108297^{T}; ****M. bolletii* CIP 108541^{T} (D'après Macheras et al, 2014)

II.2. *Mycobacterium abscessus subsp abscessus*

II.2.1. Les différents morphotypes

Mycobacterium abscessus est une bactérie qui existe sous la forme de deux morphotypes distincts présentant chacun des propriétés physiologiques et pathologiques spécifiques.

II.2.1.1. Le morphotype lisse

Le morphotype lisse (Smooth ou S) possède, sur milieu solide, une forme ronde et crémeuse, qui est rendue possible grâce aux GPL présents à la surface du bacille, insérés dans la mycomembrane (Figure 9). Ce sont ces lipides de surface qui confèrent au morphotype lisse ses propriétés physiopathologiques. Ce morphotype S est capable de former des biofilms (communauté multicellulaire adhérant entre eux et à une surface et marquée par la sécrétion d'une matrice adhésive et protectrice), ce qui permet de diminuer la pénétration d'agents anti-microbiens ou des effecteurs du système immunitaire au sein du regroupement ainsi que de faciliter les échanges intercellulaires, ce qui participe à la persistance de ce morphotype. Il est également très mobile et est capable de glisser sur la gélose d'une boîte de pétri (sliding motility) toujours grâce à la présence de GPL à la surface du bacille (Bernut et al. 2014). Le morphotype S est considéré comme la forme colonisante et peut transiter vers la forme rugueuse au cours de la maladie. Ce morphotype est généralement retrouvé dans les phases précoces de l'infection (Bernut et al. 2016).

II.2.1.2. Le morphotype rugueux

Le morphotype rugueux (Rough ou R), de forme irrégulière et craquelée sur milieu solide, se caractérise par l'absence partielle ou totale de GPL à sa surface (Figure 9). Malgré cette absence de GPL à sa surface et l'hypothèse qu'ils étaient nécessaires à la formation du biofilm, Clary et al. ont récemment montré que les bacilles de type R pouvaient être impliqués dans des biofilms (Clary et al. 2018). Cette absence de GPL dans la mycomembrane du morphotype R peut être expliquée en partie grâce à l'identification de mutations dans le locus comprenant les gènes impliqués dans la synthèse de ceux-ci (Pawlik et al. 2013) mais également dans les gènes codant pour le transporteur MmpL4a/MmpL4b (Bernut et al. 2016). Cela permet à d'autres lipides ou protéines d'être démasqués comme les PIM et les lipoprotéines (Roux et al. 2011) qui sont

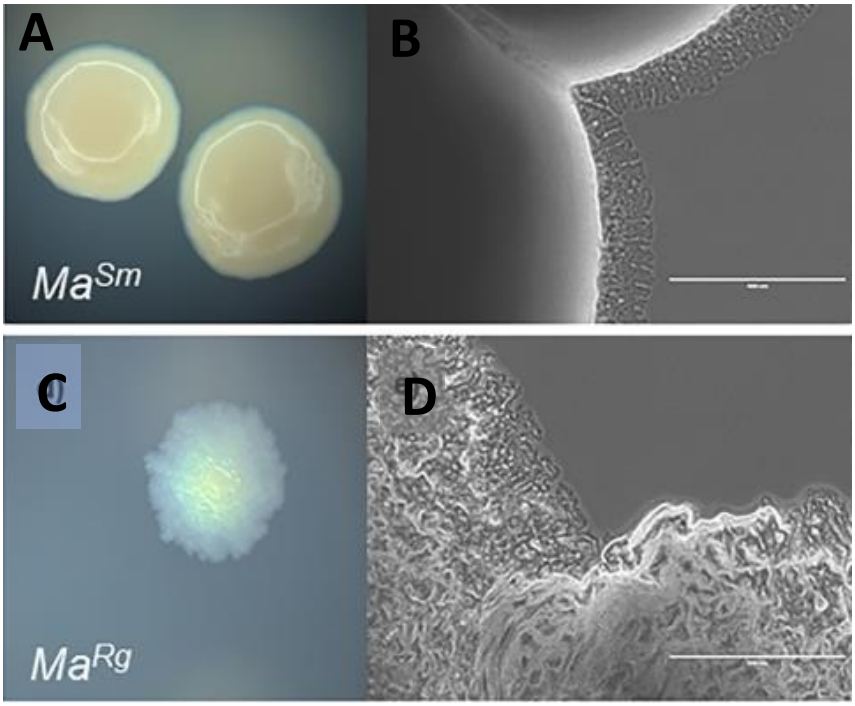

Figure 9. Caractérisation des morphotypes lisse et rugueux caractéristiques de *M. abscessus.*

(A et C) Morphologie des colonies de *M. abscessus* sur milieu agar 7H10. **(B et D)** à faible zoom, le morphotype R forme des cordes visibles. (Adapté de Clary et al. 2018)

reconnus par les Toll-Like Receptor 2 (TLR2) pour déclencher l'inflammation. Il a également été montré que les molécules de TPP présentes dans la mycomembrane étaient, elles-aussi, impliquées dans la formation d'agrégats bactériens appelés « cordes » (Llorens-Fons et al. 2017). Ces cordes de grande taille ne peuvent plus être phagocytées par les cellules du système immunitaire inné tels que les macrophages ou les neutrophiles (Bernut et al. 2014). Cette organisation structurale diminue également la pénétration des molécules anti-microbiennes. Ces caractéristiques font du morphotype R la forme hypervirulente qui est surtout retrouvée dans les phases d'infection aigüe (Catherinot et al. 2009; Jonsson et al. 2007).

II.3. Physiopathologie de l'infection

II.3.1. Infection du macrophage/amibe par *M. abscessus*

L'infection du macrophage par le morphotype S conduit à l'internalisation de plusieurs bacilles individuels. Les GPL présents à la surface de la bactérie masquant des récepteurs de type TLR empêchent la mise en place de la réponse inflammatoire en limitant la surproduction de cytokines pro-inflammatoires et donc le recrutement de nouvelles cellules immunitaires au site de l'infection (Roux et al. 2016). Ils vont également empêcher la fusion des lysosomes avec le phagosome ce qui empêche l'acidification du phagosome, et la destruction des bactéries, *via* des systèmes de sécrétion de type VII, Esx-4 (Laencina et al. 2018).

La réponse inflammatoire est atténuée car les GPL interagissent avec la cyclophiline D, responsable de l'apoptose dans les cellules phagocytaires (Whang et al. 2017). La bactérie va donc survivre dans le macrophage et pouvoir se répliquer jusqu'à ce que la quantité de bactéries intracellulaires soit trop importante et que la cellule hôte meurt, relarguant les bactéries dans le milieu extracellulaire et permettant la réinfection de nouvelles cellules phagocytaires. Le morphotype S peut s'échapper du phagosome vers le cytoplasme cellulaire et permettre une destruction plus rapide du macrophage infecté (Laencina et al. 2018). Le morphotype S est considéré comme une forme persistante (Figure 10). A l'inverse, le morphotype R ne possédant pas ou peu de GPL à sa surface, va être internalisé sous la forme d'agrégats créant alors un « social phagosome ». Ses récepteurs de surface étant démasqués, une forte réponse immunitaire va être induite grâce à la reconnaissance des PIM par les récepteurs de type TLR de la cellule (Roux et al. 2011). La fusion du lysosome avec le phagosome n'est pas inhibée et conduit donc à l'acidification du phagosome. Dans ce cas précis, l'apoptose de la cellule est activée conduisant à la mort cellulaire, on observe donc une lyse plus importante lors de l'infection avec

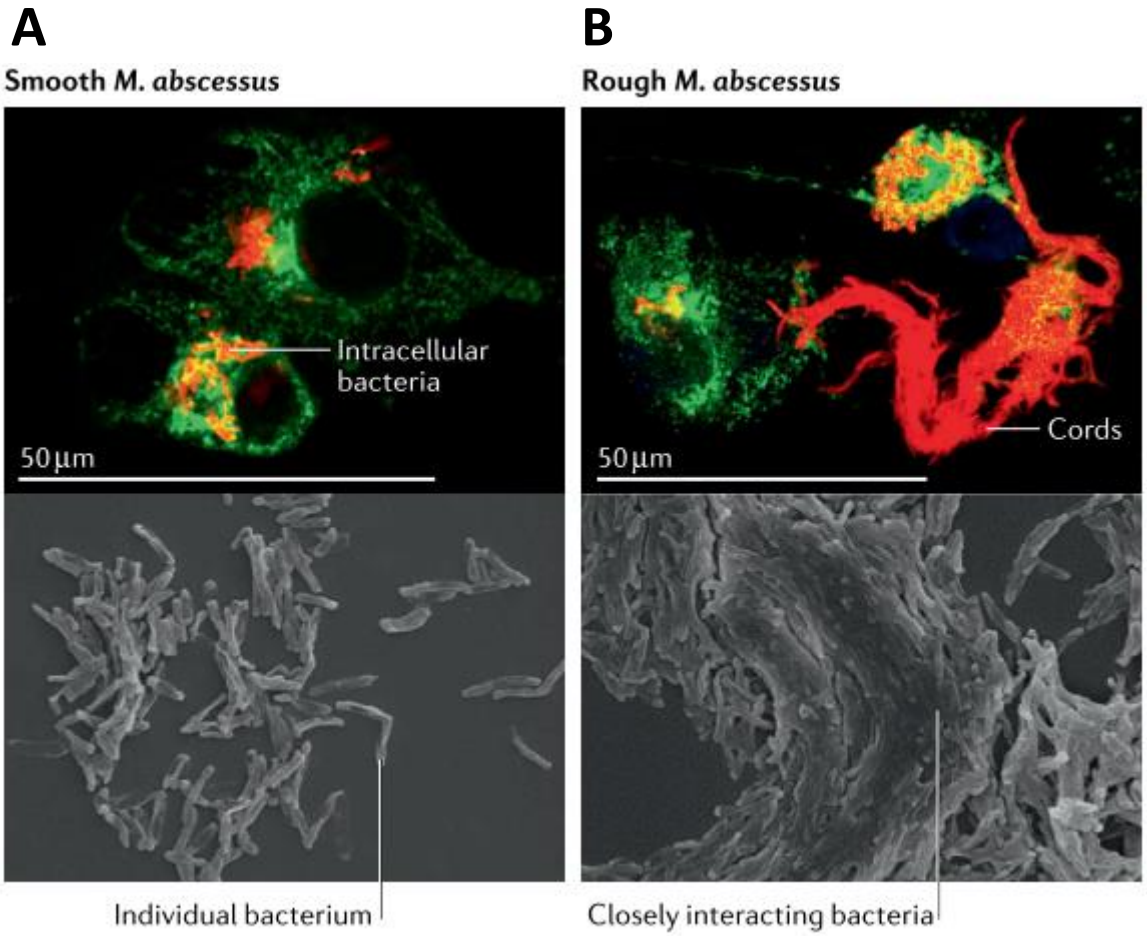

Figure 10. Représentation de *M. abscessus* intracellulaire dans des macrophages infectés.

(A) Le morphotype S est représenté par un mode de survie intracellulaire et avec des bacilles individuels interagissant peu les uns avec les autres**. (B)** Le morphotype R est représenté avec un mode de survie à la fois intracellulaire et extracellulaire sous forme de cordes (en haut), des agrégats formés par des bacilles collés les uns aux autres (en bas). (D'après Johansen et al, 2020)

le morphotype R (Figure 10) (Whang et al. 2017). La capacité du morphotype R à former des cordes compliquera également la (re)phagocytose de ces agrégats pouvant atteindre jusqu'à 100µm de long, qui ne peuvent alors plus être phagocytés par ces cellules immunitaires. Globalement, une réponse inflammatoire exacerbée et une destruction plus rapide des macrophages infectés seront observées qui sont caractéristiques de l'hypervirulence induite durant l'infection par le morphotype R.

II.3.2. Infection chez le poisson-zèbre par *M. abscessus*

Le poisson zèbre (*Danio rerio*) est un modèle utilisé au laboratoire pour étudier la chronologie de l'infection par *M. abscessus* ainsi que les mécanismes de pathogénèse. Les embryons de poisson zèbre sont infectés par micro-injection de bactéries dans la veine caudale à 30h post-fécondation. Grâce à des bactéries exprimant constitutivement une protéine fluorescente et à la transparence des larves, le suivi de l'infection au cours du temps est alors possible en utilisant un microscope à épifluorescence (Figure 11). Dans ce modèle d'étude, les interactions entre les bacilles et les cellules immunitaires sont observables car le système immunitaire inné se met en place rapidement lors des phases précoces du développement de l'embryon (Torraca et al. 2014). En utilisant une lignée transgénique exprimant des cellules immunitaires fluorescentes (macrophages ou neutrophiles), il devient aisé d'observer les interactions hôtes/pathogènes (Bernut et al. 2017).

Lors de l'infection par le morphotype S, un recrutement des cellules immunitaires vers le lieu de l'infection puis une phagocytose rapide des bacilles sont observées. L'infection est alors contenue par le système immunitaire, donc qualifiée de chronique et le taux de survie des embryons observé reste très élevé (90%).

Lors de l'infection par le morphotype R, on observe également un recrutement des cellules immunitaires vers le foyer infectieux mais les bactéries étant déjà agrégées, nombre d'entre elles ne pourront être phagocytées. Les autres seront phagocytées par les macrophages qui vont alors entrer massivement en apoptose entraînant un recrutement excessif de cellules immunitaires qui tenteront de contenir l'infection en formant un granulome. Si l'infection ne parvient pas à être contrôlée, alors les bactéries vont former des cordes dans le milieu extracellulaire qui seront trop volumineuses pour pouvoir être phagocytées conduisant à une surproduction de cytokines, la formation d'un abcès et la dégradation des tissus alentours

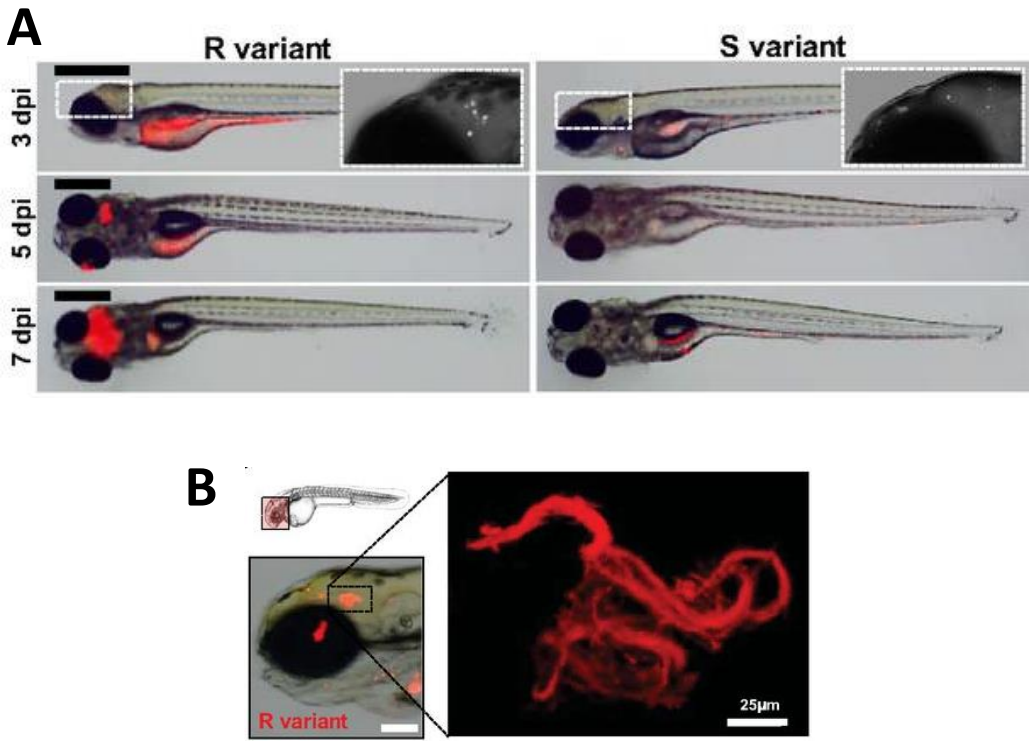

Figure 11. Modèle d'infection du poisson zèbre *Danio rerio* par *M. abscessus*.

(A) Visualisation spatiotemporelle de l'infection par les morphotypes S et R de *M. abscessus*. Les bactéries expriment la protéine fluorescente rouge mCherry. **(B)** Image d'un embryon infecté par le morphotype R. L'image agrandie montre une photo d'une corde prise au microscope confocal. (Adapté de Bernut et al. 2014)

menant à la mort de l'embryon (Bernut et al. 2014). Le taux de survie des embryons observé lors de ces infections est faible (35%), ce qui appuie le caractère hypervirulent de ce morphotype R.

Classiquement, ce modèle est utilisé pour déterminer la virulence d'une souche ou en observer différents paramètres tels que la survie des embryons, le nombre/l'apparition de granulome/abcès et la charge bactérienne par détermination du nombre de pixels fluorescents par embryon. L'efficacité d'une molécule anti-microbienne peut également être mesurée grâce à ces paramètres, sur différents temps après infection par le variant R.

II.3.3. Infection chez la souris immunocompétente et immunodéprimée par *M. abscessus*

L'infection de la souris par *Mycobacterium abscessus* a nécessité beaucoup d'efforts au cours de ces dernières années car l'infection chez la souris blanche (lignée Balb/c) conduit à une forte diminution (disparition) de la charge bactérienne au bout de 3 à 4 semaines (Bernut et al. 2014). Différentes voies d'infection ont été envisagées : intra-veineuse (IV), gavage, aérosol, billes mais aucune d'entre elles ne sont parvenues à établir une infection persistante dans la souris.

Ces raisons ont conduit différentes équipes de recherche à mettre d'autres modèles souris au point : Nude, Gamma interféron KO (GKO), A/J (déficience en fonction macrophagique), beige (mutation sur le chromosome 13), Swiss et C57BL/6J. La charge bactérienne diminue toujours au cours du temps dans tous ces modèles ce qui ne permet pas d'évaluer précisément l'activité de molécules anti-microbiennes actives contre *M. abscessus in vivo* (Lerat et al. 2014). D'autres modèles souris ont été testés : Severe Combined ImmunoDeficiency (SCID), Granulocyte Macrophage Colony Stimulating Factor (GMCSF) pour lesquels l'infection bactérienne est visible jusqu'à 40 jours sans que la charge bactérienne ne diminue au cours du temps (Obregón-Henao et al. 2015). Il existe également un modèle ΔCFTR (S489X avec correction par CFTR humain) sur un fond génétique C57BL/6J mais il ne permet d'observer l'infection que pendant au maximum 15 jours (Caverly et al. 2015).

Plus récemment, un nouveau modèle d'étude a été mis au point. Les souris C3HeB/FeJ sont immunocompétentes et permettent d'observer une charge bactérienne constante jusqu'à 3 semaines, voire 5 à 7 semaines dans le cas d'un traitement aux corticostéroïdes. Ces souris possèdent une mutation dans le locus *sstI* (super susceptible to tuberculosis I) et vont exhiber

des symptômes au niveau pulmonaire tels que des granulomes après l'infection avec une faible diminution de la charge bactérienne (Maggioncalda et al. 2020).

Ce modèle permet d'analyser l'évolution de la charge bactérienne dans le foie, la rate et les poumons afin de suivre la chronologie de l'infection et la répartition de la charge bactérienne dans l'organisme étudié.

II.3.4. Infection à *M. abscessus* chez l'Homme

Les infections causées par des MNT sont diverses et se distinguent par deux grands groupes : les infections extra-pulmonaires et les infections pulmonaires.

II.3.4.1. Infections extra-pulmonaires

Les infections extra-pulmonaires dues aux infections par des MNT touchent principalement la peau et les tissus mous (Figure 12).

Elles apparaissent souvent après des actes chirurgicaux ou des tatouages. C'est principalement l'utilisation d'instruments contaminés qui permet à ces bactéries de traverser l'épiderme et d'aller se nicher dans les couches plus profondes de la peau (Bechara et al. 2010) mais aussi lors d'injection de toxine botulique (Chen et al. 2019).

La plupart du temps, ces infections entraînent des abcès et des lésions ulcératives, qui peuvent plus rarement entraîner une infection disséminée. Ce type d'infections intervient surtout chez les personnes ayant des prédispositions responsables d'une immunodépression (Lee et al. 2015). Elles peuvent également intervenir lorsque l'épiderme est endommagé comme dans le cas des grands brûlés (Vaghaiwalla et al. 2014).

Si l'infection arrive à traverser la barrière hémato-encéphalique, il sera alors possible de retrouver une infection du système nerveux central (SNC) (Talati et al. 2008).

II.3.4.2. Infections pulmonaires

Les infections pulmonaires sont les formes les plus courantes d'infections par les MNT et ce type d'infection est présent sur tous les continents en différentes proportions. La part des infections

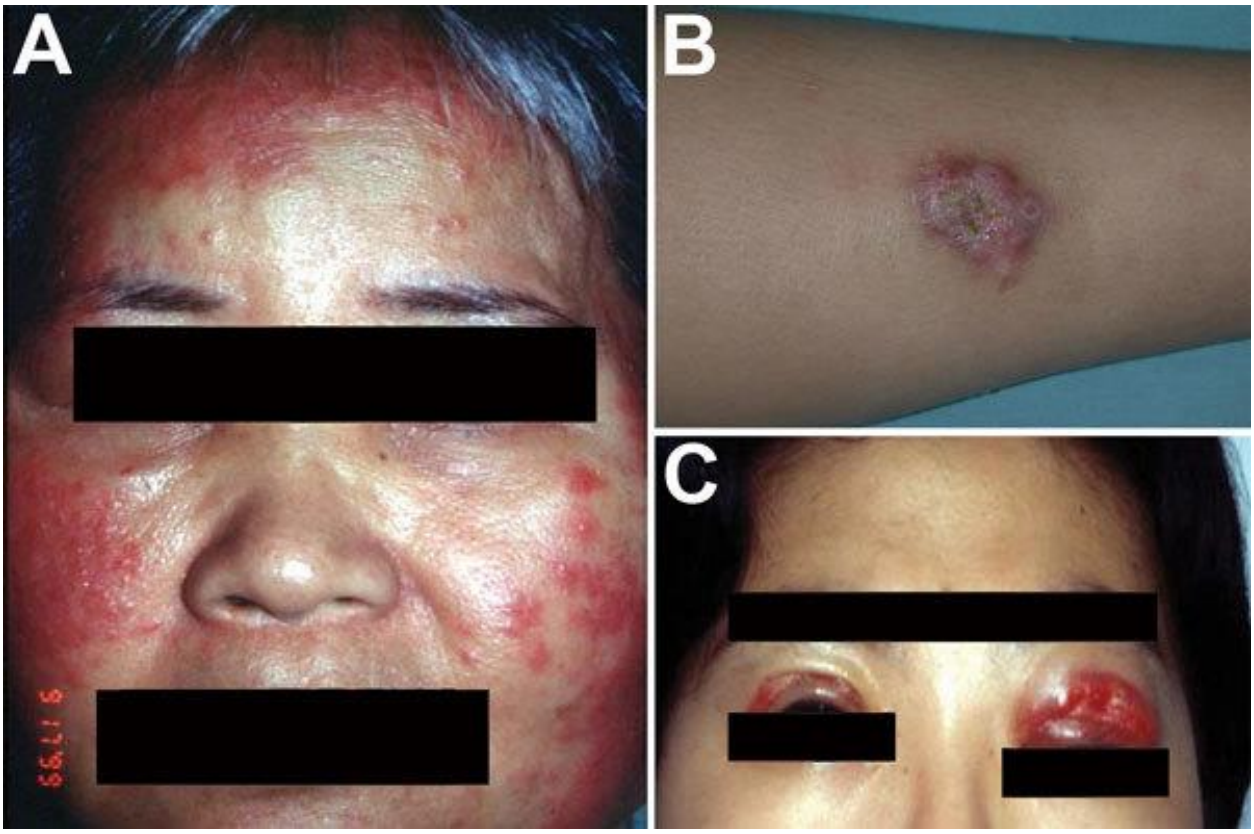

Figure 12. Exemples d'infections extra-pulmonaires à *M. abscessus.*

(A) Une infection à *M. abscessus* au niveau de la peau du visage suite à une lymphadénite. **(B)** Un nodule sous-cutané. **(C)** Une infection des muqueuses sous les paupières supérieures développée une semaine après une intervention de chirurgie esthétique. (D'après Lee et al, 2015)

à *M. abscessus* parmi les infections des MNT est plus élevée dans des pays occidentaux tels que la France, le Royaume-Uni ou les États-Unis que dans les pays orientaux tels que la Chine (Mougari et al. 2016).

Les principaux symptômes sont une toux récurrente et persistante avec production excessive de mucus, hémoptysie, une dyspnée ainsi que de la fièvre et une perte de poids caractéristique. La plupart du temps ces symptômes persistent et la maladie devient chronique. La maladie peut ensuite évoluer avec des formes plus sévères telles que la bronchiectasie nodulaire ou la bronchiectasie fibro-cavitaire, ces formes vont dégrader de façon irréversible les poumons des malades en formant une fibrose ce qui va détériorer grandement leur fonction respiratoire (Figure 13) (https://www.blf.org.uk/support-for-you/non-tuberculous-mycobacterial-infection-ntm).

Ces infections touchent principalement des personnes dites « à risque » qui possèdent des prédispositions médicales même si presque un tiers de ces infections surviennent chez des personnes ne présentant aucun problème de santé majeur (Griffith et al. 1993).

II.3.4.3. Facteurs de risques

Ces prédispositions qui augmentent le risque de la survenue d'infection à *M. abscessus* et aux NTM en général sont appelés facteurs de risques et peuvent être de deux types : d'origine environnementale et non génétique ou d'origine génétique.

II.3.4.3.1. Les troubles pulmonaires chroniques d'origines environnementales et non génétiques

Les troubles pulmonaires d'origine environnementale et non génétique prédisposent à l'infection par *M. abscessus* car ils fragilisent tous le système respiratoire qui est le principal lieu d'infection du corps humain par ce pathogène. Ces facteurs sont très variés et comprennent tout ce qui vient de l'extérieur et qui fragilise les poumons :

-Les broncho-pneumopathies chroniques obstructives (BPCO), qui elles-mêmes englobent deux maladies que sont la bronchite chronique et l'emphysème pulmonaire.

-Les pneumoconioses, qui correspondent à un ensemble de maladies résultant de l'inhalation et de la fixation de particules solides dans les poumons (amiante, silice, charbon…).

-Avoir contracté la tuberculose, les dégâts pulmonaires résultant de la tuberculose pouvant augmenter le risque de contracter une infection aux MNT.

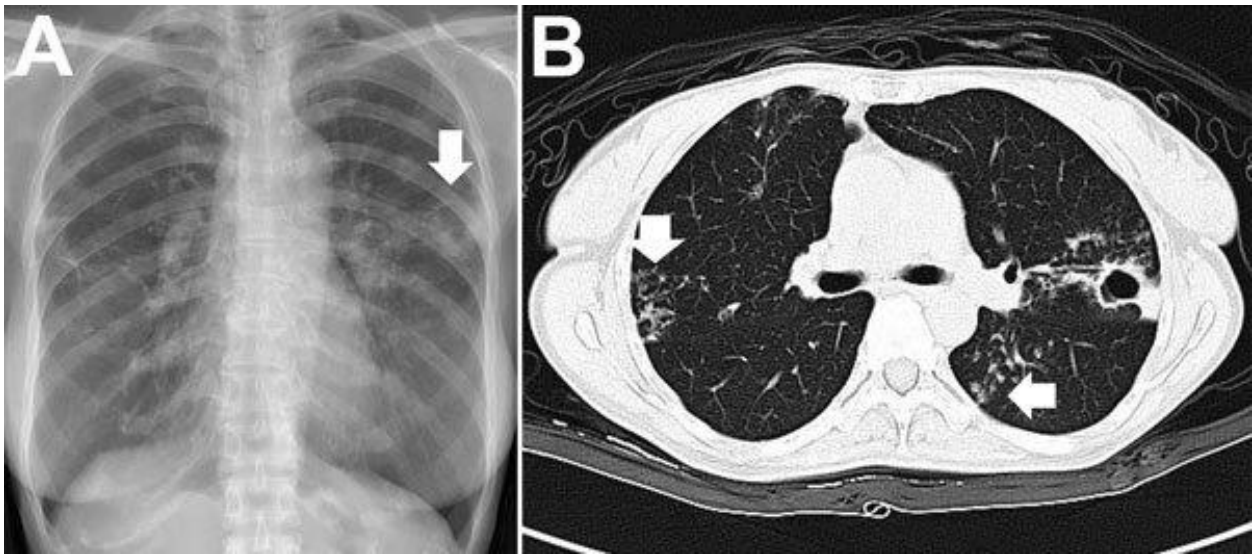

Figure 13. Exemple d'infections pulmonaires causées par des infections à *M. abscessus.*

(A) Radiographie du torse d'un patient ayant une infection à *M. abscessus*, la flèche indique un nodule pulmonaire. **(B)** Tomographie du tronc du patient, la flèche horizontale indique un nodule et la verticale une bronchiectasie. (d'après Lee et al, 2015)

-Des reflux gastro-œsophagiens, les reflux gastriques très acides vont inflammer l'œsophage ainsi que les voies aériennes supérieures ce qui va favoriser les infections aux MNT (Koh et al. 2007). Le Virus de l'Immunodéficience Humaine (VIH) ou le traitement avec des immunosuppresseurs, ainsi que l'affaiblissement du système immunitaire en général semble favoriser les infections aux MNT (Hannah et al. 2020).

II.3.4.3.2. Les troubles pulmonaires chroniques d'origine génétique

D'autres troubles au niveau pulmonaire sont dus à des anomalies génétiques.

II.3.4.3.2.1. L'exemple de la mucoviscidose et bronchiectasie

La mucoviscidose représente la plus grande part dans ces troubles. En effet, cette maladie génétique récessive dont l'incidence est estimée à 1 sur 2500 naissances, est causée par des mutations au niveau du gène *cftr* (Cystic Fibrosis Transmembrane Regulator) situé sur le chromosome 7, qui code pour la protéine CFTR. CFTR est un canal chlore transmembranaire exprimé dans la zone apicale des cellules épithéliales présentes dans divers organes du corps (foie, sinus, poumons, pancréas) (Leitch and Rodgers 2013). La fonction de cette protéine est de maintenir un équilibre au niveau des ions entre les compartiments intracellulaires et extracellulaires. Il existe 6 classes de mutations identifiées qui donnent lieu à différents phénotypes, certains ne montrent aucune transcription d'ARNm, d'autres une protéine exprimée mais mal repliée, non adressée à la membrane plasmique ou encore une protéine insérée dans la membrane mais non fonctionnelle. Des modulateurs du CFTR ont été découverts récemment et permettent de restaurer partiellement la fonction du canal chlore selon la classe de mutation. Plusieurs molécules sont efficaces contre les différentes mutations dont la plus fréquente est la F508del (Lopes-Pacheco 2016).

L'absence de cette protéine au niveau apical des cellules épithéliales pulmonaires provoque un changement de la composition du mucus présent à la surface de ces cellules. Ce mucus va devenir épais et visqueux empêchant alors la fonction mucociliaire permettant le renouvellement de celui-ci et créant ainsi un terrain propice aux infections polymicrobiennes chroniques (Pier et al. 1996) (Figure 14). Cette forme du mucus va également rendre compliqué l'accès à cette zone des cellules immunitaires qui permettent, en temps normal, de contrôler la colonisation par les espèces bactériennes (Figure 15). De plus, ces canaux CFTR sont également

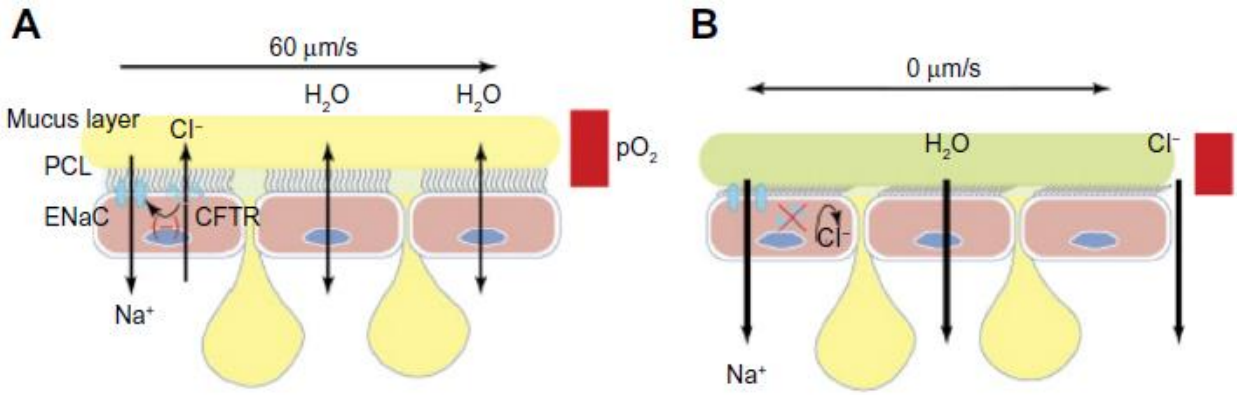

Figure 14. Facteurs impliquant une diminution de l'activité mucociliaire dans un contexte de mucoviscidose.

(A) Contexte normal, il y a un équilibre avec le Na+ qui entre dans la cellule et le Cl- qui est expulsé par le canal CFTR fonctionnel. L'activité mucociliaire est normale et le mucus est fluide et mobile à une vitesse de 60µm/s. **(B)** Contexte mucoviscidose, le Cl^- n'est plus exporté vers le milieu extérieur ce qui entraîne un déséquilibre ionique et l'arrêt de l'activité mucociliaire et un épaississement du mucus qui reste immobile. (D'après Vallières et Elborn, 2014)

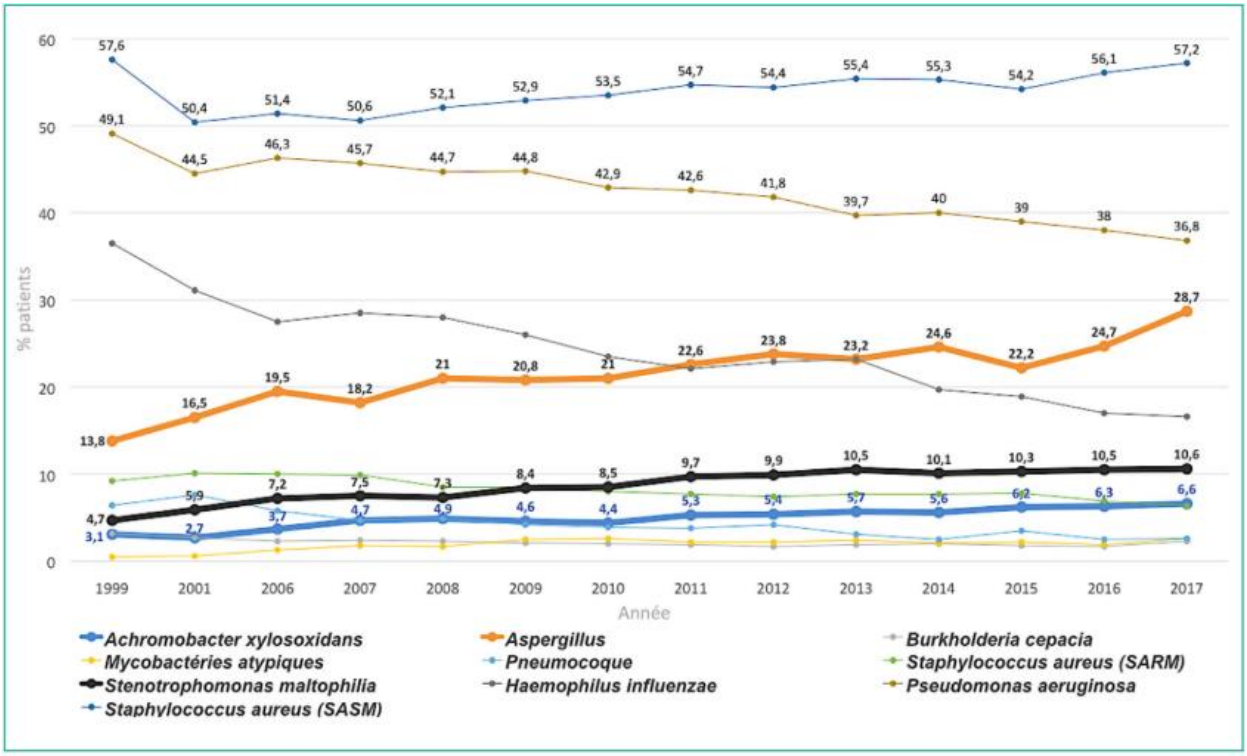

Figure 15. Evolution des pourcentages de patients atteints de mucoviscidose colonisés par différent pathogènes sur la période 1999-2017.

S. aureus et *P. aeruginosa* (bleu et marron) restent les principaux pathogènes qui colonisent les malades atteints de mucoviscidose mais les mycobactéries atypiques (MNT)(en jaune) augmentent très légèrement sur cette période. (D'après Menetrey et al, 2020)

impliqués dans l'internalisation des bactéries telles que *Pseudomonas aeruginosa* et des mutations dans ce gène (F508del) semblent rendre le canal muté inapte à internaliser les bactéries qui vont alors pouvoir se multiplier dans le milieu extérieur (Pier et al. 1996).

Il a également été montré dans un modèle zebrafish que l'absence de CFTR a pour conséquence une diminution de la production de ROS par la NADPH oxydase Nox2 favorisant la survie de *M. abscessus* dans les phagosomes. Les bactéries vont ainsi se multiplier de façon incontrôlée jusqu'à lyse des cellules pour enfin continuer de se multiplier dans le compartiment extracellulaire sous forme de cordes extracellulaires aboutissant à une infection aigüe et létale (Bernut et al. 2019).

D'autres troubles peuvent également favoriser ces infections comme la bronchiectasie, ce phénomène correspond à une détérioration du tissu pulmonaire, qui s'accompagne d'une difficulté à évacuer le mucus pulmonaire ainsi qu'une diminution des défenses immunitaires. Dans certains cas, une fibrose pulmonaire peut être observée. Tous ces facteurs favorisent la colonisation par des espèces bactériennes pathogènes opportunistes.

III. Traitement des infections à *M. abscessus*

Les infections à *M. abscessus* sont de véritables défis à relever pour les médecins car cette bactérie est naturellement résistante à la plupart des classes antibiotiques utilisées en clinique. Chaque année une antibiothérapie recommandée est publiée au journal officiel.

III.1. Antibiothérapie recommandée

L'antibiothérapie recommandée contre les infections à *M. abscessus* est une trithérapie : on associe un aminoglycoside (amikacine (AMK)) à une β-lactamine (imipénème (IPM) ou céfoxitine (CFX)) et un macrolide (clarithromycine ou azithromycine) pendant au moins 12 mois. Le risque de rechute reste très élevé en particulier dû au terrain propice à l'infection de ces patients (environ 40%).

En 2016, les associations européenne et américaine de lutte contre la mucoviscidose ont proposé un nouveau régime thérapeutique divisé en deux phases. La première dite intensive où l'on utilise la trithérapie en remplaçant les macrolides par la tigécycline (TGC) si la bactérie est résistante à ceux-ci. Elle dure de 1 à 3 mois. Vient ensuite la phase dite de prolongation, qui

Tableau 1. Traitements recommandés contre les infections à *M. abscessus* en fonction de la sensibilité aux macrolides. (D'après Daley et al, 2020)

Macrolide susceptibility pattern		Number of drugs[+]	Preferred drugs	Frequency of dosing
Mutational[#]	Inducible[¶]			
Susceptible	Susceptible	Initial phase ⩾3	*Parenteral (choose 1–2)* Amikacin Imipenem (or Cefoxitin) Tigecycline *Oral (choose 2)* Azithromycin (clarithromycin)[§] Clofazimine Linezolid	Daily (3 times weekly may be used for aminoglycosides)
		Continuation phase ⩾2	*Oral/inhaled (choose 2–3)* Azithromycin (clarithromycin)[§] Clofazimine Linezolid Inhaled amikacin	
Susceptible	Resistant	Initial phase ⩾4	*Parenteral (choose 2–3)* Amikacin Imipenem (or Cefoxitin) Tigecycline *Oral (choose 2–3)* Azithromycin (clarithromycin)[f] Clofazimine Linezolid	Daily (3 times weekly may be used for aminoglycosides)
		Continuation phase ⩾2	*Oral/inhaled (choose 2–3)* Azithromycin (clarithromycin)[f] Clofazimine Linezolid Inhaled amikacin	
Resistant	Susceptible or resistant	Initial phase ⩾4	*Parenteral (choose 2–3)* Amikacin Imipenem (or Cefoxitin) Tigecycline *Oral (choose 2–3)* Azithromycin (clarithromycin)[f] Clofazimine Linezolid	Daily (3 times weekly may be used for aminoglycosides)
		Continuation phase ⩾2	*Oral/inhaled (choose 2–3)* Azithromycin (clarithromycin)[f] Clofazimine Linezolid Inhaled amikacin	

[#]: mutational resistance: none present: isolate determined to be phenotypically susceptible at 3–5 days of incubation in culture. Present: isolate determined to be phenotypically resistant at 3–5 days of incubation or sequencing identifies *rrl* mutation know to confer resistance. [¶]: inducible resistance: functional *erm*(41) gene: isolate determined to be resistant after 14 days of incubation or sequencing identifies functional gene sequence. Nonfunctional *erm*(41) gene: isolate determined to be susceptible after 14 days of incubation or sequencing identifies truncated sequence or C28 mutation (in subspecies *abscessus*). [+]: initial phase refers to the time that the parenteral agents are being given. Continuation phase refers to the subsequent phase of therapy that typically includes oral antimicrobial agents sometimes paired with inhaled agents. [§]: azithromycin (clarithromycin) is active in this setting and should be used whenever possible. [f]: azithromycin (clarithromycin) activity is unlikely but can be added for its immunomodulatory effects but should not be counted as active against *M. abscessus* with a functional *erm*(41) gene. In this setting, frequent sputum cultures should be obtained to detect potentially new organisms like *M. avium* complex.

s'échelonne sur au moins 12 mois et durant laquelle de nouvelles classes d'antibiotiques sont testées afin d'éradiquer l'infection comme le linézolide (LNZ), la moxifloxacine (MOX) ou encore la CFZ. Ces recommandations viennent d'être reconfirmées cette année (Tableau 1)(Daley et al. 2020).

III.2. Les β-lactamines

Les β-lactamines forment la plus ancienne famille d'antibiotiques, regroupant plusieurs classes d'antibiotiques : les pénicillines, les céphalosporines et les carbapénèmes. Toutes ont le même mécanisme d'action : elles inhibent la dernière étape de synthèse du peptidoglycane avec d'un côté la CFX (céphalosporine de 2ème génération) qui inhibe les D-D transpeptidases par compétition avec leur substrat et d'un autre côté l'IPM (carbapénème) qui inhibe les L-D transpeptidases par compétition avec leur substrat (Cho et al. 2014). L'imipénème semble plus efficace *in vitro* contre les infections à *M. abscessus* du fait de sa faible cinétique de dégradation par sa β-lactamase naturelle Bla_{mab} (Dubée et al. 2015).

III.3. Les aminoglycosides

Les aminoglycosides (ou aminosides) les plus connus sont la streptomycine (STP), la kanamycine (KAN) et la gentamicine (GEN). Leur mécanisme d'action consiste à perturber la traduction protéique au niveau du ribosome. Ils interagissent avec l'ARNr 16S de la petite sous unité 30S du ribosome (Cabañas et al. 1978). La fixation de la molécule sur l'ARNr au niveau du site A de décodage va entraîner des erreurs de traduction et des protéines non viables qui devront être éliminées par la cellule (Figure 16). Cette accumulation de déchets au niveau du cytosol va créer un fort stress oxydatif et membranaire (Ying et al. 2019).

L'amikacine appartient également à cette famille mais elle est inactivée par différentes enzymes bactériennes. Cependant des effets indésirables sont souvent observés lors de l'utilisation de ces antibiotiques comme la perte de l'ouïe ou une toxicité rénale. Ces effets indésirables peuvent être contournés en administrant l'amikacine sous forme liposomale par aérosol pour qu'elle soit délivrée directement au niveau des voies respiratoires (Colin and Ali-Dinar 2010).

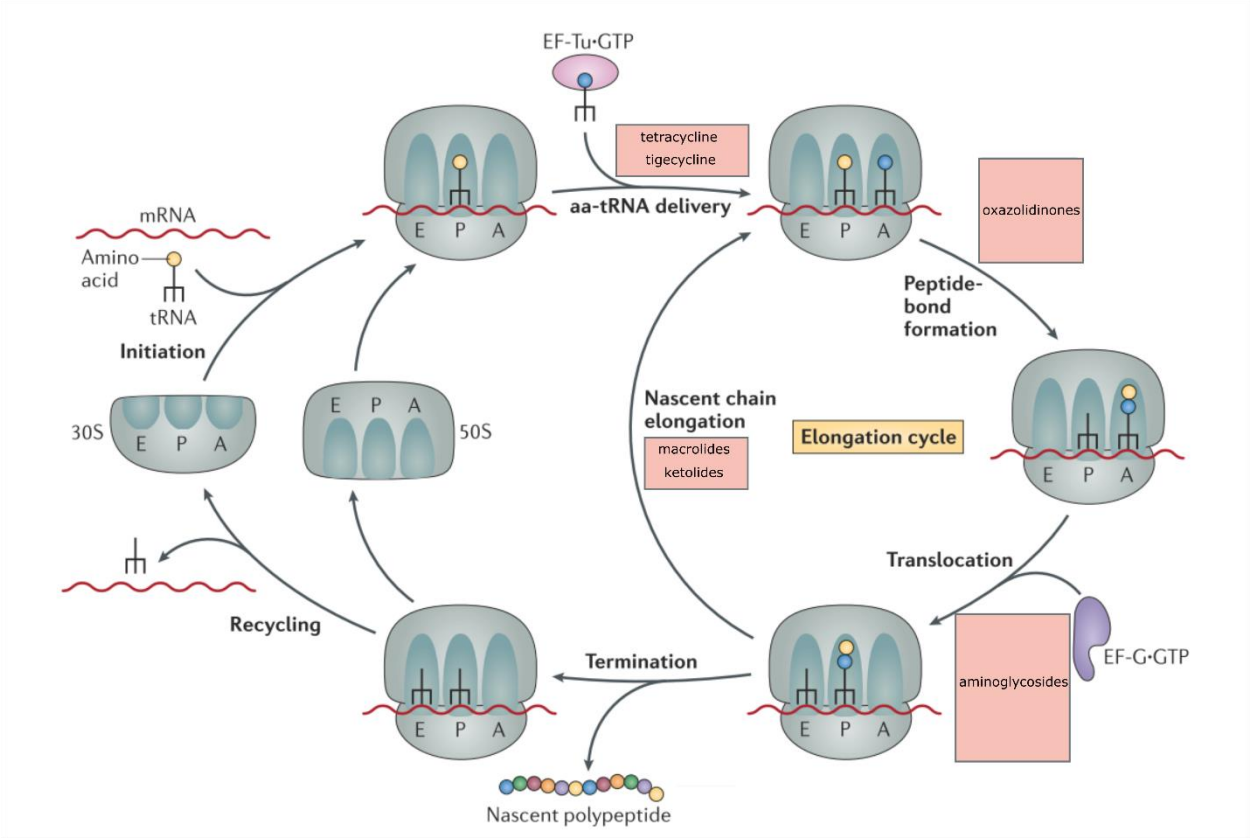

Figure 16. Cycle de traduction des protéines bactériennes et les différents antibiotiques permettant de l'inhiber.

Les différentes familles d'antibiotiques ciblant le ribosome bactérien agissent à différentes étapes de celui-ci. Les tétracyclines et les glycylcylines vont empêcher l'arrivée des ARNt au niveau du site A du ribosome, les oxazolidinones vont empêcher les acides aminés de s'attacher entre eux entre les sites P et A, les aminoglycosides vont empêcher la translocation du néo peptide au sein du ribosome et enfin les macrolides vont bloquer l'élongation du peptide.

III.4. Les macrolides

Les macrolides sont une classe d'antibiotiques inhibant également la synthèse protéique, la plus connue étant l'érythromycine (ERY). Leur mécanisme d'action consiste à interagir avec l'ARNr 23S de la grande sous unité 50S du ribosome. Ils vont empêcher l'ajout d'acide aminé porté par l'ARNt en obstruant la voie d'accès à la chaîne polypeptidique néosynthétisée (Figure 16) (Poehlsgaard and Douthwaite 2005). La clarithromycine (CLR) et l'azithromycine (AZR) sont toutes deux des molécules dérivées de l'ERY, elles diffèrent uniquement par la taille de leur cycle lactone (14 contre 15 respectivement) ce qui confère à l'AZR une demi-vie deux fois plus longue.

Cependant plusieurs auteurs ont déconseillé une utilisation prolongée de l'AZR à cause de ses effets immunomodulateurs, elle inhibe l'autophagie, la fusion phagolysosomale ainsi que la voie IFN-γ et TNFα qui jouent un grand rôle dans l'élimination des bacilles par le système immunitaire (Renna et al. 2011).

Tout cela montre que si les doses utilisées ne sont pas assez élevées alors ces antibiotiques ne seront pas efficaces mais pourraient même favoriser l'infection par les mycobactéries.

III.5. Les tétracyclines et leurs dérivés

Les tétracyclines sont des molécules dont le mécanisme consiste à interagir avec la petite sous unité 30S du ribosome et inhiber l'entrée de l'ARNt au niveau du site A (Figure 16) (Maxwell 1968). Globalement, ce sont de mauvais candidats pour les traitements des infections à *M. abscessus* car leur activité *in vitro* et leur pénétration dans la bactérie demeurent très faibles. La minocycline (MIN), une tétracycline de 2ème génération, reste la molécule la plus active contre *M. abscessus in vitro* mais les études démontrent qu'elle reste très peu efficace. Elle pourrait être envisagée dans le traitement mais uniquement contre des souches sensibles (Ruth et al. 2018).

Un autre dérivé de tétracycline, une glycylcycline, la TGC a montré quant à elle une très bonne activité *in vitro* et un très bon taux d'absorption et d'accumulation intracellulaire, ce qui en fait un bon candidat pour le traitement des infections à *M. abscessus* pendant la phase de prolongation. De plus, elle semble insensible à tous les mécanismes de résistance connus chez *M. abscessus* pour contrer les tétracyclines (Ferro et al. 2016).

Plus récemment, l'omadacycline, une nouvelle molécule dérivée des tétracyclines montre une bonne activité contre les MNT dont *M. abscessus* avec des effets indésirables considérablement réduits par rapport à la TGC (Kaushik et al. 2019; Bax et al. 2019).

III.6. Les phénazines

La CFZ est une phénazine qui est utilisée dans le traitement des infections à *M. leprae*. Elle a été repositionnée dans le traitement des infections à *M. tuberculosis* multi résistantes et est actuellement encore testée en clinique pour prouver son efficacité (Mirnejad et al. 2018). Son mécanisme d'action chez *M. abscessus* n'a pas été démontré mais il a été montré chez *M. smegmatis* qu'elle est pro-activée par la NADH déshydrogénase (NDH-2) (enzyme du métabolisme énergétique), ce qui entraînerait une surproduction de ROS qui serait alors fatale pour le bacille (Yano et al. 2011). Plusieurs effets indésirables comme des douleurs abdominales, des troubles intestinaux ainsi que l'apparition d'une coloration rouge sur diverses parties du corps sont susceptibles de remettre en cause son utilisation en routine (Holdiness 1989).

Une administration par aérosol a été testée chez la souris et les résultats montrent que la quantité de CFZ au niveau pulmonaire était bien supérieure que lors d'une administration orale et les sujets présentaient une meilleure tolérance au traitement (Banaschewski et al. 2019).

III.7. Les fluoroquinolones

Les fluoroquinolones sont des molécules dérivées de l'acide nalidixique découvert en 1962. Leur mécanisme d'action repose sur une interaction avec la gyrase/topoisomérase II qui est une enzyme indispensable dans la réplication du chromosome bactérien. Une autre cible est la topoisomérase IV, responsable de la séparation des deux chromosomes lors de la séparation des deux cellules filles (Drlica and Malik 2005).

La MOX est une fluoroquinolone de 4ème génération qui est efficace contre *M. abscessus* mais son utilisation n'est pas recommandée en routine car l'émergence de mutations acquises dans les gènes codant pour la gyrase (*gyrA/gyrB)* est fréquente et les effets indésirables avec ces molécules sont nombreux (Kim et al. 2018).

III.8. Les oxazolidinones

Les oxazolidinones sont des molécules de synthèse dont la plus connues est le LNZ. Leur mécanisme d'action consiste à interagir avec les sous-unités 30S et 50S du ribosome pour inhiber le complexe d'initiation 70S (Figure 15) (Hashemian et al. 2018). Le tédizolide (TDZ), un analogue du LNZ, a montré une bonne activité contre des isolats clinique de *M. abscessus in vitro* mais

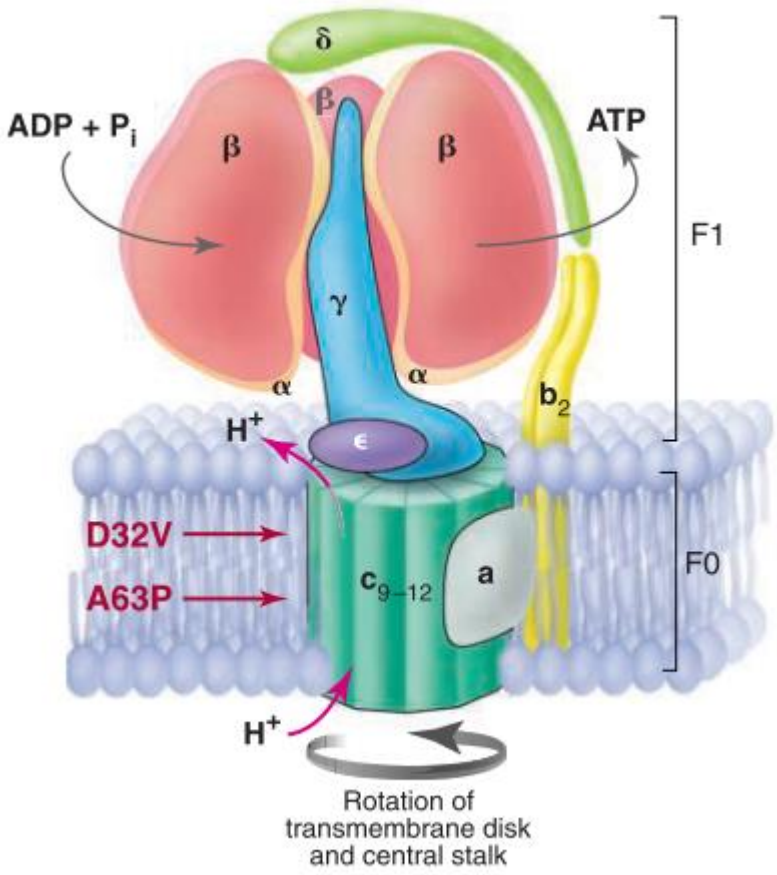

Figure 17. Structure de l'ATP synthase de *M. tuberculosis*, cible des diarylquinolines.

L'ATP synthase est une protéine transmembranaire composé de deux parties, F0 et F1. Les diarylquinolines vont inhiber la rotation de la sous unité c et donc la production d'énergie. Les mutations D32V et A63P confèrent une résistance aux diarylquinolines. (D'après Cole et Alzari, 2005)

également en association avec d'autres molécules dans un modèle d'infection de macrophages (Le Run et al. 2019; Compain et al. 2018).

III.9. Présentation d'autres possibilités thérapeutiques

Les recherches récentes ont permis de mettre en lumière d'autres possibilités de traitement des infections à *M. abscessus*, principalement du repositionnement de molécules mais également la découverte de nouvelles molécules et enfin des traitements alternatifs.

III.9.1. Les rifamycines

Les rifamycines comprennent des antibiotiques utilisés dans le traitement des infections à *M. tuberculosis* tels que la rifampicine (RIF). Leur mécanisme d'action consiste à interagir avec la sous-unité β de l'ARN polymérase codée par le gène *rpoB*. Plus précisément elles vont se lier par des interactions de type Van Der Vaals à la sous-unité β de l'ARN polymérase pour bloquer l'interaction entre la polymérase et l'ADN (Campbell et al. 2001). La RIF n'a aucune activité contre *M. abscessus* du fait de la présence de nombreuses enzymes la rendant inopérante.

La rifabutine (RFB), une nouvelle molécule semi-synthétique a montré une activité bien supérieure à la RIF contre *M. abscessus* car elle est moins susceptible aux mécanismes de résistance présents chez *M. abscessus* (mécanismes décrits dans la partie IV.2.1.3 Les rifamycines)(Dinah Binte Aziz et al. 2017). Il a également été montré qu'elle possède une activité synergique avec d'autres antibiotiques utilisés dans le traitement de *M. abscessus* (Le Run et al. 2019).

III.9.2. Les aminoglycosides non-conventionnels

Les aminoglycosides sont des antibiotiques de première ligne dans le traitement des infections à *M. abscessus* qui ont déjà été présentés précédemment.

Toutefois la tobramycine, un aminoglycoside particulier non-conventionnel existe et possède une meilleure activité *in vitro* que l'amikacine (Maurer et al. 2014). Cette molécule fonctionne sur le même principe que les aminoglycosides classiques mais est inactivée par les enzymes impliquées dans la résistance aux aminoglycosides ce qui limite son utilisation en clinique (Rominski et al. 2017).

Tableau 2. Principaux inhibiteurs de MmpL3 actifs contre *M. abscessus* (Adapté de *Sethiya et al.*).

	Structure	MIC_{99} *M. abscessus*	Références
1	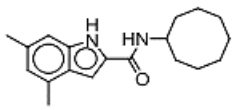	0,063 µg/mL	(Franz et al. 2017)
2	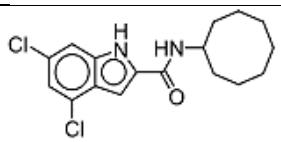	0,125 µg/mL	(Kozikowski et al. 2017)
3	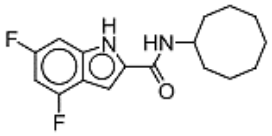	0,125 µg/mL	(Kozikowski et al. 2017)
4	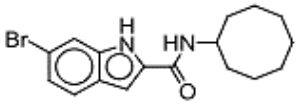	0,125 µg/mL	(Kozikowski et al. 2017)
5	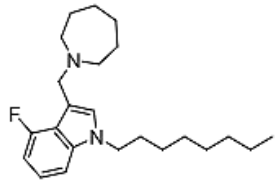	19 µM	(Yang et al. 2017)
7	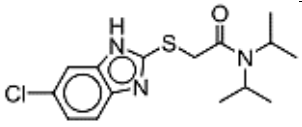	MIC_{50} = 25 µM	(Williams et al. 2019)
8	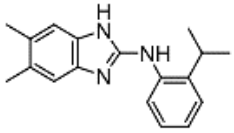	31,25 µM	(Dal Molin et al. 2019)
9	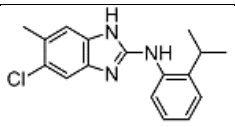	31,25 µM	(Dal Molin et al. 2019)
10	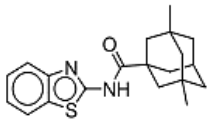	1 µg/mL	(Graham et al. 2018)
11	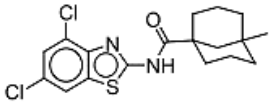	0,03 µg/ml	(Graham et al. 2018)
12	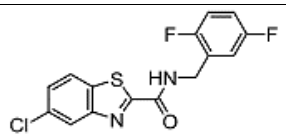	N.D.	(Shah et al. 2014)
13	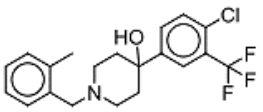	0,125 µg/ml	(Dupont et al. 2016; 2019)

III.9.3. Les diarylquinolines

Les diarylquinolines sont une nouvelle famille d'antibiotique utilisée en clinique depuis 2012 dans le traitement des infections à *M. tuberculosis* multi-résistantes aux antibiotiques. La BDQ a montré une forte activité *in vitro* contre *M. abscessus* (Brown-Elliott and Wallace 2019) et également *in vivo* dans un modèle d'infection de poisson zèbre (Dupont et al. 2017). Leur mécanisme d'action repose sur l'inhibition de l'ATP synthase, ce qui perturbe le métabolisme énergétique de la bactérie. Elles bloquent la rotation de l'anneau formé par les sous unités c. Des mutations sur les résidus acide aspartique 32 (D32) et alanine 64 (A64) confèrent une résistance à la BDQ (Figure 17). La rotation de cet anneau transmembranaire est indispensable au passage des électrons qui sont, eux, nécessaires à la production d'ATP (Preiss et al. 2015). D'autres travaux ont montré qu'une cible secondaire était la sous unité ε de l'ATP synthase (Kundu et al. 2016).

Récemment, *Luo et al.* ont montré que la BDQ était capable d'inhiber également l'ATP synthase humaine. Cette découverte alerte sur un éventuel risque de toxicité pour les personnes ayant des pathologies sous-jacentes au niveau cardiaque (Luo et al. 2020).

III.9.4. Les inhibiteurs de MmpL3

Depuis quelques années, MmpL3 est une nouvelle cible très étudiée dans la lutte contre les mycobactéries. Cette protéine appartenant à la grande famille des MmpL et à la super famille des transporteurs membranaires RND. Sa principale fonction est de transporter les TMM à travers la membrane plasmique grâce à la force protomotrice. Plus précisément, elle aurait une fonction de flippase qui permettrait aux TMM de basculer d'un versant à l'autre de la membrane plasmique (Xu et al. 2017). Une étude a montré qu'en plus des TMM elle pouvait transporter divers phospholipides, tels que des phosphatidylethanolamines (Belardinelli et al. 2016). MmpL3 est essentielle à la biosynthèse des TDM et à la mycolylation de l'arabinogalactane et une réduction de son expression entraîne une forte réduction de la viabilité des bacilles ainsi que de leur virulence, ce qui en fait une bonne cible thérapeutique (Figure 18) (Degiacomi et al. 2017; Grzegorzewicz et al. 2012; Viljoen et al. 2017). Une inhibition par des molécules chimiques entraîne une accumulation cytoplasmique des TMM et une diminution de la quantité de TDM et d'Arabinogalactane mycolylé (mAG) (Kozikowski et al. 2017). Le peu d'information concernant le mécanisme d'action de ces molécules a été étayé par la publication de la structure

cristallographique de la protéine MmpL3 de *M. smegmatis* (Zhang et al. 2019). Il semble que deux types d'inhibiteurs se distinguent : le premier comprend des inhibiteurs qui empêchent

Tableau 2. suite

14	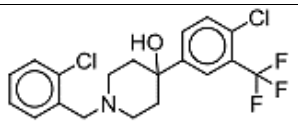	0,125 µg/ml	(de Ruyck et al. 2020)
15	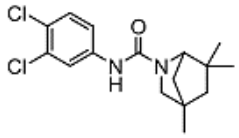	>62,5 µM	(Dal Molin et al. 2019)
16	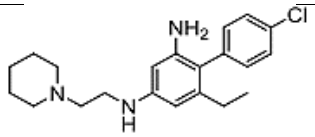	>31,25 µM	(Dal Molin et al. 2019)
17	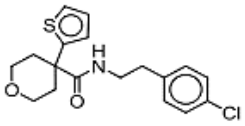	MIC_{50} = 6,25 µM	(Zheng et al. 2018)
18	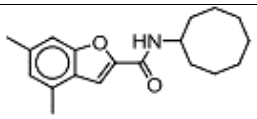	0,5 µg/ml	(Kozikowski et al. 2017)
19	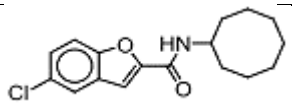	0,5 µg/ml	(Kozikowski et al. 2017)
20	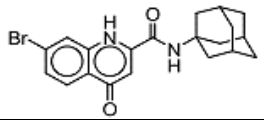	>159 µM	(Alsayed et al. 2020)
21	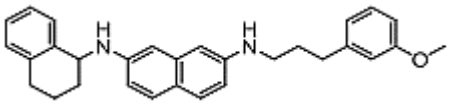	>31,25 µM	(Dal Molin et al. 2019)
22	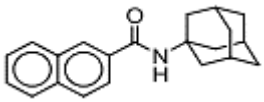	>209 µM	(Alsayed et al. 2020)
23	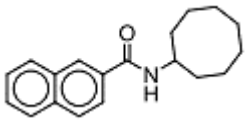	>209 µM	(Alsayed et al. 2020)
24	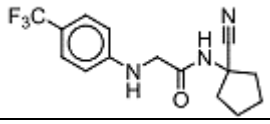	12 µM	(Williams et al. 2018)

directement le transport des lipides tandis que le second comprend des molécules qui altèrent la force protomotrice. Il a été observé que plusieurs familles chimiques distinctes sont capables d'inhiber cette protéine tels que des dérivés de pipéridinol (Dupont et al. 2016), les indole-2-carboxamides (Kozikowski et al. 2017), les dérivés du pyrrole (BM212), les adamantyl urée (AU1235), les N-adamantan-2-yl-N=-[(E)-3,7-dimethyl-octa-2,6-dienyl]-ethane-1,2-diamine (SQ109), de tetrahydropyrazolo[1,5-a]pyrimidine-3-carboxamide (THPP) (W. Li et al. 2019; Remuiñán et al. 2013; Grzegorzewicz et al. 2012) (Tableau 2).

Depuis, plusieurs sites de liaison ont été découverts et permettent de mieux comprendre l'action de ces inhibiteurs. Plusieurs de ces inhibiteurs ont montré une grande activité vis-à-vis de *M. abscessus in vitro* mais également dans des modèles d'infection de macrophages. Ils doivent maintenant être testés dans des modèles d'étude pré-cliniques.

III.9.5. Associations d'antibiotiques et synergies pour le traitement de *M. abscessus*

Une autre perspective de traitement est l'association d'antibiotiques, cette dernière consiste à utiliser des molécules ayant une activité synergique afin d'obtenir une activité égale ou supérieure à celle retrouvée lorsqu'on utilise ces deux molécules prises séparément. Cela permet également de diminuer les concentrations d'antibiotiques utilisées et de ce fait de diminuer les effets indésirables causés par l'utilisation prolongée de ces molécules. D'un point de vue des résistances, l'utilisation de plusieurs molécules en association va permettre de réduire l'émergence de résistances croisées et ainsi de lutter plus efficacement contre l'infection à *M. abscessus.* Lors d'infections multiples, l'association d'antibiotiques va permettre d'élargir le spectre d'activité utilisé afin d'être efficace contre plusieurs familles de pathogènes.

Beaucoup d'informations sont disponibles concernant des effets synergiques *in vitro* et certaines sont plus intéressantes du fait de leur transposabilité chez l'Homme en clinique.
Plusieurs d'entre elles concernent les macrolides, qui posent problème à cause d'un mécanisme de résistance inductible présent chez cette bactérie (Partie IV.2.2 Les enzymes protégeant la cible : l'exemple d'Erm41). Plusieurs équipes ont donc testé différentes associations incluant les macrolides, comme par exemple la CLR avec le LNZ, la TGC, la vancomycine (VAN) ou encore la MOX (Cremades et al. 2009; Zhang et al. 2017). Dans le cas de VAN, l'antibiotique n'est pas efficace seul contre *M. abscessus* mais lorsqu'on l'associe à un macrolide, l'effet des deux molécules est amélioré même contre des souches pré-exposées aux macrolides (Tableau 3) (Mukherjee et al. 2017).

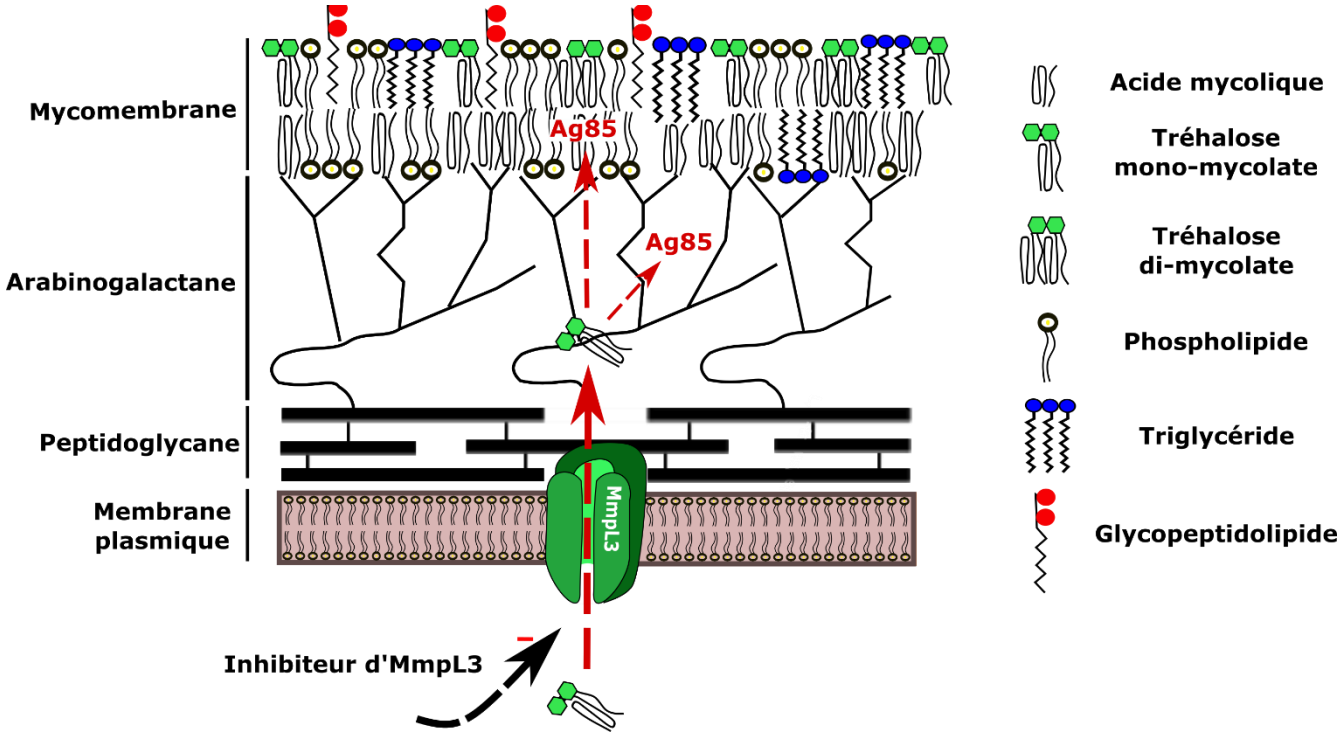

Figure 18. Mécanisme d'action des inhibiteurs de MmpL3.

Les inhibiteurs de MmpL3 vont inhiber l'activité de cette protéine dont le rôle est de transporter les TMM à travers la membrane plasmique pour qu'ils soient ensuite pris en charge par les protéines su complexe Ag85 qui les associeront soit à l'arabinogalactane, soit à la mycomembrane sous forme de TDM. (D'après Raynaud et Kremer, 2020)

Classiquement, deux molécules anti-microbiennes sont utilisées pour réaliser ces associations mais certaines molécules n'ayant aucune activité anti-microbienne peuvent également potentialiser l'effet d'un antibiotique. C'est le cas du vérapamil (VER), un inhibiteur de canaux calciques utilisé dans le traitement des maladies cardiaques. Cette molécule ne possède aucune activité antibiotique en soi et pourtant lorsqu'utilisée en association avec la bédaquiline contre *M. tuberculosis*, elle permet de potentialiser son effet *in vitro* (Gupta et al. 2014).

D'autres molécules de ce type sont les inhibiteurs de β-lactamase, ils permettent de potentialiser l'effet des β-lactamines, tels que l'acide clavulanique, l'avibactam ou le rélébactam. Ces molécules ont démontré leur efficacité *in vitro* et *in vivo* dans le zebrafish (Lefebvre et al. 2017; Le Run et al. 2020; Soroka et al. 2017; Dubee et al. 2015) (Tableau 3).

III.9.6. Traitement alternatifs envisageables : les bactériophages

Une autre stratégie a récemment émergé pour les traitements des infections anti-*M. abscessus*, dans l'optique d'une ère post-antibiotique : la phagothérapie. L'utilisation de phages lytiques pour traiter les infections bactériennes est empirique car leur découverte remonte au début du 20ème siècle par Félix d'Hérelle, bien avant celle des antibiotiques. Leur utilisation sous forme de cocktail pour traiter les infections ne date pas d'hier car dans des pays comme la Géorgie, leur utilisation est très fréquente.

Le recours à la phagothérapie intéresse déjà les chercheurs et les médecins pour soigner différentes infections causées par des pathogènes tels que *Pseudomonas aeruginosa* ou *Streptococcus pneumoniae*. Plusieurs études sont mises en place pour évaluer l'efficacité d'un tel traitement en clinique.

D'autres études cliniques ont été réalisées avec les phages, comme « phagoburn » (www.phagoburn.eu) qui proposait de traiter en prophylaxie les grands brûlés en appliquant directement des phages au niveau topique pour prévenir de l'infection par les staphylocoques principalement. Une autre étude clinique nommée « Phosa » (https://fr.pherecydes-pharma.com/recherche-collaborative-phosa.html) visait à traiter les infections ostéoarticulaires en traitant avec des phages contre les staphylocoques.

Récemment, un article a décrit l'utilisation d'un cocktail de bactériophages dans le traitement d'une jeune fille atteinte de mucoviscidose, doublement transplantée au niveau pulmonaire et ayant contracté une infection à une souche de *M. massiliense* multi-résistante aux antibiotiques. Après une année d'antibiothérapie en testant différentes associations, aucune

Tableau 3. Différentes combinaisons entre molécules ayant une relation synergique (Adapté de thèse de Matthias Richard).

	Combinaisons	Type d'étude	Références
1	clarithromycine + linézolide	*In vitro*	(Cremades et al. 2009)
2	clarithromycine + tigécycline	*In vitro*	(Z. Zhang et al. 2017; Huang et al. 2013)
3	clarithromycine + vancomycine	*In vitro*	(Mukherjee et al. 2017)
4	clarithromycine + moxifloxacine	*In vitro*, macrophage, *in vivo* (souris)	(G. E. Choi et al. 2012; Z. Zhang et al. 2017)
5	azithromycine + moxifloxacine	*In vitro*, macrophage, *in vivo* (souris)	(G. E. Choi et al. 2012)
6	clarithromycine + linézolide + moxifloxacine/lévofloxacine/gatifloxacine	*In vitro*	(Cremades et al. 2009)
7	clarithromycine + ciprofloxacine + rifabutine	*In vitro*	(Cremades et al. 2009)
8	imipénème + clarithromycine	*In vitro*	(Miyasaka et al. 2007)
9	imipénème + lévofloxacine	*In vitro*	(Miyasaka et al. 2007)
10	amikacine + clofazimine	*In vitro*	(Shen et al. 2010; Van Ingen et al. 2012)
11	amikacine + linézolide	*In vitro*	(Z. Zhang et al. 2018)
12	tigécycline + clofazimine	*In vitro*	(Singh et al. 2014)
13	tigécycline + linézolide	*In vitro,* drosophile	(Z. Zhang et al. 2018; C. T. Oh et al. 2014)
14	tigécycline + teicoplanine	*In vitro*	(Dinah B. Aziz et al. 2018)
15	rifampicine + doripénème/biapénème	*In vitro*	(Kaushik et al. 2015)
16	rifabutine + imipénème	*In vitro*	(Cheng et al. 2019a)
17	rifabutine + tigécycline	*In vitro*	(Cheng et al. 2019a)
18	rifabutine + tigécycline + clarithromycine	*In vitro*	(Pryjma et al. 2018)
19	amoxicilline + avibactam	*In vitro,* macrophage, zebrafish	(Dubée et al. 2015)

amélioration n'a été dénotée et des dysfonctionnements aux niveaux hépatique et rénal sont survenus. Une phagothérapie a été tentée, dans le cadre d'un traitement compassionnel. Tout d'abord, une phagothèque a été testée afin d'identifier des phages les plus actifs contre cette souche. Ainsi, un cocktail de trois phages lytiques a été mis au point, puis administré par voie intra-veineuse plusieurs fois par jour. Au bout de 10 mois, une nette diminution de la charge bactérienne a été observée ainsi qu'une nette amélioration des fonctions rénale et hépatique (Dedrick et al. 2019).

La phagothérapie semble compliquée à mettre en place en routine en clinique et restera vraisemblablement limitée dans le cadre d'une médecine personnalisée du fait de la grande spécificité des phages vis-à-vis des souches bactériennes.

IV. Les différents mécanismes de résistance aux antibiotiques chez *M. abscessus*

M. abscessus est naturellement très résistante aux antibiotiques. Ces résistances se font par plusieurs biais : tout d'abord les résistances acquises, qui correspondent aux mutations accumulées lors de la réplication de l'ADN pendant la division cellulaire et qui surviennent dans des gènes codant pour les cibles des antibiotiques ou des gènes impliqués dans l'activation d'antibiotiques. Ensuite, les mécanismes de résistance innée correspondent à des mécanismes présents constitutivement chez la bactérie.

IV.1. Mécanismes et résistances acquises

IV.1.1. Polymorphisme nucléotidique, génétique et mutations acquises

Le polymorphisme nucléotidique permet d'expliquer pourquoi la plupart des antibiotiques de première ligne utilisés contre *M. tuberculosis* ne fonctionnent pas contre *M. abscessus*. En effet, par exemple l'isoniazide (INH), qui cible InhA, un acteur indispensable de la voie de synthèse des acides mycoliques. Chez *M. tuberculosis,* l'INH requiert une activation de sa forme précoce par KatG, une catalase/peroxydase qui convertit le pro INH en un métabolite actif qui va inhiber InhA et la synthèse des acides mycoliques (Wiseman et al. 2010). Or chez *M. abscessus*, le gène *katG*, différant légèrement de celui retrouvé chez *M. tuberculosis*, ne peut pas activer l'isoniazide ce qui ne permet pas d'inhiber InhA chez *M. abscessus* (Luthra et al. 2018).

Un autre inhibiteur d'inhA, l'éthionamide (ETH) (Banerjee et al. 1994), requiert également une activation avant d'être efficace. Chez *M. tuberculosis*, c'est la monooxygénase EthA qui active

Tableau 3. Suite

	Combinaisons	Type d'étude	Références
20	céftaroline + avibactam	*In vitro,* macrophage	(Lefebvre et al. 2016)
21	imipénème + avibactam + amikacine	*In vitro,* macrophage, zebrafish	(Lefebvre et al. 2017)
22	tébipénème/ertapénème/panipénème + avibactam	*In vitro*	(Kaushik et al. 2017)
23	doripénème/faropénème/méropénème/biapénème + avibactam	*In vitro*	(Kaushik et al. 2017)
24	céfalotine/cefuroxime/cefamandole/ceftriaxone + avibactam	*In vitro*	(Dubée et al. 2015)
25	méropénème + acide clavulanique	*In vitro*	(Kaushik et al. 2015)

l'ETH et d'autres molécules telles que le thiacétazone (TAC) et ses dérivés (Dover et al. 2007). Chez *M. abscessus,* EthA n'est pas capable d'activer l'ETH alors qu'elle parvient à activer d'autres antibiotiques tels que le TAC et ses analogues (Halloum et al. 2017).

Ce polymorphisme intervient également dans le cas de l'éthambutol (EMB), cet antibiotique cible des enzymes modifiant la paroi, notamment les arabinosyltransférases qui permettent l'arabinosylation de l'arabinogalactane et du LAM (Zhang et al. 2003). Il a été montré des différences d'acides aminés au niveau de la protéine EmbB chez *M. abscessus* par rapport à celle présente chez *M. tuberculosis*. Ces changements d'acides aminés (I303G et L304M) induisent un haut niveau de résistance à l'EMB chez *M. abscessus* et chez d'autres MNT (Nessar et al. 2012).

Le dernier exemple est celui des fluoroquinolones, qui ciblent l'ADN gyrase, constituée des sous-unités GyrA et GyrB, dans lesquelles on retrouve les QRDRs (Quinolone Resistance-Determining Regions). Des changements d'acides aminés sont fréquemment observés dans ces régions chez *M. tuberculosis* et la plupart des mycobactéries pathogènes, leur permettant de résister aux quinolones (Guillemin et al. 1998; Matrat et al. 2008).

Les résistances observées chez *M. abscessus* peuvent être acquises par exemple lors d'exposition à des doses d'antibiotiques trop faibles mais également à une mauvaise observance du traitement. Cela va entraîner la sélection d'une population bactérienne résistante qui était déjà présente au préalable mais non prédominante car ses modifications génétiques n'étaient pas favorables au milieu sans antibiotique. Avec la pression antibiotique, ce phénotype devient favorable et émerge, résultant dans une population bactérienne totalement résistante à l'antibiotique (Blair et al. 2015).

Ces mutations dans les gènes codant pour les cibles des antibiotiques interviennent surtout lorsque la pression de sélection est grande et qu'aucun autre mécanisme de résistance n'est présent pour contrer l'antibiotique. Pour les macrolides, les mutations responsables de la résistance ont été localisées dans le gène *rrl* codant pour la sous unité 23S du ribosome au niveau de deux adénines aux positions 2058 et 2059 impliquées dans des liaisons hydrogènes permettant de stabiliser la fixation de l'antibiotique au ribosome (Carvalho et al. 2018). On observe ces mutations en particulier chez la sous-espèce *M. massiliense* chez laquelle le mécanisme de résistance inductible *via* la méthyltransférase Erm(41) n'est pas actif car la séquence de cette dernière est tronquée. Concernant le reste des sous-espèces du complexe

M. abscessus, ces mutations interviennent très rarement sauf dans le cas de souches sequovar T28C pour lesquelles une substitution de nucléotide dans la séquence de *erm(41)* rend cette dernière non fonctionnelle (Liu et al. 2017).

Pour les aminoglycosides, on observe également des mutations dans la cible de ces antibiotiques, le gène *rrs* codant pour la sous-unité 16S du ribosome. Les différentes molécules de la famille des aminoglycosides ne se fixent pas au même niveau de la sous-unité 16S du ribosome. Il existe tout de même des acides aminés impliqués dans la plupart des sites de liaison comme les adénines en position 1408, 1492, 1493 et la guanine en position 1494 (Prammananan et al. 1998; Wu et al. 2019). Comme pour les macrolides, ces mutations semblent être des évènements assez rares du fait que *M. abscessus* possède d'autres mécanismes de résistance aux aminoglycosides tels que des enzymes qui modifient directement ces antibiotiques ou encore des pompes à efflux pour les évacuer hors du cytoplasme.

IV.2. Mécanismes et résistances innées :

IV.2.1. Les enzymes modifiant les antibiotiques ou leurs cibles

M. abscessus possède intrinsèquement une batterie d'enzymes capable de modifier directement les antibiotiques ou leur cible afin de diminuer fortement l'affinité de ces antibiotiques pour ces dernières.

IV.2.1.1. Les β-lactamines

La résistance de *M. abscessus* aux β-lactamines est médiée par l'activité de sa β-lactamase Bla_{mab} de classe A. Elle possède une bonne activité pénicillinase, céphalosporinase (sauf pour la CFX qu'elle ne peut pas hydrolyser) et carbapénèmase (sauf pour l'IPM dont l'hydrolyse est très lente ce qui permet à cet antibiotique d'être efficace pendant un certain temps) (Soroka et al. 2017).

En revanche, elle possède une très bonne activité même en présence d'inhibiteurs tels que l'acide clavulanique ou le tazobactam. Des inhibiteurs comme l'avibactam permettent une forte inhibition de Bla_{mab} (Dubée et al. 2015) mais les inhibiteurs de dernière génération tels que le rélébactam permettent une meilleure inhibition de Bla_{mab} et donc une meilleure activité des β-lactamines contre *M. abscessus* (Le Run et al. 2020).

IV.2.1.2. Les aminoglycosides

La résistance de *M. abscessus* face aux aminoglycosides est principalement due aux enzymes modifiant ces antibiotiques. La première famille d'enzymes est la famille Eis (enchanced intracellular survival). Elles sont au nombre de deux chez *M. abscessus*, Eis1 et Eis2, respectivement codées par les gènes *MAB_4124* et *MAB_4532c*, et expriment une activité acétyltransférase (Rominski et al. 2017). Il a été montré pour la protéine Eis de *M. tuberculosis* que cette fonction participe à la survie intracellulaire du bacille. Le mécanisme d'action a été décrit et montre qu'Eis bloque l'autophagie, la maturation phagosomale, l'apoptose et diminue la production de cytokines inflammatoires (Kim et al. 2012).

Une étude sur Eis2 de *M. abscessus* a montré que les séquences étaient assez différentes mais que les structures tridimensionnelles des deux protéines étaient tout de même assez proches (Ung et al. 2019). Une autre étude a démontré son implication dans la survie intracellulaire chez *M. abscessus* dans les macrophages ainsi que dans les amibes (Dubois et al. 2019). Le spectre d'acétylation de Eis2 est assez large puisqu'il regroupe la plupart des aminoglycosides tels que la kanamycine A, la kanamycine B, l'AMK, l'hygromycine B etc…

Eis1, quant à elle, possède une fonction acétyltransférase mais ne peut pas acétyler les aminoglycosides. Elle pourrait tout de même participer à la survie intracellulaire (Ung et al. 2020).

La seconde famille d'enzyme est connue sous le nom de Aminoglycoside 2'-Acétyltransférase (AAC(2')). Elle est codée par le gène *MAB_4395*, et l'inactivation de ce gène conduit à une sensibilité accrue à certains antibiotiques de la famille des aminoglycosides. Elle possède également une fonction acétyl-transférase qui lui permet d'acétyler des aminoglycosides en position 2' du cycle 1 en transférant un groupement acétyle d'une molécule d'acétyl-CoA. Elle est capable d'inactiver la gentamicine C, la kanamycine B ainsi que la tobramycine (Maurer et al. 2014).

Un troisième type d'enzyme responsable de la résistance de *M. abscessus* aux aminoglycosides est codé par le gène *MAB_2385.* Cette enzyme possède une fonction 3''-O-phosphotransférase principalement responsable de l'inactivation de la streptomycine (STP) (Ramón-García et al. 2006). Elle a été identifiée lors d'une étude d'homologie avec une autre phosphotransférase Aph(3'')-Ic, et est responsable de l'inactivation de la STP chez *M. fortuitum*. Un mutant *ΔMAB_2385* présente une sensibilité accrue à la streptomycine (Dal Molin et al. 2018).

Grâce à une étude phylogénétique, d'autres acétyltransférases et phosphotransférases ont été identifiées et pourraient être impliquées, elles aussi, dans la résistance aux aminoglycosides et dans la survie intracellulaire (Luthra et al. 2018).

IV.2.1.3. Les rifamycines

La résistance aux rifamycines implique plusieurs mécanismes distincts, le premier est lié à l'hydrophobicité de la mycomembrane et à sa composition (Becker et al. 2017). En effet, plusieurs rifamycines, telles que la RIF et la rifapentine, ne parviennent pas ou mal à traverser cette barrière protectrice pour atteindre l'ARN polymérase dans le cytoplasme de la bactérie car leur taille est trop importante pour être importées activement par les porines et doivent donc traverser la paroi de manière passive. Ces molécules sont également sujettes à l'auto-oxydation à l'intérieur comme à l'extérieur de la bactérie du fait de la présence de motif hydroquinone sur leur cycle naphtyle. De plus, au niveau du cytoplasme de *M. abscessus* sont retrouvées deux enzymes permettant d'inactiver ces molécules (Ganapathy et al. 2019).

La première est une monooxygénase, Rox_{mab}, qui va conduire à leur dégradation. Elle va oxygéner la molécule en position 2 du cycle naphtyle ce qui va entraîner l'ouverture du cycle et la linéarisation de la molécule, provoquant la perte de sa forme « en panier » qui est indispensable pour se lier à l'ARN polymérase (Koteva et al. 2018).

La seconde est une ADP-ribosyltransférase codée par le gène *MAB_0591*, Arr_{mab}, qui va conduire à leur inactivation enzymatique. En effet, un mutant Δ*MAB_0591* est beaucoup plus sensible aux rifamycines que la souche sauvage. Par ailleurs, l'expression de cette enzyme chez des espèces naturellement sensibles comme *E. coli* ou *M. tuberculosis* induit une résistance aux rifamycines. Chez *M. abscessus*, Arr_{mab}, modifie le C23 de la RIF pour la rendre inactive. Dans cette étude, les auteurs discutent également l'importance du C25 de ces molécules qui permet d'augmenter leur activité. Ils suggèrent également la synthèse de nouvelles rifamycines optimisées dont la diffusion au niveau du cytoplasme serait améliorée ainsi que des affinités réduites aux différentes enzymes impliquées dans la résistance (Rominski et al. 2017; Combrink et al. 2019) (Figure 19).

Un autre analogue des rifamycines, la RFB (Figure 19), possède une meilleure activité *in vitro*. Sa structure légèrement différente des rifamycines classiques lui permet de résister à l'autooxygénation ainsi qu'à l'oxygénation par Rox_{mab}. Cette molécule est moins sensible à l'ADP-ribosylation par Arr_{mab} que la rifampicine (Ganapathy et al. 2019).

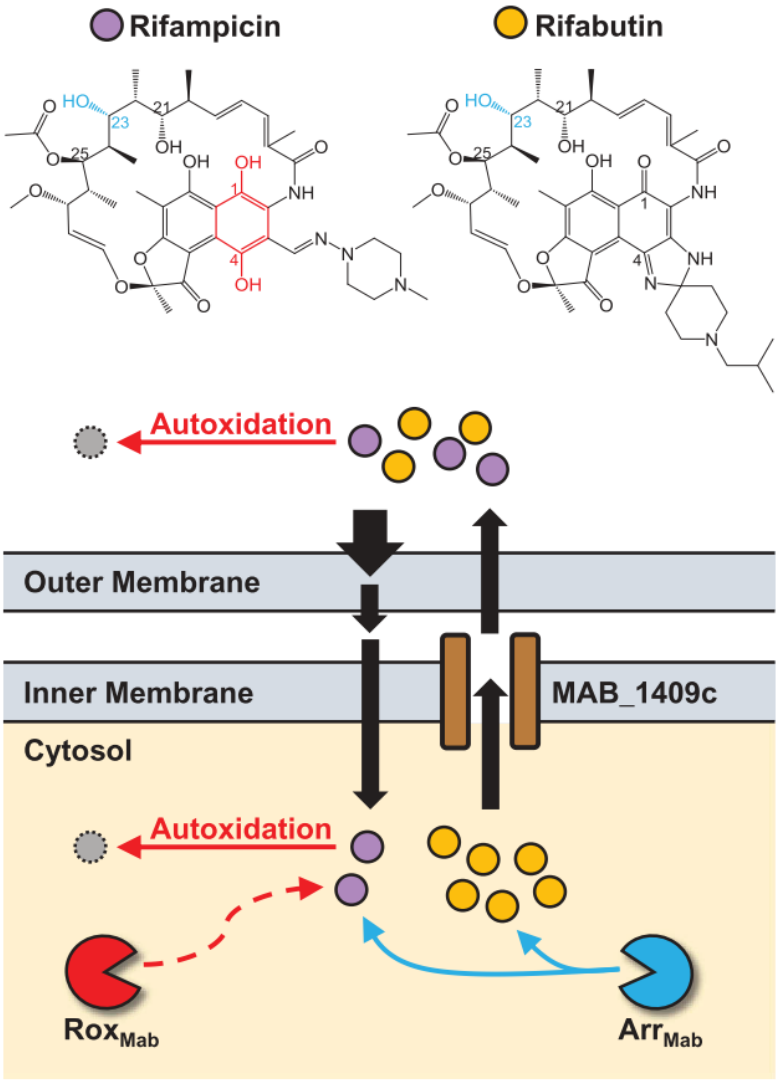

Figure 19. Résumé des différents mécanismes de résistance aux rifamycines présents chez *M. abscessus.*

Les mécanismes de résistance aux rifamycines sont nombreux chez *M. abscessus*, on retrouve notamment les deux enzymes qui modifient directement ces molécules Arr_{mab} va ADP-ribosyler alors Rox_{mab} va les monooxygéner, ces deux modifications vont conduire à leur inactivation. On retrouve également une pompe à efflux de type Tap (MAB_1409c) mais aussi la mycomembrane qui est très imperméable surtout à la rifampicine.

IV.2.1.4. Les tétracyclines

Les tétracyclines sont une classe d'antibiotiques très peu actifs sur *M. abscessus.* Ceci est dû en grande partie au mécanisme de résistance associé à MabTetX, codée par le gène *MAB_1496c.* MABTetX possède une fonction monooxygénase FAD-dépendante qui va permettre l'inactivation des tétracyclines. L'expression de ce gène est régulée par la protéine MabTetRx qui est codée par le gène *MAB_1497c*. En absence de substrat (antibiotique), le TetR va se fixer sur la région promotrice de l'opéron *MAB_1496c/MAB_1497c* et réprimer sa transcription. En présence de substrat, le TetR va subir un changement conformationnel qui va entraîner la libération de l'ADN au niveau de la région promotrice de l'opéron et permettre l'expression de celui-ci. Il a été montré que MabTetX est responsable de l'hydroxylation de la tétracycline et de la doxycycline chez *M. abscessus*. *Rudra et al.* ont également réalisé un mutant Δ*MAB_1496c* et ont montré que ces mutants sont plus sensibles aux tétracyclines. Ce mécanisme représente le mécanisme intrinsèque principal de résistance aux tétracyclines mais certaines molécules proches des tétracyclines, mais avec de légères modifications au niveau structural permettent de contourner ce mécanisme (Rudra et al. 2018).

La TGC, une glycylcycline, possède une chaîne 2-tert-butylglycylamido qui la protège de l'hydroxylation par MabTetX. Elle est utilisée en clinique actuellement dans le traitement des infections à *M. abscessus* mais possède un certain nombre d'effets indésirables. D'autres molécules analogues, telle que l'omadacycline sont actuellement testées et prometteuses car elles entraînent moins d'effets indésirables que la TGC (Kaushik et al. 2019; Bax et al. 2019).

IV.2.2. Les enzymes protégeant la cible : l'exemple d'Erm41

Les exemples concernant les enzymes capables de modifier les antibiotiques sont nombreux chez *M. abscessus* mais il existe également une enzyme capable de modifier directement la cible des macrolides. La méthyltransférase Erm41 (erythromycin resistance methylase), codée par le gène *MAB_2297*, est capable de transférer des groupements méthyles sur l'adénine en position 2048 de l'ARNr 23S situé dans la boucle du centre peptidyltranférase. Cette mutation empêche la fixation des macrolides à cet emplacement en diminuant considérablement leur affinité pour ce site de fixation. Ce type de méthyltransférase est présent chez un certain nombre d'espèces mycobactériennes (Nash et al. 2009). Ce mécanisme présente un problème important car la résistance est induite au cours du temps et peut être indétectable

au début du traitement. Or les macrolides sont des antibiotiques de première ligne dans le traitement des infections à *M. abscessus*. Il est donc nécessaire d'identifier rapidement les souches sensibles des souches résistantes. Pour cela, le gène *erm41* est systématiquement séquencé puis selon le génotype, le traitement sera adapté. Certaines souches ne nécessitent même pas d'être séquencées, c'est le cas de *M. massiliense* dont le gène *erm41* est tronqué et la protéine est non fonctionnelle. Les souches de *M. massiliense* sont donc sensibles aux macrolides (Brown-Elliott et al. 2015).

Plus récemment, un autre mécanisme de résistance aux macrolides a été découvert et dont le principal acteur est la protéine HflX, une GTPase associée au ribosome codée par le gène *MAB_3042c*. Le mécanisme proposé serait que HflX détecterait les ribosomes inactifs du fait de la liaison d'un macrolide à celui-ci et déclenchait le démantèlement du ribosome 70S en plusieurs sous-unités puis séquestrerait les sous-unités 50S toujours liées aux macrolides pour les empêcher d'assembler à nouveau des ribosomes qui seraient, au final, improductifs. Une autre hypothèse serait que la fonction GTPase de HlfX favoriserait le détachement des macrolides des sous-unités 50S du ribosome, puis, après détachement d'HflX, l'assemblage de nouveaux ribosomes actifs. Toutefois, ce système semble induire un niveau de résistance plus faible que celui d'Erm(41) mais l'addition de ces deux mécanismes de résistance est une arme redoutable pour *M. abscessus* afin de lutter contre l'action des macrolides (Rudra et al. 2020).

IV.2.3. Les pompes à efflux

IV.2.3.1. L'export de la bédaquiline et de la clofazimine

L'export de la BDQ ainsi que de la CFZ chez *M. abscessus* s'effectue à l'aide d'un mécanisme unique régulé par une protéine de la famille TetR. Ainsi, le gène *MAB_2299c* code pour une protéine TetR se fixant sur sa région promotrice, réprimant ainsi son expression. Ce TetR est en opéron avec les gènes *MAB_2300/MAB_2301* qui codent pour un couple MmpS/MmpL qui agirait comme une pompe à efflux. Lorsque de la BDQ ou de la CFZ pénètre dans la bactérie, les molécules vont se fixer sur le TetR, qui va alors se détacher du promoteur, entraînant la transcription des trois gènes en aval de la région promotrice. Les protéines MmpS/MmpL vont alors être produites à haut niveau et extruder les antibiotiques tandis que le TetR se refixe sur son ADN (Richard et al. 2019) (Figure 20).

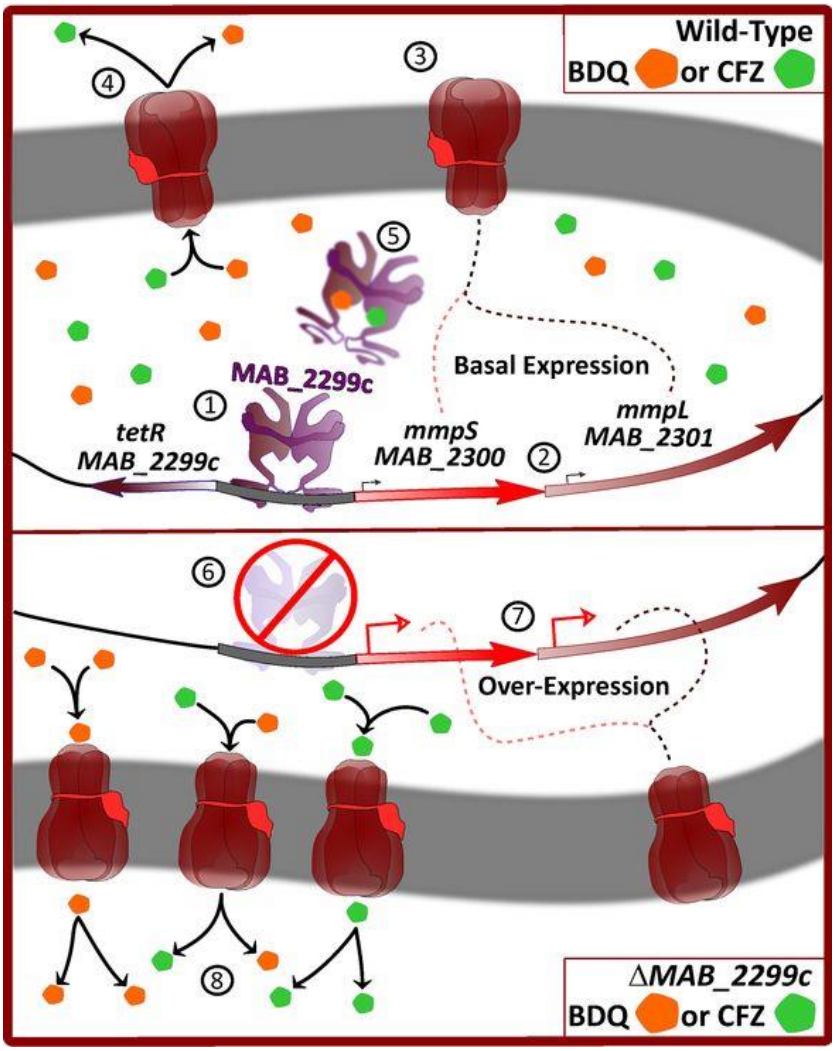

Figure 20. Mécanisme de régulation TetR conduisant à une résistance croisée entre la clofazimine et la bédaquiline chez *M. abscessus*.

En absence d'antibiotique, le tetR reste fixé sur l'ADN (1) et réprime l'expression de l'opéron *mmps/mmpl* (2) qui est alors exprimé basalement (3). Lorsqu'il y a présence d'antibiotiques, ceux-ci vont se fixer sur le tetR (5), ce qui va conduire à la libération de l'ADN (6) et à la surexpression du couple *mmps/mmpl* (7). (D'après Gutierrez et al, 2019)

De plus, ce TetR (*MAB_2299c*) peut également se fixer sur la région promotrice d'un second couple MmpS/MmpL, *MAB_1134c/MAB_1135c*, fonctionnant sur le même principe et étant également impliqué dans la résistance intrinsèque à la CFZ et à la BDQ (Gutiérrez et al. 2019).

IV.2.3.2. L'export du linézolide

La résistance au LNZ est souvent retrouvée dans les isolats cliniques et implique souvent une mutation au niveau du site de liaison de l'antibiotique sur l'ARNr 23S. D'autres mécanismes ont été décrits impliquant notamment des mutations dans des régulateurs d'expression des pompes à efflux, entraînant leur surexpression. La première est LmrS, qui appartient à la famille MFS. La seconde est MmpL10 qui est codée par le gène *MAB_4746*, une pompe à efflux de la famille RND (Ye et al. 2019).

IV.2.3.3. L'export des analogues structuraux du thiacétazone

Le TAC est une molécule utilisée autrefois contre *M. tuberculosis* même si son activité reste limitée contre celle-ci. Des améliorations au niveau moléculaire ont été réalisées pour augmenter son activité, et ces nouveaux composés (D6, D15 et D17) ont également montré une bonne activité contre *M. abscessus.* Des mutants résistants spontanés ont été isolés et les mutations responsables de la résistance aux dérivés du TAC ont été identifiées dans un régulateur MAB_4384 (un membre de la famille TetR) qui régule l'expression des gènes *MAB_4383c/4382c* codant pour un couple MmpS/MmpL qui agirait comme une pompe à efflux pour extruder les analogues du TAC (Halloum et al. 2017).

L'ensemble de ces mécanismes de résistance innés chez *M. abscessus* forment un véritable arsenal pour lutter contre les antibiotiques (Figure 21).

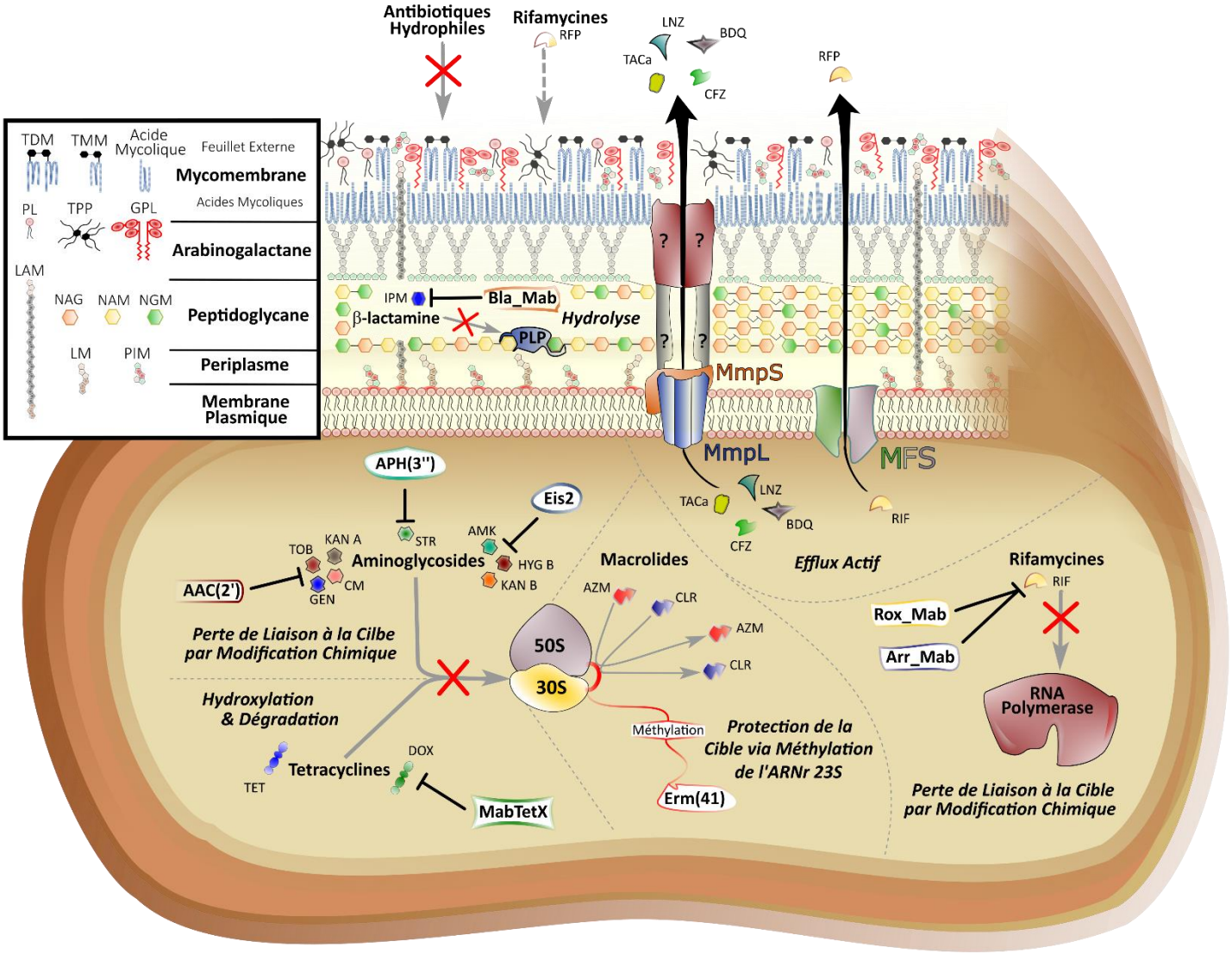

Figure 21. Mécanismes de résistance innés à diverses classes d'antibiotiques chez *M. abscessus.*

Les mécanismes de résistance innés présents sont présents sous différentes formes. On trouve tout d'abord la mycomembrane très hydrophobe qui va empêcher les molécules hydrophiles de pénétrer dans le bacille et ralentit l'absorption de molécules telles que les rifamycines. Au sein de celle-ci, la β-lactamase Bla_{MAB} va hydrolyser les β-lactamines et les inactiver. Dans la membrane plasmique, plusieurs types de pompes à efflux sont enchâssés : les MmpL qui vont extruder la BDQ, la CFZ, le LNZ et les analogues du TAC tandis que les MFS (MAB_{Tap}) va extruder les rifamycines. Dans le cytoplasme, toute une batterie d'enzymes sont présentes, AAC(2'), APH(3'') et Eis2 sont impliquées dans la résistances aux aminoglycosides. MabTetX est responsable de la résistance aux tétracyclines. Erm(41) va méthyler la cible des macrolides et réduire leur affinité pour celle-ci. Enfin, Arr_{Mab} et Rox_{Mab} sont impliquées dans la résistance aux rifamycines. (D'après thèse de Matthias Richard).

OBJECTIFS

Les traitements utilisés contre les infections à *M. abscessus* ne sont actuellement pas optimisés et plusieurs mécanismes intrinsèques, en plus de mutations acquises, empêchent ces traitements d'être vraiment efficaces, ce qui conduit souvent à des échecs thérapeutiques. De plus, l'émergence des infections aux MNT, et plus précisément à *M. abscessus,* est devenue une priorité pour les autorités de santé publique. Cette inefficacité thérapeutique des molécules utilisées dans les traitements oblige à identifier rapidement de nouvelles molécules plus efficaces contre *M. abscessus.* Pour cela, deux solutions sont possibles :

- Découvrir des molécules capables d'inhiber de nouvelles cibles pharmacologiques
- Repositionner des molécules déjà utilisées dans le traitement d'autres pathologies.

La découverte de nouvelles molécules implique de collaborer avec des chimistes qui synthétisent des banques de composés. L'objectif de mon travail a consisté à tester une banque de composés dérivés de benzimidazoles mise à disposition par l'équipe du Pr Gobis (Gdansk, Pologne). Après avoir identifié les composés phares (les plus actifs contre la bactérie), ces derniers ont été testés dans différents modèles d'études, tout d'abord *in vitro* directement contre la souche de référence ainsi que des isolats cliniques, puis dans un modèle d'infection macrophagique et enfin dans un modèle d'infection de zebrafish. En parallèle, des mutants résistants spontanés ont été générés en présence de hautes doses de composés afin de confirmer, par des approches génétiques, la cible de ces composés chez *M. abscessus*. Cette étude a permis d'identifier de nouveaux inhibiteurs de MmpL3, un transporteur lipidique membranaire ayant pour fonction la translocation du TMM vers la membrane externe.

Le repositionnement de molécule se base sur le principe de tester des molécules déjà utilisées en clinique dans le traitement d'autres infections, et ciblant certaines bactéries, qui pourraient également avoir une activité sur *M. abscessus*. Par exemple, la CFZ, utilisée normalement dans le traitement des infections à *M. leprae*, a déjà été repositionnée dans le traitement des infections à *M. abscessus* car elle a montré une très bonne activité contre cette dernière. Un autre avantage du repositionnement est le fait que toutes ces molécules déjà présentes sur le marché ont passé tous les tests pré-cliniques sur les animaux et les études cliniques chez l'Homme, ce qui leur permet d'être utilisées directement dans le traitement des infections pulmonaires à *M. abscessus*. Dans cette optique, nous nous sommes intéressés à la bédaquiline qui est utilisée dans le traitement des infections à *M. tuberculosis,* plus particulièrement contre les souches multi-résistantes aux antibiotiques. *Dupont et al.* ont déjà démontré son efficacité *in vitro* et *in vivo* (dans un modèle d'infection de zebrafish) contre *M.*

abscessus. Nous nous sommes intéressés à l'identification de potentielles synergies impliquant la BDQ ainsi qu'à son efficacité dans un modèle pré-clinique murin C3HeB/FeJ.

La RFB a récemment été proposée dans le cadre d'un repositionnement dans le traitement des infections à *M. abscessus*. A l'origine, cette rifamycine est utilisée dans le traitement des infections à *M. tuberculosis*. Ses différences structurales par rapport aux autres rifamycines en font un excellent candidat contre *M. abscessus* car elle n'est pas (ou peu) inactivée par l'ADP-ribosyltransférase codée par le gène arr_{mab}. L'objectif est de tester l'activité de la RFB contre *M. abscessus in vitro,* dans un modèle d'infection macrophagique ainsi que dans un modèle d'infection de zebrafish. Nous avons également tenté d'identifier la cible de la rifabutine chez *M. abscessus* grâce à la génération de mutants résistants spontanés.

L'identification de synergies potentielles entre antibiotiques représente également une manière intéressante d'améliorer les traitements car elles permettent, en utilisant deux molécules à des concentrations plus faibles, d'obtenir un effet similaire ou supérieur à celui obtenu en utilisant les molécules prises séparément. L'objectif de ce travail a consisté à tester les différentes combinaisons d'antibiotiques associant des indole-2-carboxamides (inhibiteurs de MmpL3) avec des antibiotiques utilisés en clinique. Tout d'abord, j'ai déterminé les FICI (Fractional Inhibitory Concentration Index) de ces associations, qui ont été confirmés *in vitro* par détermination de CFU et dans un modèle d'infection macrophagique.

L'ensemble de ces résultats est présenté dans la partie VI Résultats sous forme de publications.

RESULTATS

Article 1: "Active Benzimidazole Derivatives Targeting the MmpL3 Transporter in *Mycobacterium abscessus*."

Clément Raynaud, Wassim Daher, Matt D. Johansen, Françoise Roquet-Banères, Mickael Blaise, Oluseye K. Onajole, Alan P. Kozikowski, Jean-Louis Herrmann, Jaroslaw Dziadek, Katarzyna Gobis, and Laurent, 2020, *ACS Infectious Diseases*. https://doi.org/10.1021/acsinfecdis.9b00389. (Raynaud et al. 2020)

Des molécules dérivées de benzimidazoles ont été synthétisées par l'équipe du Pr Gobis et testées comme agents anti-tuberculeux (Gobis et al. 2014; 2015). L'activité de ces molécules contre *M. tuberculosis* a également été évaluée par cette même équipe et les résultats ont montré que certaines molécules phares étaient très actives *in vitro* contre *M. tuberculosis*. La cible, MmpL3, a été identifiée grâce à la génération de mutants spontanés et au séquençage complet du génome de ces mutants, puis le mécanisme d'action a été confirmé par chromatographie sur couche mince des acides mycoliques radiomarqués au ^{14}C (Korycka-Machała et al. 2019).

Ce travail est résumé dans une « Nouvelle » publiée dans Médecine/Sciences (Raynaud and Kremer 2020) qui est présentée à la suite de l'article.

ACS Infectious Diseases

Article

Cite This: ACS Infect. Dis. 2020, 6, 324−337

pubs.acs.org/journal/aidcbc

Active Benzimidazole Derivatives Targeting the MmpL3 Transporter in *Mycobacterium abscessus*

Clément Raynaud,[†] Wassim Daher,[†] Matt D. Johansen,[†] Françoise Roquet-Banères,[†] Mickael Blaise,[†] Oluseye K. Onajole,[‡] Alan P. Kozikowski,[§] Jean-Louis Herrmann,[∥,⊥] Jaroslaw Dziadek,[#] Katarzyna Gobis,[▽] and Laurent Kremer*[,†,•]

[†]Centre National de la Recherche Scientifique UMR 9004, Institut de Recherche en Infectiologie de Montpellier (IRIM), Université de Montpellier, 1919 route de Mende, 34293 Montpellier, France

[‡]Department of Biological, Physical and Health Sciences, Roosevelt University, 425 S. Wabash Avenue, Chicago, Illinois 60605, United States

[§]StarWise Therapeutics LLC, 2020 N. Lincoln Park West, Chicago, Illinois 60614, United States

[∥]2I, UVSQ, INSERM UMR1173, Université Paris-Saclay, 2 avenue de la Source de la Bièvre, 78180 Montigny-Le-Bretonneux, France

[⊥]APHP, GHU-Paris Saclay, Hôpital Raymond Poincaré, Garches, France

[#]Institute for Medical Biology, Polish Academy of Sciences, Lodowa 106, Łódź 93-232, Poland

[▽]Department of Organic Chemistry, Medical University of Gdansk, 107 Gen. Hallera Avenue, 80-416 Gdansk, Poland

[•]INSERM, IRIM, 34293 Montpellier, France

Supporting Information

ABSTRACT: The prevalence of pulmonary infections due to nontuberculous mycobacteria such as *Mycobacterium abscessus* has been increasing and surpassing tuberculosis (TB) in some industrialized countries. Because of intrinsic resistance to most antibiotics that drastically limits conventional chemotherapeutic treatment options, new anti-*M. abscessus* therapeutics are urgently needed against this emerging pathogen. Extensive screening of a library of benzimidazole derivatives that were previously shown to be active against *Mycobacterium tuberculosis* led to the identification of a lead compound exhibiting very potent in vitro activity against a wide panel of *M. abscessus* clinical strains. Designated EJMCh-6, this compound, a 2-(2-cyclohexylethyl)-5,6-dimethyl-1*H*-benzo[*d*]-imidazole), also exerted very strong activity against intramacrophage-residing *M. abscessus*. Moreover, the treatment of infected zebrafish embryos with EJMCh-6 was correlated with significantly increased embryo survival and a decrease in the bacterial burden as compared to those for untreated fish. Insights into the mechanism of action were inferred from the generation of spontaneous benzimidazole-resistant strains and the identification of a large set of missense mutations in MmpL3, the mycolic acid transporter in mycobacteria. Overexpression of the mutated *mmpL3* alleles in a susceptible *M. abscessus* strain was associated with high resistance levels to EJMCh-6 and to other known MmpL3 inhibitors. Mapping the mutations conferring resistance on an MmpL3 three-dimensional homology model defined a potential EJMCh-6-binding cavity. These data emphasize a yet unexploited chemical structure class against *M. abscessus* with promising translational development for the treatment of *M. abscessus* lung diseases.

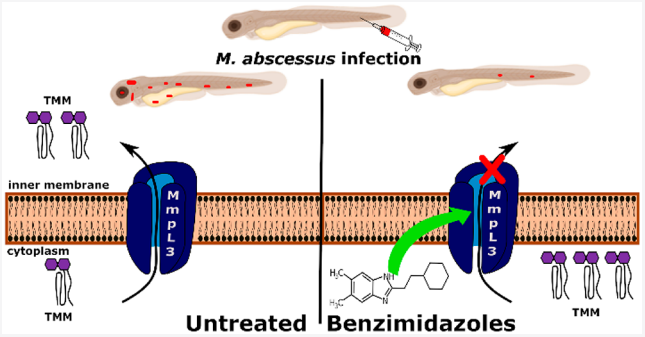

KEYWORDS: *Mycobacterium abscessus, benzimidazole, mycolic acid, MmpL3, therapeutic activity, zebrafish*

Although the incidence of tuberculosis is decreasing in developed countries, infections with nontuberculous mycobacteria (NTM) represent an increasing health concern. In developing countries, the misdiagnosis of NTM infections is common because of a clinical presentation similar to that of TB and following the microscopic examination of samples.[1] NTM are environmental mycobacteria displaying various degrees of virulence and associated with a wide spectrum of clinical manifestations. The *Mycobacterium avium* complex and the *Mycobacterium abscessus* complex are the most frequently encountered pathogens associated with NTM pulmonary diseases.[2,3] *M. abscessus* infections are particularly frequent in

Received: October 9, 2019
Published: December 20, 2019

DOI: 10.1021/acsinfecdis.9b00389
ACS Infect. Dis. 2020, 6, 324−337

Table 1. Library of Benzimidazole Analogs Tested and Their MIC against *M. tuberculosis*[a] and *M. abscessus* Determined after 4 Days at 30 °C in CaMH

No	Symbol	Structure	MIC (μg/mL) *M. tuberculosis*[a]		MIC (μg/mL) *M. abscessus*
			$H_{37}Rv$	Spec. 210	CIP104536^T (S)
1	BMC-2g	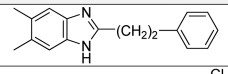	1.5	1.5	4
2	BMC-2i	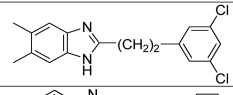	0.75	1.5	0.25
3	BMC-2j	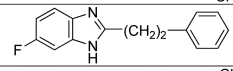	25	50	64
4	BMC-2l	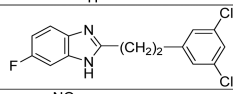	>100	>100	8
5	BMC-2a	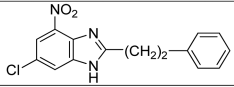	>100	>100	>128
6	BMC-2c	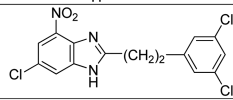	25	100	>128
7	BMC-2h	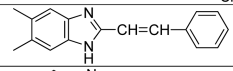	6.25	6.25	4
8	BMC-2k	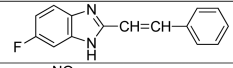	50	25	>128
9	BMC-2b	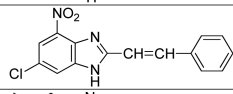	50	>100	>128
10	BMC-3a	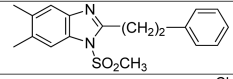	25	25	>128
11	BMC-3c	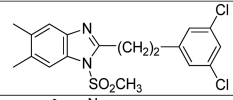	12.5	12.5	>128
12	BMC-3d	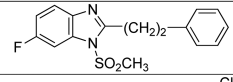	100	>100	>128
13	BMC-3f	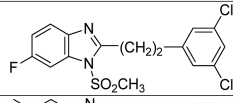	50	50	>128
14	BMC-3g	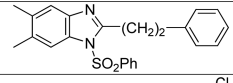	50	50	32
15	BMC-3i	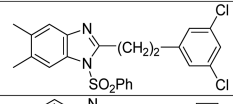	25	25	128
16	BMC-3j	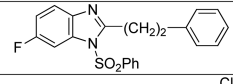	>100	>100	128
17	BMC-3l	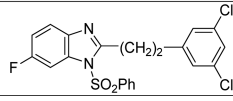	25	25	>128
18	BMC-3b	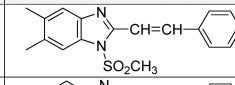	>100	>100	>128
19	BMC-3e	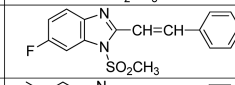	50	50	>128
20	BMC-3h	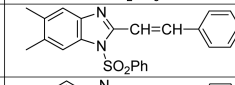	>100	>100	>128
21	BMC-3k	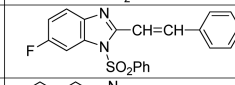	50	100	>128
22	BMC-2d	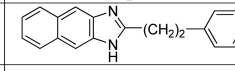	>100	>100	>128
23	BMC-2f	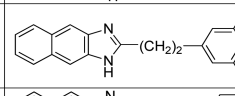	6.25	6.25	>128
24	BMC-2e	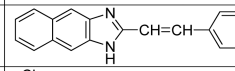	25	25	>128
25	EJMCh-14	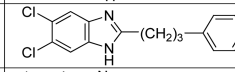	6.2	6.2	1
26	EJMCh-13	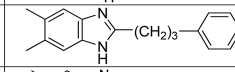	12.5	6.25	0.25
27	EJMCh-11	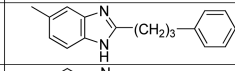	25	100	8
28	EJMCh-12	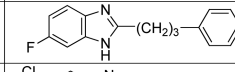	12.5	50	32
29	EJMCh-10	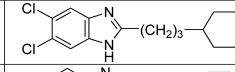	12.5	6.25	0.5
30	EJMCh-8	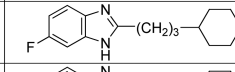	6.2	6.2	>128
31	EJMCh-15	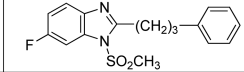	50	50	>128
32	EJMCh-16	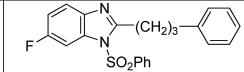	100	50	>128
33	EJMCh-3	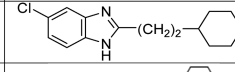	0.75	0.75	2
34	EJMCh-4	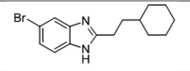	0.6	ND	4
35	EJMCh-6	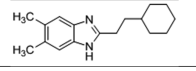	0.08	ND	0.125

[a]MIC values against *M. tuberculosis* were taken from refs 20 and 21. ND, not determined.

patients with underlying lung disorders, notably in the context of bronchiectasis or cystic fibrosis (CF). Importantly, a recent genomic survey suggested that a majority of *M. abscessus* infections among CF patients are acquired through aerosol transmission of recently emerging dominant circulating clones.[4] In CF patients, *M. abscessus* accelerates inflammatory lung damage, leading to increased morbidity and mortality.[5,6] The peculiar link between a dysfunctional CFTR and vulnerability to *M. abscessus* infection has recently been addressed using a CFTR-depleted zebrafish model, recapitulating CF immunopathogenesis, which showed that the loss of CFTR increases susceptibility to infection as a consequence of a defect in the macrophage oxidative response.[7]

M. abscessus lung diseases are very difficult to treat because of the intrinsic or induced drug resistance mechanisms developed by these microorganisms, making them highly resistant to most available antimicrobials and antitubercular drugs.[8−11] This developed drug resistome includes the acquisition of mutations in target genes, a low permeability of the *M. abscessus* cell envelope, defective drug-activating systems converting prodrugs

DOI: 10.1021/acsinfecdis.9b00389
ACS Infect. Dis. 2020, 6, 324−337

to metabolically active molecules, the induction of drug efflux pumps, and the expression of drug-modifying enzymes.[8,11,12] Resistance to most classes of antibiotics leads to poor treatment outcomes and lengthy treatment durations accompanied by side effects such as drug toxicity. The recommended treatment regimen includes a combination of a macrolide (clarithromycin or azithromycin), an aminoglycoside (amikacin), and an intravenous β-lactam (cefoxitin or imipenem) for at least 12 months,[13] resulting in a cure rate of only 25−40% in the case of macrolide resistance, which occurs in 40−60% of the isolates.[14] In addition, failure to eradicate *M. abscessus* can be a contraindication for lung transplantation in CF treatment centers, leaving patients without any therapeutic options. Therefore, it is imperative that we continue to explore and develop more effective and safer drugs for the treatment of *M. abscessus* lung infections.

Because *M. tuberculosis* and *M. abscessus* share many common biochemical pathways, it is likely that compounds inhibiting biosynthetic pathways in *M. tuberculosis* may also be active against *M. abscessus*. Therefore, the screening of chemical libraries generated against TB in previous drug discovery programs may represent a useful approach to rapidly populating the *M. abscessus* drug pipeline with attractive drug candidates. We have previously validated this approach and discovered a new chemical scaffold that is active against *M. abscessus* from a known set of potent nontoxic antitubercular hits.[15] The lead compound designated PIPD1 showed selective activity against *M. abscessus* both in vitro and in vivo by targeting essential mycolic acid transporter MmpL3.[16] These results prompted us to further explore this strategy by testing a library of indole-2-carboxamide derivatives that were previously reported for their strong activity against *M. tuberculosis*,[17] which led to the identification of active lead compounds against *M. abscessus* also targeting MmpL3.[18] The sequencing analysis of *mmpL3* in spontaneous resistant mutants selected on either PIPD1 or on the indole-2-carboxamides (lead compounds **6** and **12**) revealed a common Ala309Pro substitution in transmembrane domain 5. Additionally, the overexpression of MmpL3 carrying the Ala309Pro mutation in *M. abscessus* wild-type bacteria conferred high-level resistance to PIPD1 and to the indole-2-carboxamides, confirming their target.[16,18] Together, these studies support the susceptibility of MmpL3 to different classes of inhibitors.[19] Recently, a new series of 2-(2-phenalkyl)-1*H*-benzo[*d*]imidazoles were examined, exhibiting a very low cytotoxic effect on eukaryotic cells and very high antitubercular activity[20,21] through the inhibition of mycolic acid transport. In *M. tuberculosis*, mutations in *mmpL3* were associated with high resistance levels against these compounds.[22] Moreover, overexpression of the mutated *mmpL3* alleles in a susceptible *M. tuberculosis* strain resulted in increased resistance to these compounds. Supporting these findings, two of these compounds [EJMCh-4 (5-bromo-2-(2-cyclohexylethyl)-1*H*-benzo[*d*]-imidazole) and EJMCh-6 (2-(2-cyclohexylethyl)-5,6-dimethyl-1*H*-benzo[*d*]imidazole)] were found to block trehalose monomycolate (TMM) transport across the plasma membrane, resulting in decreased trehalose dimycolate (TDM) production and arabinogalactan mycolylation.[22]

In this study, we investigate the efficacy of the benzimidazoles against *M. abscessus*. We describe the structure−activity relationship of benzimidazole analogs against *M. abscessus* and report their activity in vitro, in macrophage infection assays, and in a zebrafish model of *M. abscessus* infection. Through a combination of genetic studies, we also provide biological evidence that benzimidazole analogs target mycolic acid transport by targeting MmpL3 in *M. abscessus*. Our results indicate the vast potential for the translational development of this new structural class of inhibitors for the treatment of *M. abscessus* infections in CF patients.

RESULTS

Activity of Benzimidazole Analogs. MmpL3 has been extensively studied in recent years as a promising susceptible target in both *M. tuberculosis* and *M. abscessus*, and many different chemical entities very active against *M. abscessus* in vitro and in vivo and targeting MmpL3 have been reported.[16,18,19,23−26] On the basis of our previous work reporting the potent activity of benzimidazoles against *M. tuberculosis* by targeting MmpL3,[22] we evaluated the efficacy of a library of 35 benzimidazole derivatives against *M. abscessus* and attempted to address their mode of action in this mycobacterial species. Screening of this chemical library against the reference strain, *M. abscessus* CIP104536^T (S variant), identified compounds with no activity (MIC > 128 μg/mL), moderate activity (2 < MIC < 64 μg/mL), or very high activity (0.125 < MIC < 1) (Table 1). Notably, EJMCh-6 (MIC of 0.125 μg/mL), EJMCh-13 (MIC of 0.25 μg/mL), and BMC-2i (MIC of 0.25 μg/mL) were the most active compounds against *M. abscessus*, although EJMCh-13 was less efficient against *M. tuberculosis*.

The combined results against *M. tuberculosis* and *M. abscessus* (Table 1) allowed the inference of some plausible relationships between individual structural elements and antimycobacterial activity. First, the presence of a hydrogen atom at the N-1 nitrogen seems to be crucial to the activity of these compounds. Conversely, substitution with an alkyl or arylsulfonyl group reduced the chemical activity. This relationship was observed for the BMC-2g and BMC-3a pair. Because of the electron-withdrawing properties of the sulfonyl functional group, it would be advisible to check how the substitution of the proton in this position by alkyl or aryl is affecting the activity. The presence of substituents at the benzimidazole core was also of great importance, with the highest activity of derivatives possessing two methyl groups in the C-5 and C-6 positions, hence the higher activity of BMC-2g and BMC-2i as compared to that of BMC-2j, BMC-2l, BMC-2a, and BMC-2c. It seems that the weak electron-donor effect of methyl groups, caused by hyperconjugation, promoted greater activity than the strongly electronegative nature of halogen atoms or the nitro group. The saturation of the linker seems to be of no greater benefit for activity (BMC-2j and BMC-2k), especially in the case of the *M. abscessus* strain. Similarly, lengthening the linker by a methylene group did not significantly affect the activity of the compounds (BMC-2g and EJMCh-13 or BMC-2j and EJMCh-12). Compounds with a saturated cyclohexane ring at the end of the linker showed higher activity than compounds possessing a benzene ring (BMC-2g and EJMCh-6). However, this association was more related to strains of *M. tuberculosis* because the opposite relationship was observed in *M. abscessus* (EJMCh-12 and EJMCh-8).

EJMCh-6 Inhibits *M. abscessus* Growth in Vitro. Exposure of exponentially growing *M. abscessus* to increasing concentrations of EJMCh-6, corresponding to 1×, 4×, and 8× MIC (0.125 μg/mL) or to 1× MIC of imipenem (IPM; 16 μg/mL), showed growth inhibition (Figure 1). The CFU numbers after 48 h of treatment were only slightly lower than those of the inoculum and were reduced by approximately 1 log at 72 h following treatment with the highest dose, suggesting that

DOI: 10.1021/acsinfecdis.9b00389
ACS Infect. Dis. 2020, 6, 324−337

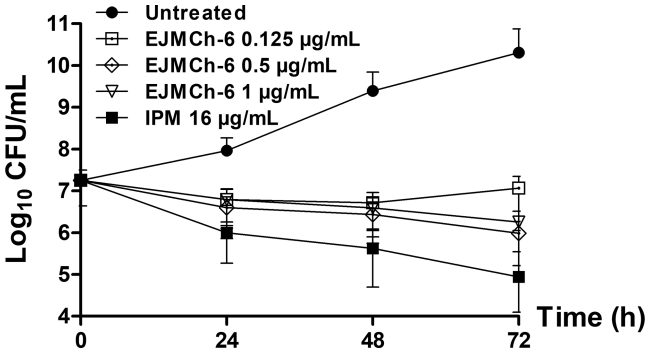

Figure 1. In vitro activity of EJMCh-6. Growth inhibition of *M. abscessus* CIP104536^T S exposed to 1×, 4×, and 8× MIC of EJMCh-6 or to 1× MIC of IPM in CaMH broth at 30 °C. At various time points, bacteria were plated on LB agar and further incubated at 37 °C for 4 days prior to CFU determination. The results for each drug concentration are representative of three independent experiments. Results are expressed as mean $\log_{10}$ values ± SD.

EJMCh-6 is bacteriostatic in vitro (Figure 1). Exposure to IPM, an active β-lactam drug against *M. abscessus*,[27] was associated with a more pronounced killing effect.

Activity of EJMCh-6 against *M. abscessus* Clinical Isolates. The activity of EJMCh-6 was next tested using a wide panel of clinical isolates belonging to the *M. abscessus* complex, which comprises three distinct subspecies groups: *M. abscessus* subsp. *abscessus*, *M. abscessus* subsp. *massiliense*, and *M. abscessus* subsp. *bolletii*, which have been shown to respond differently to antibiotics.[28] This compound showed very potent activity against the various strains and subspecies, regardless of whether they were isolated from CF patients or non-CF patients, with MIC values ranging from 0.031 to 1 μg/mL (Table 2). These values were much lower than those of commonly used drugs in a clinical setting such as IPM (MIC ranging from 8 to 64 μg/mL), sutezolid (MIC ranging from 1 to 16 μg/mL), and linezolid (MIC ranging from 1 to 32 μg/mL) (Table 2). All clinical isolates responded equally well to EJMCh-4 (MIC of 2 μg/mL), a validated analogue shown to block TMM transport across the

Table 2. Comparison of the Activity of Sutezolid, Linezolid, EJMCh-4, EJMCh-6, and Imipenem against Clinical Isolates from CF (Cystic Fibrosis) and Non-CF Patients[a]

strain	morphotype	source	imipenem	sutezolid	linezolid	EJMCh-4	EJMCh-6
M. abscessus							
CIP104536	S	non-CF	16	16	32	2	0.125
3321	S	non-CF	16	16	16	2	0.25
1298	S	CF	8	4	4	2	0.25
2587	S	CF	16	16	32	2	0.125
2069	S	non-CF	8	16	32	2	0.25
CF	S	not reported	8	8	16	2	0.5
2524	R	CF	16	4	8	2	0.125
2648	R	CF	32	4	8	2	0.5
3022	R	non-CF	32	8	8	2	0.25
5175	R	CF	16	ND	ND	4	0.25
CIP104536	R	non-CF	16	4	8	2	0.031
CF	R	not reported	8	ND	ND	2	0.5
M. massiliense							
CIP108297	R	Addison's disease	32	4	8	2	0.25
210	R	CF	16	2	16	2	0.125
179	R	CF	8	1	0.5	2	0.125
CIP108297	S	Addison's disease	16	4	16	2	0.125
140	S	CF	32	4	16	2	0.125
185	S	CF	16	8	16	2	0.5
107	S	CF	32	8	16	2	0.25
122	S	CF	16	4	8	2	0.125
120	S	CF	16	16	32	2	0.062
212	S	CF	16	16	32	2	0.25
100	S	CF	32	4	16	2	0.5
111	S	CF	16	2	16	2	0.5
M. bolletii							
CIP108541	S	not reported	8	16	32	2	1
114	S	CF	16	4	8	2	1
17	S	CF	32	16	32	2	1
116	S	CF	16	4	16	2	0.5
97	S	CF	16	8	16	2	0.5
112	R	CF	16	8	16	2	0.5
19	R	non-CF	8	ND	ND	4	0.5
10	R	not reported	32	1	1	2	0.062
108	R	CF	64	8	16	2	0.5

[a]The MIC was determined in CaMH broth for different subspecies belonging to the *M. abscessus* complex. Values are shown in μg/mL. ND = not determined.

DOI: 10.1021/acsinfecdis.9b00389
ACS Infect. Dis. 2020, 6, 324−337

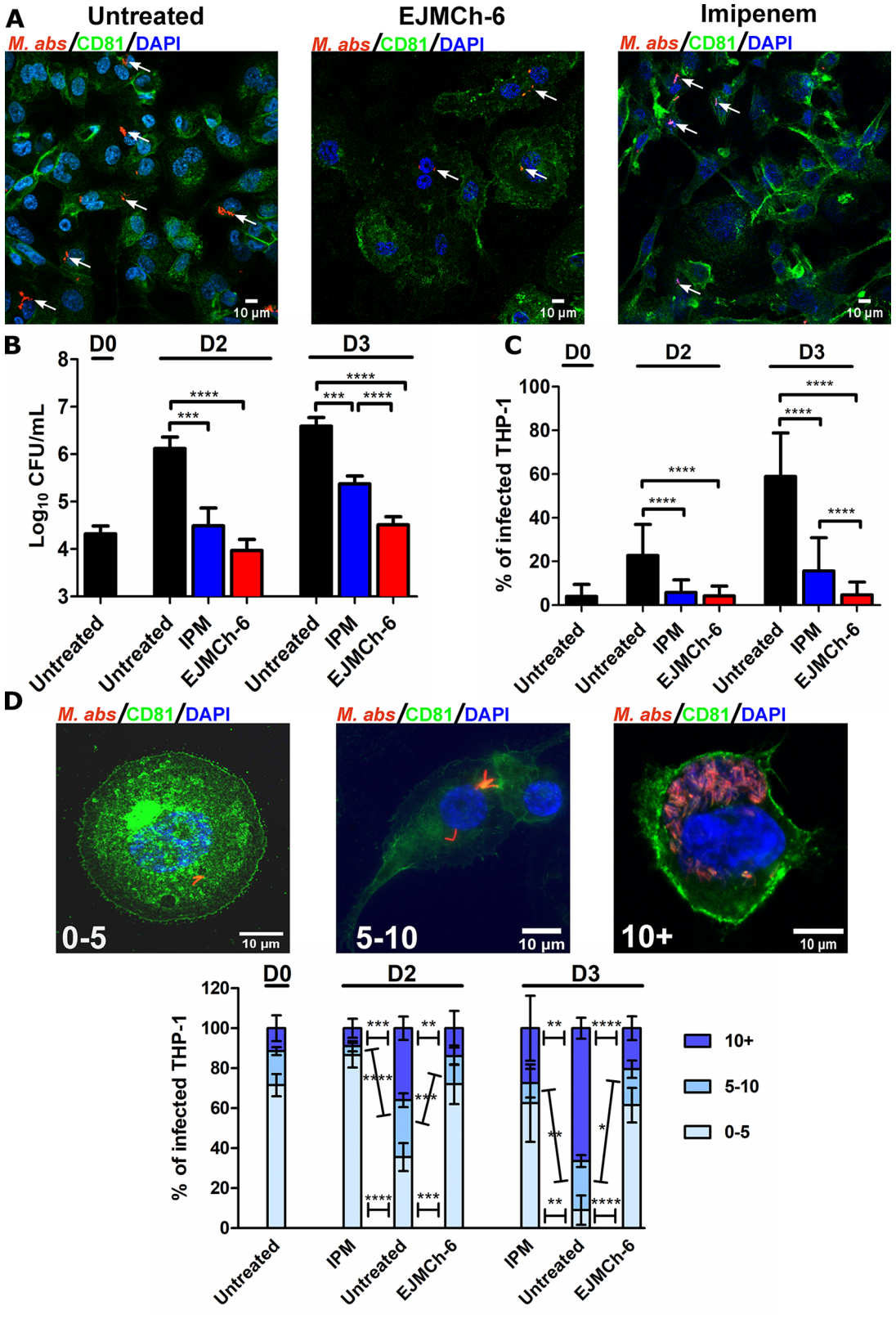

Figure 2. Intracellular activity of EJMCh-6 on *M. abscessus*-infected THP-1 cells. Macrophages were infected with *M. abscessus* S-morphotype expressing tdTomato (MOI of 2:1) for 2 h prior to treatment with IPM (96 μg/mL) or EJMCh-6 (3 μg/mL). (A) Three immunofluorescent fields were taken 2 days postinfection at 40× magnification showing macrophages infected with fluorescent *M. abscessus* (red). The surface of the macrophages was detected using anti-CD81 antibodies (green). The nuclei were stained with DAPI (blue). White arrows depict intracellular mycobacteria. (B) CFU were determined at days 2 and 3 postinfection, respectively. Data are mean values ± SD for three independent experiments. Data were analyzed using the one-tailed Mann−Whitney *t* test. (C) Percentage of infected THP-1 macrophages at days 2 and 3 postinfection. Data are mean values ± SD for three independent experiments. Data was analyzed using a one-tailed Mann−Whitney *t* test. (D) Analysis of the percentage of macrophage categories infected with different numbers of bacilli. The first image illustrates a macrophage containing fewer than 5 bacilli, the second

DOI: 10.1021/acsinfecdis.9b00389
ACS Infect. Dis. 2020, 6, 324−337

Figure 2. continued

encompasses 5 to 10 bacilli, and the third comprises >10 bacilli (upper panels). The surface of macrophages was detected using anti-CD81 antibodies (green). The nuclei were stained with DAPI (blue). The macrophage categories were counted at 2 and 3 dpi in the absence of antibiotics or in the presence of either IPM or EJMCh-6 (lower panel). The percentages of macrophages containing different numbers of bacilli (0−5, 5−10, and >10) are represented on the *y* axis. Values are means ± SD for three independent experiments performed each time in triplicate. Data were analyzed using the one-tailed nonpaired *t* test.

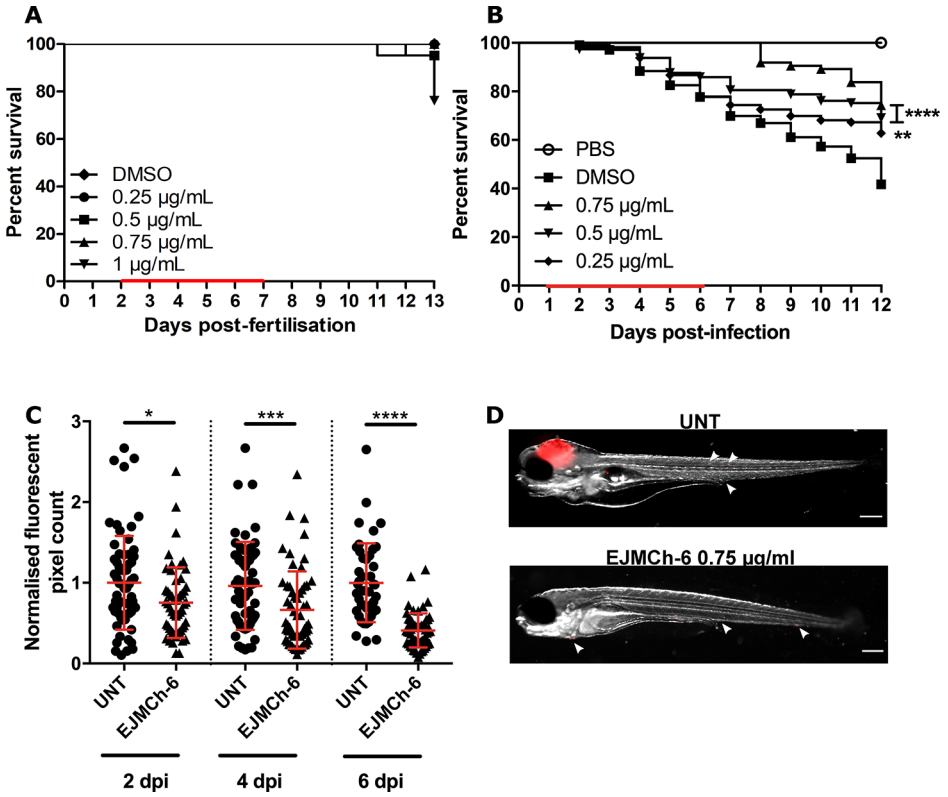

Figure 3. EJMCh-6 displays high therapeutic activity against *M. abscessus* in an embryonic zebrafish infection model. (A) Groups of uninfected embryos were immersed in water containing increasing concentrations of EJMCh-6 (ranging from 0.25 to 1 μg/mL) for 5 days. The red bar indicates the duration of treatment. The graph shows the survival of the EJMCh-6-treated and untreated (DMSO) embryos over a 13-day period. (B) Zebrafish embryos 30 h postfertilization were infected with approximately 250−300 CFU of *M. abscessus* CIP104536^T (R variant) expressing tdTomato via caudal vein injection. A standard PBS injection control was included for each experiment. At 1 dpi, embryos were randomly split into equal groups of approximately 20 embryos per group, and varying concentrations of EJMCh-6 (0.25, 0.5, and 0.75 μg/mL) were added to the water. DMSO was included as a positive control group. For a 5 day period (as indicated by the red bar), drugs were changed daily, after which embryos were washed twice in fresh embryo water and maintained in embryo water. Embryo survival was monitored daily over a 12-day period. Each treatment group was compared against the DMSO positive control group with significant differences calculated using the log rank (Mantel−Cox) statistical test for survival curves. (C) The bacterial burden was quantified by a fluorescent pixel count determination using *ImageJ* software, with each data point representing a single embryo. Error bars represent the standard deviation. Statistical significance was determined by the Student's *t* test. The plots represent a pool of 3 experiments containing approximately 20 embryos each. (D) Representative embryos from the untreated group (upper panel) and from the treated group with 0.75 μg/mL EJMCh-6 at 6 dpi. White arrowheads show tdTomato-expressing bacteria. Scale bars represent 500 μm. *$P \leq 0.05$, ** $P \leq 0.01$, *** $P \leq 0.001$, and **** $P \leq 0.0001$.

plasma membrane in *M. tuberculosis*.[22] The S and R morphotypes of *M. abscessus* were equally sensitive to EJMCh-4 and EJMCh-6. Overall, these results demonstrate that benzimidazole analogs exert potent activity against the *M. abscessus* complex, including isolates from CF patients.

Efficacy of EJMCh-6 against Intracellular *M. abscessus*. Previous work indicated that the benzimidazole derivatives, particularly EJMCh-6, exhibited low cytotoxicity toward human lung cancer cell line A549 and the LLC-PK1 pig kidney epithelial cell line.[20] Herein, we evaluated the eventual cytotoxicity of benzimidazoles in human THP-1 macrophages, incubated for 48 h with increasing concentrations of EJMCh-6 or BMC-2i. As shown in Figure S1, the latter showed reduced levels of toxicity as compared to EJMCh-6, although both compounds exhibited toxicity only at high concentrations (CC_{50} = 89 μg/mL for EJMCh-6 and 154 μg/mL for BMC-2i), leading to selectivity indexes (SI = CC_{50}/MIC) of 712 for EJMCh-6 and 616 for BMC-2i. SDS was included as a positive control for macrophage death. On the basis of the low cytotoxicity, we next examined the intracellular efficacy of EJMCh-6 in THP-1 cells infected with *M. abscessus* S expressing tdTomato. Following infection, macrophages were treated with 250 μg/mL amikacin for 2 h to prevent extracellular bacterial growth and were treated with IPM (96 μg/mL) or EJMCh-6 (3 μg/mL). Untreated infected macrophages were included as a negative control for intracellular bacterial replication. At 0, 2, and 3 dpi, macrophages were stained with

DOI: 10.1021/acsinfecdis.9b00389
ACS Infect. Dis. 2020, 6, 324−337

anti-CD81 and DAPI and observed under an epifluorescence microscope. Microscopic observations revealed a marked decrease in the number of bacilli inside the macrophages treated with either EJMCh-6 or IPM (Figure 2A). In parallel, macrophages were lyzed and plated to determine the intracellular bacterial loads following drug treatment. When left untreated for 48 h, there was a 1.5 to 2 log increase in the number of intracellular *M. abscessus*, consistent with previous reports.[27] In contrast, exposure to either IPM or EJMCh-6 significantly impeded multiplication of the bacilli within the macrophages (Figure 2B). Treatment with EJMCh-6 significantly reduced the intracellular *M. abscessus* load to a higher extent than IPM after 72 h. Furthermore, a quantitative analysis confirmed the pronounced reduction in the number of infected THP-1 cells treated with EJMCh-6 or IPM at 2 dpi, and this effect was further exacerbated at 3 dpi with a stronger effect of EJMCh-6 over IPM as compared to the untreated control cells (Figure 2C). To address whether drug treatment alters the intracellular bacterial loads, infected macrophages were classified into three categories based on their bacterial content: poorly infected (<5 bacilli), moderately infected (5−10 bacilli), and heavily infected (>10 bacilli) macrophages as illustrated in Figure 2D (upper panels). Infected macrophages were then individually observed under the microscope and assigned to one of the three categories. This quantitative analysis clearly showed that treatment with IPM or EJMCH-6 significantly reduced the percentage of moderately and heavily infected THP-1 cells and increased the number in the poorly infected category as compared to the number of untreated cells at 2 dpi (Figure 2D, lower panel). A similar trend was observed at 3 dpi, whereby the EJMCh-6-treated cell population was characterized by a very high proportion of poorly infected cells containing fewer than 5 bacilli (around 60%) and about 20% of moderately and heavily infected cells containing more than 5 bacilli. In contrast, the untreated group was composed of more than 60% of heavily infected macrophages at 3 dpi. Taken together, these results clearly indicate that EJMCh-6 enters human macrophages, impedes bacterial replication, and prevents macrophage reinfection.

EJMCh-6 Treatment Increases the Protection of Zebrafish Infected with *M. abscessus*. An acute *M. abscessus* model of infection in zebrafish has been developed to test the potency of drug treatments in a living vertebrate.[29−31] Initial experiments indicated that EJMCh-6 failed to interfere with larval development and/or to induce toxicity in zebrafish embryos at concentrations below 1 μg/mL (final concentration in fish water) when treatment was applied for 5 days with a daily renewal of the compound (Figure 3A). Next, red fluorescent tdTomato-expressing *M. abscessus* (R variant) was injected into the caudal vein of embryos 30 h postfertilization (hpf) and transferred to 24-well plates. EJMCh-6 was directly added 1 day postinfection (dpi) to the water containing the infected zebrafish, with EJMCh-6-supplemented water changed on a daily basis for 5 days. Survival of the embryos was recorded daily for 12 days. A significant and dose-dependent reduction in mortality rates of the embryos exposed to 0.25, 0.5, or 0.75 μg/mL EJMCh-6 was observed as compared to the untreated infection group (Figure 3B). In the presence of 0.75 μg/mL EJMCh-6, the highest dose tested, around 80% of the treated embryos survived at 12 dpi as compared to 40% of the untreated group, indicating that EJMCh-6 protects zebrafish from being killed by *M. abscessus*. The determination of the bacterial loads, reflected by fluorescent pixel counts (FPC), showed significantly fewer bacilli in the EJMCh-6-treated embryos than in the untreated infection group (Figure 3C). This reduced bacterial burden, already visible at 2 dpi, was even more pronounced at 4 and 6 dpi. This was corroborated by whole embryo imaging showing the presence of large abscesses in the brain of the untreated fish, which are not found in the EJMCh-6-treated embryos, although single bacilli or small bacterial clumps can be observed (Figure 3D).

Mutations in MmpL3 Confer Resistance to EJMCh-6. Recent work in *M. tuberculosis* identified multiple mutations in *mmpL3* associated with high resistance levels to the benzimidazoles.[22] Furthermore, the overexpression of mutated *mmpL3* alleles in a susceptible *M. tuberculosis* strain resulted in increased resistance, supporting the hypothesis that EJMCh-6 targets the mycolic acid transporter. This prompted us to sequence the *MAB_4508* gene, encoding the MmpL3 protein in *M. abscessus*, in spontaneous EJMCh-6-resistant mutants selected on plates containing 1.25 μg/mL EJMCh-6. In an initial experiment, two resistors (EJMCh-6^R1 and EJMCh-6^R3) were isolated, exhibiting 8- and 2-fold-increased resistance levels (MICs of 2 and 0.5 μg/mL) respectively, as compared to the parental strain (Table 3). Comparative analysis of the sequences with the parental strain identified a single nucleotide polymorphism (SNP) in *mmpL3* in both resistors. In EJMCh-6^R1, a C974T was found, resulting in an amino acid replacement at position 325 (T325I), whereas in EJMCh-6^R3 another SNP (T607G) occurred, leading to an amino acid change at position 203 (L203R). To further extend the number and diversity of SNP in *mmpL3* associated with resistance to the benzimidazoles, 12 additional mutants were selected on EJMCh-6 (EJMCh-6^R4 to EJMCh-6^R16), uncovering L678R, L551S, V247G, and V299A (Table 3). Spontaneous mutants were then selected on plates containing 2.5 or 5 μg/mL BMC-2i. This led to the selection of nine additional resistors using the R parental strain (BMC-$2i^R$1 to BMC-$2i^R$11) characterized by very high MIC upshifts (>16 μg/mL) for BMC-2i (Table 3). Among them, seven mutants were harboring the Y620C mutation in MmpL3; one, the A309P mutation; and one, the L551F mutation. As expected, all nine mutants were slightly cross-resistant to EJMCh-6. Some of these mutations were previously reported in *M. abscessus* strains resistant to PIPD1[16] or to indolcarboxamides[18] that were previously shown to target MmpL3. The frequencies of resistance to EJMCh-6 and BMC-2i (determined at concentrations equivalent to 10× MIC) were estimated to be 5×10^{-8} and 4×10^{-8}, respectively. We then tested the susceptibility profile of additional *M. abscessus* mutants resistant to PIPD1[16] and presenting additional SNP in *mmpL3*. These strains, designated PIPD1^{R}1 to PIPD1^{R}21, were all cross-resistant to EJMCh-6 or BMC-2i, although the MIC upshift varied considerably from one mutant to another, with the A309P substitution inducing the highest resistance profile to all three inhibitors (Table 3). Overall, these results uncover a wide panel of missense mutations in MmpL3 conferring resistance to the benzimidazole derivatives in *M. abscessus*.

Genetic Validation of *mmpL3* as the Target of EJMCh-6. To further validate *mmpL3* as a target of EJMCh-6, various *mmpL3* alleles carrying point mutations were cloned under the control of the *hsp60* promoter in a multicopy plasmid and were introduced into *M. abscessus* prior to MIC determination. While overexpression of the WT MmpL3 protein did not result in increased resistance to EJMCh-6, overproduction of the mutated protein harboring L551F, V617F, T325I, V547G, or A309P led to a 4- to >64-fold upshift in the MIC value (Table 4).

DOI: 10.1021/acsinfecdis.9b00389
ACS Infect. Dis. 2020, 6, 324−337

Table 3. Mutations in *mmpL3* Conferring Resistance to Indole-2 Carboxamide Cpd12, EJMCh-6, or BMC-2i[a]

strain	MIC (μg/mL)			mutation in MAB_4508	
	Cpd12	EJMCh-6	BMC-2i	SNP	AA change
CIP104536^T (R)	0.125	0.125	0.25		
CIP104536^T (S)	0.125	0.25	0.5		
selection on PIPD1[b]					
PIPD1^{R}1	>16	>16	>16	G925C	A309P
PIPD1^{R}2	0.063	>16	>16	T779C	L260P
PIPD1^{R}3	0.125	1	>16	T1652C	L551S
PIPD1^{R}5	0.125	0.5	>16	G38C	R11P
PIPD1^{R}6	0.25	1	>16	T1838C	V613A
PIPD1^{R}8	0.25	1	>16	C1211T	P404L
PIPD1^{R}9	0.25	2	>16	C974T	T325I
PIPD1^{R}12	0.125	1	>16	G1653C	L551F
PIPD1^{R}13	0.125	2	>16	T1647G	V547G
PIPD1^{R}14	0.25	1	>16	C974T	T325I
PIPD1^{R}21	0.06	0.5	>16	G1849T	V617F
selection on EJMCh-6[c]					
EJMCh-6^{R}1	0.125	2	>16	C974T	T325I
EJMCh-6^{R}3	0.125	0.5	>16	T607G	L203R
EJMCh-6^{R}4	0.063	2	>16	T2033C	L678R
EJMCh-6^{R}5	0.063	2	>16	T2033C	L678R
EJMCh-6^{R}6	0.063	2	>16	T2033C	L678R
EJMCh-6^{R}7	0.063	2	>16	T2033C	L678R
EJMCh-6^{R}8	0.063	2	>16	T2033C	L678R
EJMCh-6^{R}9	0.063	2	>16	T1653C	L551S
EJMCh-6^{R}11	0.125	1	>16	T1653C	L551S
EJMCh-6^{R}12	0.25	2	>16	T1653C	L551S
EJMCh-6^{R}13	0.25	2	>16	C974T	T325I
EJMCh-6^{R}14	0.063	2	1	T740G	V247G
EJMCh-6^{R}15	0.063	2	1	T740G	V247G
EJMCh-6^{R}16	0.125	0.5	>16	T896C	V299A
selection on BMC-2i[d]					
BMC-2i^{R}1	0.063	2	>16	A1859T	Y620C
BMC-2i^R 3	0.063	0.5	>16	A1859T	Y620C
BMC-2i^{R}4	0.063	0.5	>16	A1859T	Y620C
BMC-2i^{R}5	>16	>16	>16	G925C	A309P
BMC-2i^{R}7	0.063	0.5	>16	A1859T	Y620C
BMC-2i^{R}8	0.063	0.5	>16	A1859T	Y620C
BMC-2i^{R}9	0.063	0.5	>16	A1859T	Y620C
BMC-2i^{R}10	0.125	0.5	>16	G1653T	L551F
BMC-2i^{R}11	0.125	0.5	>16	A1859T	Y620C

[a]Spontaneous resistant mutants were derived from *M. abscessus* CIP104536^T (S) or (R) against PIPD1, EJMCh-6, or BMC-2i as indicated. MIC was determined after 4 days at 30 °C in CaMH. Mutations were determined by sequencing the *mmpL3* gene. [b]Mutants R1, R2, R3, R5, R6, R8, and R9 were derived from CIP104536^T (S), whereas R12, R13, R14, and R21 were derived from CIP104536^T (R).[16] [c]Mutants EJMCh-6^{R}1 to EJMCh-6^{R}9 were derived from CIP104536^T (S), and EJMCh-6^{R}11 to EJMCh-6^{R}16 were derived from CIP104536^T (R). [d]All mutants BMC-2i^R were derived from CIP104536^T (R).

As expected, comparable results were obtained when testing BMC-2i against this panel of strains. AU1235, a well-established MmpL3 inhibitor,[32] exhibited high MIC levels against all strains expressing the mutated *mmpL3* alleles, and in general, the resistance levels were more pronounced (MIC > 16 μg/mL) than those observed with EJMCh-6. Regarding Cpd12, an indole-2 carboxamide previously reported to target mycolic acid transport in *M. abscessus*,[18] an increase in the MIC value was detected only with the strain overproducing the MmpL3_A309P variant, a finding supported by the fact that spontaneous mutants selected on Cpd12 identified only the A309P mutation.[18] This is in contrast, however, to the large number of mutations selected in spontaneous mutants selected on PIPD1[16] or EJMCh-6/BMC-2i (Table 2). The effect of these mutations was restricted to MmpL3 inhibitors because the MIC of amikacin remained comparable in all of the strains (Table 4). Collectively, these results indicate that the single transfer of point mutations in MmpL3 identified in the EJMCh-6 spontaneously resistant strains confers cross-resistance to multiple MmpL3 inhibitors, suggesting that these compounds share the same target and mechanism of action.

Mapping the EJMCh-6-Resistant Mutations on an MmpL3 Structural Model Unravels a Potential Drug-Binding Pocket. To assess the potential mode of action of EJMCh-6 at the molecular level, the various mutations identified in the spontaneously resistant mutants were mapped onto a *M. abscessus* MmpL3 three-dimensional homology model that was generated using the crystal structure of *M. smegmatis* MmpL3 as a template.[33] The 15 mutations are scattered over 7 different transmembrane helices (TM) (Figure 4A), first on TM2 (L203R), with L260P found on TM4 and two mutations concerning TM5 (V299A and A309P). TM6 and TM7 also carry single point mutations, T325I and P404L, whereas both TM8 (V547G and L551S or L551F) and TM10 (V613A, V617F, and Y620C) display three mutations. Three residues not located in TM regions are mutated, notably N-terminus R11P, V247G residing in the loop between TM3 and TM4, and L678R in the loop separating TM11 and TM12. To propose a mechanism of action of the drug, docking studies with EJMCh-6 were performed using the MmpL3 homology model. Because residues A309, V547, L551, V613A, V617F, and Y620 are in close proximity, it was therefore tempting to hypothesize that these residues may form a potential binding pocket for EJMCh-6. We could not, however, dock EJMCh-6 without clashes in this area. Various drug scaffolds have been found in the same cavity in several cocrystal structures of *M. smegmatis* MmpL3,[33] indicating that they are directly interacting with MmpL3, a view supported by recent biochemical studies.[34] Guided by this available structural information, both EJMCh-6 and BMC-2i were docked in the same binding pocket. Eighteen residues from TM4 (I258, I262, D265, Y266, and F269), TM5 (T298, V299, S302, and I306), TM10 (V618, G621, L622, D625, and F629), TM11 (I658, A662, and L666), and TM12 (L688) delineate a large binding cavity (Figure 4B–D). Most of these amino acids are hydrophobic, and the recognition of EJMCh-6/BMC-2i appears to be mainly driven by hydrophobic interactions, although D625 and Y626 establish, via their side chains, hydrogen bonds with the inhibitors. This is of interest because these two residues are highly conserved in the members of the MmpL family of proteins and are essential to TMM transport in MmpL3 through their likely role in the proton relay.[33,35,36] It is therefore tempting to speculate that binding of EJMCh-6/BMC-2i in this pocket perturbs the proton relay and, consequently, the capacity of the pump to be energized, which may lead to the cessation of mycolic acid transport across the inner membrane.

However, most mutations found in spontaneously resistant strains are not in close proximity to the EJMCh-6-binding pocket. Only the V299A mutation concerns an amino acid proposed to be involved in hydrophobic interaction with the drug (Figure 4C,D). The V299A change could nonetheless have an effect, albeit weak, on the interaction due to the loss of

DOI: 10.1021/acsinfecdis.9b00389
ACS Infect. Dis. 2020, 6, 324−337

Table 4. MIC (μg/mL) Determination of Amikacin, EJMCh-6, BMC-2i, AU1235, and Cpd12 against Different Strains of *M. abscessus* Overexpressing Various *mmpL3* Mutated Alleles, Determined in CaMH

strains	pMV261	+*mmpL3* (WT)	+*mmpL3* (L551F)	+*mmpL3* (V617F)	+*mmpL3* (T325I)	+*mmpL3* (V547G)	+*mmpL3* (A309P)
Amikacin	16	16	16	16	16	16	32
EJMCh-6	0.25	0.25	2	1	2	2	>16
BMC-2i	1	1	>16	>16	>16	>16	>16
AU1235	0.6	0.3	>16	>16	>16	>16	>16
Cpd12	0.063	0.063	0.125	0.03	0.125	0.125	>16

bulkiness of the side chain that would lower the strength of the hydrophobic interaction, thereby reducing the MmpL3/inhibitor affinity. This is consistent with bacteriological data where this mutation only slightly affects the MIC (2 to 4 times higher MIC in comparison to the wild-type progenitor). Regarding the remaining mutations, it appears very speculative at this stage to propose the mechanistic effect with respect to drug resistance because they are far away from the drug binding site. One probable hypothesis is that these mutations trigger long distance structural rearrangements that affect the drug-binding affinity.

DISCUSSION

MmpL3 represents the only essential MmpL member in *M. tuberculosis*[37] and in *M. smegmatis*.[38] This MmpL is crucial in the translocation of mycolic acids in the form of trehalose-monomycolate (TMM) across the plasma membrane, subsequently allowing TMM to be converted to trehalose dimycolate (TDM), and in the mycolylation of arabinogalactan (AG).[32,38] Through metabolic labeling with [1,2-^{14}C]acetic acid, followed by apolar lipid extraction and subsequent separation of the lipids on TLC, we showed that EJMCh-6 inhibits TDM biosynthesis as well as mycolylation of AG by targeting MmpL3 in *M. tuberculosis*.[22] On the basis of previous work in *M. tuberculosis* and the results generated in this study, it is highly likely that EJMCh-6 targets the transport of mycolic acid in *M. abscessus*. This is supported by various complementary findings: (i) the identification of a wide panel of point mutations mapping MmpL3 associated with various degrees of resistance to EJMCh-6, (ii) spontaneous EJMCh-6-resistant mutants that are cross-resistant to previously characterized MmpL3 inhibitors, (iii) increased resistance to EJMCh-6 in *M. abscessus* strains overproducing mutated *mmpL3* alleles, and (iv) docking studies revealing the binding of EJMCh-6 in a cavity, which is shown to accommodate other inhibitors in the crystal structure of MmpL3 from *M. smegmatis*.[33] Since the original discovery of the piperidinol-containing PIPD1 compound,[16] numerous studies have described and characterized structurally unrelated chemical entities targeting MmpL3 in *M. abscessus*, including indole-2-carboxamides[18,19,39] or benzothiazole amides.[25,40] The present study adds benzimidazoles to the growing list of molecules targeting MmpL3 in *M. abscessus*,[24] although it remains to be established whether these compounds physically interact and inhibit the mycolic acid flippase activity of MmpL3.

In a recent screen aimed to identify new compounds active against NTMs, 10 hits showing strong activity against *M. avium* and *M. abscessus* were identified.[23] Among them, PIPD1 and indo-2-carboxamides were identified, thus validating previous screens. Interestingly, a benzimidazole compound, MMV687730, was also identified and was previously reported to target FtsZ in *M. tuberculosis*, thereby inhibiting the assembly of FtsZ and destabilizing the FtsZ polymer.[41,42] From a chemical point of view, MMV687730 is a trisubstituted benzimidazole that differs considerably from the structure of EJMCh-6 or the other benzimidazoles analogs assessed in this study, presumably explaining why these compounds are acting on different targets. However, one cannot exclude the possibility that, in addition to MmpL3, EJMCh-6 also targets FtsZ.

EJMCh-6 was found to be extremely active against a vast panel of clinical strains, regardless of whether they were isolated from CF or non-CF patients. The efficacy of EJMCh-6 was also independent of the morphotype and the *M. abscessus* subspecies, providing promising findings for the clinical inclusion of this compound against all members of the *M. abscessus* complex. This latter aspect is of interest because *M. abscessus* subsp. *abscessus*, subsp. *massiliense*, and subsp. *bolletii* can exhibit different drug susceptibility profiles to antibiotics.[43,44] Importantly, EJMCh-6 shows high potent activity both against extracellular and intracellular bacilli. This was further verified using the zebrafish model, displaying significant reduction in the bacterial burden and improved larval survival in a dose-dependent manner. These in vivo data warrant further investigation in preclinical mouse models. In this context, the oral administration of two MmpL3 inhibitors within the indole-2-carboxamide family has recently been shown to significantly reduce the bacterial loads in the lungs and spleen of *M. abscessus*-infected SCID mice.[26]

To date, MmpL3 appears to be one of the most promising antimycobacterial targets for subsequent therapeutic developments. Multiple chemical scaffolds have recently been shown to inhibit MmpL3 activity in *M. tuberculosis* and in *M. abscessus*, opening a new pharmacological area centered on the inhibition of mycolic acid transport.[16,17,32,45−50] In addition, several studies indicated that MmpL3 inhibitors can also act synergistically with other antitubercular drugs, which is of interest in reducing the duration of TB treatments.[51] Whether the benzimidazole analogs reported here show synergistic activity with drugs used in clinical settings for the treatment of *M. abscessus* diseases remains to be addressed.

In summary, this study further substantiates mycolic acid transport as a vulnerable site of inhibition to be further exploited for the rational design of active compounds against *M. abscessus*, acknowledged as one of the most drug-resistant mycobacterial species for which current therapeutic options remain highly challenging.[8,52] Our work has shown that benzimidazole derivatives represent a new and very promising molecular scaffold targeting MmpL3 in the *M. abscessus* complex. Of particular interest from a medicinal chemistry and drug development perspective, benzimidazole analogs are easy to prepare, allowing subsequent chemical improvements that would translate into new analogs with optimized pharmacological properties. Thus, the elucidation of the crystal structure of the MmpL3/EJMCh-6 complex and the use of functional assays[53,54] would greatly assist in guiding future structure−activity relationship studies to generate a new generation of analogs with enhanced activity.

DOI: 10.1021/acsinfecdis.9b00389
ACS Infect. Dis. 2020, 6, 324−337

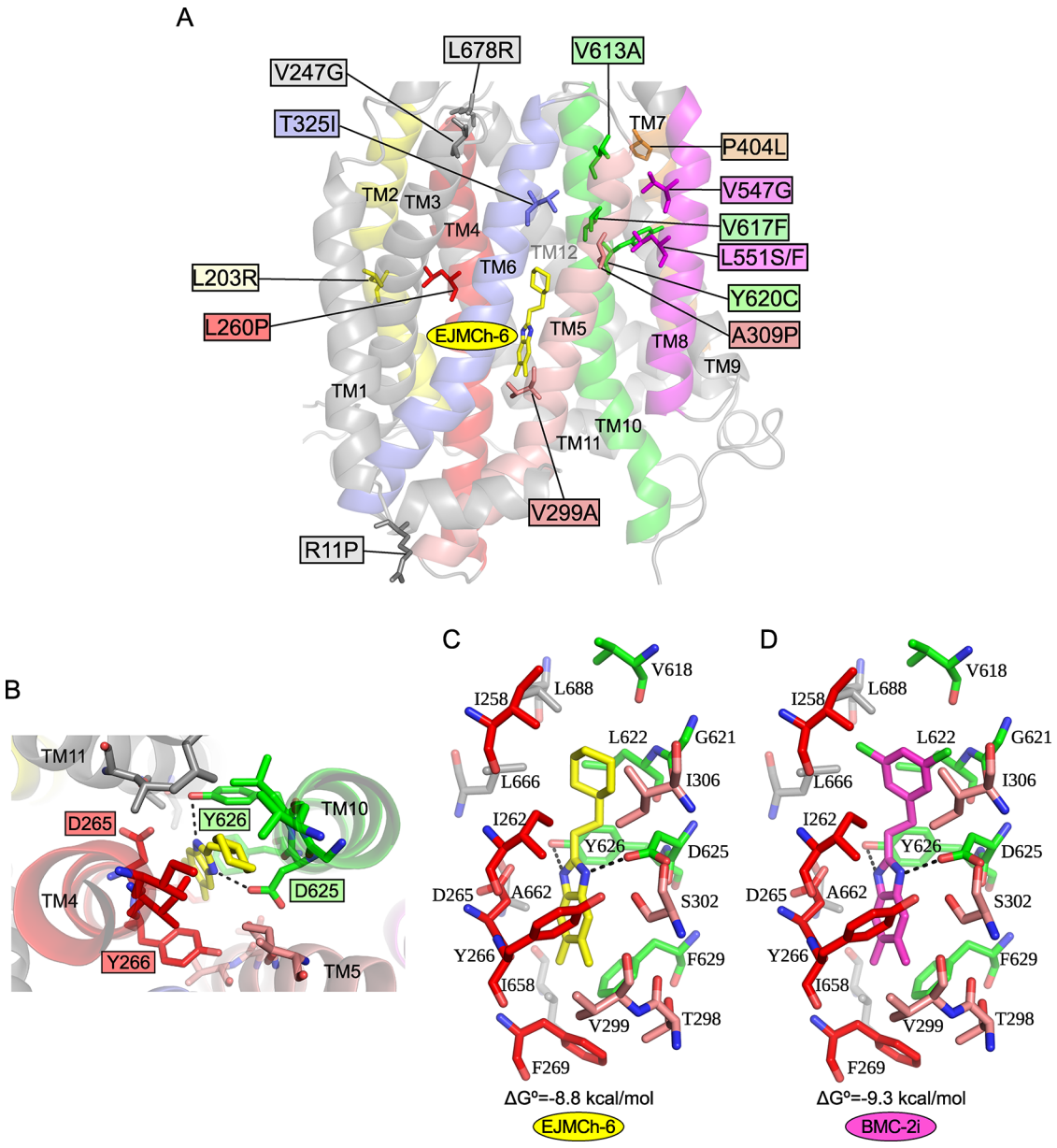

Figure 4. Mapping the EJMCh-6-resistant mutations on a MmpL3 structural model and identification of the potential drug-binding pocket. (A) Mapping of the mutations found in spontaneously resistant mutants to EJMCh-6 and BMC-2i on a *M. abscessus* MmpL3 three-dimensional homology model. Only the transmembrane helices (TMs) are shown. Mutated residues are displayed as sticks and annotated in colored boxes. All the TMs are colored gray with the exception of those carrying mutations that confer resistance to EJMCh-6/BMC-2i, notably, TM2 (yellow), TM4 (red), TM5 (salmon), TM6 (blue), TM7 (orange), TM8 (magenta), and TM10 (green). EJMCh-6 is shown as yellow sticks. Residues that are not positioned on TM but are found in spontaneously resistant mutants are shown as gray sticks. EJMCh-6 and BMC-2i were docked (only EJMCh-6 is represented in this view), as indicated in the Methods section. (B) Top view of the residues forming the proposed EJMCh-6 binding pocket. Residues and TM follow the same color code as in (A). Only the four residues proposed to be essential to MmpL3 function (D265, Y266, D625, and Y626)[33,36] are annotated in colored boxes. D625 and Y626 in TM10 are potentially interacting with EJMCh-6 by hydrogen bonds, as depicted by black dashed lines. Mapping of the potential binding sites for EJMCh-6 (yellow) (C) and BMC-2i (magenta) (D). Residues 5 Å apart from any atom in the drug are represented as mostly interacting via hydrophobic interactions, with the exception of D625 and Y626 appearing to make hydrogen bonds with the amine group of the drugs. The binding energy for the two compounds is indicated as ΔG° in kcal/mol. The color code used is the same as the one mentioned above.

CONCLUSIONS

We present here a new lead compound, EJMCh-6, which holds promise for the development of a novel therapeutic agent against *M. abscessus*. Optimal drug formulation developments are now required for direct intrapulmonary delivery via aerosol, which is particularly warranted for the treatment of lung infections in CF patients.

METHODS

Synthesis of Benzimidazole Derivatives. Compounds related to the BMC and EJMCh series were synthesized according to the method described earlier.[20,21] Cpd12 was produced as reported previously.[18] AU1235 was purchased from MedChemTronica (Sweden). All compounds were dissolved in DMSO.

DOI: 10.1021/acsinfecdis.9b00389
ACS Infect. Dis. 2020, 6, 324−337

Bacterial Strains and Growth Media. *M. abscessus*-CIP104536^T, *M. bolletii* CIP108541^T, and *M. massiliense* CIP108297^T reference strains were used along with a series of clinical isolates reported previously.[55,56] Cultures were routinely grown and maintained at 30 °C in Middlebrook 7H9 broth (BD Difco), 0.05% Tween 80 (Sigma-Aldrich), 10% oleic acid, albumin, dextrose, and catalase (OADC enrichment; BD Difco) (7H9$^{T/OADC}$) or in Middlebrook 7H10 agar (BD Difco) containing 10% OADC enrichment (7H10^{OADC}). Media were supplemented either with 500 μg/mL hygromycin for strains carrying pTEC27 (Addgene, plasmid 30182), allowing tdTomato expression, or with 200 μg/mL kanamycin when harboring pMV261 derivatives. Drug susceptibility assays were carried out with cultures grown in cation-adjusted Mueller-Hinton broth (CaMHB; Sigma-Aldrich). Strains used in this study are listed in Table S1.

Drug Susceptibility Testing. The minimal inhibitory concentrations (MICs) were determined according to the CLSI guidelines.[57] The broth microdilution method was used in CaMHB with an inoculum of 5 × 10^6 CFU/mL in an exponential growth phase. Drug dilutions (100 μL) were added to 100 μL of bacterial suspension and incubated for 3−5 days at 30 °C. MIC were recorded by visual inspection. Assays were completed in triplicate in three independent experiments.

In Vitro Growth Inhibition Assay. To follow growth inhibition kinetics, microtiter plates were set up as for MIC determination. Briefly, serial dilutions of the bacterial suspensions were plated after 0, 24, 48, and 72 h of exposure to increasing drug concentrations. Colony-forming units (CFU) were counted after 4 days of incubation at 37 °C. The results from each drug concentration are representative of at least three independent experiments.

Intramacrophage Killing Assay. THP-1 macrophages were grown in RPMI medium supplemented with 10% fetal bovine serum (Sigma-Aldrich) (RPMI^{FBS}) and incubated at 37 °C with 5% CO_2. THP-1 monocytes were differentiated in macrophages in the presence of 20 ng/mL phorbol myristate acetate in 24-well flat-bottom tissue culture microplates (10^5 cells/mL) and incubated for 48 h at 37 °C with 5% CO_2. Infection with *M. abscessus* carrying pTEC27 (MOI 2:1) was performed at 37 °C in the presence of 5% CO_2 for 2 h. Cells were carefully washed three times with 1× phosphate-buffered saline (PBS) and then incubated with RPMI^{FBS} supplemented with 250 μg/mL amikacin for 2 h to kill extracellular bacteria. Macrophages were then washed three times with PBS prior to the addition of 500 μL of RPMI^{FBS} alone (negative control) or 500 μL of RPMI^{FBS} containing EJMCh-6 or IPM. At various time points, macrophages were washed three times with PBS and lysed with 100 μL of 1% Triton X-100. A cell lysis suspension was made up to a total volume of 1 mL with PBS, and serial dilutions were plated to monitor the intracellular bacterial counts. Experiments were completed in triplicate in three independent experiments.

Immunofluorescent Staining of Infected THP-1 Macrophages with tdTomato Red Fluorescent *M. abscessus*. For microscopy-based infectivity assays, THP-1 cells were cultured on coverslips in 24-well plates at a density of 10^5 cells/mL and incubated for 48 h at 37 °C with 5% CO_2. THP-1 macrophages were infected with tdTomato expressing *M. abscessus* (MOI 2:1) for 2 h. Following infection, cells were washed, treated with amikacin to kill extracellular bacteria, and then incubated with EJMCh-6 or IPM, as described above. Fixation was performed at days 0, 2, and 3 postinfection using 4% paraformaldehyde in PBS for 20 min, and the cells were permeabilized using 0.2% Triton X-100 for 20 min. After blocking with 2% BSA in PBS supplemented with 0.2% Triton X-100 for 20 min, cells were incubated with anti-CD81 antibody (Becton Dickinson; dilution 1:1000) for 1 h and subsequently incubated with an Alexa Fluor 488-conjugated antimouse secondary antibody (Molecular Probes, Invitrogen). Cells were then stained with 1 μg/mL 4′,6-diamidino-2-phenylindole (DAPI; Becton Dickinson) for 5 min, washed with PBS, mounted onto microscope slides using Immu-mount (Calbiochem), and examined using a confocal microscope using a 63× objective (Zeiss LSM880). The average proportion of macrophages containing fewer than <5, 5−10, or >10 bacteria was quantified using Zeiss Axiovision software. Images were acquired by focusing on combined signals (CD81 in green and red fluorescent *M. abscessus*) and captured on a Zeiss Axioimager confocal microscope equipped with a 63× oil objective and processed using Zeiss Axiovision software. Quantification and scoring of the numbers of bacilli present within macrophages were performed using *ImageJ*. Equal parameters for the capture and scoring of images were consistently applied to all samples. For each condition, around 900 infected macrophages were analyzed.

Zebrafish Drug Treatment. Experiments on zebrafish were conducted according to the Comité d'Ethique pour l'Expérimentation Animale de la Région Languedoc Roussillon under the reference CEEALR36-1145. Experiments were performed using the golden mutant.[58] Embryos were obtained and maintained as described.[59] Embryo age is expressed as hours postfertilization (hpf). Red fluorescent *M. abscessus* CIP104536^T (R) expressing tdTomato was prepared and microinjected into the caudal vein (2 to 3 nL containing ∼100 bacteria/nL) in 30 hpf embryos previously dechorionated and anesthetized with tricaine, as described earlier.[60] The bacterial inoculum was checked a posteriori by injecting 2 nL in sterile PBS^T and plating on 7H10^{OADC}. Infected embryos were transferred into 24-well plates (2 embryos/well) and incubated at 28.5 °C to monitor the kinetics of infection and embryo survival. Survival curves were determined by counting dead larvae on a daily basis for up to 12 days, with the experiment concluded when uninfected embryos started to die. EJMCh-6 treatment of infected embryos and uninfected embryos (used as negative controls of toxicity) was started at 24 hpi (hours postinfection) for 5 days. The drug-containing solution was renewed daily. Bacterial loads in live embryos were determined by anesthetising embryos in tricaine as previously described, mounting on 3% (w/v) methylcellulose solution, and taking fluorescent images using a Zeiss Axio Zoom.V16 coupled with an Axiocam 503 mono (Zeiss). Fluorescence pixel count (FPC) measurements were made using the "Analyze particles" function in *ImageJ*.[60] All experiments were conducted at least three times independently.

Selection of Resistant *M. abscessus* Mutants and Target Identification. Exponentially growing *M. abscessus* CIP104536^T S or R cultures were plated on LB agar containing either 1.25 μg/mL EJMCh-6 or 2.5 to 5 μg/mL BMC-2i. After 1 week of incubation at 37 °C, individual colonies were selected, grown in CaMH broth medium, individually assessed for MIC determination, and scored for resistance to EJMCh-6, BMC-2i, and Cpd12. Identification of SNPs in the resistant strains was done by PCR amplification using MAB_4508f 5′-GGCCAC-CGTCTTTACCAATA-3′ and MAB_4508r 5′-GTGCCG-TACCTGAATGTCCT-3′ to produce a 3549 bp amplicon for full-coverage sequencing of the *MAB_4508 (mmpL3)* gene.

DOI: 10.1021/acsinfecdis.9b00389
ACS Infect. Dis. 2020, 6, 324−337

DNA Constructs. All plasmids used in this study are listed with relevant details in Table S2. The pMV261 derivatives allowing the expression of the *mmpL3* alleles (carrying the T325I, L551F, V547G, V617F, and A309P mutations) under the control of the constitutive *hsp60* promoter were reported previously.[16,18]

Homology Modeling and Docking. The three-dimensional homology model of *M. abscessus* MmpL3 (MAB_4508) was generated using the Swiss-Model server[61] and the crystal structure of *M. smegmatis* MmpL3 as a template (PDB code 6ajj). The model geometry was further optimized using the Phenix package.[62] EJMCh-6 and BMC-2i in silico docking was performed with *PyRx* software[63] running *AutoDock Vina*[64] and using the homology model of *M. abscessus* MmpL3 as a receptor and keeping all of the amino acids as rigid. Docking was carried out using the following grid parameters: center $X = 10.5$, $Y = 6.1$, and $Z = 18.2$ and dimensions (Å) $X = 16.1$, $Y = 15.3$, and $Z = 22.1$.

Statistical Analyses. Statistical analyses were performed on *Prism 5.0* (Graphpad) and detailed for each figure legend. *$P \leq 0.05$, ** $P \leq 0.01$, *** $P \leq 0.001$, and **** $P \leq 0.0001$.

■ ASSOCIATED CONTENT

Supporting Information

The Supporting Information is available free of charge at https://pubs.acs.org/doi/10.1021/acsinfecdis.9b00389.

Lists of bacterial strains and plasmids used in this study; cytotoxicity of EJMCh-6 and BMC-2i on THP-1 macrophages (PDF)

■ AUTHOR INFORMATION

Corresponding Author

*Tel: (+33) 4 34 35 94 47. E-mail: laurent.kremer@irim.cnrs.fr.

ORCID

Laurent Kremer: 0000-0002-6604-4458

Notes

The authors declare no competing financial interest.

■ ACKNOWLEDGMENTS

This study was supported by the Association Gregory Lemarchal and Vaincre la Mucoviscidose (RIF20180502320) and by the National Science Centre (Krakow, Poland) on the basis of decision number DEC-2017/25/B/NZ7/00124. M.D.J. received a postdoctoral fellowship granted by Labex EpiGenMed, an "Investissements d'avenir" program (ANR-10-LABX-12-01).

■ REFERENCES

(1) Raju, R. M., Raju, S. M., Zhao, Y., and Rubin, E. J. (2016) Leveraging Advances in Tuberculosis Diagnosis and Treatment to Address Nontuberculous Mycobacterial Disease. *Emerging Infect. Dis. 22* (3), 365−369.

(2) Park, I. K., and Olivier, K. N. (2015) Nontuberculous Mycobacteria in Cystic Fibrosis and Non-Cystic Fibrosis Bronchiectasis. *Semin. Respir. Crit. Care Med. 36* (2), 217−224.

(3) van Ingen, J., Wagner, D., Gallagher, J., Morimoto, K., Lange, C., Haworth, C. S., Floto, R. A., Adjemian, J., Prevots, D. R., and Griffith, D. E. (2017) Poor Adherence to Management Guidelines in Nontuberculous Mycobacterial Pulmonary Diseases. *Eur. Respir. J. 49* (2), 1601855.

(4) Bryant, J. M., Grogono, D. M., Rodriguez-Rincon, D., Everall, I., Brown, K. P., Moreno, P., Verma, D., Hill, E., Drijkoningen, J., Gilligan, P., Esther, C. R., Noone, P. G., Giddings, O., Bell, S. C., Thomson, R., Wainwright, C. E., Coulter, C., Pandey, S., Wood, M. E., Stockwell, R. E., Ramsay, K. A., Sherrard, L. J., Kidd, T. J., Jabbour, N., Johnson, G. R., Knibbs, L. D., Morawska, L., Sly, P. D., Jones, A., Bilton, D., Laurenson, I., Ruddy, M., Bourke, S., Bowler, I. C., Chapman, S. J., Clayton, A., Cullen, M., Daniels, T., Dempsey, O., Denton, M., Desai, M., Drew, R. J., Edenborough, F., Evans, J., Folb, J., Humphrey, H., Isalska, B., Jensen-Fangel, S., Jönsson, B., Jones, A. M., Katzenstein, T. L., Lillebaek, T., MacGregor, G., Mayell, S., Millar, M., Modha, D., Nash, E. F., O'Brien, C., O'Brien, D., Ohri, C., Pao, C. S., Peckham, D., Perrin, F., Perry, A., Pressler, T., Prtak, L., Qvist, T., Robb, A., Rodgers, H., Schaffer, K., Shafi, N., van Ingen, J., Walshaw, M., Watson, D., West, N., Whitehouse, J., Haworth, C. S., Harris, S. R., Ordway, D., Parkhill, J., and Floto, R. A. (2016) Emergence and Spread of a Human-Transmissible Multidrug-Resistant Nontuberculous Mycobacterium. *Science 354* (6313), 751−757.

(5) Catherinot, E., Roux, A.-L., Macheras, E., Hubert, D., Matmar, M., Dannhoffer, L., Chinet, T., Morand, P., Poyart, C., Heym, B., Rottman, M., Gaillard, J. L., and Herrmann, J. L. (2009) Acute Respiratory Failure Involving an R Variant of *Mycobacterium abscessus*. *J. Clin. Microbiol. 47* (1), 271−274.

(6) Esther, C. R., Esserman, D. A., Gilligan, P., Kerr, A., and Noone, P. G. (2010) Chronic *Mycobacterium abscessus* Infection and Lung Function Decline in Cystic Fibrosis. *J. Cystic Fibrosis 9* (2), 117−123.

(7) Bernut, A., Dupont, C., Ogryzko, N. V., Neyret, A., Herrmann, J.-L., Floto, R. A., Renshaw, S. A., and Kremer, L. (2019) CFTR Protects against *Mycobacterium abscessus* Infection by Fine-Tuning Host Oxidative Defenses. *Cell Rep. 26* (7), 1828−1840.

(8) Nessar, R., Cambau, E., Reyrat, J. M., Murray, A., and Gicquel, B. (2012) *Mycobacterium abscessus*: A New Antibiotic Nightmare. *J. Antimicrob. Chemother. 67* (4), 810−818.

(9) van Ingen, J., Boeree, M. J., van Soolingen, D., and Mouton, J. W. (2012) Resistance Mechanisms and Drug Susceptibility Testing of Nontuberculous Mycobacteria. *Drug Resist. Updates 15* (3), 149−161.

(10) Brown-Elliott, B. A., Nash, K. A., and Wallace, R. J. (2012) Antimicrobial Susceptibility Testing, Drug Resistance Mechanisms, and Therapy of Infections with Nontuberculous Mycobacteria. *Clin. Microbiol. Rev. 25* (3), 545−582.

(11) Lopeman, R., Harrison, J., Desai, M., and Cox, J. (2019) *Mycobacterium abscessus*: Environmental Bacterium Turned Clinical Nightmare. *Microorganisms 7* (3), 90.

(12) Luthra, S., Rominski, A., and Sander, P. The Role of Antibiotic-Target-Modifying and Antibiotic-Modifying Enzymes in *Mycobacterium abscessus* Drug Resistance. *Front. Microbiol.* 2018, *9*, DOI: 10.3389/fmicb.2018.02179.

(13) Floto, R. A., Olivier, K. N., Saiman, L., Daley, C. L., Herrmann, J.-L., Nick, J. A., Noone, P. G., Bilton, D., Corris, P., Gibson, R. L., Hempstead, S. E., Koetz, K., Sabadosa, K. A., Sermet-Gaudelus, I., Smyth, A. R., van Ingen, J., Wallace, R. J., Winthrop, K. L., Marshall, B. C., and Haworth, C. S. (2016) US Cystic Fibrosis Foundation and European Cystic Fibrosis Society Consensus Recommendations for the Management of Non-Tuberculous Mycobacteria in Individuals with Cystic Fibrosis: Executive Summary. *Thorax 71* (1), 88−90.

(14) Roux, A. L., Catherinot, E., Soismier, N., Heym, B., Bellis, G., Lemonnier, L., Chiron, R., Fauroux, B., Le Bourgeois, M., Munck, A., Pin, I., Sermet, I., Gutierrez, C., Véziris, N., Jarlier, V., Cambau, E., Herrmann, J. L., Guillemot, D., and Gaillard, J. L. (2015) OMA group. Comparing *Mycobacterium massiliense* and *Mycobacterium abscessus* Lung Infections in Cystic Fibrosis Patients. *J. Cystic Fibrosis 14* (1), 63−69.

(15) Ballell, L., Bates, R. H., Young, R. J., Alvarez-Gomez, D., Alvarez-Ruiz, E., Barroso, V., Blanco, D., Crespo, B., Escribano, J., González, R., Lozano, S., Huss, S., Santos-Villarejo, A., Martín-Plaza, J. J., Mendoza, A., Rebollo-Lopez, M. J., Remuiñan-Blanco, M., Lavandera, J. L., Pérez-Herran, E., Gamo-Benito, F. J., García-Bustos, J. F., Barros, D., Castro, J. P., and Cammack, N. (2013) Fueling Open-Source Drug Discovery: 177 Small-Molecule Leads against Tuberculosis. *ChemMedChem 8* (2), 313−321.

(16) Dupont, C., Viljoen, A., Dubar, F., Blaise, M., Bernut, A., Pawlik, A., Bouchier, C., Brosch, R., Guérardel, Y., Lelièvre, J., Ballell, L., Herrmann, J. L., Biot, C., and Kremer, L. (2016) A New Piperidinol

Derivative Targeting Mycolic Acid Transport in *Mycobacterium abscessus*. *Mol. Microbiol. 101* (3), 515−529.
(17) Lun, S., Guo, H., Onajole, O. K., Pieroni, M., Gunosewoyo, H., Chen, G., Tipparaju, S. K., Ammerman, N. C., Kozikowski, A. P., and Bishai, W. R. (2013) Indoleamides Are Active against Drug-Resistant *Mycobacterium tuberculosis*. *Nat. Commun. 4*, 2907.
(18) Kozikowski, A. P., Onajole, O. K., Stec, J., Dupont, C., Viljoen, A., Richard, M., Chaira, T., Lun, S., Bishai, W., Raj, V. S., Ordway, D., and Kremer, L. (2017) Targeting Mycolic Acid Transport by Indole-2-Carboxamides for the Treatment of *Mycobacterium abscessus* Infections. *J. Med. Chem. 60* (13), 5876−5888.
(19) Viljoen, A., Herrmann, J.-L., Onajole, O. K., Stec, J., Kozikowski, A. P., and Kremer, L. (2017) Controlling Extra- and Intramacrophagic *Mycobacterium abscessus* by Targeting Mycolic Acid Transport. *Front. Cell. Infect. Microbiol. 7*, 388.
(20) Gobis, K., Foks, H., Serocki, M., Augustynowicz-Kopeć, E., and Napiórkowska, A. (2015) Synthesis and Evaluation of *in vitro* Antimycobacterial Activity of Novel 1H-Benzo[d]Imidazole Derivatives and Analogues. *Eur. J. Med. Chem. 89*, 13−20.
(21) Gobis, K., Foks, H., Suchan, K., Augustynowicz-Kopeć, E., Napiórkowska, A., and Bojanowski, K. (2015) Novel 2-(2-Phenalkyl)-1H-Benzo[d]Imidazoles as Antitubercular Agents. Synthesis, Biological Evaluation and Structure-activity Relationship. *Bioorg. Med. Chem. 23* (9), 2112−2120.
(22) Korycka-Machała, M., Viljoen, A., Pawełczyk, J., Borówka, P., Dziadek, B., Gobis, K., Brzostek, A., Kawka, M., Blaise, M., Strapagiel, D., Kremer, L., and Dziadek, J. (2019) 1H-Benzo[d]Imidazole Derivatives Affect MmpL3 i*n Mycobacterium tuberculosis*. *Antimicrob. Agents Chemother. 63*, No. e00441-19.
(23) Low, J. L., Wu, M.-L., Aziz, D. B., Laleu, B., and Dick, T. (2017) Screening of TB Actives for Activity against Nontuberculous Mycobacteria Delivers High Hit Rates. *Front. Microbiol. 8*, 1539.
(24) Li, W., Yazidi, A., Pandya, A. N., Hegde, P., Tong, W., Calado Nogueira de Moura, V., North, E. J., Sygusch, J., and Jackson, M. (2018) MmpL3 as a Target for the Treatment of Drug-Resistant Nontuberculous Mycobacterial Infections. *Front. Microbiol. 9*, 1547.
(25) Shetty, A., Xu, Z., Lakshmanan, U., Hill, J., Choong, M. L., Chng, S.-S., Yamada, Y., Poulsen, A., Dick, T., and Gengenbacher, M. (2018) Novel Acetamide Indirectly Targets Mycobacterial Transporter MmpL3 by Proton Motive Force Disruption. *Front. Microbiol. 9*, 2960.
(26) Pandya, A. N., Prathipati, P. K., Hegde, P., Li, W., Graham, K. F., Mandal, S., Drescher, K. M., Destache, C. J., Ordway, D., Jackson, M., and North, E. L. Indole-2-Carboxamides Are Active against *Mycobacterium abscessus* in a Mouse Model of Acute Infection. *Antimicrob. Agents Chemother.* 2019, *63* (3), DOI: 10.1128/AAC.02245-18.
(27) Lefebvre, A.-L., Le Moigne, V., Bernut, A., Veckerlé, C., Compain, F., Herrmann, J.-L., Kremer, L., Arthur, M., and Mainardi, J.-L. Inhibition of the *β*-Lactamase BlaMab by Avibactam Improves the *in vitro* and in vivo Efficacy of Imipenem against *Mycobacterium abscessus*. *Antimicrob. Agents Chemother.* 2017, *61* (4), DOI: 10.1128/AAC.02440-16.
(28) Bastian, S., Veziris, N., Roux, A.-L., Brossier, F., Gaillard, J.-L., Jarlier, V., and Cambau, E. (2011) Assessment of Clarithromycin Susceptibility in Strains Belonging to the *Mycobacterium abscessus* Group by *erm(41)* and *rrl* Sequencing. *Antimicrob. Agents Chemother. 55* (2), 775−781.
(29) Bernut, A., Le Moigne, V., Lesne, T., Lutfalla, G., Herrmann, J.-L., and Kremer, L. (2014) *In vivo* Assessment of Drug Efficacy against *Mycobacterium abscessus* Using the Embryonic Zebrafish Test System. *Antimicrob. Agents Chemother. 58* (7), 4054−4063.
(30) Dubée, V., Bernut, A., Cortes, M., Lesne, T., Dorchene, D., Lefebvre, A.-L., Hugonnet, J.-E., Gutmann, L., Mainardi, J.-L., Herrmann, J.-L., Gaillard, J. L., Kremer, L., and Arthur, M. (2014) *β*-Lactamase Inhibition by Avibactam in *Mycobacterium abscessus*. *J. Antimicrob. Chemother. 70* (4), 1051−1058.
(31) Dupont, C., Viljoen, A., Thomas, S., Roquet-Banères, F., Herrmann, J.-L., Pethe, K., and Kremer, L. Bedaquiline Inhibits the ATP Synthase in *Mycobacterium abscessus* and Is Effective in Infected Zebrafish. *Antimicrob. Agents Chemother.* 2017, *61* (11), DOI: 10.1128/AAC.01225-17.
(32) Grzegorzewicz, A. E., Pham, H., Gundi, V. A. K. B., Scherman, M. S., North, E. J., Hess, T., Jones, V., Gruppo, V., Born, S. E. M., Korduláková, J., Chavadi, S. S., Morisseau, C., Lenaerts, A. J., Lee, R. E., McNeil, M. R., and Jackson, M. (2012) Inhibition of Mycolic Acid Transport across the *Mycobacterium tuberculosis* Plasma Membrane. *Nat. Chem. Biol. 8* (4), 334−341.
(33) Zhang, B., Li, J., Yang, X., Wu, L., Zhang, J., Yang, Y., Zhao, Y., Zhang, L., Yang, X., Yang, X., Cheng, X., Liu, Z., Jiang, B., Jiang, H., Guddat, L. W., Yang, H., and Rao, Z. (2019) Crystal Structures of Membrane Transporter MmpL3, an Anti-TB Drug Target. *Cell 176* (3), 636−648.
(34) Li, W., Stevens, C. M., Pandya, A. N., Darzynkiewicz, Z., Bhattarai, P., Tong, W., Gonzalez-Juarrero, M., North, E. J., Zgurskaya, H. I., and Jackson, M. (2019) Direct Inhibition of MmpL3 by Novel Antitubercular Compounds. *ACS Infect. Dis. 5*, 1001.
(35) Belardinelli, J. M., Yazidi, A., Yang, L., Fabre, L., Li, W., Jacques, B., Angala, S. K., Rouiller, I., Zgurskaya, H. I., Sygusch, J., and Jackson, M. (2016) Structure-Function Profile of MmpL3, the Essential Mycolic Acid Transporter from *Mycobacterium tuberculosis*. *ACS Infect. Dis. 2* (10), 702−713.
(36) Bernut, A., Viljoen, A., Dupont, C., Sapriel, G., Blaise, M., Bouchier, C., Brosch, R., de Chastellier, C., Herrmann, J.-L., and Kremer, L. (2016) Insights into the Smooth-to-Rough Transitioning in *Mycobacterium bolletii* Unravels a Functional Tyr Residue Conserved in All Mycobacterial MmpL Family Members. *Mol. Microbiol. 99* (5), 866−883.
(37) Domenech, P., Reed, M. B., and Barry, C. E. (2005) Contribution of the *Mycobacterium tuberculosis* MmpL Protein Family to Virulence and Drug Resistance. *Infect. Immun. 73* (6), 3492−3501.
(38) Varela, C., Rittmann, D., Singh, A., Krumbach, K., Bhatt, K., Eggeling, L., Besra, G. S., and Bhatt, A. (2012) MmpL Genes Are Associated with Mycolic Acid Metabolism in Mycobacteria and Corynebacteria. *Chem. Biol. 19* (4), 498−506.
(39) Franz, N. D., Belardinelli, J. M., Kaminski, M. A., Dunn, L. C., Calado Nogueira de Moura, V., Blaha, M. A., Truong, D. D., Li, W., Jackson, M., and North, E. J. (2017) Design, Synthesis and Evaluation of Indole-2-Carboxamides with Pan Anti-Mycobacterial Activity. *Bioorg. Med. Chem. 25* (14), 3746−3755.
(40) De Groote, M. A., Jarvis, T. C., Wong, C., Graham, J., Hoang, T., Young, C. L., Ribble, W., Day, J., Li, W., Jackson, M., Gonzalez-Juarrero, M., Sun, X., and Ochsner, U. A. (2018) Optimization and Lead Selection of Benzothiazole Amide Analogs Toward a Novel Antimycobacterial Agent. *Front. Microbiol. 9*, 2231.
(41) Kumar, K., Awasthi, D., Berger, W. T., Tonge, P. J., Slayden, R. A., and Ojima, I. (2010) Discovery of Anti-TB Agents That Target the Cell-Division Protein FtsZ. *Future Med. Chem. 2* (8), 1305−1323.
(42) Kumar, K., Awasthi, D., Lee, S.-Y., Zanardi, I., Ruzsicska, B., Knudson, S., Tonge, P. J., Slayden, R. A., and Ojima, I. (2011) Novel Trisubstituted Benzimidazoles, Targeting Mtb FtsZ, as a New Class of Antitubercular Agents. *J. Med. Chem. 54* (1), 374−381.
(43) Koh, W.-J., Jeon, K., Lee, N. Y., Kim, B.-J., Kook, Y.-H., Lee, S.-H., Park, Y. K., Kim, C. K., Shin, S. J., Huitt, G. A., Daley, C. L., and Kwon, O. J. (2011) Clinical Significance of Differentiation of *Mycobacterium massiliense* from *Mycobacterium abscessus*. *Am. J. Respir. Crit. Care Med. 183* (3), 405−410.
(44) Harada, T., Akiyama, Y., Kurashima, A., Nagai, H., Tsuyuguchi, K., Fujii, T., Yano, S., Shigeto, E., Kuraoka, T., Kajiki, A., Kobashi, Y., Kokubu, F., Sato, A., Yoshida, S., Iwamoto, T., and Saito, H. (2012) Clinical and Microbiological Differences between *Mycobacterium abscessus* and *Mycobacterium massiliense* Lung Diseases. *J. Clin. Microbiol. 50* (11), 3556−3561.
(45) La Rosa, V., Poce, G., Canseco, J. O., Buroni, S., Pasca, M. R., Biava, M., Raju, R. M., Porretta, G. C., Alfonso, S., Battilocchio, C., Javid, B., Sorrentino, F., Ioerger, T. R., Sacchettini, J. C., Manetti, F., Botta, M., De Logu, A., Rubin, E. J., and De Rossi, E. (2012) MmpL3 Is the Cellular Target of the Antitubercular Pyrrole Derivative BM212. *Antimicrob. Agents Chemother. 56* (1), 324−331.

(46) Tahlan, K., Wilson, R., Kastrinsky, D. B., Arora, K., Nair, V., Fischer, E., Barnes, S. W., Walker, J. R., Alland, D., Barry, C. E., and Boshoff, H. I. (2012) SQ109 Targets MmpL3, a Membrane Transporter of Trehalose Monomycolate Involved in Mycolic Acid Donation to the Cell Wall Core of *Mycobacterium tuberculosis*. *Antimicrob. Agents Chemother. 56* (4), 1797−1809.
(47) Rao, S. P. S., Lakshminarayana, S. B., Kondreddi, R. R., Herve, M., Camacho, L. R., Bifani, P., Kalapala, S. K., Jiricek, J., Ma, N. L., Tan, B. H., Ng, S. H., Nanjundappa, M., Ravindran, S., Seah, P. G., Thayalan, P., Lim, S. H., Lee, B. H., Goh, A., Barnes, W. S., Chen, Z., Gagaring, K., Chatterjee, A. K., Pethe, K., Kuhen, K., Walker, J., Feng, G., Babu, S., Zhang, L., Blasco, F., Beer, D., Weaver, M., Dartois, V., Glynne, R., Dick, T., Smith, P. W., Diagana, T. T., and Manjunatha, U. H. (2013) Indolcarboxamide Is a Preclinical Candidate for Treating Multidrug-Resistant Tuberculosis. *Sci. Transl. Med. 5* (214), 214ra168.
(48) Bailo, R., Bhatt, A., and Aínsa, J. A. (2015) Lipid Transport in *Mycobacterium tuberculosis* and Its Implications in Virulence and Drug Development. *Biochem. Pharmacol. 96* (3), 159−167.
(49) Foss, M. H., Pou, S., Davidson, P. M., Dunaj, J. L., Winter, R. W., Pou, S., Licon, M. H., Doh, J. K., Li, Y., Kelly, J. X., Dodean, R. A., Koop, D. R., Riscoe, M. K., and Purdy, G. E. (2016) Diphenylether-Modified 1,2-Diamines with Improved Drug Properties for Development against *Mycobacterium tuberculosis*. *ACS Infect. Dis. 2* (7), 500−508.
(50) Zheng, H., Williams, J. T., Coulson, G. B., Haiderer, E. R., and Abramovitch, R. B. (2018) HC2091 Kills *Mycobacterium tuberculosis* by Targeting the MmpL3 Mycolic Acid Transporter. *Antimicrob. Agents Chemother. 62* (7), e02459-17.
(51) Li, W., Sanchez-Hidalgo, A., Jones, V., de Moura, V. C. N., North, E. J., and Jackson, M. Synergistic Interactions of MmpL3 Inhibitors with Antitubercular Compounds *In vitro*. *Antimicrob. Agents Chemother.* 2017, *61* (4), DOI: 10.1128/AAC.02399-16.
(52) Medjahed, H., Gaillard, J.-L., and Reyrat, J.-M. (2010) *Mycobacterium abscessus*: A New Player in the Mycobacterial Field. *Trends Microbiol. 18* (3), 117−123.
(53) Xu, Z., Meshcheryakov, V. A., Poce, G., and Chng, S.-S. (2017) MmpL3 Is the Flippase for Mycolic Acids in Mycobacteria. *Proc. Natl. Acad. Sci. U. S. A. 114* (30), 7993−7998.
(54) Dupont, C., Chen, Y., Xu, Z., Roquet-Banères, F., Blaise, M., Witt, A.-K., Dubar, F., Biot, C., Guérardel, Y., Maurer, F. P., Chng, S. S., and Kremer, L. (2019) A Piperidinol-Containing Molecule Is Active against *Mycobacterium tuberculosis* by Inhibiting the Mycolic Acid Flippase Activity of MmpL3. *J. Biol. Chem. 294*, 17512−17523.
(55) Singh, S., Bouzinbi, N., Chaturvedi, V., Godreuil, S., and Kremer, L. (2014) *In vitro* Evaluation of a New Drug Combination against Clinical Isolates Belonging to the *Mycobacterium abscessus* Complex. *Clin. Microbiol. Infect. 20* (12), O1124−1127.
(56) Halloum, I., Viljoen, A., Khanna, V., Craig, D., Bouchier, C., Brosch, R., Coxon, G., and Kremer, L. Resistance to Thiacetazone Derivatives Active against *Mycobacterium abscessus* Involves Mutations in the MmpL5 Transcriptional Repressor MAB_4384. *Antimicrob. Agents Chemother.* 2017, *61* (4), DOI: 10.1128/AAC.02509-16.
(57) Woods, G. L., Brown-Elliott, B. A., Conville, P. S., Desmond, E. P., Hall, G. S., Lin, G., Pfyffer, G. E., Ridderhof, J. C., Siddiqi, S. H., and Wallace, R. J. *Susceptibility Testing of Mycobacteria, Nocardiae and Other Aerobic Actinomycetes: Approved Standard*, 2nd ed. (M24-A2); Clinical and Laboratory Standards Institute: Wayne, PA, 2011.
(58) Lamason, R. L., Mohideen, M.-A. P. K., Mest, J. R., Wong, A. C., Norton, H. L., Aros, M. C., Jurynec, M. J., Mao, X., Humphreville, V. R., Humbert, J. E., Sinha, S., Moore, J. L., Jagadeeswaran, P., Zhao, W., Ning, G., Makalowska, I., McKeigue, P. M., O'donnell, D., Kittles, R., Parra, E. J., Mangini, N. J., Grunwald, D. J., Shriver, M. D., Canfield, V. A., and Cheng, K. C. (2005) SLC24A5, a Putative Cation Exchanger, Affects Pigmentation in Zebrafish and Humans. *Science 310* (5755), 1782−1786.
(59) Bernut, A., Herrmann, J.-L., Kissa, K., Dubremetz, J.-F., Gaillard, J.-L., Lutfalla, G., and Kremer, L. (2014) *Mycobacterium abscessus* Cording Prevents Phagocytosis and Promotes Abscess Formation. *Proc. Natl. Acad. Sci. U. S. A. 111* (10), E943−952.
(60) Bernut, A., Dupont, C., Sahuquet, A., Herrmann, J.-L., Lutfalla, G., and Kremer, L. (2015) Deciphering and Imaging Pathogenesis and Cording of *Mycobacterium abscessus* in Zebrafish Embryos. *J. Visualized Exp. 103* (103), No. e53130.
(61) Waterhouse, A., Bertoni, M., Bienert, S., Studer, G., Tauriello, G., Gumienny, R., Heer, F. T., de Beer, T. A. P., Rempfer, C., Bordoli, L., Lepore, R., and Schwede, T. (2018) SWISS-MODEL: Homology Modelling of Protein Structures and Complexes. *Nucleic Acids Res. 46* (W1), W296−W303.
(62) Adams, P. D., Afonine, P. V., Bunkóczi, G., Chen, V. B., Davis, I. W., Echols, N., Headd, J. J., Hung, L.-W., Kapral, G. J., Grosse-Kunstleve, R. W., McCoy, A. J., Moriarty, N. W., Oeffner, R., Read, R. J., Richardson, D. C., Richardson, J. S., Terwilliger, T. C., and Zwart, P. H. (2010) PHENIX: A Comprehensive Python-Based System for Macromolecular Structure Solution. *Acta Crystallogr., Sect. D: Biol. Crystallogr. 66* (2), 213−221.
(63) Dallakyan, S., and Olson, A. J. (2015) Small-Molecule Library Screening by Docking with PyRx. *Methods Mol. Biol. 1263*, 243−250.
(64) Trott, O., and Olson, A. J. (2010) AutoDock Vina: Improving the Speed and Accuracy of Docking with a New Scoring Function, Efficient Optimization, and Multithreading. *J. Comput. Chem. 31* (2), 455−461.

Supporting Information

Active benzimidazole derivatives targeting the MmpL3 transporter in *Mycobacterium abscessus*

Clément Raynaud[1], Wassim Daher[1], Matt D. Johansen[1], Françoise Roquet-Banères[1], Mickael Blaise[1], Oluseye K. Onajole[3], Alan P. Kozikowski[4], Jean-Louis Herrmann[5,6], Jaroslaw Dziadek[7], Katarzyna Gobis[8], and Laurent Kremer[1,2,#]

[1]Centre National de la Recherche Scientifique UMR 9004, Institut de Recherche en Infectiologie de Montpellier (IRIM), Université de Montpellier, 1919 route de Mende, 34293, Montpellier, France.

[2]INSERM, IRIM, 34293 Montpellier, France.

[3]Department of Biological, Physical and Health Sciences, Roosevelt University, 425 S. Wabash Avenue, Chicago, IL 60605, USA.

[4]StarWise Therapeutics LLC, 2020 N Lincoln Park West, Chicago, Illinois 60614

[5]2I, UVSQ, INSERM UMR1173, Université Paris-Saclay, 2 avenue de la Source de la Bièvre - 78180 Montigny-Le-Bretonneux, France.

[6]APHP, GHU-Paris Saclay, Hôpital Raymond Poincaré, Garches, France

[7]Institute for Medical Biology, Polish Academy of Sciences, Lodowa 106, Łódź 93-232, Poland

[8]Department of Organic Chemistry, Medical University of Gdansk, 107 Gen. Hallera Ave., 80-416 Gdansk, Poland.

[#]To whom correspondence should be addressed:

Tel: (+33) 4 34 35 94 47; E-mail: laurent.kremer@irim.cnrs.fr

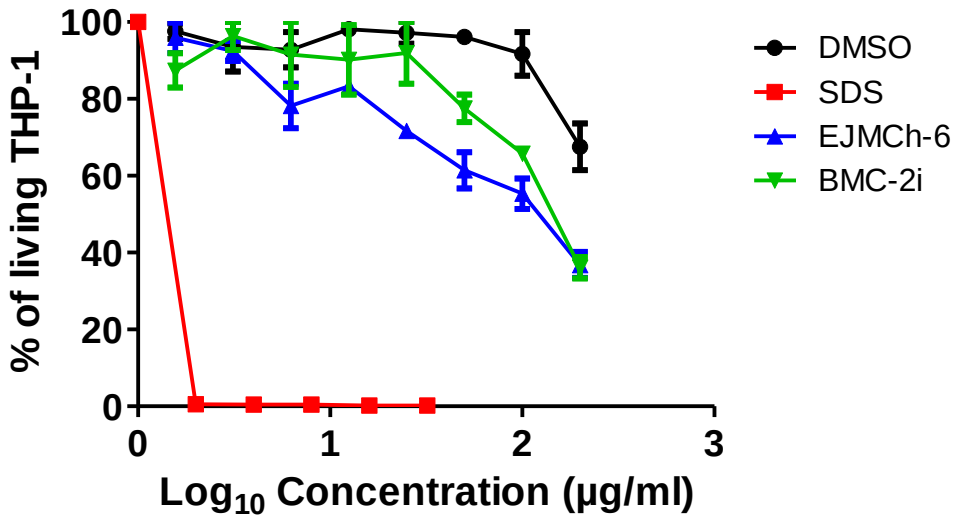

Figure S1. Cytotoxicity of EJMCh-6 and BMC-2i on THP-1 macrophages. THP-1 cells were differentiated with PMA for 48 hrs, exposed to increasing concentration of either EJMCh-6 or BMC-2i (starting at 200 µg/ml) for an additional 48 hrs at 37°C with 5% CO_2. SDS was used as a positive killing control. Results are representative of 3 independent experiments done in duplicate.

Table S1. List of bacterial strains used in this study.

Name	Description	Marker	Reference
***M. abscessus* S**	*Mabs sensu stricto*, strain CIP104536^T, smooth	_	Laboratoire de Référence des Mycobactéries
***M. abscessus* R**	*Mabs,* strain CIP104536^T, rough	_	Laboratoire de Référence des Mycobactéries
PIPD1_R1, R2, R3, R5, R6, R8 and R9, R12, R13, R14, R21	*Mabs* PIPD1-resistant mutants produced in the R variant	_	(1)
EJMCh-6^R 1 and EJMCh-6^R 3	*Mabs* EJMCh_6 resistant mutants produced in the S variant	_	This study
***M. abscessus* S pMV261**	*Mabs* S carrying the pMV261 empty vector	Kan	(1)
***M. abscessus* S pMV261-MAB_4508(WT)**	*Mabs* S carrying the pMV261-MAB_4508 vector, over-expressing MAB_4508 (MmpL3)	Kan	(1)
***M. abscessus* S pMV261-MAB_4508(T325I)**	*Mabs* S carrying the pMV261-MAB_4508 vector, over-expressing MAB_4508 (MmpL3) with a T325I mutation	Kan	(1)
***M. abscessus* S pMV261-MAB_4508(L551F)**	*Mabs* S carrying the pMV261-MAB_4508 vector, over-expressing MAB_4508 (MmpL3) with a L551F mutation	Kan	(1)
***M. abscessus* S pMV261-MAB_4508(V547G)**	*Mabs* S carrying the pMV261-MAB_4508 vector, over-expressing MAB_4508 (MmpL3) with a V547G mutation	Kan	(1)
***M. abscessus* S pMV261-MAB_4508(V617F)**	*Mabs* S carrying the pMV261-MAB_4508 vector, over-expressing MAB_4508 (MmpL3) with a V617F mutation	Kan	(1)
***M. abscessus* S pMV261-MAB_4508(A309P)**	*Mabs* S carrying the pMV261-MAB_4508 vector, over-expressing MAB_4508 (MmpL3) with a A309P mutation	Kan	(2)
***E. coli* XL1 blue**	recA1 endA1 gyrA96 thi-1 hsdR17 supE44 relA1 lac [F´ proAB lacIq ZΔM15 Tn10 (Tetr)]	TetR	Stratagene

Table S2. List of plasmids used in this study.

Name	Description	Marker	Reference
pMV261	Multi-copy *E. coli*/mycobacterial shuttle vector. Cloned genes are under the control of the constitutive *hsp60* promoter	Kan	(3)
pMV261-MAB_4508(WT)	MAB_4508 open reading frame introduced into pMV261 downstream of the hsp60 promoter.	Kan	(1)
pMV261-MAB_4508(T325I)	MAB_4508 open reading frame, with T325I mutation, introduced into pMV261 downstream of the hsp60 promoter.	Kan	(1)
pMV261-MAB_4508(L551F)	MAB_4508 open reading frame, with L551F mutation, introduced into pMV261 downstream of the hsp60 promoter.	Kan	(1)
pMV261-MAB_4508(V547G)	MAB_4508 open reading frame, with V547G mutation, introduced into pMV261 downstream of the hsp60 promoter.	Kan	(1)
pMV261-MAB_4508(V617F)	MAB_4508 open reading frame, with V617F mutation, introduced into pMV261 downstream of the hsp60 promoter.	Kan	(1)
pMV261-MAB_4508(A309P)	MAB_4508 open reading frame, with A309P mutation, introduced into pMV261 downstream of the hsp60 promoter.	Kan	(2)
pTEC27	Multi-copy *E. coli*/mycobacterial shuttle vector to express tdTomato under the control of a strong mycobacterial promoter.	Hyg	Addgene (plasmid 30182)

References

1. Dupont C, Viljoen A, Dubar F, Blaise M, Bernut A, Pawlik A, Bouchier C, Brosch R, Guérardel Y, Lelièvre J, Ballell L, Herrmann J-L, Biot C, Kremer L. 2016. A new piperidinol derivative targeting mycolic acid transport in Mycobacterium abscessus. Mol Microbiol 101:515–529.

2. Kozikowski AP, Onajole OK, Stec J, Dupont C, Viljoen A, Richard M, Chaira T, Lun S, Bishai W, Raj VS, Ordway D, Kremer L. 2017. Targeting Mycolic Acid Transport by Indole-2-carboxamides for the Treatment of Mycobacterium abscessus Infections. J Med Chem 60:5876–5888.

3. Stover CK, de la Cruz VF, Fuerst TR, Burlein JE, Benson LA, Bennett LT, Bansal GP, Young JF, Lee MH, Hatfull GF. 1991. New use of BCG for recombinant vaccines. Nature 351:456–460.

NOUVELLE

Un nouvel espoir pour traiter les infections persistantes à *Mycobacterium abscessus* ?

Clément Raynaud, Laurent Kremer

CNRS UMR 9004, Institut de Recherche en Infectiologie de Montpellier (IRIM), Université de Montpellier, 1919 route de Mende, 34293 Montpellier, France
laurent.kremer@irim.cnrs.fr

› Les bactéries du genre *Mycobacterium*, ou mycobactéries, se divisent en deux groupes principaux : les mycobactéries à croissance lente, dont font partie plusieurs espèces pathogènes strictes telles que *M. tuberculosis* ou *M. leprae*, respectivement responsables de la tuberculose et de la lèpre, et les mycobactéries à croissance rapide, qui comprennent des espèces pathogènes opportunistes telles que *M. fortuitum* ou *M. abscessus* [1]. Cette dernière est responsable d'infections cutanées ou des tissus mous, mais les principales formes sévères sont pulmonaires, notamment chez des personnes ayant des prédispositions particulières et des maladies sous-jacentes (bronchiectasie, mucoviscidose, etc.). Chez les patients atteints de mucoviscidose, les infections pulmonaires causées par des mycobactéries non tuberculeuses sont relativement fréquentes (10 à 14 % des cas), et plus de 50 % d'entre elles sont causées par le complexe *M. abscessus* [2]. Ce complexe comprend trois sous-espèces, *M. abscessus stricto sensu*, *M. bolletii* et *M. massiliense*, qui diffèrent par leur sensibilité à certains antibiotiques. Toutes trois peuvent exister sous la forme de deux morphotypes distincts : 1) le morphotype lisse, qui se caractérise par l'abondante production de lipides de surface, les glycopeptidolipides (GPL), lesquels participent à la motilité des bacilles sur un milieu gélosé et à la formation de pellicules à l'interface liquide/air, apparentées à des biofilms, et 2) le morphotype rugueux, qui se caractérise par la faible production ou l'absence de GPL à la surface des bactéries. Le caractère très hydrophobe des formes rugueuses stimule la formation d'agrégats bactériens aboutissant à la formation de cordes, très difficiles à dissocier et résistantes à la phagocytose par les macrophages et les granulocytes neutrophiles [3] (➜) ainsi qu'à de nombreux agents antiseptiques.

(➜) Voir la Nouvelle de A. Bernut *et al.*, *m/s* n° 5, mai 2014, page 499

Par ailleurs, l'infection par la forme rugueuse de ces bactéries est souvent associée à un déclin de la fonction pulmonaire chez les patients atteints de mucoviscidose [4], et cette forme est considérée comme la plus virulente dans divers modèles animaux.

Une espèce hautement résistante à de nombreux antibiotiques

M. abscessus est naturellement résistante à la plupart des familles d'antibiotiques utilisées en clinique, y compris à la quasi-totalité des agents antituberculeux, ce qui complique considérablement le traitement des infections par cette bactérie. Si la thérapie comprend généralement l'administration d'une

m/s n° 8-9, vol. 36, août-septembre 2020
https://doi.org/ 10.1051/medsci/2020138

β-lactamine (imipénème ou céfoxitine) associée à un macrolide (clarithromycine ou azithromycine) et à un aminoglycoside (amikacine) pendant plusieurs mois, le risque de rechute reste très élevé du fait d'un terrain propice à l'infection pulmonaire ou de l'induction de mécanismes de résistance aux antibiotiques.

La résistance de *M. abscessus* aux antibiotiques implique de nombreux mécanismes de résistance innée [1] : 1) une panoplie d'enzymes qui modifient l'antibiotique (acétyl-transférases, β-lactamase et ADP-ribosyl-transférase, qui inactivent les aminoglycosides, β-lactamines et rifamycines, respectivement), 2) des enzymes qui modifient la cible des antibiotiques (méthyl-transférase qui modifie la sous-unité 23S du ribosome, empêchant la fixation des macrolides), et 3) des pompes à efflux capables de transporter certains antibiotiques, comme la bédaquiline et la clofazimine, vers l'extérieur de la bactérie. A cela s'ajoutent des mutations acquises durant les périodes prolongées de traitement des patients infectés. En pratique clinique, des mutations ont notamment été observées dans les gènes *rrs* et *rrl*, codant les ARNr 16S et 23S, et impliqués respectivement dans la résistance aux aminoglycosides et aux macrolides. L'ensemble de ces mécanismes de résistance englobe toutes les classes d'antibiotiques utilisées pour traiter les infections pulmonaires à *M. abscessus*. Dès lors, il apparaît urgent de développer de nouveaux traitements, en recourant à des molécules existantes déjà utilisées contre d'autres maladies (stratégie de *drug repositioning*) ou en identifiant de nouvelles entités chimiques agissant sur de nouvelles cibles thérapeutiques.

Le transporteur d'acides mycoliques MmpL3 : une nouvelle cible d'intérêt pharmacologique

La paroi des mycobactéries regorge de lipides complexes participant à la virulence. Ils sont généralement synthétisés dans le cytoplasme et exportés à la surface du bacille par l'intermédiaire de transporteurs membranaires de la famille MmpL (*mycobacterial membrane protein large*) [5]. Les GPL, par exemple, sont transportés à travers la membrane plasmique par MmpL4a et MmpL4b, tandis que d'autres MmpL participent à l'efflux de certains antibiotiques. Les acides mycoliques sont des acides gras essentiels à très longue chaîne carbonée, qui sont synthétisés dans le cytoplasme sous la forme de tréhalose mono-mycolate (TMM). Le TMM est transporté par la protéine MmpL3 vers la mycomembrane, où il servira de substrat aux mycolyl-transférases du complexe Ag85 (*antigen 85*), soit pour être estérifié sur l'arabinane de l'arabinogalactane, soit pour servir à la synthèse de tréhalose di-mycolate (TDM), qui s'insèrera dans le feuillet externe de la mycomembrane *(Figure 1)*. Du fait de la nature essentielle du gène *mmpL3* pour la survie des mycobactéries et de l'absence de gènes orthologues chez les mammifères, de nombreuses études, réalisées tout d'abord chez *M. tuberculosis,* ont permis d'identifier plusieurs familles de composés capables

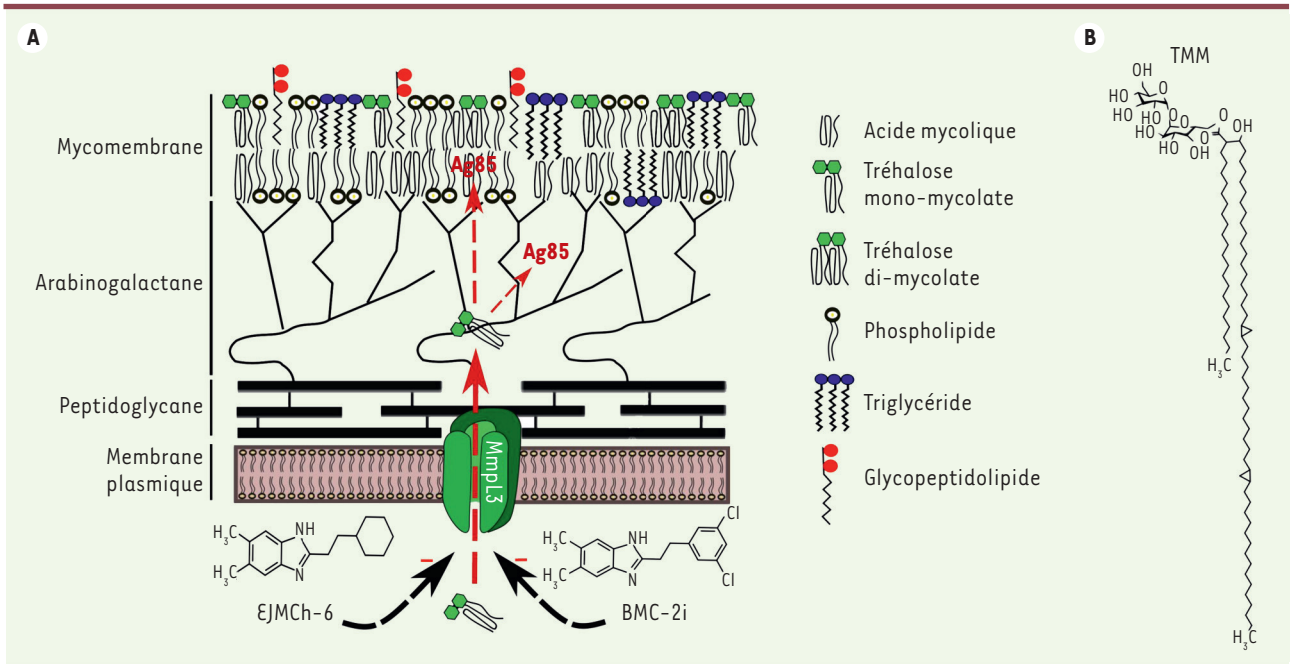

Figure 1. ***Vue schématique de la paroi de Mycobacterium abscessus et mode d'action des inhibiteurs de MmpL3. (A)*** EJMCh-6 et BMC-2i inhibent le transport du tréhalose mono-mycolate (TMM), qui sert de substrat aux protéines du complexe Ag85 pour mycolyler l'arabinogalactane ou produire du tréhalose di-mycolate (TDM), qui s'insère dans la membrane bactérienne externe. ***(B)*** Structure du TMM.

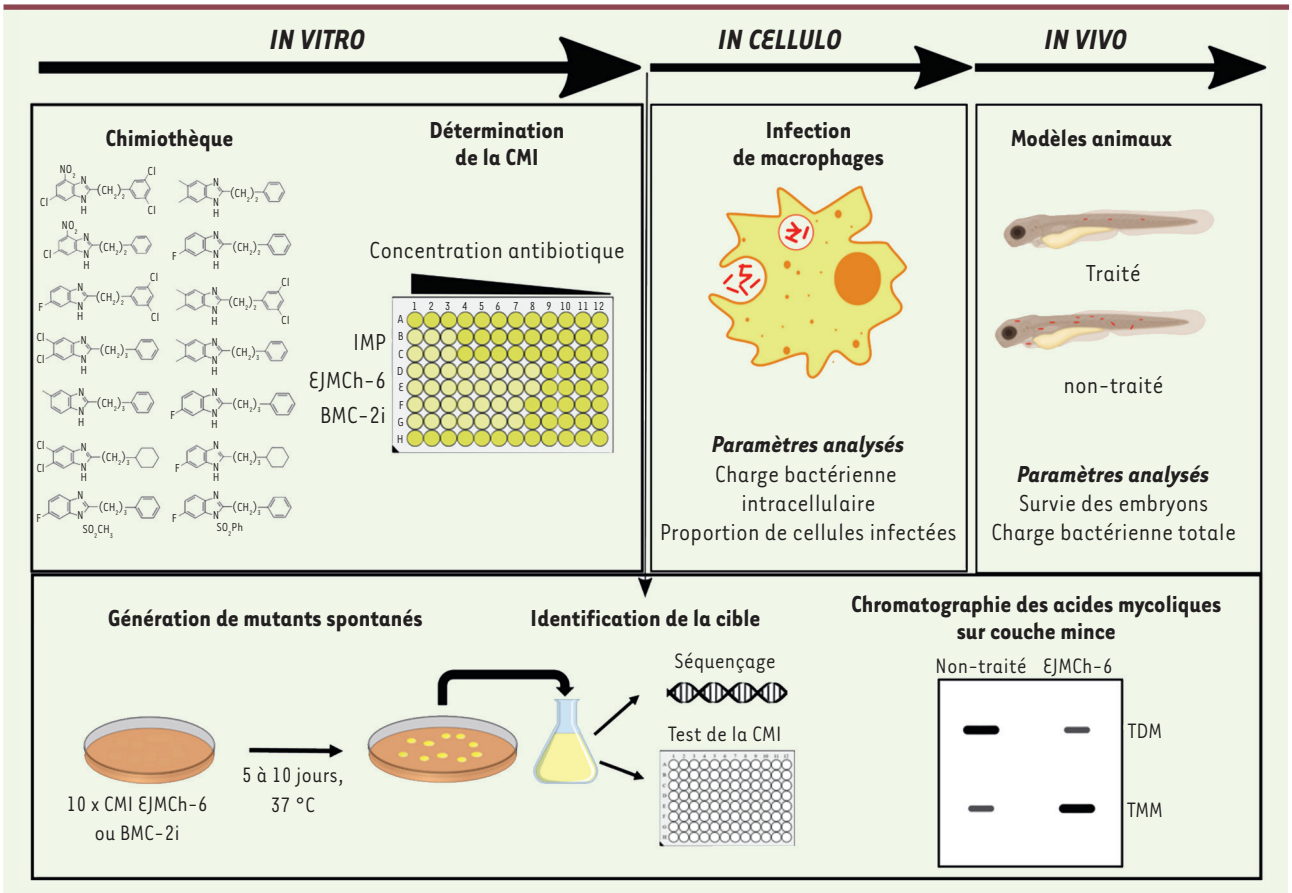

Figure 2. ***Principales étapes depuis l'identification des composés phares EJMCh-6 et BMC-2i à partir d'une « chimiothèque » de dérivés du benzimidazole jusqu'aux tests précliniques chez l'embryon du poisson-zèbre (Danio rerio).*** L'approche utilisée pour l'identification de la cible de ces composés (le transporteur d'acides mycoliques MmpL3), combinant à la fois des études génétiques et biochimiques, est également représentée. IMP, imipénème ; CMI, concentration minimale inhibitrice.

d'inhiber la translocation du TMM en bloquant l'activité flippase[1] de MmpL3. Récemment, plusieurs entités chimiques présentant une forte activité contre *M. abscessus* et inhibant MmpL3 ont été décrites, incluant des dérivés de pipéridinol [6], des indole-2-carboxamides [7] et des dérivés du benzimidazole [8].

Activité des benzimidazoles sur les formes intracellulaires et extracellulaires de *M. abscessus*

Les benzimidazoles ont d'abord été synthétisés dans le but d'inhiber la croissance de *M. tuberculosis* [9], ce qui suggérait la possibilité d'un effet comparable chez *M. abscessus*. Le criblage d'une chimiothèque de 34 dérivés du benzimidazole a permis d'identifier deux composés phares, EJMCh-6 et BMC-2i, possédant des concentrations minimales inhibitrices très basses (0,125 et 0,25 µg/mL, respectivement) vis-à-vis de la souche de référence de *M. abscessus*, CIP104536 *(Figure 2)*. EJMCh-6 montre également une très bonne activité contre un large panel d'isolats cliniques de cette bactérie, d'origines diverses, notamment issus de patients atteints de mucoviscidose. Aucune différence de susceptibilité à EJMCh-6 n'a été observée entre les morphotypes lisse et rugueux de *M. abscessus*. Par ailleurs, l'exposition à EJMCh-6 de macrophages humains infectés par cette bactérie se traduit par une très nette diminution du nombre de bactéries intracellulaires à des concentrations de ce composé pour lesquelles aucune cytotoxicité apparente n'est observée sur des macrophages sains. Enfin, l'efficacité thérapeutique du composé EJMCh-6 a été testée avec succès chez l'embryon du poisson-zèbre (*Danio rerio*) infecté par le variant rugueux de *M. abscessus*, qui est la forme la plus virulente de la bactérie dans ce modèle animal [3]. Le traitement s'accompagne d'une amélioration considérable de la survie des embryons infectés, consécutive à une nette diminution de la charge bactérienne dans les embryons *(Figure 2)*. Pour confirmer que MmpL3 est la cible de EJMCh-6 et de BMC-2i, des mutants bactériens spontanés résistants à ces deux composés ont été sélectionnés *in vitro*, et le séquençage de *mmpL3* a révélé l'existence de neuf mutations ponctuelles

[1] Les flippases sont des enzymes qui participent au maintien de l'asymétrie de la double couche lipidique de la membrane cytoplasmique en transportant des lipides d'une couche à l'autre.

distinctes chez ces mutants *(Figure 2)*. De plus, l'introduction de différents allèles de *mmpL3* renfermant ces mutations ponctuelles dans une souche sensible à EJMCh-6 confère à cette souche une résistance accrue à EJMCh-6 et BMC-2i [8]. Par ailleurs, l'analyse du profil lipidique d'une culture de *M. tuberculosis* traitée avec EJMCh-6 s'accompagne d'une diminution de la synthèse de TDM au profit d'une accumulation du TMM [9]. Ainsi, l'ensemble de ces résultats indique que EJMCh-6 inhibe la translocation du TMM en ciblant MmpL3 chez les mycobactéries.

Vers de nouveaux développements précliniques ?

Plusieurs classes d'inhibiteurs de MmpL3 ont montré une activité synergique avec des molécules utilisées en clinique, en particulier les β-lactamines, dans des tests *in vitro* [10], ce qui permettrait d'utiliser *in vivo* des doses d'antibiotique réduites et d'obtenir une activité antimycobactérienne similaire, voire meilleure que lorsque ces molécules sont utilisées individuellement. Une conséquence importante de la réduction des doses d'antibiotiques efficaces est de limiter à la fois les effets secondaires liés à une exposition prolongée à ces antibiotiques, mais aussi de prévenir l'émergence de souches résistantes. Cependant, l'activité synergique de EJMCh-6 et de BMC-2i avec d'autres antibiotiques (imipénème, céfoxitine) utilisés en clinique reste à vérifier expérimentalement.

Enfin, grâce à la structure cristallographique de la protéine MmpL3 de *M. smegmatis* publiée récemment [11], et à un modèle prédictif de celle de *M. abscessus* [8], il devient possible d'entreprendre des études de type relation structure-activité afin de produire, en lien avec des chimistes, de nouveaux dérivés de EJMCh-6 aux propriétés pharmacologiques et physicochimiques améliorées.

Une prochaine étape dans l'évaluation de ces composés consistera à évaluer leurs propriétés pharmacocinétiques et toxicologiques dans un modèle animal plus complexe que le poisson-zèbre. Depuis quelques années en effet, plusieurs modèles murins immunodéprimés ont été décrits pour étudier la physiopathologie infectieuse de *M. abscessus*. Récemment, un modèle de souris immunocompétentes, C3HeB/FeJ, propice à une infection par *M. abscessus* persistant jusqu'à 25 jours, a été rapporté et utilisé avec succès pour démontrer l'activité thérapeutique de la bédaquiline *in vivo* [12]. Les résultats très prometteurs de tous ces travaux ouvrent désormais la voie d'une alternative thérapeutique contre les infections pulmonaires à *M. abscessus*. ◊

New hopes for the treatment of persistent *Mycobacterium abscessus* infections?

REMERCIEMENTS

Ce travail a bénéficié d'une aide des associations Vaincre la mucoviscidose et Grégory Lemarchal ainsi que du programme Équipe FRM de la Fondation pour la recherche médicale.

LIENS D'INTÉRÊT

Les auteurs déclarent n'avoir aucun lien d'intérêt concernant les données publiées dans cet article.

RÉFÉRENCES

1. Johansen MD, Herrmann JL, Kremer L. Non-tuberculous mycobacteria and the rise of *Mycobacterium abscessus*. *Nat Rev Microbiol* 2020 ; https://doi.org/10.1038/s41579-020-0331-1.
2. Mougari F, Guglielmetti L, Raskine L, *et al*. Infections caused by *Mycobacterium abscessus*: epidemiology, diagnostic tools and treatment. *Exp Rev Anti-Inf Ther* 2016 ; 14 : 1139-54.
3. Bernut A, Herrmann JL, Lutfalla G, Kremer L. Les cordes mycobactériennes : un nouveau moyen d'échappement au système immunitaire ? *Med Sci (Paris)* 2014 ; 30 : 499-502.
4. Catherinot E, Roux AL, Macheras E, *et al*. Acute respiratory failure involving an R variant of *Mycobacterium abscessus*. *J Clin Microbiol* 2009 ; 47 : 271-4.
5. Chalut C. MmpL transporter-mediated export of cell-wall associated lipids and siderophores in mycobacteria. *Tuberculosis (Edinb)* 2016 ; 100 : 32-45.
6. Dupont C, Viljoen A, Dubar F, *et al.* A new piperidinol derivative targeting mycolic acid transport in *Mycobacterium abscessus*. *Mol Microbiol* 2016 ; 101 : 515-29.
7. Kozikowski A, Onajole OK, Stec J, *et al.* Targeting mycolic acid transport by indole-2-carboxamides for the treatment of *Mycobacterium abscessus* infections. *J Med Chem* 2017 ; 60 : 5876-88.
8. Raynaud C, Daher W, Johansen MD, *et al*. Active benzimidazole derivatives targeting the MmpL3 transporter in *Mycobacterium abscessus*. *ACS Inf Dis* 2020 ; 6 : 324-37.
9. Korycka-Machała M, Viljoen A, Pawełczyk J, *et al*. ^{1}H-Benzo[*d*]imidazole derivatives affect MmpL3 in *Mycobacterium tuberculosis*. *Antimicrob Agents Chemother* 2019 ; 63 : e00441-19.
10. Li W, Sanchez-Hidalgo A, Jones V, *et al*. Synergistic interactions of MmpL3 inhibitors with antitubercular compounds *in vitro*. *Antimicrob Agents Chemother* 2017 ; 61 : e02399-16.
11. Zhang B, Li J, Yang X, *et al*. Crystal structures of membrane transporter MmpL3, an anti-TB drug target. *Cell* 2019 ; 176 : 636-48.e13.
12. Le Moigne V, Raynaud C, Moreau F, *et al*. Efficacy of bedaquiline, alone or in combination with imipenem, against *Mycobacterium abscessus* in C3HeB/FeJ mice. *Antimicrob Agents Chemother* 2020 ; 64 : e00114-20.

Article 2: "Synergistic Interactions of indole-2-carboxamides and β-Lactam Antibiotics Against *Mycobacterium abscessus* "

Clément Raynaud, Wassim Daher, Françoise Roquet-Banères, Diane Ordway, Alan P. Kozikowski, Laurent Kremer, 2020, *Antimicrobial Agents and Chemotherapy* 64 (5): 1–8. https://doi.org/10.1128/AAC.02548-19. (Raynaud et al. 2020)

Les indoles-2-carboxamides sont des molécules qui appartiennent à la famille des inhibiteurs de MmpL3 et ont été décrites comme ayant une excellente activité *in vitro* et dans un modèle d'infection macrophagique contre *M. abscessus* (Kozikowski et al. 2017). L'imipénème et la céfoxitine appartiennent tous deux à la famille des β-lactamines et ont déjà leur place dans le traitement des infections à *M. abscessus.* Récemment *Li et al.* ont identifié des synergies entre des inhibiteurs de MmpL3 et des molécules anti-tuberculeuses chez *M. tuberculosis* (Li et al. 2017).

Dans ce travail, nous avons d'abord évalué les interactions entre deux inhibiteurs de MmpL3 et différents antibiotiques (IPM, CFX, sutézolide (STZ) et CFZ) en utilisant la technique de la plaque « checkerboard » en deux dimensions qui a permis de déterminer les FICI, paramètre reflétant la force des interactions entre ces différentes molécules. Des synergies ont été identifiées pour les combinaisons impliquant les inhibiteurs de MmpL3 et les β-lactamines (IPM et CFX) avec des FICI inférieurs à 0,5. Afin de confirmer ces synergies, nous avons mis en présence différentes concentrations des différentes molécules puis après 5 jours, dénombré les CFU (colony forming unit) sur milieu solide. La quantité de bactéries viables étaient bien moindre en présence des deux antibiotiques par rapport aux conditions renfermant les antibiotiques seuls.

Dans un second temps, ces combinaisons ont été testées dans un modèle d'infection de macrophages où sont déterminées les CFU intracellulaires ainsi que le nombre de cellules infectées. L'utilisation de combinaisons inhibiteur de MmpL3/β-lactamine a entraîné une forte diminution des CFU intracellulaires ainsi que du nombre de macrophages infectés par rapport aux molécules seules.

Ce travail met en exergue un effet synergique intéressant entre des inhibiteurs de MmpL3 et des β-lactamines car ce type d'effet permet de réduire les concentrations d'antibiotiques et d'augmenter leur efficacité. D'un point de vue clinique, cela permettrait de diminuer les effets indésirables observés avec certaines molécules mais également de limiter l'émergence de résistances croisées aux antibiotiques.

AMERICAN SOCIETY FOR MICROBIOLOGY | Antimicrobial Agents and Chemotherapy®

MECHANISMS OF ACTION: PHYSIOLOGICAL EFFECTS

Synergistic Interactions of Indole-2-Carboxamides and β-Lactam Antibiotics against *Mycobacterium abscessus*

Clément Raynaud,[a] Wassim Daher,[a] Françoise Roquet-Banères,[a] Matt D. Johansen,[a] Jozef Stec,[c] Oluseye K. Onajole,[d] Diane Ordway,[e] Alan P. Kozikowski,[f] Laurent Kremer[a,b]

[a]Centre National de la Recherche Scientifique UMR 9004, Institut de Recherche en Infectiologie de Montpellier (IRIM), Université de Montpellier, Montpellier, France
[b]INSERM, IRIM, Montpellier, France
[c]Department of Pharmaceutical Sciences, College of Pharmacy, Marshall B. Ketchum University, Fullerton, California, USA
[d]Department of Biological, Physical and Health Sciences, Roosevelt University, Chicago, Illinois, USA
[e]Colorado State University, Department of Microbiology, Immunology & Pathology, Mycobacteria Research Laboratory, Fort Collins, Colorado, USA
[f]StarWise Therapeutics LLC, Chicago, Illinois, USA

ABSTRACT New drugs or therapeutic combinations are urgently needed against *Mycobacterium abscessus*. Previously, we demonstrated the potent activity of indole-2-carboxamides 6 and 12 against *M. abscessus*. We show here that these compounds act synergistically with imipenem and cefoxitin *in vitro* and increase the bactericidal activity of the β-lactams against *M. abscessus*. In addition, compound 12 also displays synergism with imipenem and cefoxitin within infected macrophages. The clinical potential of these new drug combinations requires further evaluation.

KEYWORDS *Mycobacterium abscessus*, indole-2-carboxamide, β-lactam, MmpL3, drug synergism, macrophage, therapeutic activity

Mycobacterium abscessus is a fast-growing mycobacterial species found particularly frequently in patients with cystic fibrosis (CF), bronchiectasis, and chronic obstructive pulmonary diseases (COPD) (1, 2). In the context of CF and COPD, *M. abscessus* has emerged as an important opportunistic pathogen responsible for significant mortality (3). However, treatment of *M. abscessus* lung disease remains particularly challenging, largely due to intrinsic resistance of *M. abscessus* to most antibiotic classes (1, 2). The typical treatment regimen includes a combination of macrolides, aminoglycosides, and intravenous β-lactams (cefoxitin or imipenem) for at least 12 months (2). There is no reliable therapeutic strategy for the treatment of *M. abscessus* pulmonary infections, and the lengthy treatment duration and drug toxicity effects are often accompanied by severe undesirable outcomes. Thus, there is an unmet clinical need for new drug regimens with improved efficacy to treat these infections. Along with the development of repurposed drugs, the drug pipeline has recently been fueled with chemical entities acting on new targets in *M. abscessus*, such as the mycolic acid transporter MmpL3, which is inhibited by a wide range of structurally unrelated small molecules (4). Chemical inhibition of MmpL3 abolishes the export of trehalose monomycolate to the outer membrane, leading to significant bacterial growth inhibition. In *M. abscessus*, these chemotypes include a piperidinol-based compound (PIPD1) (5), benzimidazoles (6), and indole-2-carboxamide derivatives (7, 8). They exhibit high levels of activity against clinical isolates *in vitro*, in macrophages, in zebrafish, and in an acute murine model of *M. abscessus* infection (5–7, 9). Due to their pronounced role in modulating the cell wall architecture and composition, it may be speculated that chemical inhibition of MmpL3 would increase the efficacy of other drugs. Although this has been reported in *M. tuberculosis*, whereby the indole carboxamides and adamantyl-

Citation Raynaud C, Daher W, Roquet-Banères F, Johansen MD, Stec J, Onajole OK, Ordway D, Kozikowski AP, Kremer L. 2020. Synergistic interactions of indole-2-carboxamides and β-lactam antibiotics against *Mycobacterium abscessus*. Antimicrob Agents Chemother 64:e02548-19. https://doi.org/10.1128/AAC.02548-19.

Address correspondence to Laurent Kremer, laurent.kremer@irim.cnrs.fr.

Received 20 December 2019
Returned for modification 24 January 2020
Accepted 6 February 2020
Accepted manuscript posted online 10 February 2020
Published 21 April 2020

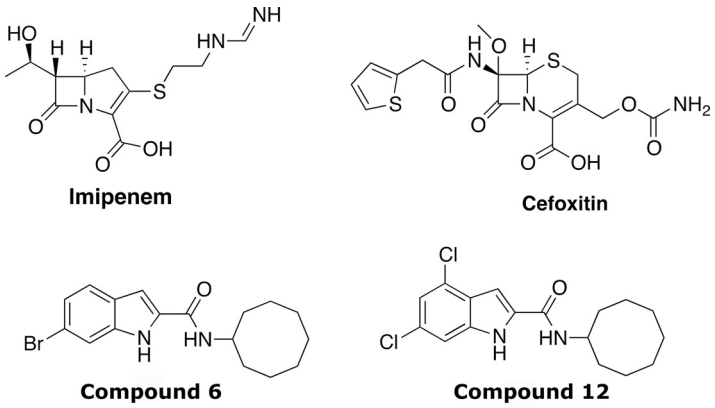

FIG 1 Structures of imipenem, cefoxitin, and the lead indole carboxamides 6 and 12 used in this study.

ureas act synergistically with rifampin, bedaquiline, clofazimine, and β-lactams (10), to date this has not been investigated in *M. abscessus*.

Indole carboxamides 6 and 12 (Fig. 1) present favorable absorption, distribution, metabolism, and excretion (ADME) properties (7, 11), and the ease of obtaining them in high yields prompted us to investigate their interaction profiles with different classes of antibiotics active against *M. abscessus* and/or used as part of clinical treatment regimens. These include sutezolid, an oxazolidinone that inhibits bacterial translation (12), clofazimine, which affects energy metabolism (13), and particularly, β-lactams (the cephalosporin cefoxitin [FOX] and the carbapenem imipenem [IPM]), which inhibit peptidoglycan biosynthesis and are reported to act in synergy with different drugs against *M. abscessus* (14, 15) (Fig. 1). The MICs were determined according to the CLSI guidelines (16) in cation-adjusted Mueller-Hinton broth (CaMHB; Sigma-Aldrich). Pair combinations between Cpd6 and Cpd12 with other drugs were tested in CaMHB in a typical checkerboard assay (17) with resazurin reduction as a metabolic readout. This allowed us to establish the fractional inhibitory concentration index (FICI) of each drug combination, where the FICI was determined using the following formula: MIC_A with B/MIC_A alone + MIC_B with A/MIC_B alone; values ≤ 0.5 were considered synergistic, those from 0.5 to 4 were considered indifferent, and those ≥ 4, antagonist (10). While Cpd12 showed a FICI value of ≤ 0.5 with IPM or FOX, indicative of synergistic interactions, no interaction (indifference) was recorded with clofazimine or sutezolid. A similar interaction profile was observed when combining these drugs with Cpd6 (Table 1).

To determine the optimal concentration of Cpd12 showing no or little activity against *M. abscessus* CIP104536^T (S variant), cultures were exposed to concentrations ranging from 0.03 to 0.125 μg/ml Cpd12 prior to CFU determination at 5 days postexposure. While at the MIC (0.125 μg/ml) there was an ~6 to 7 log drop in the CFU

TABLE 1 Interaction of Cpd6 and Cpd12 with other antibiotics against *M. abscessus* CIP104536^T (smooth strain) assessed by checkerboards REMA in CaMHB[a]

		Interaction with Cpd12			Interaction with Cpd6		
Compound	MIC (μg/ml)	FICI (mean)	SD	Outcome	FICI (mean)	SD	Outcome
Cpd12	0.125						
Cpd6	0.25						
SUT	16	0.84	±0.27	Indifferent	0.62	±0	Indifferent
IPM	16	0.5	±0.18	Synergistic	0.5	±0	Synergistic
FOX	64	0.45	±0.14	Synergistic	0.44	±0.16	Synergistic
CFZ	0.5	0.88	±0.18	Indifferent	0.88	±0.18	Indifferent

[a]Results are the mean of the FICI ± SD of 3 independent experiments. SUT, sutezolid; IPM, imipenem; FOX, cefoxitin; CFZ, clofazimine.

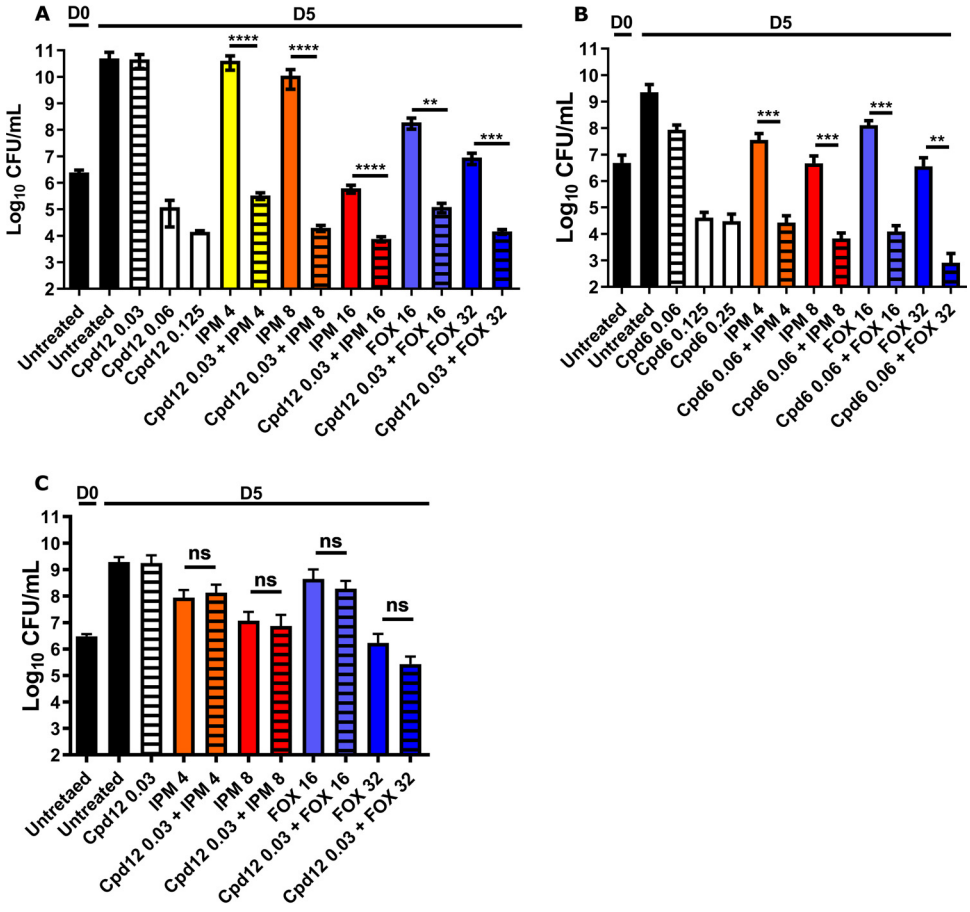

FIG 2 Synergistic activity of indole-2-carboxamide derivatives with IPM and FOX *in vitro*. CFU counts of Cpd12 (A) and Cpd6 (B) given alone and in combination with imipenem (IPM) or cefoxitin (FOX). *M. abscessus* cultures were incubated at 30°C in CaMHB for 5 days in the presence of the indicated compounds (μg/ml) and plated on LB agar prior to CFU enumeration. (C) For CFU determination, the *M. abscessus* mutant A309P (spontaneous resistant strain to Cpd12 carrying the A309P mutation in MmpL3) was exposed to the indicated antibiotics (μg/ml) at 30°C in CaMHB for 5 days. Graphs represent the mean of three independent experiments completed in triplicate. Data are expressed as the mean ± standard deviation (SD). The statistical test used is a nonparametric Mann-Whitney *t* test in which the combinations were compared to the drugs alone. ns, nonsignificant; **, $P \leq 0.01$; ***, $P \leq 0.001$.

counts, no decrease was observed at 0.03 μg/ml (Fig. 2A). This concentration was thus chosen to investigate the potential synergistic activity of Cpd12 with β-lactams. IPM was used at 4, 8, and 16 μg/ml, and FOX was used at 16 and 32 μg/ml, corresponding to concentrations 4- and 2-fold lower than their MICs, respectively (Table 1). At these sub-MIC levels, Cpd12 plus IPM decreased CFU counts by ~4 to 6 log compared to Cpd12 or IPM alone. Similarly, FOX alone at 16 and 32 μg/ml was accompanied by a reduction in the CFU counts, while the addition of 0.03 μg/ml Cpd12 further reduced the CFU by ~2 to 3 log (Fig. 2A). Comparable results were obtained when assessing the synergistic activity of Cpd6 with IPM or FOX (Fig. 2B). At 0.06 μg/ml and 0.125 μg/ml Cpd6, the CFU were reduced by ~1 and 5 log, respectively, and no further decrease in the CFU was observed at 0.25 μg/ml. The addition of 4 μg/ml or 8 μg/ml IPM to 0.06 μg/ml Cpd6 resulted in an ~3 log decrease in the CFU compared to IPM alone. Similarly, the simultaneous addition of 0.06 μg/ml Cpd6 to FOX (at 16 or 32 μg/ml) exacerbated the effect of FOX, leading to an ~4 log decrease in the CFU compared to FOX alone (Fig. 2B). To assess whether these interactions are due to the chemical inhibition of MmpL3, the CFU killing assay was repeated using a strain highly resistant to both Cpd12 and Cpd6 due to the presence of an A309P missense mutation in MmpL3 ($MIC_{Cpd12/Cpd6}$ of 32 μg/ml, [7]). Figure 2C shows that the Cpd12 plus IPM or Cpd12 plus FOX synergistic interactions were abolished, indi-

cating that inhibition of MmpL3 is necessary to establish drug synergism with the β-lactams. This confirms a previous study demonstrating that synergistic interactions between the indole carboxamides NITD-304 and NITD-349 with other clinically relevant drugs are diminished in an MmpL3 mutant of *M. tuberculosis* resistant to indole carboxamides (10).

The *M. abscessus* complex comprises three subspecies, *M. abscessus* subsp. *abscessus*, *M. abscessus* subsp. *bolletii*, and *M. abscessus* subsp. *massiliense* (18), displaying different drug susceptibility profiles. We therefore tested the activity of the Cpd12/β-lactam combinations against a panel of *M. abscessus* complex clinical isolates (19, 20) by determining the CFU counts of two *M. abscessus* subsp. *abscessus* strains (1298 and 2587), two *M. abscessus* subsp. *bolletii* strains (97 and 116), and two *M. abscessus* subsp. *massiliense* strains (120 and 122). In general, the combination of Cpd12 plus IPM or Cpd12 plus FOX resulted in significantly reduced CFU counts compared to the cultures exposed to Cpd12, IPM, or FOX alone. However, the 6 strains responded differently to each of these drug combinations (Fig. 3). Overall, CFU determination was in direct agreement with the checkerboard results and indicates that low concentrations of Cpd6 and Cpd12 improve the activity of IPM or FOX against the *M. abscessus* complex *in vitro*.

The activity of IPM and FOX alone or in combination with Cpd12 was next evaluated using THP-1 macrophages infected with *M. abscessus* CIP104536^T (S variant) carrying pTEC27, as previously described (6). Infected cells were either left untreated or exposed for 2 days to Cpd12, IPM, or FOX alone or in combination, lysed, and plated for subsequent intracellular bacterial load determination. While IPM and FOX displayed only minor effects at the concentrations tested, the addition of 0.06 μg/ml Cpd12 significantly reduced the bacterial burden by ~0.5 log (Fig. 4A). This effect was further exacerbated (1 log reduction) when 0.25 μg/ml Cpd12 was used. A microscopy-based infectivity assay reported earlier (6, 21) was subsequently used to quantify the impact of drug treatment on the percentage of infected THP-1 cells. The results confirm the pronounced reduction in the number of infected macrophages treated with Cpd12 plus IPM or Cpd12 plus FOX (~50% decrease with 0.06 μg/ml Cpd12) compared to cells treated with the drugs alone at day 2 postinfection (Fig. 4B and C). Collectively, these findings suggest that the Cpd12/IPM and Cpd12/FOX combinations are effective on intracellular *M. abscessus*.

IPM use is usually associated with improved outcome for the treatment of *M. abscessus* pulmonary disease (22), and IPM combined with other antibiotics exerts a synergistic or additive effect contributing to its success (14, 15). However, resistance to IPM is also emerging, highlighting the limiting application of IPM in the treatment of *M. abscessus* infections (23, 24). The present results highlight the therapeutic potential of the Cpd12/IPM combination against a panel of clinical *M. abscessus* complex isolates. This combination may help lower the effective dose of IPM, thus possibly limiting the emergence of IPM-resistant strains. Similarly, the use of indole carboxamides as companion drugs further reduces the effective concentrations of FOX, restricting the eventual emergence of *M. abscessus*-resistant mutants. A plausible hypothesis explaining this synergistic activity may rely on the fact that the indole carboxamides, through inhibition of mycolic acid transport at the bacterial surface, disorganize and disrupt the mycomembrane, which accelerates the penetration of the β-lactam drugs to reach their targets (the L,D-transpeptidase for IPM and the D,D-transpeptidase for FOX), leading to inhibition of peptidoglycan synthesis. Conversely, inhibition of the peptidoglycan transpeptide linkages by the β-lactams may also facilitate the access of Cpd6 or Cpd12 to their inner membrane target. However, other underlying mechanisms may be responsible for the observed synergistic effects, and further research is required.

In summary, indole-2-caboxamides represent a promising chemotype improving the activity of FOX and IPM, two recommended drugs for the treatment of *M. abscessus* pulmonary infections (2). Future studies should evaluate whether β-lactamase inhibitors (25, 26) would further improve the observed synergistic

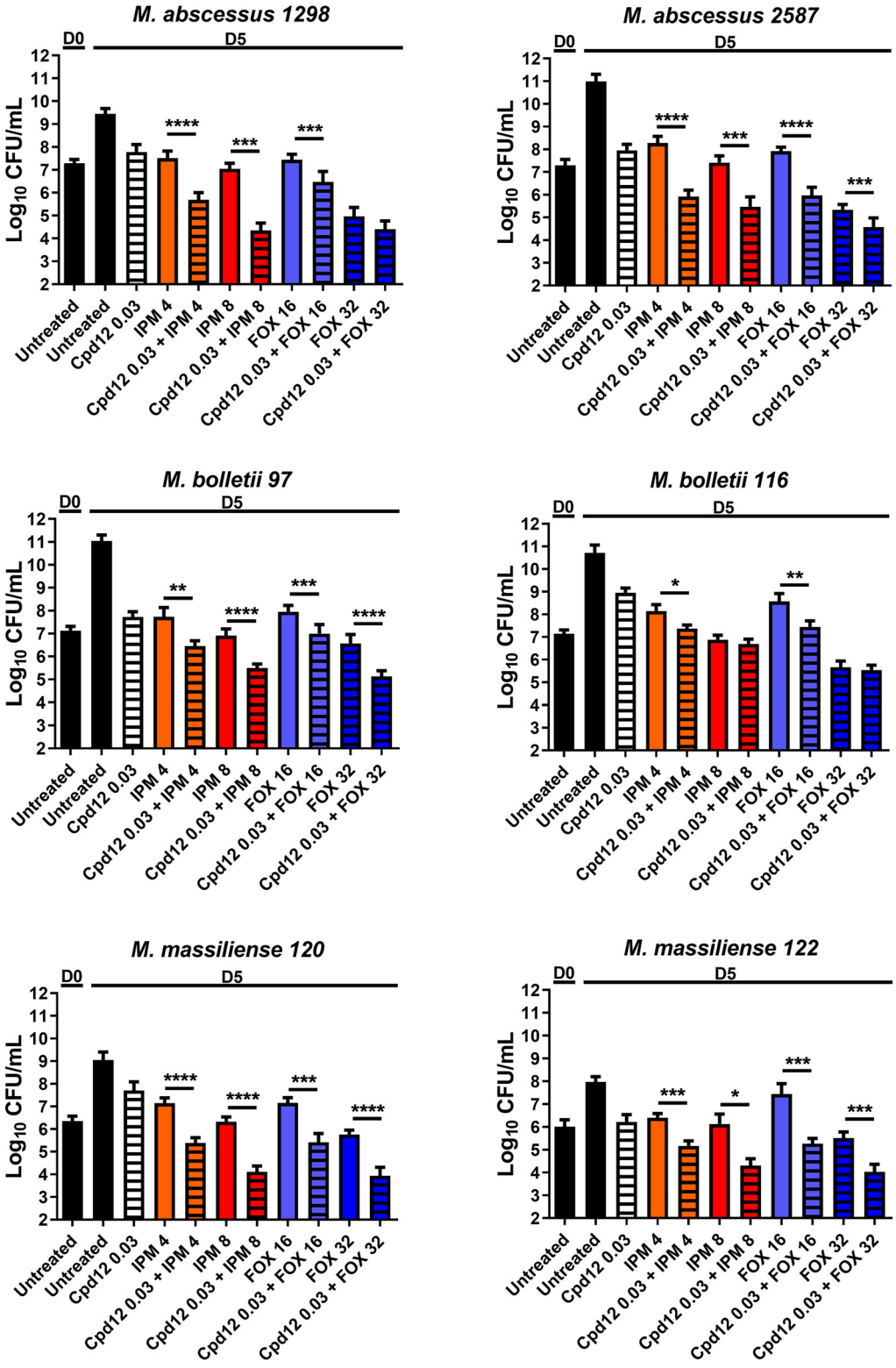

FIG 3 CFU determination of clinical isolates exposed to Cpd12 given alone or in combination with imipenem (IPM) or cefoxitin (FOX). *M. abscessus* cultures were incubated at 30°C in CaMHB for 5 days in the presence of the indicated compounds (μg/ml) and plated on LB agar prior to CFU enumeration. Data are expressed as the mean ± SD from three independent experiments completed in triplicate. The statistical test used is a nonparametric Mann-Whitney *t* test in which the combinations were compared to the drugs alone. *, $P \leq 0.05$; **, $P \leq 0.01$; ***, $P \leq 0.001$; ****, $P < 0.0001$.

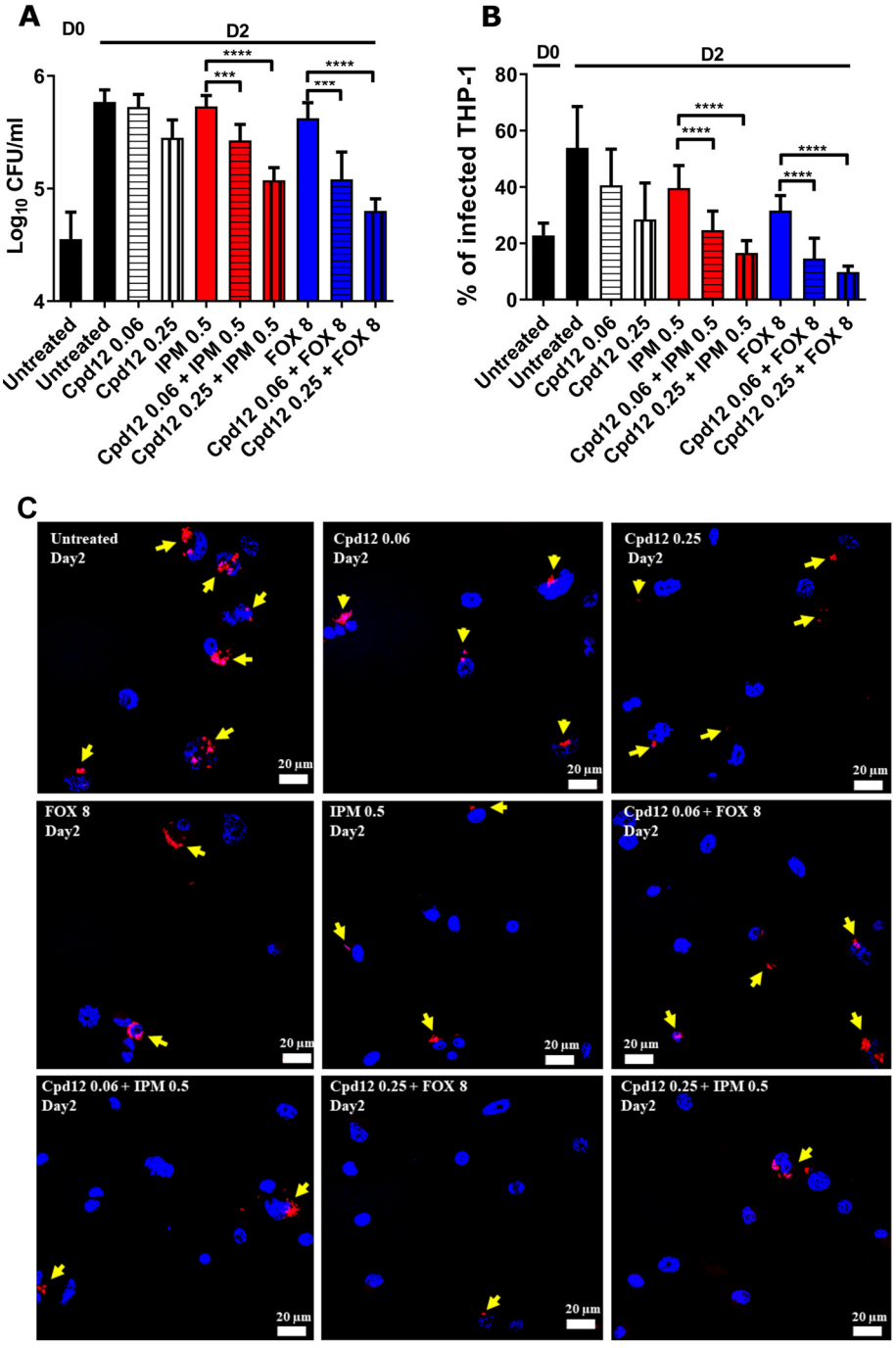

FIG 4 Impact of Cpd12 alone or in combination on intracellular-residing *M. abscessus*. THP-1 macrophages were infected with *M. abscessus* S expressing TdTomato (multiplicity of infection [MOI] of 2:1) and treated with the indicated compounds (μg/ml). (A) CFU were determined at day 0 and day 2 postinfection. Data represents the mean ± SD of three independent experiments completed in triplicate. For statistical analysis, a nonparametric Mann-Whitney *t* test was performed. ***, $P \leq 0.001$; ****, $P < 0.0001$. (B) Percentage of infected THP-1 macrophages at day 0 and day 2 postinfection. Data shown are mean values ± SD for one representative experiment completed in triplicate. One-way analysis of variance (ANOVA) Kruskal-Wallis was used as a statistical test. ****, $P < 0.0001$. (C) Immunofluorescent fields were taken at day 2 postinfection at magnification 40× (using confocal microscopy) showing the nuclei of macrophages (DAPI in blue) infected with red-fluorescent *M. abscessus* in the absence or in the presence of the drugs used alone or in combination. Yellow arrows emphasize red-fluorescent *M. abscessus* (tdTomato) within macrophages. Only intracellular bacteria that were individually observed under the microscope were recorded.

interactions. Our results indicate that the Cpd12/β-lactam combinations are highly effective within macrophages by reducing the intracellular bacterial burden and the percentage of infected cells, emphasizing the need for further evaluation in preclinical animal models.

Data availability. All data are available upon request.

ACKNOWLEDGMENTS

This study was supported by funding from the Association Gregory Lemarchal and Vaincre la Mucoviscidose (RIF20180502320) to L.K. M.D.J. received a postdoctoral fellowship granted by Labex EpiGenMed, an "Investissements d'Avenir" program (ANR-10-LABX-12-01).

The authors have no conflict of interest to declare.

REFERENCES

1. Griffith DE, Aksamit T, Brown-Elliott BA, Catanzaro A, Daley C, Gordin F, Holland SM, Horsburgh R, Huitt G, Iademarco MF, Iseman M, Olivier K, Ruoss S, von Reyn CF, Wallace RJ, Winthrop K, ATS Mycobacterial Diseases Subcommittee, American Thoracic Society, Infectious Disease Society of America. 2007. An official ATS/IDSA statement: diagnosis, treatment, and prevention of nontuberculous mycobacterial diseases. Am J Respir Crit Care Med 175:367–416. https://doi.org/10.1164/rccm.200604-571ST.
2. Floto RA, Olivier KN, Saiman L, Daley CL, Herrmann J-L, Nick JA, Noone PG, Bilton D, Corris P, Gibson RL, Hempstead SE, Koetz K, Sabadosa KA, Sermet-Gaudelus I, Smyth AR, van Ingen J, Wallace RJ, Winthrop KL, Marshall BC, Haworth CS. 2016. US Cystic Fibrosis Foundation and European Cystic Fibrosis Society consensus recommendations for the management of non-tuberculous mycobacteria in individuals with cystic fibrosis: executive summary. Thorax 71:88–90. https://doi.org/10.1136/thoraxjnl-2015-207983.
3. Brode SK, Daley CL, Marras TK. 2014. The epidemiologic relationship between tuberculosis and non-tuberculous mycobacterial disease: a systematic review. Int J Tuber Lung Dis 18:1370–1377. https://doi.org/10.5588/ijtld.14.0120.
4. Li W, Yazidi A, Pandya AN, Hegde P, Tong W, Calado Nogueira de Moura V, North EJ, Sygusch J, Jackson M. 2018. MmpL3 as a target for the treatment of drug-resistant nontuberculous mycobacterial infections. Front Microbiol 9:1547. https://doi.org/10.3389/fmicb.2018.01547.
5. Dupont C, Viljoen A, Dubar F, Blaise M, Bernut A, Pawlik A, Bouchier C, Brosch R, Guérardel Y, Lelièvre J, Ballell L, Herrmann J-L, Biot C, Kremer L. 2016. A new piperidinol derivative targeting mycolic acid transport in *Mycobacterium abscessus*. Mol Microbiol 101:515–529. https://doi.org/10.1111/mmi.13406.
6. Raynaud C, Daher W, Johansen MD, Roquet-Baneres F, Blaise M, Onajole OK, Kozikowski AP, Herrmann JL, Dziadek J, Gobis K, Kremer L. 2020. Active benzimidazole derivatives targeting the MmpL3 transporter in *Mycobacterium abscessus*. ACS Infect Dis 6:324–337. https://doi.org/10.1021/acsinfecdis.9b00389.
7. Kozikowski AP, Onajole OK, Stec J, Dupont C, Viljoen A, Richard M, Chaira T, Lun S, Bishai W, Raj VS, Ordway D, Kremer L. 2017. Targeting mycolic acid transport by indole-2-carboxamides for the treatment of *Mycobacterium abscessus* infections. J Med Chem 60:5876–5888. https://doi.org/10.1021/acs.jmedchem.7b00582.
8. Franz ND, Belardinelli JM, Kaminski MA, Dunn LC, Calado Nogueira de Moura V, Blaha MA, Truong DD, Li W, Jackson M, North EJ. 2017. Design, synthesis and evaluation of indole-2-carboxamides with pan anti-mycobacterial activity. Bioorg Med Chem 25:3746–3755. https://doi.org/10.1016/j.bmc.2017.05.015.
9. Pandya AN, Prathipati PK, Hegde P, Li W, Graham KF, Mandal S, Drescher KM, Destache CJ, Ordway D, Jackson M, North EJ. 2019. Indole-2-carboxamides are active against *Mycobacterium abscessus* in a mouse model of acute infection. Antimicrob Agents Chemother 63:e02245-18. https://doi.org/10.1128/AAC.02245-18.
10. Li W, Sanchez-Hidalgo A, Jones V, de Moura VCN, North EJ, Jackson M. 2017. Synergistic interactions of MmpL3 inhibitors with antitubercular compounds *in vitro*. Antimicrob Agents Chemother 61:e02399-16. https://doi.org/10.1128/AAC.02399-16.
11. Stec J, Onajole OK, Lun S, Guo H, Merenbloom B, Vistoli G, Bishai WR, Kozikowski AP. 2016. Indole-2-carboxamide-based MmpL3 inhibitors show exceptional antitubercular activity in an animal model of tuberculosis infection. J Med Chem 59:6232–6247. https://doi.org/10.1021/acs.jmedchem.6b00415.
12. Shaw KJ, Barbachyn MR. 2011. The oxazolidinones: past, present, and future. Ann N Y Acad Sci 1241:48–70. https://doi.org/10.1111/j.1749-6632.2011.06330.x.
13. Richard M, Gutiérrez AV, Viljoen A, Rodriguez-Rincon D, Roquet-Baneres F, Blaise M, Everall I, Parkhill J, Floto RA, Kremer L. 2018. Mutations in the MAB_2299c TetR regulator confer cross-resistance to clofazimine and bedaquiline in *Mycobacterium abscessus*. Antimicrob Agents Chemother 63:e01316-18. https://doi.org/10.1128/AAC.01316-18.
14. Miyasaka T, Kunishima H, Komatsu M, Tamai K, Mitsutake K, Kanemitsu K, Ohisa Y, Yanagisawa H, Kaku M. 2007. *In vitro* efficacy of imipenem in combination with six antimicrobial agents against *Mycobacterium abscessus*. Int J Antimicrob Agents 30:255–258. https://doi.org/10.1016/j.ijantimicag.2007.05.003.
15. Le Run E, Arthur M, Mainardi J-L. 2018. *In vitro* and intracellular activity of imipenem combined with rifabutin and avibactam against *Mycobacterium abscessus*. Antimicrob Agents Chemother 62:e00623-18. https://doi.org/10.1128/AAC.00623-18.
16. Woods GL, Brown-Elliott BA, Conville PS, Desmond EP, Hall GS, Lin G, Pfyffer GE, Ridderhof JC, Siddiqi SH, Wallace RJ. 2011. Susceptibility testing of mycobacteria, nocardiae and other aerobic actinomycetes: approved standard. 2nd ed. M24-A2. Clinical and Laboratory Standards Institute, Wayne, PA.
17. Odds FC. 2003. Synergy, antagonism, and what the chequerboard puts between them. J Antimicrob Chemother 52:1. https://doi.org/10.1093/jac/dkg301.
18. Adekambi T, Sassi M, van Ingen J, Drancourt M. 2017. Reinstating *Mycobacterium massiliense* and *Mycobacterium bolletii* as species of the *Mycobacterium abscessus* complex. Int J Syst Evol Microbiol 67:2726–2730. https://doi.org/10.1099/ijsem.0.002011.
19. Singh S, Bouzinbi N, Chaturvedi V, Godreuil S, Kremer L. 2014. *In vitro* evaluation of a new drug combination against clinical isolates belonging to the *Mycobacterium abscessus* complex. Clin Microbiol Infect 20:O1124–1127. https://doi.org/10.1111/1469-0691.12780.
20. Halloum I, Viljoen A, Khanna V, Craig D, Bouchier C, Brosch R, Coxon G, Kremer L. 2017. Resistance to thiacetazone derivatives active against *Mycobacterium abscessus* involves mutations in the MmpL5 transcriptional repressor MAB_4384. Antimicrob Agents Chemother 61:e02509-16. https://doi.org/10.1128/AAC.02509-16.
21. Viljoen A, Raynaud C, Johansen MD, Roquet-Banères F, Herrmann J-L, Daher W, Kremer L. 2019. Verapamil improves the activity of bedaquiline against *Mycobacterium abscessus in vitro* and in macrophages. Antimicrob Agents Chemother 63:e00705-19. https://doi.org/10.1128/AAC.00705-19.
22. Kwak N, Dalcolmo MP, Daley CL, Eather G, Gayoso R, Hasegawa N, Jhun BW, Koh W-J, Namkoong H, Park J, Thomson R, van Ingen J, Zweijpfenning SMH, Yim J-J. 2019. *Mycobacterium abscessus* pulmonary disease: individual patient data meta-analysis. Eur Respir J 54:1801991. https://doi.org/10.1183/13993003.01991-2018.
23. Lee M-C, Sun P-L, Wu T-L, Wang L-H, Yang C-H, Chung W-H, Kuo A-J, Liu T-P, Lu J-J, Chiu C-H, Lai H-C, Chen N-Y, Yang J-H, Wu T-S. 2017. Antimicrobial resistance in *Mycobacterium abscessus* complex isolated from patients with skin and soft tissue infections at a tertiary teaching

hospital in Taiwan. J Antimicrob Chemother 72:2782–2786. https://doi.org/10.1093/jac/dkx212.
24. Li B, Yang S, Chu H, Zhang Z, Liu W, Luo L, Ma W, Xu X. 2017. Relationship between antibiotic susceptibility and genotype in *Mycobacterium abscessus* clinical isolates. Front Microbiol 8:1739. https://doi.org/10.3389/fmicb.2017.01739.
25. Dubée V, Bernut A, Cortes M, Lesne T, Dorchene D, Lefebvre A-L, Hugonnet J-E, Gutmann L, Mainardi J-L, Herrmann J-L, Gaillard J-L, Kremer L, Arthur M. 2015. β-Lactamase inhibition by avibactam in *Mycobacterium abscessus*. J Antimicrob Chemother 70:1051–1058. https://doi.org/10.1093/jac/dku510.
26. Kaushik A, Ammerman NC, Lee J, Martins O, Kreiswirth BN, Lamichhane G, Parrish NM, Nuermberger EL. 2019. *In vitro* activity of the new β-lactamase inhibitors relebactam and vaborbactam in combination with β-lactams against *Mycobacterium abscessus* complex clinical isolates. Antimicrob Agents Chemother 63:e02623-18. https://doi.org/10.1128/AAC.02623-18.

Article 3: "Verapamil Improves the Activity of Bedaquiline Against *Mycobacterium abscessus* In Vitro and in Macrophages."

Albertus Viljoen, Clément Raynaud, Wassim Daher, Matt D. Johansen, Françoise Roquet-Banères, Jean-Louis Herrmann, Laurent Kremer, 2019, *Antimicrobial Agents and Chemotherapy* 63 (9): 1–6. https://doi.org/10.1128/AAC.00705-19. (Viljoen et al. 2019)

La BDQ est un antibiotique de la famille des diarylquinolines et sa cible est l'ATP synthase. Son utilisation en clinique est surtout réservée au traitement des infections par des souches de *M. tuberculosis* multi-résistantes aux antibiotiques. Le VER, une molécule utilisée pour traiter des maladies cardiaques, a été utilisée pour potentialiser l'activité de la BDQ car il est également connu pour inhiber les pompes à efflux (Chen et al. 2018). Des études ont montré qu'il était capable d'améliorer l'activité de la BDQ contre *M. tuberculosis in vitro* (Gupta et al. 2014), et ces résultats ont été confirmés *in vivo* dans un modèle souris BALB/c (Gupta et al. 2015). Récemment, notre équipe a montré l'efficacité de la BDQ contre *M. abscessus in vitro* contre les souches de référence ainsi que des isolats cliniques et *in vivo* dans un modèle d'infection de zebrafish. Le gène *atpE* a également été identifié comme cible de la bédaquiline chez *M. abscessus* (Dupont et al. 2017).

Toutes ces études nous ont conduit à tester l'efficacité de l'association BDQ/VER contre *M. abscessus*. Tout d'abord, la CMI de la BDQ a été déterminée contre la souche de référence avec et sans vérapamil et une forte diminution de la concentration minimale inhibitrice (CMI) a été observée en présence du vérapamil. Dans un second temps, la même expérience a été réalisée avec des isolats cliniques et a permis de mettre en évidence une diminution de la CMI contre toutes les souches cliniques testées. Cette association a également été testée vis-à-vis de plusieurs mutants résistant (*ΔMAB_2299)* ou plus sensible (*ΔMAB_2299ΔMAB_2300-2301)* à la BDQ (Richard et al. 2019). Les résultats ont montré que le mutant *ΔMAB_2299* était moins résistant à la BDQ en présence de VER et que le mutant *ΔMAB_2299ΔMAB_2300-2301* présentait une sensibilité accrue à la BDQ en présence de VER. Enfin cette combinaison a été testée dans un modèle d'infection de macrophages. Nos résultats ont montré qu'en présence de VER la BDQ possédait une activité augmentée contre *M. abscessus,* à la fois en termes de charge bactérienne intracellulaire et au regard du nombre de cellules infectées**.** Dans cette étude, je me suis principalement focalisé sur la partie infection de macrophages.

AMERICAN SOCIETY FOR MICROBIOLOGY | Antimicrobial Agents and Chemotherapy®

Verapamil Improves the Activity of Bedaquiline against *Mycobacterium abscessus In Vitro* and in Macrophages

Albertus Viljoen,[a]* Clément Raynaud,[a] Matt D. Johansen,[a] Françoise Roquet-Banères,[a] Jean-Louis Herrmann,[b] Wassim Daher,[a,c] Laurent Kremer[a,c]

[a]Institut de Recherche en Infectiologie de Montpellier, Université de Montpellier, CNRS UMR 9004, Montpellier, France
[b]2I, INSERM, UVSQ, Université Paris-Saclay, Versailles, France
[c]INSERM, IRIM, Montpellier, France

ABSTRACT Due to intrinsic multidrug resistance, pulmonary infections with *Mycobacterium abscessus* are extremely difficult to treat. Previously, we demonstrated that bedaquiline is highly effective against *Mycobacterium abscessus* both *in vitro* and *in vivo*. Here, we report that verapamil improves the efficacy of bedaquiline activity against *M. abscessus* clinical isolates and low-level resistant strains, both *in vitro* and in macrophages. Verapamil may have clinical potential as adjunctive therapy provided that sufficiently high doses can be safely achieved.

KEYWORDS ATP synthase, MmpL, *Mycobacterium abscessus*, bedaquiline, drug resistance, efflux pump, verapamil

The *Mycobacterium abscessus* complex, comprising three subspecies, *M. abscessus sensu stricto*, *M. bolletii*, and *M. massiliense* (1, 2), represents the most important cause of pulmonary infections by rapidly growing nontuberculous mycobacteria (NTM) in patients with chronic lung diseases, such as bronchiectasis and cystic fibrosis (CF) (3, 4). Chronic *M. abscessus* infection in these patients correlates with greater rates of pulmonary function decline compared to patients without NTM infections (5, 6). Moreover, pulmonary infections with *M. abscessus* remain extremely difficult to treat, with a cure rate of only 25 to 58% (7, 8). In addition, prolonged treatment regimes not only induce severe side effects in patients but also cause a high economic burden to society (9).

Clofazimine (CFZ) and bedaquiline (BDQ) are currently being evaluated in clinical trials against *M. abscessus* pulmonary infections as repositioned drugs with gaining interest. BDQ is a diarylquinoline approved by the U.S. Food and Drug Administration and the European Medicines Agency for the treatment of multidrug-resistant tuberculosis (10). We and others have recently shown that BDQ exhibits very low MIC values against NTM, including clinical *M. abscessus* strains from CF and non-CF patients (11–13). To determine the cooperative potential of BDQ with companion drugs for new treatment regimens against *M. abscessus*, evaluation of combinations of BDQ and other antimicrobials in synergism is necessary. In this context, we tested whether verapamil (VER), a cationic amphiphilic membrane stress inducer, previously shown to potentiate the effect of BDQ in *M. tuberculosis* (14, 15), increases the efficacy of BDQ in *M. abscessus*.

On Middlebrook 7H10 agar supplemented with oleic acid-albumin-dextrose-catalase (OADC) enrichment (7H10^{OADC}), VER alone at 50 μg/ml did not impact on *M. abscessus* growth but clearly augmented growth inhibition by BDQ, although it did not for CFZ (Fig. 1A). A similar augmentative effect was not observed with the efflux inhibitor, reserpine (Fig. 1A). These results were reproduced in cation-adjusted Mueller-Hinton broth, the CLSI-recommended medium for antimicrobial testing against NTM (16)

Citation Viljoen A, Raynaud C, Johansen MD, Roquet-Banères F, Herrmann J-L, Daher W, Kremer L. 2019. Verapamil improves the activity of bedaquiline against *Mycobacterium abscessus in vitro* and in macrophages. Antimicrob Agents Chemother 63:e00705-19. https://doi.org/10.1128/AAC.00705-19.

Address correspondence to Laurent Kremer, laurent.kremer@irim.cnrs.fr.

* Present address: Albertus Viljoen, Louvain Institute of Biomolecular Science and Technology, Université Catholique de Louvain, Croix du Sud, Louvain-la-Neuve, Belgium.

Received 2 April 2019
Returned for modification 23 April 2019
Accepted 10 June 2019
Accepted manuscript posted online 17 June 2019
Published 23 August 2019

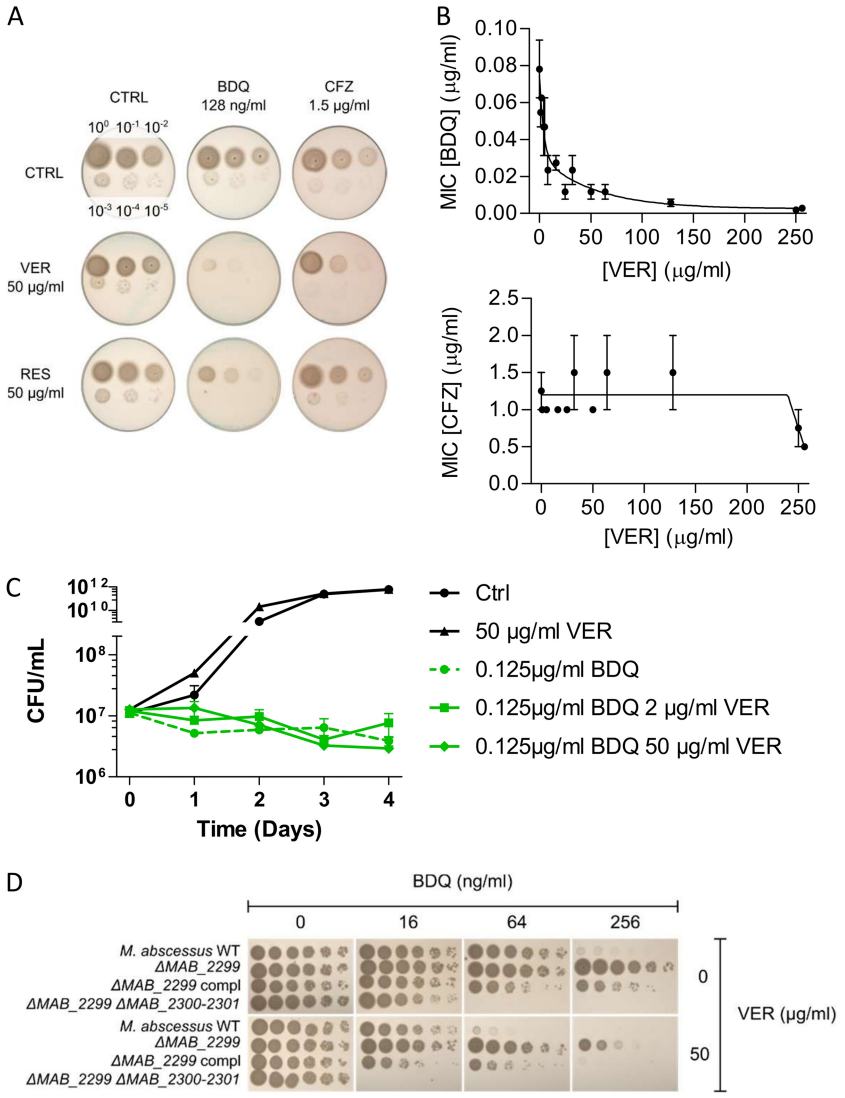

FIG 1 VER potentiates the *in vitro* efficacy of BDQ against *M. abscessus*. (A) Assessment of BDQ and clofazimine (CFZ) MICs against *M. abscessus* in the presence of verapamil (VER) or reserpine (RES) in 7H10^{OADC} agar medium. An exponential-phase culture of *M. abscessus* CIP104536^{T} (smooth variant) was serially 10-fold diluted, and 5-μl volumes of each dilution were spotted onto the agar plates, which were then incubated at 37°C for 4 days before pictures were taken. (B) Line graph showing a hyperbolic decrease in BDQ MIC as the VER concentration is increased (top panel). No decrease in CFZ MIC against *M. abscessus* is observed by addition of increasing concentrations of VER (bottom panel). These MIC determinations were done in cation-adjusted Mueller-Hinton broth at 30°C. Symbols and error bars represent means and standard errors of the mean calculated from at least two independent experiments. (C) Growth kinetics of *M. abscessus* in cation-adjusted Mueller-Hinton broth containing (or not) 0.125 μg/ml BDQ, as well as 0, 2, or 50 μg/ml VER. (D) Assessment in the presence of VER of BDQ MICs against *M. abscessus* mutants that overexpress (Δ*MAB_2299c*) or lack the MAB_2300-MAB_2301 BDQ-efflux pump (Δ*MAB_2299c* Δ*MAB_2300-2301*). An exponential-phase culture of each strain was serially 10-fold diluted, and 5-μl volumes of each dilution were spotted onto the agar plates, which were then incubated at 37°C for 4 days before pictures were taken.

(Fig. 1B). Moreover, varying the concentration of BDQ over that of VER showed a hyperbolic relationship between the MIC of BDQ and the concentration of VER that was suggestive of a strong synergistic effect between the two compounds (Fig. 1B, upper panel). Importantly, high concentrations of up to 250 μg/ml VER did not affect *M. abscessus* growth (data not shown), while concentrations as low as 2 to 4 μg/ml resulted in an ~2-fold decrease in the BDQ MIC (Fig. 1B, upper panel). In the context of well documented toxicity of VER (17, 18), the maximal range of systemic verapamil concentrations that have been achieved in the clinic by rapid continuous intravenous

TABLE 1 MICs of BDQ in cation-adjusted Mueller-Hinton broth at 30°C without verapamil (0 VER) or with 50 μg/ml verapamil (50 VER) for 17 clinical isolates from CF and non-CF patients belonging to the *M. abscessus* complex[a]

			BDQ MIC (ng/ml)				
			Replicate 1		Replicate 2		
Isolate	Morphotype	Source	0 VER	50 VER	0 VER	50 VER	Fold change
M. abscessus							
CIP104536^T	S	Non-CF	64	16	64	8	4–8
1298	S	CF	64	8	32	8	4–8
2069	S	Non-CF	64	8	64	8	8
3321	S	Non-CF	32	8	32	8	4
2587	S	CF	32	8	32	4	4–8
2648	R	CF	64	8	32	4	8
2524	R	CF	64	8	128	16	8
3022	R	Non-CF	128	64	64	16	2–4
M. massiliense							
210	R	CF	64	16	64	16	4
179	R	CF	64	8	64	8	8
140	S	CF	64	8	64	8	8
185	S	CF	128	16	128	16	8
M. bolletii							
114	S	CF	128	16	128	16	8
116	S	CF	32	4	32	4	8
17	S	Non-CF	32	4	32	4	8
112	R	CF	64	4	64	4	16
19	R	Non-CF	32	4	64	16	4–8
108	R	CF	32	8	32	8	4

[a]The fold change in BDQ MIC in the presence of verapamil compared to in its absence is shown. The experiment was completed in duplicate, with technical replicates included in each experiment. Morphotype: R, resistant; S, susceptible.

infusion without major toxicity is in the order of 2 μg/ml (19). To investigate whether VER and BDQ in combination exert a bacteriostatic or bactericidal activity against *M. abscessus*, we determined the growth kinetics of the bacteria in the presence of BDQ at 1× MIC (0.125 μg/ml) in the presence of VER. As shown in Fig. 1C, VER at 50 μg/ml failed to exert an additive bactericidal effect along with BDQ against *M. abscessus* (Fig. 1C).

Next, we tested the potency of the VER/BDQ combination against a wide range of *M. abscessus* clinical isolates, including isolates from all three *M. abscessus* subspecies, and obtained from both non-CF and CF patients. As shown in Table 1, VER drastically improved the efficacy of BDQ against all isolates tested, with an improvement of the BDQ MIC in the presence of VER ranging between 4- and 8-fold. These results are in line with previous studies demonstrating that VER decreases the MIC of BDQ against *M. tuberculosis in vitro* (14, 15, 20). However, the addition of VER to the medium failed to change the MIC of the clinically used drugs amikacin, imipenem, or cefoxitin (see Table S1 in the supplemental material). This highlights the specificity of VER in potentiating the effect of BDQ and indicates that VER has no beneficial value when combined with other *M. abscessus* drugs.

We recently identified a TetR repressor, MAB_2299c, responsible for low-level resistance to BDQ and CFZ in *M. abscessus* (21). Loss-of-function mutations or targeted deletion of *MAB_2299c* led to overexpression of the *MAB_2300-MAB_2301*-encoded MmpS-MmpL efflux pump system. This resulted in the exclusion of BDQ and CFZ and, hence, a low level of resistance toward these antibiotics. On the other hand, targeted deletion of *MAB_2300-MAB_2301* led to a 4-fold decrease in the already low MIC of BDQ against *M. abscessus*, implicating the MAB_2300-MAB_2301 efflux pump in intrinsic resistance to BDQ. We exploited these strains (Table S2) to address whether VER's potentiating action in BDQ sensitivity is dependent upon the BDQ efflux mechanism encoded by *MAB_2300-MAB_2301*. As shown in Fig. 1D and Table 2, VER still exerted a

TABLE 2 MICs of BDQ in 7H10^{OADC} agar at 37°C without verapamil (0 VER) or with 50 μg/ml (50 VER) or 250 μg/ml (250 VER) verapamil against genetically modified *M. abscessus* strains either overexpressing the *MAB_2300-2301*-encoded MmpS-MmpL efflux pump (Δ*MAB_2299c* deletion mutant or CFZ-R6 carrying a point mutation in *MAB_2299c*) or in which the gene set has been deleted (Δ*MAB_2299c* Δ*MAB_2300-2301*)[a]

Strain	BDQ MIC (ng/ml)				
	0 VER	50 VER	Fold change (50 VER)	250 VER	Fold change (250 VER)
Wild type	256	64	4	16	16
Δ*MAB_2299c*	512	256	2	64	8
Δ*MAB_2299c* Compl	256	64	4	32	8
Δ*MAB_2299c* Δ*MAB_2300-2301*	32	8	4	4	8
CFZ-R6	512	256	2	64	8

[a]The fold change values shown represent the BDQ MIC in the presence of verapamil (for 50 VER and 250 VER each) compared to in its absence. Data shown are representative of three independent experiments. 7H10^{OADC}, Middlebrook 7H10 supplemented with OADC.

potentiating effect on BDQ sensitivity in strains that normally exhibit low-level resistance to BDQ due to MAB_2300-MAB_2301 overexpression (Δ*MAB_2299c* and CFZ-R6), as well as in a BDQ-hypersensitive strain lacking both *MAB_2299c* and MAB_2300-MAB_2301 (Δ*MAB_2299c* Δ*MAB_2300-2301*). These results indicate that the VER/BDQ combination may be successful in mitigating low-level BDQ resistance. Moreover, the latter strain became extremely susceptible to BDQ/VER exposure (BDQ MIC of 4 to 8 ng/ml), apparently excluding this efflux pump as a target of VER. That VER augments the activity of BDQ in *M. tuberculosis* through its deleterious effect on membrane energetics, rather than by directly inhibiting efflux, was recently reported (22). However, VER at 50 μg/ml did not increase the sensitivity toward BDQ of *M. abscessus* AtpE target mutants (*atpE* with a mutation at D29V [*atpE*^{D29V}] and *atpE*^{A64P}), expressing high-level resistance to BDQ (13) (Fig. S1), consistent with previous work in *M. tuberculosis* (23).

To further demonstrate the potential of VER to improve BDQ treatment outcomes during infection, we assayed the VER/BDQ combination in a THP-1 macrophage infection model. The cytotoxicity of VER was first examined using a procedure described elsewhere (24). As can be seen in Fig. 2A, VER exhibited a relatively low level of toxicity against differentiated THP-1 macrophages, with a 50% inhibitory concentration (IC_{50}) of 42 μg/ml. We thus decided to fix the concentration of VER to one-half the IC_{50} in BDQ/VER cotreatment experiments against *M. abscessus*-infected macrophages. Cells were infected with *M. abscessus* (multiplicity of infection [MOI] of 2:1) at 37°C in 5% CO_2 for 2 h, followed by three gentle washes with phosphate-buffered saline (PBS) and an incubation with fetal bovine serum-supplemented RPMI (Gibco) medium (RPMI^{FBS}) containing 250 μg/ml amikacin for 2 h to kill remaining extracellular bacteria, prior to the addition of RPMI^{FBS} alone (negative control) or containing increasing concentrations of BDQ alone or in combination with 20 μg/ml VER. At 2 days postinfection, macrophages were extensively washed with PBS and lysed with 1% (vol/vol) Triton X-100, and serial dilutions were plated to monitor the intracellular viable bacterial units. As shown in Fig. 2B, after 2 days of treatment, VER significantly restricted intracellular growth of *M. abscessus* at 0.06 and 0.25 μg/ml BDQ. Furthermore, to determine the percentage of infected macrophages, cells were infected with tdTomato-expressing *M. abscessus* (25) (MOI of 2:1) prior to treatment with medium containing increasing concentrations of BDQ alone or in combination with 20 μg/ml VER. Fixation was performed using 4% paraformaldehyde in PBS for 20 min, and samples were examined using a confocal microscope (63× objective; Zeiss, LSM880). For each condition, hundreds of macrophages were counted to determine the percentage of infected cells. A pronounced reduction in the number of infected THP-1 cells treated with increasing concentrations of BDQ at 2 days postinfection compared to untreated controls was observed, and this effect was further exacerbated by the addition of 20 μg/ml VER, particularly in the presence of low BDQ doses (0.06 and 0.25 μg/ml) (Fig. 2C). These results are in agreement with previous reports on potentiation of BDQ activity against *M. tuberculosis* by VER in macrophages and in the mouse model of infection (15, 20, 26).

In summary, we illustrated, for the first time, the potential of a membrane stress

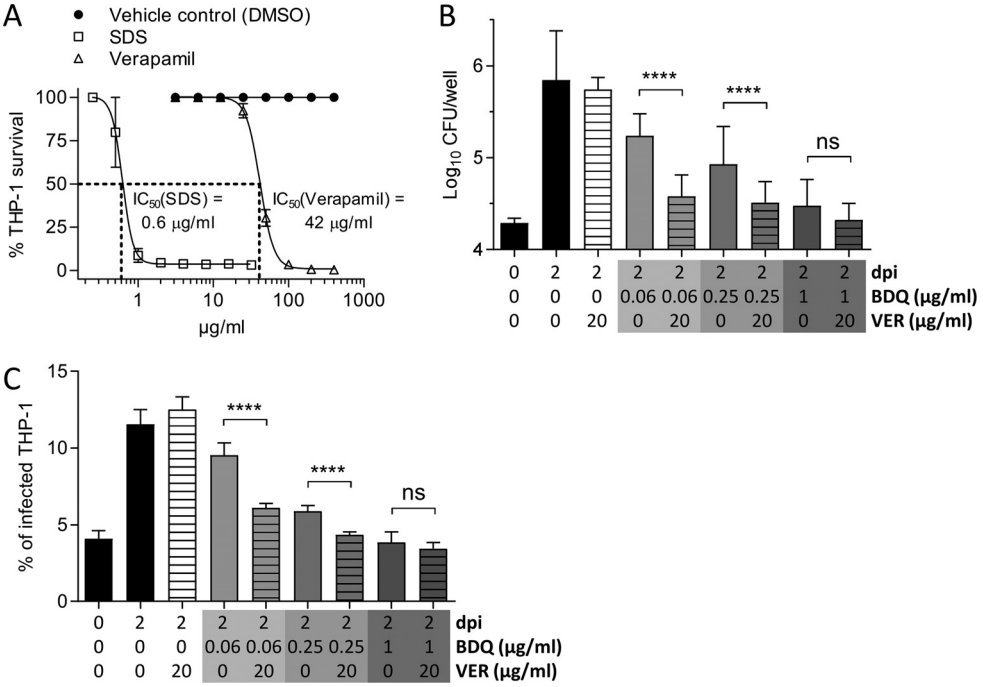

FIG 2 Augmentation by VER of BDQ activity against *M. abscessus* in macrophages. (A) Cytotoxicity assay of VER toward THP-1 macrophages. SDS was included as a control compound that is known to be toxic to the cells at low concentrations. (B) *M. abscessus*-infected THP-1 macrophages were treated with different concentrations of BDQ without or with 20 μg/ml VER and incubated for 2 days before they were lysed, the lysates were plated, and CFU enumerations were performed. Histograms and error bars represent medians and 95% confidence intervals calculated from three independent experiments done in triplicate. Differences between treatments were assessed by a two-tailed Mann Whitney test. ****, $P < 0.0001$; ns, nonsignificant. (C) THP-1 macrophages were infected with *M. abscessus* expressing tdTomato, treated with different concentrations of BDQ without or with VER, and incubated for 2 days before they were observed under a confocal microscope and the percentage of infected macrophages determined. Histograms and error bars represent medians and 95% confidence intervals calculated from three independent experiments completed in triplicate. Differences between treatments were assessed by a two-tailed Mann-Whitney test. ****, $P < 0.0001$; ns, nonsignificant.

inducer, VER, to increase BDQ sensitivity in *M. abscessus*, and we also confirmed that VER has adjunctive activity in macrophages. Due to limitations on the verapamil plasma concentrations that are obtained by oral verapamil dosing (27), its potential might be limited in clinical settings to improve outcomes of BDQ treatment in *M. abscessus* infections. However, this study, along with previous reports that VER augments BDQ activity against *M. tuberculosis* (14, 15), proves that pharmacological potential exists to improve the activity of BDQ against tuberculous and nontuberculous mycobacteria. Subsequent investigations should be initiated to discover analogous compounds to VER that have reduced toxicity and that act in a similar manner to increase the sensitivity of mycobacteria to BDQ.

SUPPLEMENTAL MATERIAL

Supplemental material for this article may be found at https://doi.org/10.1128/AAC.00705-19.

SUPPLEMENTAL FILE 1, PDF file, 0.7 MB.

ACKNOWLEDGMENTS

This study was supported by the Fondation pour la Recherche Médicale (grant DEQ20150331719 to L.K.) and the Association Gregory Lemarchal and Vaincre la Mucoviscidose (grant RIF20180502320 to C.R.). M.D.J. received a postdoctoral fellowship granted by Labex EpiGenMed, an Investissements d'Avenir program (ANR-10-LABX-12-01). The funders had no role in study design, data collection, interpretation, or the decision to submit the work for publication.

The authors have no conflict of interest to declare.

REFERENCES

1. Choo SW, Wee WY, Ngeow YF, Mitchell W, Tan JL, Wong GJ, Zhao Y, Xiao J. 2014. Genomic reconnaissance of clinical isolates of emerging human pathogen *Mycobacterium abscessus* reveals high evolutionary potential. Sci Rep 4:4061. https://doi.org/10.1038/srep04061.
2. Tan JL, Ngeow YF, Choo SW. 2015. Support from phylogenomic networks and subspecies signatures for separation of *Mycobacterium massiliense* from *Mycobacterium bolletii*. J Clin Microbiol 53:3042–3046. https://doi.org/10.1128/JCM.00541-15.
3. Griffith DE, Aksamit T, Brown-Elliott BA, Catanzaro A, Daley C, Gordin F, Holland SM, Horsburgh R, Huitt G, Iademarco MF, Iseman M, Olivier K, Ruoss S, von Reyn CF, Wallace RJ, Winthrop K, ATS Mycobacterial Diseases Subcommittee, American Thoracic Society, Infectious Disease Society of America. 2007. An official ATS/IDSA statement: diagnosis, treatment, and prevention of nontuberculous mycobacterial diseases. Am J Respir Crit Care Med 175:367–416. https://doi.org/10.1164/rccm.200604-571ST.
4. Floto RA, Olivier KN, Saiman L, Daley CL, Herrmann J-L, Nick JA, Noone PG, Bilton D, Corris P, Gibson RL, Hempstead SE, Koetz K, Sabadosa KA, Sermet-Gaudelus I, Smyth AR, van Ingen J, Wallace RJ, Winthrop KL, Marshall BC, Haworth CS. 2016. U.S. Cystic Fibrosis Foundation and European Cystic Fibrosis Society consensus recommendations for the management of non-tuberculous mycobacteria in individuals with cystic fibrosis: executive summary. Thorax 71:88–90. https://doi.org/10.1136/thoraxjnl-2015-207983.
5. Esther CR, Esserman DA, Gilligan P, Kerr A, Noone PG. 2010. Chronic *Mycobacterium abscessus* infection and lung function decline in cystic fibrosis. J Cyst Fibros 9:117–123. https://doi.org/10.1016/j.jcf.2009.12.001.
6. Catherinot E, Roux A-L, Macheras E, Hubert D, Matmar M, Dannhoffer L, Chinet T, Morand P, Poyart C, Heym B, Rottman M, Gaillard J-L, Herrmann J-L. 2009. Acute respiratory failure involving an R variant of *Mycobacterium abscessus*. J Clin Microbiol 47:271–274. https://doi.org/10.1128/JCM.01478-08.
7. Jeon K, Kwon OJ, Lee NY, Kim B-J, Kook Y-H, Lee S-H, Park YK, Kim CK, Koh W-J. 2009. Antibiotic treatment of *Mycobacterium abscessus* lung disease: a retrospective analysis of 65 patients. Am J Respir Crit Care Med 180:896–902. https://doi.org/10.1164/rccm.200905-0704OC.
8. Jarand J, Levin A, Zhang L, Huitt G, Mitchell JD, Daley CL. 2011. Clinical and microbiologic outcomes in patients receiving treatment for *Mycobacterium abscessus* pulmonary disease. Clin Infect Dis 52:565–571. https://doi.org/10.1093/cid/ciq237.
9. Strollo SE, Adjemian J, Adjemian MK, Prevots DR. 2015. The burden of pulmonary nontuberculous mycobacterial disease in the United States. Ann Am Thorac Soc 12:1458–1464. https://doi.org/10.1513/AnnalsATS.201503-173OC.
10. Matteelli A, Carvalho AC, Dooley KE, Kritski A. 2010. TMC207: the first compound of a new class of potent anti-tuberculosis drugs. Future Microbiol 5:849–858. https://doi.org/10.2217/fmb.10.50.
11. Pang Y, Zheng H, Tan Y, Song Y, Zhao Y. 2017. *In vitro* activity of bedaquiline against nontuberculous mycobacteria in China. Antimicrob Agents Chemother 61:e02627-16. https://doi.org/10.1128/AAC.02627-16.
12. Vesenbeckh S, Schönfeld N, Roth A, Bettermann G, Krieger D, Bauer TT, Rüssmann H, Mauch H. 2017. Bedaquiline as a potential agent in the treatment of *Mycobacterium abscessus* infections. Eur Respir J 49:1700083. https://doi.org/10.1183/13993003.00083-2017.
13. Dupont C, Viljoen A, Thomas S, Roquet-Banères F, Herrmann J-L, Pethe K, Kremer L. 2017. Bedaquiline inhibits the ATP synthase in *Mycobacterium abscessus* and is effective in infected zebrafish. Antimicrob Agents Chemother 61:e01225-17. https://doi.org/10.1128/AAC.01225-17.
14. Gupta S, Cohen KA, Winglee K, Maiga M, Diarra B, Bishai WR. 2014. Efflux inhibition with verapamil potentiates bedaquiline in *Mycobacterium tuberculosis*. Antimicrob Agents Chemother 58:574–576. https://doi.org/10.1128/AAC.01462-13.
15. Gupta S, Tyagi S, Bishai WR. 2015. Verapamil increases the bactericidal activity of bedaquiline against *Mycobacterium tuberculosis* in a mouse model. Antimicrob Agents Chemother 59:673–676. https://doi.org/10.1128/AAC.04019-14.
16. Woods GL, Brown-Elliott BA, Conville PS, Desmond EP, Hall GS, Lin G, Pfyffer GE, Ridderhof JC, Siddiqi SH, Wallace RJ. 2011. Susceptibility testing of mycobacteria, nocardiae, and other aerobic actinomycetes: approved standard, 2nd ed. M24-A2. Clinical and Laboratory Standards Institute, Wayne, PA.
17. St-Onge M, Dubé P-A, Gosselin S, Guimont C, Godwin J, Archambault PM, Chauny J-M, Frenette AJ, Darveau M, Le Sage N, Poitras J, Provencher J, Juurlink DN, Blais R. 2014. Treatment for calcium channel blocker poisoning: a systematic review. Clin Toxicol 52:926–944. https://doi.org/10.3109/15563650.2014.965827.
18. Batalis NI, Harley RA, Schandl CA. 2007. Verapamil toxicity: an unusual case report and review of the literature. Am J Forensic Med Pathol 28:137–140. https://doi.org/10.1097/01.paf.0000257399.58935.28.
19. Toffoli G, Robieux I, Fantin D, Gigante M, Frustaci S, Nicolosi GL, De Cicco M, Boiocchi M. 1997. Non-linear pharmacokinetics of high-dose intravenous verapamil. Br J Clin Pharmacol 44:255–260. https://doi.org/10.1046/j.1365-2125.1997.t01-1-00574.x.
20. Xu J, Tasneen R, Peloquin CA, Almeida DV, Li S-Y, Barnes-Boyle K, Lu Y, Nuermberger E. 2018. Verapamil increases the bioavailability and efficacy of bedaquiline but not clofazimine in a murine model of tuberculosis. Antimicrob Agents Chemother 62:e01692-17. https://doi.org/10.1128/AAC.01692-17.
21. Richard M, Gutiérrez AV, Viljoen A, Rodriguez-Rincon D, Roquet-Baneres F, Blaise M, Everall I, Parkhill J, Floto RA, Kremer L. 2018. Mutations in the MAB_2299c TetR regulator confer cross-resistance to clofazimine and bedaquiline in *Mycobacterium abscessus*. Antimicrob Agents Chemother 63:e01316-18. https://doi.org/10.1128/AAC.01316-18.
22. Chen C, Gardete S, Jansen RS, Shetty A, Dick T, Rhee KY, Dartois V. 2018. Verapamil targets membrane energetics in *Mycobacterium tuberculosis*. Antimicrob Agents Chemother 62:e02107-17. https://doi.org/10.1128/AAC.02107-17.
23. Andries K, Villellas C, Coeck N, Thys K, Gevers T, Vranckx L, Lounis N, de Jong BC, Koul A. 2014. Acquired resistance of *Mycobacterium tuberculosis* to bedaquiline. PLoS One 9:e102135. https://doi.org/10.1371/journal.pone.0102135.
24. Lefebvre A-L, Le Moigne V, Bernut A, Veckerlé C, Compain F, Herrmann J-L, Kremer L, Arthur M, Mainardi J-L. 2017. Inhibition of the β-lactamase Bla_{Mab} by avibactam improves the *in vitro* and *in vivo* efficacy of imipenem against *Mycobacterium abscessus*. Antimicrob Agents Chemother 61:e02440-16. https://doi.org/10.1128/AAC.02440-16.
25. Bernut A, Herrmann J-L, Kissa K, Dubremetz J-F, Gaillard J-L, Lutfalla G, Kremer L. 2014. *Mycobacterium abscessus* cording prevents phagocytosis and promotes abscess formation. Proc Natl Acad Sci U S A 111:E943–E952. https://doi.org/10.1073/pnas.1321390111.
26. Adams KN, Szumowski JD, Ramakrishnan L. 2014. Verapamil, and its metabolite norverapamil, inhibit macrophage-induced, bacterial efflux pump-mediated tolerance to multiple anti-tubercular drugs. J Infect Dis 210:456–466. https://doi.org/10.1093/infdis/jiu095.
27. John DN, Fort S, Lewis MJ, Luscombe DK. 1992. Pharmacokinetics and pharmacodynamics of verapamil following sublingual and oral administration to healthy volunteers. Br J Clin Pharmacol 33:623–627. https://doi.org/10.1111/j.1365-2125.1992.tb04091.x.

Table S1. MICs (µg/ml) of amikacin (AMK), imipenem (IPM) and cefoxitin (CFX) on 7H10^{OADC} agar at 37°C without (0 VER) or with 50 µg/ml verapamil (50 VER) or 250 µg/ml verapamil (250 VER) against *M. abscessus* CIP104536^{T}.

Drug	**MIC (µg/ml)**		
	0 VER	**50 VER**	**250 VER**
BDQ	0.25	0.64	0.16
AMK	16	16	16
IMP	16	16	16
CFX	32	32	32

Table S2. List of *M. abscessus* genetically modified strains used in this study.

Strain	Description	Reference
M. abscessus S	Type strain CIP104536^T, smooth	Laboratoire de Référence des Mycobactéries
M. abscessus R	Type strain CIP104536 ^{T}, rough	Laboratoire de Référence des Mycobactéries
CFZ-R6	*In vitro* reared low-level BDQ resistant *M. abscessus*. Harbours a loss-of-function point mutation in *MAB_2299c* and over-expresses *MAB_2300* and *MAB_2301* at a transcriptional level.	(1)
Δ*MAB_2299c*	Unmarked *MAB_2299* deletion mutant in the smooth CIP104536 background. Over-expresses *MAB_2300* and *MAB_2301* at a transcriptional level.	(1)
Δ*MAB_2299c* Compl	Δ*MAB_2299c* complemented strain. *MAB_2300* and *MAB_2301* transcript levels are decreased compared to the parent strain.	(1)
Δ*MAB_2299c* Δ*MAB_2300-2301*	Unmarked *MAB_2300-MAB_2301* deletion mutant in the Δ*MAB_2299c* background. More sensitive to BDQ than WT.	(1)
atpE^{D29V}	D29V BDQ-resistance conferring mutation transferred onto the *atpE* gene by homologous recombination in the smooth CIP104536^T background. Highly resistant to BDQ.	(2)
atpE^{A64P}	A64P BDQ-resistance conferring mutation transferred onto the *atpE* gene by homologous recombination in the smooth CIP104536^T background. Highly resistant to BDQ.	(2)

REFERENCES

1. Richard M, Gutiérrez AV, Viljoen A, Rodriguez-Rincon D, Roquet-Baneres F, Blaise M, Everall I, Parkhill J, Floto RA, Kremer L. 2019. Mutations in the MAB_2299c TetR regulator confer cross-resistance to clofazimine and bedaquiline in *Mycobacterium abscessus*. Antimicrob Agents Chemother 63.

2. Dupont C, Viljoen A, Thomas S, Roquet-Banères F, Herrmann J-L, Pethe K, Kremer L. 2017. Bedaquiline inhibits the ATP synthase in *Mycobacterium abscessus* and is effective in infected zebrafish. Antimicrob Agents Chemother 61.

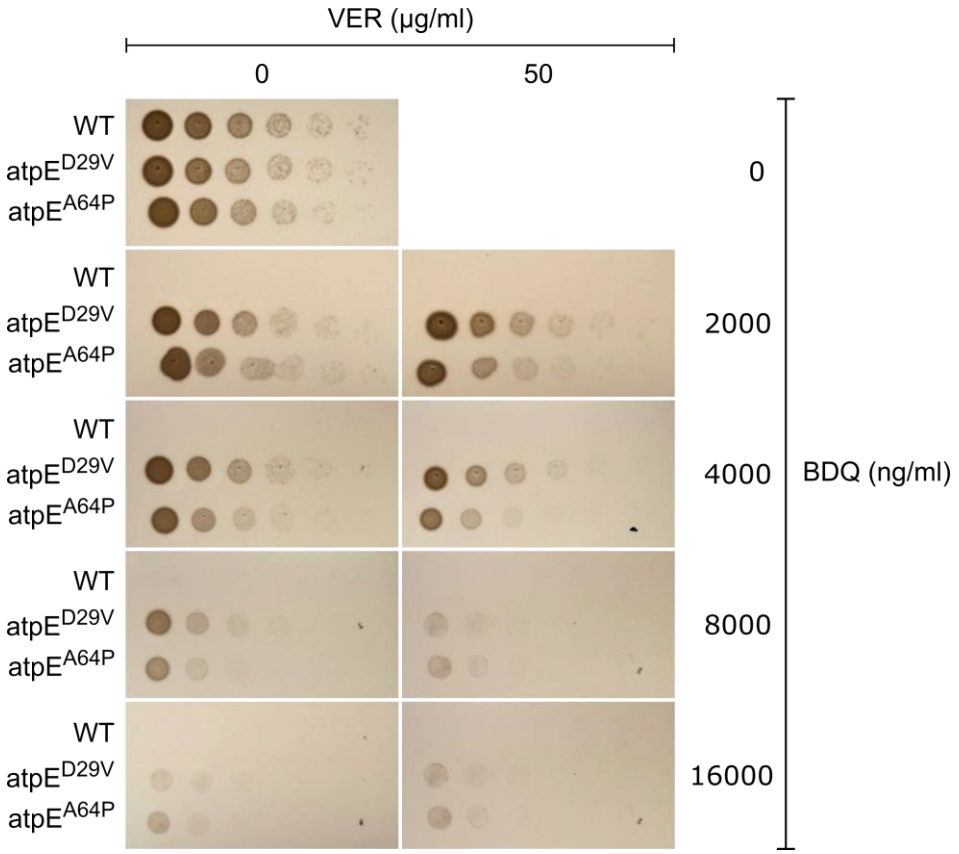

Fig. S1. Potentiation of the activity of BDQ against *M. abscessus* is lost in mutants carrying mutations in the AtpE target of BDQ. An exponential phase culture of each strain was serially ten-fold diluted and 5 µl volumes of each dilution were spotted onto the agar plates, which were then incubated at 37°C for 4 days before pictures were taken.

Article 4: "Efficacy of Bedaquiline, Alone or in Combination with Imipenem, against *Mycobacterium abscessus* in C3HeB/FeJ Mice."
Le Moigne, Vincent, Clément Raynaud, Flavie Moreau, Christian Dupont, Jérôme Nigou, Olivier Neyrolles, Laurent Kremer, and Jean Louis Herrmann, 2020, *Antimicrobial Agents and Chemotherapy* 64 (6): 1–6. https://doi.org/10.1128/AAC.00114-20. (Le Moigne et al. 2020)

Lerat et al. ont montré dans un modèle de souris immunodéprimée Nude, que la BDQ exhibait une efficacité limitée et s'accompagnait d'une faible diminution des CFU au niveau des poumons et de la rate (Lerat et al. 2014). A l'inverse, *Obregon-Henao et al.* ont montré dans d'autres modèles murins immunodéprimés (GKO et SCID) que la BDQ permettait une nette diminution des CFU dans les poumons, la rate et le foie (Obregón-Henao et al. 2015).

Ces résultats conflictuels nous ont poussé à réexaminer l'effet de la BDQ dans un autre modèle de souris immunocompétentes C3HeB/FeJ (mis en place dans le laboratoire du Pr Herrmann à Versailles) et également aux synergies potentielles entre la BDQ et des molécules utilisées contre *M. abscessus*. Dans un premier temps, nous avons déterminé les FICI des combinaisons BDQ avec différents antibiotiques (CLR, IPM, CFX et ampicilline (AMP)). Les FICI obtenus étant proches de 0,5 pour l'IPM et la CFX, nous ont conduit à évaluer ces combinaisons thérapeutiques dans un modèle souris C3HeB/FeJ. Nous avons observé une diminution modérée des CFU dans les poumons, la rate et le foie des souris traitées avec la BDQ par rapport à celles traitées avec l'AMK ou non traitées. Nous avons également testé l'association BDQ/IPM dans ce modèle murin. La charge bactérienne obtenue était légèrement inférieure ou égale à celle des souris traité uniquement par la BDQ.

Dans cette étude, je me suis essentiellement concentré sur la partie *in vitro* et la recherche des synergies potentielles entre molécules.

AMERICAN SOCIETY FOR MICROBIOLOGY | Antimicrobial Agents and Chemotherapy®

EXPERIMENTAL THERAPEUTICS

Efficacy of Bedaquiline, Alone or in Combination with Imipenem, against *Mycobacterium abscessus* in C3HeB/FeJ Mice

Vincent Le Moigne,[a] Clément Raynaud,[b] Flavie Moreau,[c] Christian Dupont,[b] Jérôme Nigou,[c] Olivier Neyrolles,[c] Laurent Kremer,[b,d] Jean-Louis Herrmann[a,e]

[a]UVSQ, INSERM, Infection et Inflammation (U1173), Université Paris-Saclay, Montigny-le-Bretonneux, France
[b]Institut de Recherche en Infectiologie de Montpellier, Centre National de la Recherche Scientifique UMR 9004, Université de Montpellier, Montpellier, France
[c]Institut de Pharmacologie et de Biologie Structurale, Université de Toulouse, CNRS, UPS, Toulouse, France
[d]INSERM, Institut de Recherche en Infectiologie de Montpellier (IRIM), Montpellier, France
[e]Hôpital Raymond Poincaré, AP-HP, GHU Paris-Saclay, Garches, France

ABSTRACT *Mycobacterium abscessus* lung infections remain difficult to treat. Recent studies have recognized the power of new combinations of antibiotics, such as bedaquiline and imipenem, although *in vitro* data have questioned this combination. We report that the efficacy of bedaquiline-imipenem combination treatment relies essentially on the activity of bedaquiline in a C3HeB/FeJ mice model of infection with a rough variant of *M. abscessus*. The addition of imipenem contributed to clearing the infection in the spleen.

KEYWORDS C3HeB/FeJ mice, *Mycobacterium abscessus*, bedaquiline, cystic fibrosis, imipenem

Mycobacterium abscessus is a rapidly growing mycobacterial species whose infections remain very difficult to treat due to the limited panel of available antibiotics (1). Among them, the β-lactams imipenem (IPM) and cefoxitin (FOX) are part of *M. abscessus* multidrug therapy, along with amikacin (AMK) and clarithromycin (CLR) (2–5). In addition, the development of specific β-lactamase inhibitors, enhancing the efficacy of IPM *in vitro* and *in vivo*, broadens the use of IPM in *M. abscessus* drug therapy (6–8). Other studies highlighted the potential of testing new drug combinations that include IPM and are associated with increased efficacy against *M. abscessus* infection (6, 9, 10); however, the relevance of the bedaquiline (BDQ) plus IPM combination has been questioned (11). BDQ targets ATP synthase and exhibits activity against a wide panel of *M. abscessus* clinical isolates *in vitro* and in infected zebrafish, although its effect is bacteriostatic only (12). A recent study suggested that by reducing the intracellular pool of ATP in *M. abscessus* isolates, BDQ suppresses the effect of IPM and FOX, although the effect of the BDQ-IPM combination was considered additive (11). This led the investigators to conclude that addition of BDQ to a β-lactam-containing regimen may negatively affect the treatment outcome (11). In comparison, data from the hollow-fiber model highlight that β-lactam is the most active and important part of the *M. abscessus* treatment regimen (13). Because these studies focused exclusively on the interaction of β-lactams and BDQ *in vitro*, confirmatory results in a preclinical animal model are warranted.

Herein, we explored the therapeutic efficacy of BDQ and IPM, alone and in combination, using the immunocompetent C3HeB/FeJ mouse model of *M. abscessus* infection. C3HeB/FeJ mice are highly susceptible to mycobacterial infections, particularly to *Mycobacterium tuberculosis* due to a deletion of the *lpr1* (intracellular pathogen resis-

Citation Le Moigne V, Raynaud C, Moreau F, Dupont C, Nigou J, Neyrolles O, Kremer L, Herrmann J-L. 2020. Efficacy of bedaquiline, alone or in combination with imipenem, against *Mycobacterium abscessus* in C3HeB/FeJ mice. Antimicrob Agents Chemother 64:e00114-20. https://doi.org/10.1128/AAC.00114-20.

Address correspondence to Vincent Le Moigne, vincent.le-moigne@uvsq.fr.

Received 17 January 2020
Returned for modification 2 March 2020
Accepted 26 March 2020
Accepted manuscript posted online 6 April 2020
Published 21 May 2020

TABLE 1 Interaction between bedaquiline and other drugs against *M. abscessus* strain CIP104536^T

Compound	MIC[a] (mg/liter)	Interaction with BDQ	
		FICI[b] score (mean ± SD)	Outcome[c]
BDQ	0.125		
IPM	16	0.55 ± 0.06	Indifferent
FOX	32	0.52 ± 0.03	Indifferent
CLR	2	0.61 ± 0.09	Indifferent
AMP	>512	0.57 ± 0.02	Indifferent

[a]MICs were evaluated by REMA (resazurin microtiter assay) checkerboard assay in CaMHB (Becton, Dickinson, Le Pont-de-Claix, France). 10^5 bacteria were diluted in Mueller-Hinton media (Sigma-Aldrich). Plates were incubated for 3 days at 30°C, after which 20 μl (10% vol/vol) of resazurin 0.025% was added to the wells; the plates were incubated overnight at 30°C.

[b]The fractional inhibitory concentration index (FICI) was calculated as follows: FICI = (MIC drug A in combination/MIC drug A alone) + (MIC drug B in combination/MIC drug B alone), where drug A was bedaquiline (BDQ) and drug B was clarithromycin (CLR) (Sigma-Aldrich, France), imipenem (IPM, Mylan S.A.S., France), cefoxitin (FOX, Panpharma, France), or ampicillin (AMP, Euromedex, France). Values are means of 4 independent experiments.

[c]Interaction between the 2 compounds was defined as synergistic when FICI was ≤0.5, indifferent when 0.5 < FICI ≤ 4, and antagonistic when FICI was >4.

tance 1) gene located within the locus *sst1* (14, 15). All animal experiments were performed according to ethical guidelines and with ethical committee (no. 047 with agreement A783223) agreement APAFIS 11465.

First, we evaluated the *in vitro* interaction between BDQ and several β-lactams or CLR against *M. abscessus* strain CIP104536 in cation-adjusted Mueller-Hinton broth (CaMHB) (Becton, Dickinson, Le Pont-de-Claix, France) using a 2-dimensional microdilution checkerboard method, as previously described (16–19). Our results confirm that the β-lactam plus BDQ combinations are indifferent, as is the case for the CLR-BDQ combination (Table 1).

Next, the performances of pulmonary and intravenous (i.v.) infection routes were compared in C3HeB/FeJ mice. Mice were infected intratracheally using agar bead-embedded bacteria to maintain a persistent infection, as reported previously for *Pseudomonas aeruginosa* (20). A significant increase in mortality was noted when mice were infected intratracheally with a solution of agar beads containing 2.10^5 CFU/mouse

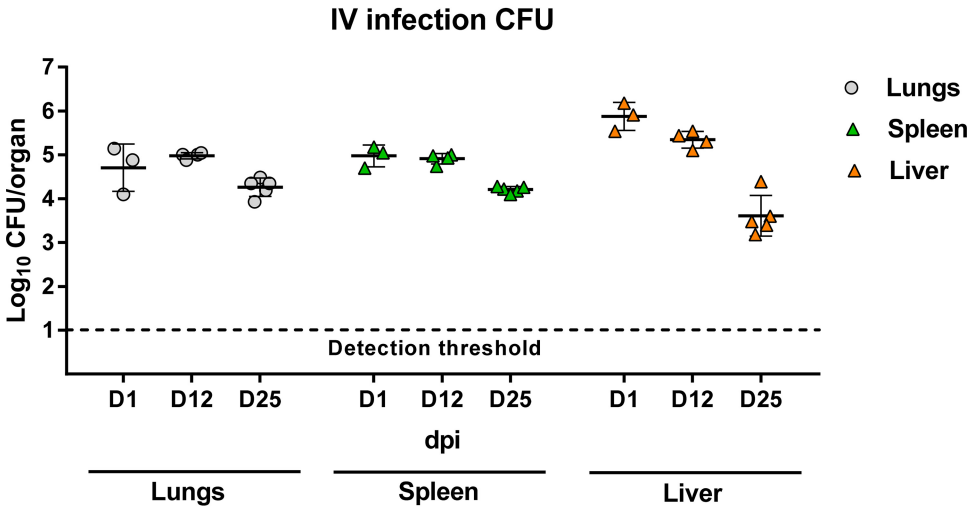

FIG 1 Bacterial persistence of *M. abscessus* strain CIP104536^T (rough variant) in lungs, spleens, and livers of C3HeB/FeJ mice after i.v. infection in the tail vein with 10^6 CFU/mouse in a total volume of 200 μl of water containing 0.9% sodium chloride. The following day, 3 mice were euthanized, and whole organs were harvested to determine baseline bacterial burden. Mouse lungs, spleens, and livers were homogenized, serially diluted, and plated onto VCAT (vancomycin, colistin sulfate, amphotericin B, and trimethoprim) chocolate agar plates (bioMérieux, France) and incubated for 5 to 6 days at 37°C before CFU counting. Results are expressed as $\log_{10}$ CFU at 1, 12, and 25 dpi.

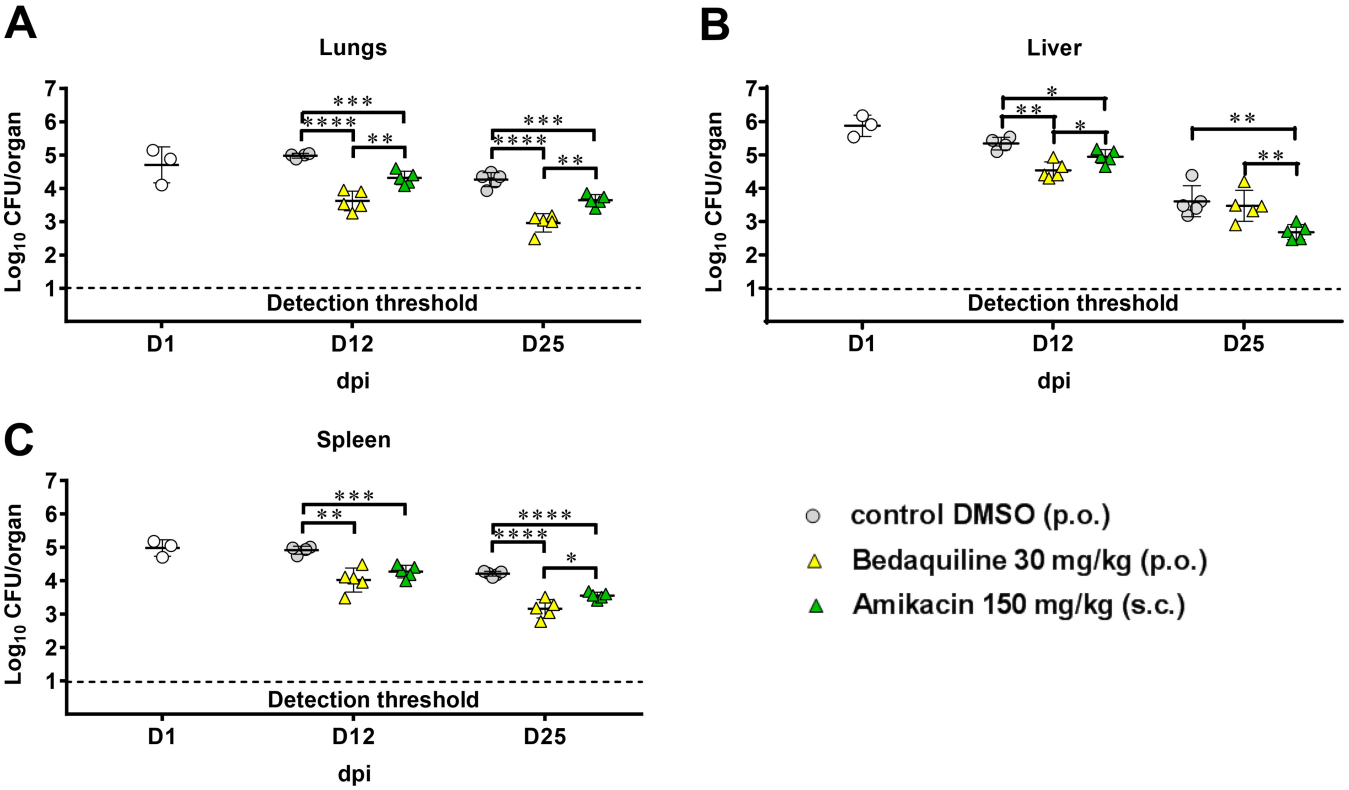

FIG 2 *M. abscessus* R-infected C3HeB/FeJ mice (9.2×10^5 CFU/mouse) treated with bedaquiline (BDQ) or amikacin (AMK). Bacterial counts in the lungs (A), liver (B), and spleen (C) of C3HeB/FeJ mice infected i.v., as described in Fig. 1. Antibiotic treatment began at 2 dpi. Mice were treated starting on day 2 for 7 days (D12) or 17 days (D25) by daily subcutaneous injections of AMK 150 mg/kg (Mylan Laboratories) in saline solution or daily oral gavage of BDQ 30 mg/kg in a total volume of 200 μl (BDQ solution in DMSO was diluted in 20% 2-hydroxypropyl-β-cyclodextrin). A control group received a daily subcutaneous injection of saline and oral gavage of DMSO containing 20% 2-hydroxypropyl-β-cyclodextrin. All solutions were administered 5 times weekly for later time point. Mice were euthanized 3 days after antibiotic cessation to allow for antibiotic clearance. Furthermore, given the long half-life and high protein binding capacity of BDQ, spleens, livers, and lungs from drug-treated and control mice were homogenized in water supplemented with 10% bovine serum albumin before dilution (30). Experimental groups of mice were evaluated for bacterial burden on day 1 (before treatment started), 12, and 25 as described in Fig. 1. Five mice were used per group. Bacterial load in each group is expressed as $\log_{10}$ CFU $\pm$ SD. Differences between means were analyzed by two-way analysis of variance (ANOVA) and the Tukey posttest, allowing for multiple comparisons. n.s., nonsignificant; *, $P < 0.05$; **, $P < 0.01$; ***, $P < 0.001$. Experiment was performed once.

in 50 μl, leading to only 40% mouse survival at 14 days postinfection (dpi) (see Fig. S1A in the supplemental material), which correlated with an important increase in the CFU at 14 dpi, suggesting accelerated bacterial growth in the lungs (see Fig. S1B). In contrast, persistence occurred for up to 25 days after i.v. infection with 10^6 CFU/mouse, as evidenced by CFU counting after plating of the organ homogenates (Fig. 1; see also Fig. S2A and B in the supplemental material), although as soon as the injected dose was $<10^6$ CFU, persistence in the organs was reduced (Fig. S2B). This represents an important improvement over results found in previously described murine models, characterized by a more rapid bacterial clearance (21–23).

The i.v. route of infection was subsequently used to evaluate and compare the activities of BDQ and AMK. Because AMK is bactericidal against *M. abscessus* isolates and BDQ is bacteriostatic *in vitro*, we wondered whether BDQ would be more effective than AMK in an *in vivo* infection model. CFU were significantly reduced in mice receiving BDQ 30 mg/kg (orally) compared with mice receiving AMK 150 mg/kg (subcutaneously) in lungs and spleen at 12 and 25 dpi (Fig. 2A and B). No significant differences were observed between the BDQ- and AMK-treated animals in the spleen at 12 dpi, but bacterial loads in these two groups were significantly lower than those in the control group (oral administration of dimethyl sulfoxide [DMSO]) (Fig. 2C).

The efficacy of BDQ in this infection model prompted us to compare it with subcutaneous IPM, alone or as a companion drug, for 15 days of treatment. No

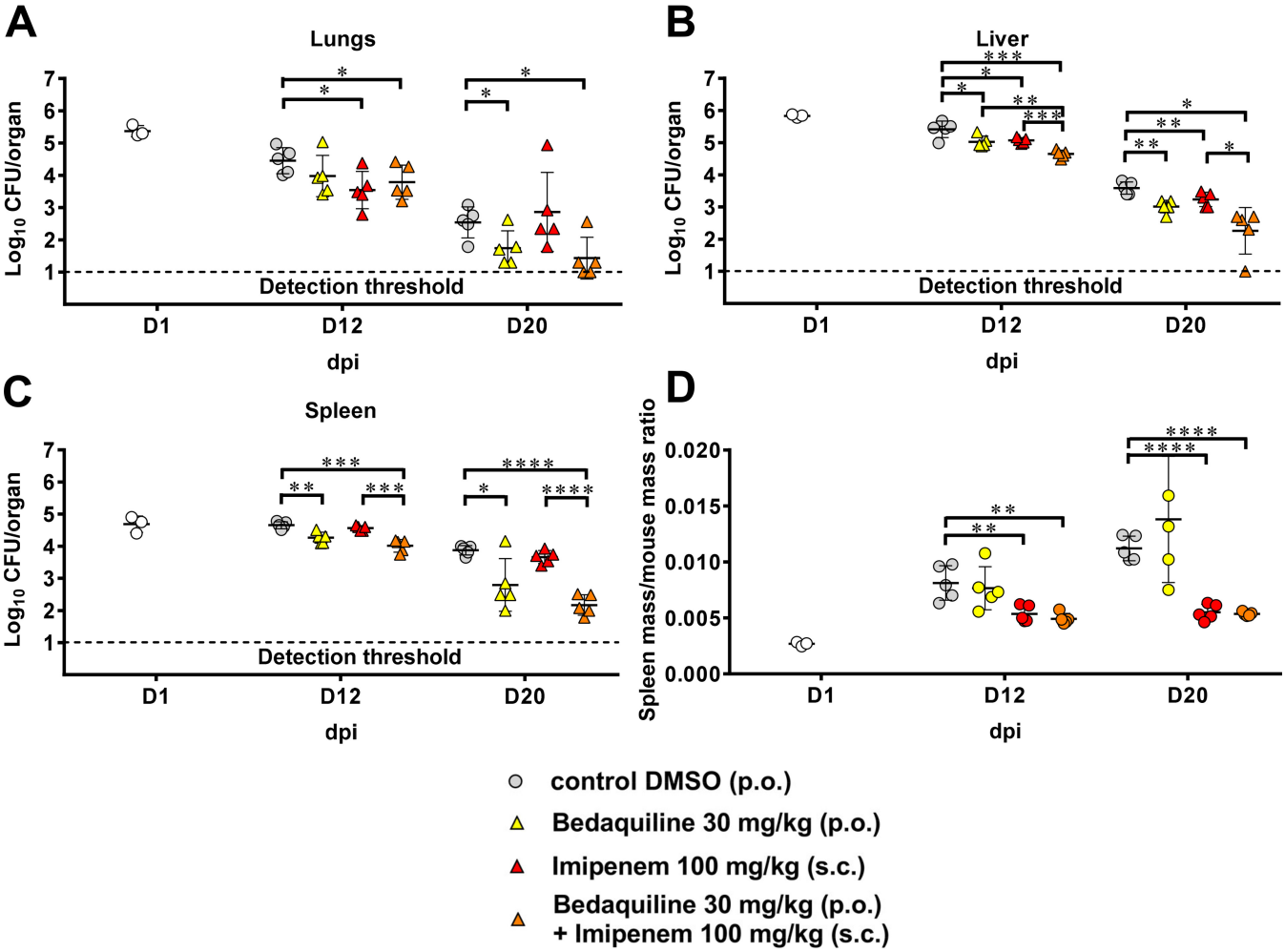

FIG 3 *M. abscessus* R-infected C3HeB/FeJ mice treated (2.7×10^5 CFU/mouse) with bedaquiline (BDQ), imipenem (IPM), or BDQ plus IPM. Bacterial loads in the lungs (A), liver (B), and spleen (C) were determined as reported in Fig. 1. Antibiotic treatment began 2 days after infection. Mice were treated starting on day 2 for 7 days (D12) or 13 days (D20) with twice-daily (i.e., every 12 h) subcutaneous injection of IPM (MSD Laboratories, France) in saline solution at 100 mg/kg or daily oral gavage of BDQ as described in Fig. 2 or IPM-BDQ. Experimental groups of mice were evaluated for bacterial burden on day 1 (before treatment started), 12, and 20 as described in Fig. 1. (D) Relative weights of spleen to mouse. Mouse spleens were weighed at 1, 12, and 20 dpi. Values represent the relative weight of each spleen relative to the weight of the mouse from which it was collected. Five mice were used per experiment. Bacterial load in each group is expressed as $\log_{10}$ CFU ± SD cells. Differences between means were analyzed by two-way ANOVA and the Tukey posttest, allowing for multiple comparisons. n.s., nonsignificant; *, $P < 0.05$; **, $P < 0.01$; ***, $P < 0.001$. Experiment was performed once.

significant differences were noticed between the animals treated with BDQ alone and the animals treated with BDQ-IPM at 12 and 20 dpi, with the exception of the liver at 12 dpi (Fig. 3A to C), indicating that the overall activity of the BDQ-IPM combination was mainly due to the intrinsic activity of BDQ. In general, BDQ alone or in combination with IPM exhibited increased activity compared with that of IPM alone in the liver and spleen but not in the lungs (Fig. 3). The spleens of treated and untreated mice were weighed as an additional marker of the effectiveness of the various treatments. These measures indicated that only treatments with BDQ plus IPM or IPM alone were associated with lower spleen weights than those of the untreated or BDQ-treated mice (Fig. 3D). Collectively, the reduced bacterial burden and the lower spleen weights represent a marker for improved outcome of the infection.

BDQ is a diarylquinoline approved by the Food and Drug Administration and the European Medicines Agency for the treatment of multidrug-resistant tuberculosis. It is bacteriostatic against *M. abscessus* isolates *in vitro*, displaying an MIC_{50} of 0.125 μg/ml and an MIC_{90} of >16 μg/ml; and epidemiological cutoff values showed that BDQ exhibits moderate activity (16, 24). Discordant results regarding the efficacy of BDQ

were generated in various immunocompromised mouse models, raising the question of the influence of immunosuppression on antibiotic efficacy (25, 26). However, efficient responses to BDQ were observed in other animal models, such as zebrafish (12). Two studies reported poor or negative results for BDQ administration against nontuberculous mycobacteria-infected patients (27, 28). However, recent studies showed that the activity of BDQ can be potentiated with adjunctive therapy, thus improving BDQ-based treatments (16, 29). This study provides evidence that treatment with the BDQ-IPM combination remains superior to treatment with IPM alone and equivalent to that with BDQ alone, as judged by the comparable bacterial clearance in the spleens of the mice treated with BDQ-IPM versus BDQ alone.

In summary, the BDQ-IPM combination enhances clearance of the infection. This also supports the importance of evaluating antibiotic activity in combination rather than separately against this highly drug-resistant mycobacterium.

SUPPLEMENTAL MATERIAL

Supplemental material is available online only.

SUPPLEMENTAL FILE 1, PDF file, 0.04 MB.

ACKNOWLEDGMENTS

Bedaquiline was a kind gift from C. Happel (NIH AIDS Reagent Program, USA) and from N. Lounis (Janssen Pharmaceuticals, Beerse, Belgium).

We acknowledge N. Véziris and J. van Ingen for helpful comments and critical reading of the manuscript. We thank the members of the Genotoul core facility ANEXPLO (IPBS, Toulouse) for animal experiments.

This study was supported by INSERM, University of Versailles Saint Quentin en Yvelines; the Association Gregory Lemarchal and Vaincre la Mucoviscidose (RIF20180502320) to L.K. and J.L.H.; the Agence Nationale de la Recherche (MyCat ANR-15-CE18-0007-02) to L.K.; CNRS, University of Toulouse, Agence Nationale de la Recherche/Program d'Investissements d'Avenir (ANR-11-EQUIPEX-0003); and the Bettencourt Schueller Foundation.

The funders had no role in study design, data collection and analysis, decision to publish, or preparation of the manuscript.

J.N., O.N., and J.L.H. designed the project and experiments. V.L.M., C.R., F.M., and C.D. performed the experiments. V.L.M., C.R., J.N., O.N., L.K., and J.L.H. wrote and corrected the manuscript.

REFERENCES

1. Kwak N, Dalcolmo MP, Daley CL, Eather G, Gayoso R, Hasegawa N, Jhun BW, Koh WJ, Namkoong H, Park J, Thomson R, van Ingen J, Zweijpfenning SMH, Yim JJ. 2019. *Mycobacterium abscessus* pulmonary disease: individual patient data meta-analysis. Eur Respir J 54:1801991. https://doi.org/10.1183/13993003.01991-2018.
2. Griffith DE, Aksamit T, Brown-Elliott BA, Catanzaro A, Daley C, Gordin F, Holland SM, Horsburgh R, Huitt G, Iademarco MF, Iseman M, Olivier K, Ruoss S, von Reyn CF, Wallace RJ, Jr, Winthrop K, ATS Mycobacterial Diseases Subcommittee, American Thoracic Society, Infectious Disease Society of America. 2007. An official ATS/IDSA statement: diagnosis, treatment, and prevention of nontuberculous mycobacterial diseases. Am J Respir Crit Care Med 175:367–416. https://doi.org/10.1164/rccm.200604-571ST.
3. Haworth CS, Banks J, Capstick T, Fisher AJ, Gorsuch T, Laurenson IF, Leitch A, Loebinger MR, Milburn HJ, Nightingale M, Ormerod P, Shingadia D, Smith D, Whitehead N, Wilson R, Floto RA. 2017. British Thoracic Society guidelines for the management of non-tuberculous mycobacterial pulmonary disease (NTM-PD). Thorax 72:ii1–ii64. https://doi.org/10.1136/thoraxjnl-2017-210927.
4. Floto RA, Olivier KN, Saiman L, Daley CL, Herrmann JL, Nick JA, Noone PG, Bilton D, Corris P, Gibson RL, Hempstead SE, Koetz K, Sabadosa KA, Sermet-Gaudelus I, Smyth AR, van Ingen J, Wallace RJ, Winthrop KL, Marshall BC, Haworth CS. 2016. US Cystic Fibrosis Foundation and European Cystic Fibrosis Society consensus recommendations for the management of non-tuberculous mycobacteria in individuals with cystic fibrosis: executive summary. Thorax 71:88–90. https://doi.org/10.1136/thoraxjnl-2015-207983.
5. Lefebvre AL, Le Moigne V, Bernut A, Veckerlé C, Compain F, Herrmann JL, Kremer L, Arthur M, Mainardi JL. 2017. Inhibition of the β-lactamase Bla_{Mab} by avibactam improves the *in vitro* and *in vivo* efficacy of imipenem against *Mycobacterium abscessus*. Antimicrob Agents Chemother 61:e02440-16. https://doi.org/10.1128/AAC.02440-16.
6. Kaushik A, Ammerman NC, Lee J, Martins O, Kreiswirth BN, Lamichhane G, Parrish NM, Nuermberger EL. 2019. *In vitro* activity of the new β-lactamase inhibitors relebactam and vaborbactam in combination with β-lactams against *Mycobacterium abscessus* complex clinical isolates. Antimicrob Agents Chemother 63:e02623-18. https://doi.org/10.1128/AAC.02623-18.
7. Dubée V, Bernut A, Cortes M, Lesne T, Dorchene D, Lefebvre AL, Hugonnet JE, Gutmann L, Mainardi JL, Herrmann JL, Gaillard JL, Kremer L, Arthur M. 2015. β-Lactamase inhibition by avibactam in *Mycobacterium abscessus*. J Antimicrob Chemother 70:1051–1058. https://doi.org/10.1093/jac/dku510.
8. Dubée V, Soroka D, Cortes M, Lefebvre AL, Gutmann L, Hugonnet JE, Arthur M, Mainardi JL. 2015. Impact of β-lactamase inhibition on the activity of ceftaroline against *Mycobacterium tuberculosis* and *Mycobacterium abscessus*. Antimicrob Agents Chemother 59:2938–2941. https://doi.org/10.1128/AAC.05080-14.

9. Le Run E, Arthur M, Mainardi JL. 2019. *In vitro* and intracellular activity of imipenem combined with tedizolid, rifabutin, and avibactam against *Mycobacterium abscessus*. Antimicrob Agents Chemother 63:e01915-18. https://doi.org/10.1128/AAC.01915-18.
10. Le Run E, Arthur M, Mainardi JL. 2018. *In vitro* and intracellular activity of imipenem combined with rifabutin and avibactam against *Mycobacterium abscessus*. Antimicrob Agents Chemother 62:e00623-18. https://doi.org/10.1128/AAC.00623-18.
11. Lindman M, Dick T. 2019. Bedaquiline eliminates bactericidal activity of β-lactams against *Mycobacterium abscessus*. Antimicrob Agents Chemother 63:e00827-19. https://doi.org/10.1128/AAC.00827-19.
12. Dupont C, Viljoen A, Thomas S, Roquet-Banères F, Herrmann JL, Pethe K, Kremer L. 2017. Bedaquiline inhibits the ATP synthase in *Mycobacterium abscessus* and is effective in infected zebrafish. Antimicrob Agents Chemother 61:e01225-17. https://doi.org/10.1128/AAC.01225-17.
13. Ferro BE, Srivastava S, Deshpande D, Pasipanodya JG, van Soolingen D, Mouton JW, van Ingen J, Gumbo T. 2016. Failure of the amikacin, cefoxitin, and clarithromycin combination regimen for treating pulmonary *Mycobacterium abscessus* infection. Antimicrob Agents Chemother 60:6374–6376. https://doi.org/10.1128/AAC.00990-16.
14. Kramnik I, Dietrich WF, Demant P, Bloom BR. 2000. Genetic control of resistance to experimental infection with virulent *Mycobacterium tuberculosis*. Proc Natl Acad Sci U S A 97:8560–8565. https://doi.org/10.1073/pnas.150227197.
15. Pan H, Yan BS, Rojas M, Shebzukhov YV, Zhou H, Kobzik L, Higgins DE, Daly MJ, Bloom BR, Kramnik I. 2005. *Ipr1* gene mediates innate immunity to tuberculosis. Nature 434:767–772. https://doi.org/10.1038/nature03419.
16. Ruth MM, Sangen JJN, Remmers K, Pennings LJ, Svensson E, Aarnoutse RE, Zweijpfenning SMH, Hoefsloot W, Kuipers S, Magis-Escurra C, Wertheim HFL, van Ingen J. 2019. A bedaquiline/clofazimine combination regimen might add activity to the treatment of clinically relevant non-tuberculous mycobacteria. J Antimicrob Chemother 74:935–943. https://doi.org/10.1093/jac/dky526.
17. Odds FC. 2003. Synergy, antagonism, and what the chequerboard puts between them. J Antimicrob Chemother 52:1. https://doi.org/10.1093/jac/dkg301.
18. Li W, Sanchez-Hidalgo A, Jones V, de Moura VC, North EJ, Jackson M. 2017. Synergistic interactions of MmpL3 inhibitors with antitubercular compounds *in vitro*. Antimicrob Agents Chemother 61:e02399-16. https://doi.org/10.1128/AAC.02399-16.
19. Clinical and Laboratory Standards Institute. 2018. Susceptibility testing of mycobacteria, Nocardiae spp., and other aerobic actinomycetes—3rd ed. CLSI standard M24. Clinical and Laboratory Standards Institute, Wayne, PA.
20. Cigana C, Lorè NI, Riva C, De Fino I, Spagnuolo L, Sipione B, Rossi G, Nonis A, Cabrini G, Bragonzi A. 2016. Tracking the immunopathological response to *Pseudomonas aeruginosa* during respiratory infections. Sci Rep 6:21465. https://doi.org/10.1038/srep21465.
21. Bernut A, Le Moigne V, Lesne T, Lutfalla G, Herrmann JL, Kremer L. 2014. *In vivo* assessment of drug efficacy against *Mycobacterium abscessus* using the embryonic zebrafish test system. Antimicrob Agents Chemother 58:4054–4063. https://doi.org/10.1128/AAC.00142-14.
22. Le Moigne V, Rottman M, Goulard C, Barteau B, Poncin I, Soismier N, Canaan S, Pitard B, Gaillard JL, Herrmann JL. 2015. Bacterial phospholipases C as vaccine candidate antigens against cystic fibrosis respiratory pathogens: the *Mycobacterium abscessus* model. Vaccine 33:2118–2124. https://doi.org/10.1016/j.vaccine.2015.03.030.
23. Ordway D, Henao-Tamayo M, Smith E, Shanley C, Harton M, Troudt J, Bai X, Basaraba RJ, Orme IM, Chan ED. 2008. Animal model of *Mycobacterium abscessus* lung infection. J Leukoc Biol 83:1502–1511. https://doi.org/10.1189/jlb.1007696.
24. Pang Y, Zheng H, Tan Y, Song Y, Zhao Y. 2017. *In vitro* activity of bedaquiline against nontuberculous mycobacteria in China. Antimicrob Agents Chemother 61:e02627-16. https://doi.org/10.1128/AAC.02627-16.
25. Lerat I, Cambau E, Roth Dit Bettoni R, Gaillard JL, Jarlier V, Truffot C, Veziris N. 2014. *In vivo* evaluation of antibiotic activity against *Mycobacterium abscessus*. J Infect Dis 209:905–912. https://doi.org/10.1093/infdis/jit614.
26. Obregón-Henao A, Arnett KA, Henao-Tamayo M, Massoudi L, Creissen E, Andries K, Lenaerts AJ, Ordway DJ. 2015. Susceptibility of *Mycobacterium abscessus* to antimycobacterial drugs in preclinical models. Antimicrob Agents Chemother 59:6904–6912. https://doi.org/10.1128/AAC.00459-15.
27. Philley JV, Wallace RJ, Jr., Benwill JL, Taskar V, Brown-Elliott BA, Thakkar F, Aksamit TR, Griffith DE. 2015. Preliminary results of bedaquiline as salvage therapy for patients with nontuberculous mycobacterial lung disease. Chest 148:499–506. https://doi.org/10.1378/chest.14-2764.
28. Zweijpfenning SMH, Schildkraut JA, Coolen JPM, Ruesen C, Koenraad E, Janssen A, Ruth MM, de Jong AS, Kuipers S, Aarnoutse RE, Magis-Escurra C, Hoefsloot W, van Ingen J. 2019. Failure with acquired resistance of an optimised bedaquiline-based treatment regimen for pulmonary *Mycobacterium avium* complex disease. Eur Respir J 54:1900118. https://doi.org/10.1183/13993003.00118-2019.
29. Viljoen A, Raynaud C, Johansen MD, Roquet-Banères F, Herrmann JL, Daher W, Kremer L. 2019. Verapamil improves the activity of bedaquiline against *Mycobacterium abscessus in vitro* and in macrophages. Antimicrob Agents Chemother 63:e00705-19. https://doi.org/10.1128/AAC.00705-19.
30. Lenaerts AJ, Hoff D, Aly S, Ehlers S, Andries K, Cantarero L, Orme IM, Basaraba RJ. 2007. Location of persisting mycobacteria in a Guinea pig model of tuberculosis revealed by r207910. Antimicrob Agents Chemother 51:3338–3345. https://doi.org/10.1128/AAC.00276-07.

Supplementary Figure 1

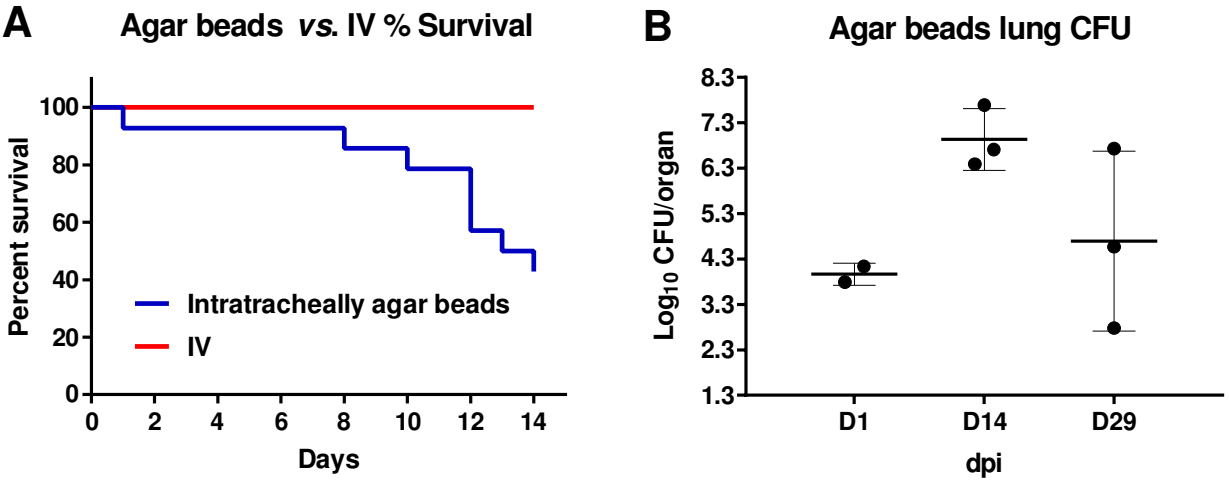

Figure 1. (A) Survival of C3HeB/FeJ mice infected intratracheally or intravenously (IV) with *M. abscessus* CIP 104536^T (smooth variant). (B) Persistence of *M. abscessus* in the lungs of intratracheally-infected C3HeB/FeJ mice. Agar beads where prepared as described previously (1). Mice were infected with a solution of agar beads containing 2.10^5 CFUs/mouse in 50 µl. Survival curves were generated over a 14 days post-infection experiment. Mouse lungs were collected and homogenized, serially diluted and plated onto VCAT (Vancomycin, Colistin sulfate, Amphotericin B, and Trimethoprim) chocolate agar plates (BioMérieux, France) and incubated for 5-6 days at 37°C prior to CFU count. Results are expressed as $\log_{10}$ units of CFU at 1, 14 and 29 dpi. Results are representative of one of two independent experiments (A and B) with similar results.

Supplementary Figure 2

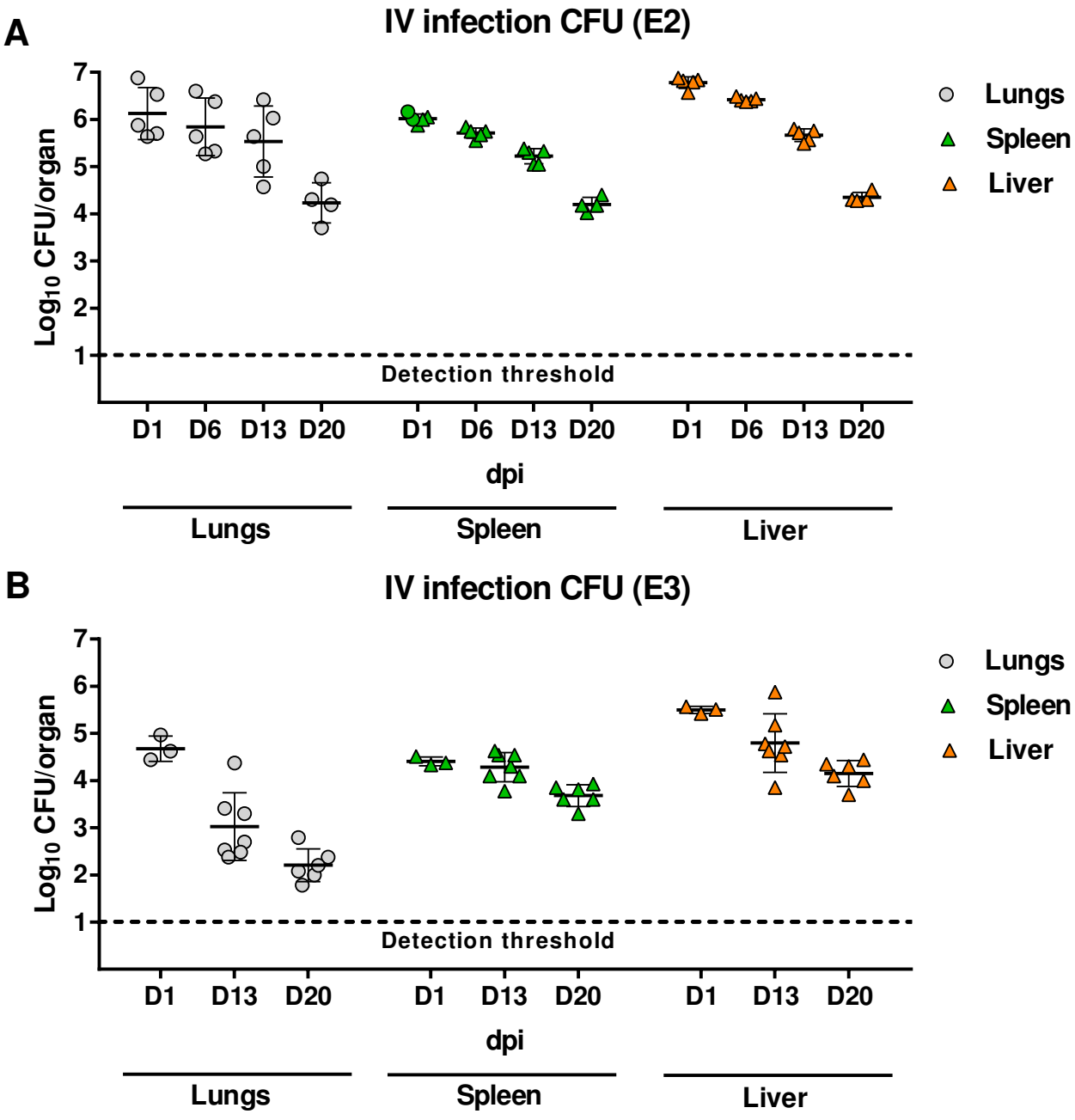

Supplementary Figure 2. Bacterial persistence of *M. abscessus* CIP 104536^T (rough variant) in the lungs, spleen and liver of C3HeB/FeJ mice after infection in the tail vein with 4.8×10^6 (A) and 3.1×10^5 CFU/mouse (B) in a total volume of 200 µl of water containing 0.9% sodium chloride. The following day, three mice were euthanized and whole organs were harvested to determine baseline bacterial burden. CFU were determined as described in Fig.S1. Results are expressed as the $\log_{10}$ units of CFU at 1, (6), 13 and 20 dpi.

REFERENCES

1. Cigana C, Lorè NI, Riva C, De Fino I, Spagnuolo L, Sipione B, Rossi G, Nonis A, Cabrini G, Bragonzi A. 2016. Tracking the immunopathological response to *Pseudomonas aeruginosa* during respiratory infections. Sci Rep 6:21465.

Article 5: "Rifabutin is bactericidal against intracellular and extracellular forms of *Mycobacterium abscessus*"

Matt D. Johansen, Wassim Daher, Françoise Roquet-Banères, Clément Raynaud, Matthéo Alcaraz, Florian P. Maurer and Laurent Kremer, 2020, *Antimicrobial Agents and Chemotherapy,* https://doi.org/10.1128/AAC.00363-20. (Johansen et al. 2020)

La RFB est une rifamycine de nouvelle génération utilisée contre *M. tuberculosis* et récemment plusieurs études ont démontré son efficacité contre *M. abscessus* ce qui en fait une excellente candidate pour être repositionnée dans le traitement de ces infections (Aziz et al. 2017; Pryjma et al. 2018a). Plus récemment, son efficacité contre *M. abscessus* a été montrée dans un modèle murin SCID renforçant l'intérêt thérapeutique pour cette molécule (Dick et al. 2020).

L'objectif de ce travail a consisté à étudier plus précisément l'efficacité de la RFB contre les différentes formes lisse et rugueuse de *M. abscessus* qu'elles soient extracellulaires et intracellulaires. Pour cela, les CMI ont été déterminées contre la souche de référence ainsi que contre des isolats cliniques. Nous avons ensuite évalué l'activité de la rifabutine contre les formes intramacrophagiques de *M. abscessus*. Enfin, la même expérience a été répétée dans un modèle d'infection de zebrafish. Par ailleurs, le gène *MAB_1408c* codant pour une pompe à efflux a été surexprimé chez *M. abscessus,* conduisant à une augmentation de la CMI de la RFB, suggérant que cette pompe à efflux pourrait extruder la RFB hors de la bactérie. Enfin, la génération de mutants résistants spontanés sélectionnés sur des hautes doses de RFB a permis d'identifier des mutations ponctuelles dans le gène *rpoB* chez *M. abscessus,* ce qui permet de confirmer que, comme chez *M. tuberculosis*, *rpoB* code pour la cible de la RFB. Dans cette étude, j'ai été plus particulièrement impliqué dans la partie infection de macrophages et dans la recherche de la cible de la RFB.

AMERICAN SOCIETY FOR MICROBIOLOGY | Antimicrobial Agents and Chemotherapy®

Rifabutin Is Bactericidal against Intracellular and Extracellular Forms of *Mycobacterium abscessus*

Matt D. Johansen,[a] Wassim Daher,[a,b] Françoise Roquet-Banères,[a] Clément Raynaud,[a] Matthéo Alcaraz,[a] Florian P. Maurer,[c,d] Laurent Kremer[a,b]

[a]Centre National de la Recherche Scientifique UMR 9004, Institut de Recherche en Infectiologie de Montpellier (IRIM), Université de Montpellier, Montpellier, France
[b]INSERM, IRIM, Montpellier, France
[c]National and WHO Supranational Reference Center for Mycobacteria, Research Center Borstel-Leibniz Lung Center, Borstel, Germany
[d]Institute of Medical Microbiology, Virology, and Hygiene, University Medical Center Hamburg-Eppendorf, Hamburg, Germany

ABSTRACT *Mycobacterium abscessus* is increasingly recognized as an emerging opportunistic pathogen causing severe lung diseases. As it is intrinsically resistant to most conventional antibiotics, there is an unmet medical need for effective treatments. Repurposing of clinically validated pharmaceuticals represents an attractive option for the development of chemotherapeutic alternatives against *M. abscessus* infections. In this context, rifabutin (RFB) has been shown to be active against *M. abscessus* and has raised renewed interest in using rifamycins for the treatment of *M. abscessus* pulmonary diseases. Here, we compared the *in vitro* and *in vivo* activity of RFB against the smooth and rough variants of *M. abscessus*, differing in their susceptibility profiles to several drugs and physiopathologial characteristics. While the activity of RFB is greater against rough strains than in smooth strains *in vitro*, suggesting a role of the glycopeptidolipid layer in susceptibility to RFB, both variants were equally susceptible to RFB inside human macrophages. RFB treatment also led to a reduction in the number and size of intracellular and extracellular mycobacterial cords. Furthermore, RFB was highly effective in a zebrafish model of infection and protected the infected larvae from *M. abscessus*-induced killing. This was corroborated by a significant reduction in the overall bacterial burden, as well as decreased numbers of abscesses and cords, two major pathophysiological traits in infected zebrafish. This study indicates that RFB is active against *M. abscessus* both *in vitro* and *in vivo*, further supporting its potential usefulness as part of combination regimens targeting this difficult-to-treat mycobacterium.

KEYWORDS *Mycobacterium abscessus*, rifabutin, macrophage, zebrafish, therapeutic activity

Nontuberculous mycobacteria (NTM) are environmental mycobacteria. Among all NTM, *Mycobacterium avium* and *Mycobacterium abscessus* represent the most frequent pathogens associated with pulmonary disease (1). *M. abscessus* is a rapidly growing NTM of increasing clinical significance, particularly in cystic fibrosis (CF) patients (2). In CF patients, infection with *M. abscessus* correlates with a more rapid decline in lung function and can represent an obstacle to subsequent lung transplantation (3–5). From a taxonomical view, the species currently comprises three subspecies, *M. abscessus* subsp. *abscessus* (here designated *M. abscessus*), *M. abscessus* subsp. *bolletii* (here designated *M. bolletii*), and *M. abscessus* subsp. *massiliense* (here designated *M. massiliense*) (6). These subspecies exhibit different clinical outcomes and drug susceptibility profiles to antibiotic treatments (7).

M. abscessus strains can exhibit either a smooth (S) or rough (R) morphotype as a consequence of the presence or absence, respectively, of bacterial surface glycopep-

Citation Johansen MD, Daher W, Roquet-Banères F, Raynaud C, Alcaraz M, Maurer FP, Kremer L. 2020. Rifabutin Is bactericidal against intracellular and extracellular forms of *Mycobacterium abscessus*. Antimicrob Agents Chemother 64:e00363-20. https://doi.org/10.1128/AAC.00363-20.

Address correspondence to Laurent Kremer, laurent.kremer@irim.cnrs.fr.

Received 25 February 2020
Returned for modification 4 May 2020
Accepted 3 August 2020
Accepted manuscript posted online 17 August 2020
Published 20 October 2020

tidolipids (GPL) (1, 8–10). These morphological distinctions are associated with important physiological differences. S variants are more hydrophilic than R variants, enabling increased sliding motility and the capacity to form biofilms (8, 9, 11), while the aggregative R variants possess a high propensity to produce large bacterial cords (11, 12). While S and R variants can be viewed as two representatives of the same isolate, which can coexist and evolve differently in response to host immunity, they express different pathophysiological traits (10). S variants are typically less virulent than the R variants (11, 13, 14), the latter being more frequently associated with severe lung diseases and persisting for years in CF patients (3, 5). Importantly, an S-to-R transition within the colonized host (5, 15) is linked to genetic polymorphisms within the GPL biosynthetic/transport locus (15, 16). Moreover, differences in the susceptibility to drug candidates have been identified between S and R variants (17, 18), highlighting the need for the improved evaluation of new compounds/drug regimens against both morphotypes.

Treatment of *M. abscessus* lung disease remains particularly challenging, largely due to intrinsic resistance to a wide panel of antimicrobial agents, including most antitubercular drugs such as rifampin (RIF) (19–22). The extensive resistome of *M. abscessus* results from a low permeability of the cell wall, absence of drug-activating systems, induction of efflux pumps, and production of a wide panel of drug-modifying enzymes (19, 22, 23). In addition, mutations in genes encoding drug targets can result in acquired drug resistance, further complicating therapy (1, 24). Treatment of infections caused by *M. abscessus* require prolonged courses of multiple antibiotics, usually combining a macrolide (azithromycin or clarithromycin), a β-lactam (imipenem or cefoxitin), and an aminoglycoside (amikacin) (25–27). Additional drugs, such as tigecycline or clofazimine, are often added to strengthen the regimen, particularly in response to toxic side effects or unsatisfactory clinical response (28). Despite intensive chemotherapy, treatment success rates typically remain around 25 to 40% in the case of macrolide resistance, which occurs in at least 40 to 60% of clinical isolates (29). Therefore, there is an urgent clinical need for new drug regimens with improved efficacy (30). While the current drug pipeline against *M. abscessus* remains poor, it has recently been fueled with the discovery of several active hits and the development of repurposed drugs (24). Among the latter, screening of libraries of approved pharmaceuticals revealed that rifabutin (RFB), a rifamycin related to the poorly active rifampicin (RIF), shows activity against *M. abscessus* (31, 32). RIF, along with many other rifamycins, is inactivated by the ADP-ribosyltransferase (Arr_{Mab}) encoded by *MAB_0591*, which ribosylates the drug at the C23 hydroxyl position (33). RFB has also been reported to be as active as clarithromycin in immunocompromised NOD/SCID mice infected with *M. abscessus* (34). However, most studies of RFB have been carried out on either S or R variants (when reported), rendering results sometimes difficult to interpret and/or to compare. Due to the coexistence of S and R variants in patients (15) and the presence of each variant in different compartments (S residing mostly in macrophages and R growing also in the form of intra- or extracellular cords), it is essential to address the activity of RFB on isogenic S/R pairs in both *in vitro* and *in vivo* studies.

The present study aimed to describe and compare the activity of RFB against S and R *M. abscessus* complex strains *in vitro* and *ex vivo* in a macrophage infection model. Due to the importance of cording, considered a marker of severity of the infection with the R variant, we also investigated the efficacy of RFB in a zebrafish model of infection.

RESULTS

Rough *M. abscessus* is more susceptible to RFB treatment than smooth *M. abscessus in vitro*. Exposure of exponentially growing *M. abscessus* CIP104536^T S and R isogenic variants to increasing concentrations of RFB, starting at 25 μg/ml for S and 6.25 μg/ml for R, resulted in a noticeable growth inhibition (Fig. 1). At the lowest concentration, the CFU at 72 h posttreatment remained comparable to that of the inoculum, suggestive of a bacteriostatic effect. However, the highest RFB concentrations for both S (200 μg/ml) and R (50 μg/ml) variants were accompanied by a 1.81- and

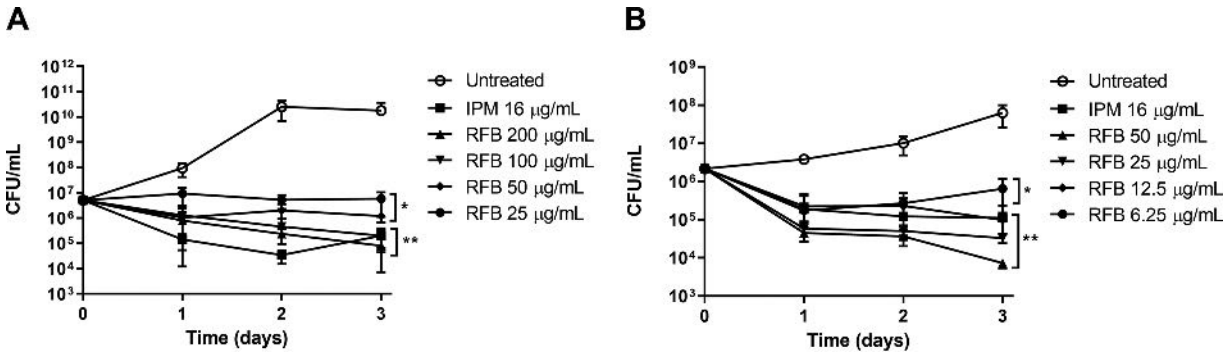

FIG 1 (A and B) *In vitro* activity of rifabutin. *M. abscessus* CIP104536^T S (A) or R (B) was exposed either to 200, 100, 50, 25, 12.5, or 6.25 μg/ml RFB or 16 μg/ml IPM in CaMHB at 30°C. At various time points, bacteria were plated on LB agar and further incubated at 30°C for 4 days prior to CFU counting. Results are expressed as the mean of triplicates ± the standard deviation (SD) and are representative of two independent experiments. *, $P \leq 0.05$; **, $P \leq 0.01$.

2.47-log reduction in the CFU counts at 72 h posttreatment, respectively (Fig. 1). While similar bactericidal effects of RFB were observed against both variants, this was achieved with lower concentrations of RFB against the R variant relative to the isogenic S variant. Overall, RFB at concentrations of 12.5 μg/ml (for the R variant) resulted in a killing effect comparable to that of imipenem (IPM) used at the MIC (16 μg/ml), which is known as an active β-lactam drug against *M. abscessus* (35) (Fig. 1).

To confirm the differences in the susceptibility to RFB, we determined the MIC of the CIP104536^T S and R variants in cation-adjusted Mueller-Hinton broth (CaMHB). Table 1 clearly shows that the S strain is 4-fold more resistant than its R counterpart. However, both variants were similarly resistant to other rifamycins (RIF, rifapentine [RPT], and rifaximin [RFX]), in agreement with previous studies (32, 34). Our MIC values, obtained in repetitive experiments with two different commercial sources of RFB, were higher than those reported earlier (32, 34) but comparable to values reported in another study (36). Consistent with other studies (31), we also noticed that the MIC values were dependent on the culture medium (see Table S1 in the supplemental material). Interestingly, MICs of RFB against S and R strains were lower in Middlebrook 7H9 broth than CaMHB, but this effect was lost when supplementing the medium with oleic acid-albumin-dextrose-catalase (OADC) enrichment. In contrast, the S and R strains displayed equal susceptibility levels to RFB in Sauton's medium.

To investigate the relationship between RFB activity and GPL production, drug susceptibility was assessed in CaMHB using the GPL-deficient Δ*mmpL4b* mutant, generated in the S background of the type strain CIP104536^T, and its complemented counterpart (14, 37, 38). The *mmpL4b* gene encodes the MmpL4b transporter, which participates in the translocation of GPL across the inner membrane (37, 39). Mutations in this gene are associated with loss of GPL and acquisition of an R morphotype (13, 37). The parental S strain, and to a lesser extent the Δ*mmpL4b*-complemented strain, showed reduced susceptibility to RFB (MIC, 32 to 64 μg/ml) compared to the *M.*

TABLE 1 Drug susceptibility/resistance profile of smooth and rough variants derived from the reference *M. abscessus* 104536^T strain to various rifamycins in CaMBH[b]

Strain	Morphotype	MIC (μg/ml)[a]			
		RFB	RIF	RPT	RFX
CIP104536 (S)	S	64	>128	>128	>128
CIP104536 (R)	R	16	>128	>128	>128
ΔMAB_mmpL4b	R	16	>128	>128	>128
ΔMAB_mmpL4b_C	S	32	>128	>128	>128
CIP104536 (S) + pMV306-MAB_1409c-HA	S	64	>128	>128	>128
CIP104536 (R) + pMV306-MAB_1409c-HA	R	64	>128	>128	>128

[a]MICs (μg/ml) were determined following the CLSI guidelines.
[b]RFB, rifabutin; RIF, rifampin; RPT, rifapentine; RFX, rifaximin.

TABLE 2 Comparison of the activity of RFB against clinical isolates from CF and non-CF patients[a]

Species and strain	Morphotype	Source	RFB MIC (μg/ml)
M. abscessus			
CIP104536	S	Non-CF	50
3321	S	Non-CF	50
1298	S	CF	50
2587	S	CF	100
2069	S	Non-CF	100
CF	S	CF	25
2524	R	CF	25
2648	R	CF	25
3022	R	Non-CF	50
5175	R	CF	25
CIP104536	R	Non-CF	25
M. massiliense			
CIP108297	R	Addison's disease	50
210	R	CF	100
179	R	CF	100
CIP108297	S	Addison's disease	100
140	S	CF	50
185	S	CF	100
107	S	CF	50
122	S	CF	100
120	S	CF	6.25
212	S	CF	100
100	S	CF	100
111	S	CF	100
M. bolletii			
CIP108541	S	None reported	100
114	S	CF	100
17	S	CF	50
116	S	CF	100
97	S	CF	100
112	R	CF	100
19	R	Non-CF	50
10	R	None reported	100
108	R	CF	25

[a]The MIC (μg/ml) was determined in cation-adjusted Mueller-Hinton broth for different subspecies belonging to the *M. abscessus* complex. Results are from 3 independent experiments. RFB, rifabutin

abscessus R strain and the GPL-deficient Δ*mmpL4b* mutant (MIC, 16 μg/ml) (Table 1). The MIC results are in agreement with the growth inhibition kinetics (Fig. 1) and suggest that the outer GPL layer influences the activity of RFB.

M. abscessus possesses numerous potential drug efflux systems (39), including MAB_1409c, a homolog of Rv1258c, previously reported to mediate efflux of RIF in *M. tuberculosis* (40). We thus addressed whether overexpression of MAB_1409c induces resistance to RFB in *M. abscessus*. *MAB_1409c* was cloned in frame with a hemagglutinin (HA) tag in the integrative vector, pMV306. The resulting construct pMV306-*MAB_1409c*-HA was introduced in both S and R variants, and the expression of MAB_1409c was confirmed by Western blotting analysis using anti-HA antibodies (Fig. S1). Drug susceptibility assessment indicated a 4-fold upshift in the MIC of RFB against the R strain carrying pMV306-*MAB_1409c*-HA, while no changes in the MIC were observed with the S strain overproducing MAB_1409c (Table 1). This suggests that increasing expression of MAB_1409c in the R variant is likely to mediate efflux of RFB, leading to reduced susceptibility to the drug.

RFB is active against S and R *M. abscessus* isolates *in vitro*. The activity of RFB was next tested using a set of clinical strains isolated from CF patients or non-CF patients. In general, the MIC of R strains were 2 to 4 times lower than those of S strains, although there were variations among the strains (Table 2). Some R strains (10, 112, 179, 210) exhibited higher MIC values (100 μg/ml) than the reference CIP104536^T R strain,

TABLE 3 Characteristics of spontaneous RFB-resistant mutants of *M. abscessus*[a]

Strain	MIC (μg/ml)	Mutation in *rpoB*	
		SNP	AA change
CIP104536^T (R)	12.5		
25.1	50	C1339T	H447Y
25.2	100	C1339G	H447D
50.1	50	C1339T	H447Y
50.2	50	C1355T	S452L

[a]MICs (μg/ml) were determined in cation-adjusted Mueller-Hinton broth. Resistant strains were derived from the rough *M. abscessus* CIP104536^T parental strain on Middlbrook 7H10 supplemented with either 25 or 50 μg/ml RFB. Single-nucleotide polymorphism identification in *rpoB* (*MAB_3869c*) and corresponding amino acid changes are also indicated. RFB, rifabutin; AA, amino acid.

while one S strain appeared particularly susceptible to RFB (*M. massiliense* 120 with a MIC of 6.25 μg/ml). These differences between strains and S/R morphotypes were not observed previously with bedaquiline (BDQ), and S and R variants were also equally sensitive to BDQ (41). Overall, these results demonstrate that RFB is active against *M. abscessus*, including isolates from CF patients, while R variants appear in general more susceptible to RFB than S variants, supporting previous findings (42).

Mutations in *rpoB* confer resistance to RFB. Although rifamycin resistance mechanisms mediated by mutations in the *rpoB* gene coding for the β-subunit of RNA polymerase have been widely described for *M. tuberculosis*, this is not the case for *M. abscessus*. Therefore, to identify the mechanism of resistance of RFB, a genetic approach involving the selection of spontaneous RFB-resistant mutants of *M. abscessus* followed by *rpoB* sequencing was applied. Four spontaneous strains were isolated in the presence of 25 or 50 μg/ml RFB, exhibiting 4- to 8-fold increased resistance levels, respectively, compared to the parental strain (Table 3). Sequencing analyses of *rpoB* identified several single nucleotide polymorphisms (SNPs) across four resistor mutants. In mutants 25.1 and 50.1, a C1339T substitution leading to an amino acid change at position 447 (H447Y) was identified. Similarly, in mutant 25.2, a C1339G replacement was found, resulting in an amino acid substitution at position 447 (H447D). Comparatively, in mutant strain 50.2, another SNP (C1355T) occurred, leading to an amino acid change at position 452 (S452L). A comparison of the growth of different resistant strains on agar plates containing increasing concentrations of RFB is shown in Fig. S2. Whereas RFB abrogated growth of the wild-type S and R strains, growth of all four resistors harboring mutations at either position 447 or 452 sustained bacterial growth at 50 μg/ml, confirming that mutations in *rpoB* confer resistance to RFB.

***M. abscessus* S and R strains are equally susceptible to RFB in macrophages.** While RFB has been shown to be active against *M. tuberculosis* in a macrophage infection model (43), this has not been thoroughly investigated for *M. abscessus*. We thus compared the intracellular efficacy of RFB in THP-1 macrophages infected with either S or R variants. First, the cytotoxicity of RFB and RIF against THP-1 cells was investigated over a 3-day exposure period to either drug. Fig. S3 clearly shows that RFB exerts significant cytotoxicity at concentrations of >25 μg/ml and that the kinetics of macrophage killing was more rapid with RFB than with RIF. Based on these results, all subsequent macrophage studies used 50 μg/ml RIF or 12.5 μg/ml RFB. Amikacin (AMK) at 50 μg/ml was added as a positive control. Dimethyl sulfoxide (DMSO)-treated macrophages were included as a negative control for intracellular bacterial replication. At 0, 1, and 3 days postinfection (dpi), macrophages were lysed and plated to determine the intracellular bacterial loads following drug treatment. Whereas the presence of DMSO or RIF failed to inhibit intramacrophage growth of *M. abscessus* S, exposure to RFB strongly decreased the intracellular bacterial loads at 1 dpi, with this effect further exacerbated at 3 dpi (Fig. 2A). As anticipated, treatment with RIF did not show any effect, in agreement with the poor activity of this compound *in vitro* (Table 1). Comparatively, AMK treatment resulted in a significantly reduced intracellular growth rate in both *M. abscessus* S and R variants between 1 and 3 dpi. Interestingly, the RFB

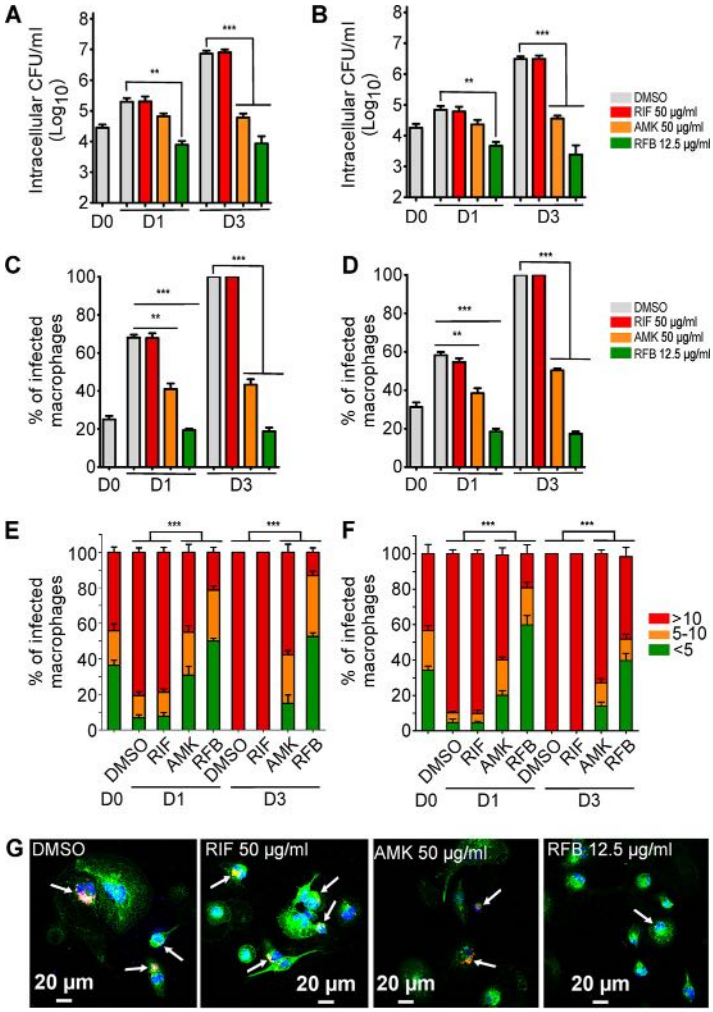

FIG 2 Intracellular activity of RFB on *M. abscessus*-infected THP-1 cells. (A and B) Macrophages were infected with (A) *M. abscessus* S-morphotype and (B) R-morphotype expressing TdTomato (MOI of 2:1) for 3 h prior to treatment with RIF (50 μg/ml), AMK (50 μg/ml), RFB (12.5 μg/ml), or DMSO. CFU were determined at 0, 1, and 3 dpi. Data are mean values ± SD for three independent experiments. Data were analyzed using a one-way analysis of variance (ANOVA) Kruskal-Wallis test. (C and D) Percentage of infected THP-1 macrophages at 0, 1, and 3 days after infection with (C) *M. abscessus* S or (D) *M. abscessus* R. Data are mean values ± SD for three independent experiments. Data were analyzed using a one-way ANOVA Kruskal-Wallis test. (E) Percentage of S-infected macrophage categories and (F) percentage of R-infected macrophage categories infected with different numbers of bacilli (<5 bacilli, 5 to 10 bacilli, and >10 bacilli). The categories were counted at 0 or at 1 and 3 days postinfection in the absence of antibiotics or in the presence of RIF or AMK at 50 μg/ml or RFB at 12.5 μg/ml. Values are means ± SD from three independent experiments performed in triplicate. (G) Four immunofluorescent fields were taken at 1 day postinfection showing macrophages infected with *M. abscessus* expressing Tdtomato (red). The surface and the endolysosomal system of the macrophages were detected using anti-CD63 antibodies (green). The nuclei were stained with DAPI (blue). White arrows indicate individual or aggregate mycobacteria. Scale bar, 20 μm. **, $P \leq 0.01$; ***; $P \leq 0.001$.

susceptibility profile for the S variant at 1 and 3 dpi was comparable to that of the R variant, with an ~3-log reduction in the CFU counts (Fig. 2A and B, respectively).

Macrophages were next infected with *M. abscessus* strains expressing Tdtomato and exposed to either DMSO, AMK, RIF, or RFB, followed by staining with anti-CD63 and DAPI (4′,6-diamidino-2-phenylindole) and observation under a confocal microscope. A quantitative analysis confirmed the marked reduction in the number of *M. abscessus* S-infected THP-1 cells treated with AMK and RFB at 1 and 3 dpi compared to RIF-treated cells or untreated control cells (Fig. 2C). A similar trend was observed when macrophages were infected with *M. abscessus* R (Fig. 2D).

Macrophages infected with the S variant were then classified into three categories based on their bacterial burden, poorly infected (<5 bacilli), moderately infected (5 to 10 bacilli), and heavily infected (>10 bacilli) macrophages. Cells containing bacilli were then individually observed under the microscope and scored to one of the three categories. The quantitative analysis indicates that exposure to RFB significantly reduces the percentage of S variant heavily infected THP-1 cells while increasing the proportion of the poorly infected category compared to the untreated cells at 1 dpi (Fig. 2E). At 3 dpi, the effect of RFB was even more pronounced, with 10% of the infected bacilli belonging to the heavily infected category and more than 50% associated with the poorly infected category. Analysis performed on cells infected with the R variant generated a similar category profile, although treatment with RFB was associated with a higher proportion of heavily infected macrophages at 3 dpi with the R variant than with the S variant (Fig. 2F). Fig. 2G illustrates the reduced number of *M. abscessus* S in infected THP-1 cells treated with RFB at 1 dpi compared to the untreated control cells (DMSO) or those treated with RIF or AMK. Collectively, these results indicate that RFB enters THP-1 macrophages and similarly impedes bacterial replication of both *M. abscessus* S and R variants.

RFB reduces the intramacrophage growth of clinical isolates. RFB has recently shown vast potential as an effective antibiotic for the treatment of *M. abscessus* infection in a NOD/SCID murine model (34). However, to date, the efficacy of RFB has only been evaluated against a limited panel of *M. abscessus* clinical isolates within an infection setting. As such, we explored the activity of RFB against S and R clinical isolates of the *M. abscessus* complex with varying MIC values against RFB within THP-1 macrophages. In support of our previous findings in infected macrophages, RFB treatment (12.5 or 25 μg/ml) was very active against all *M. abscessus* subspecies within macrophages at 1 and 3 dpi compared to day 0 and DMSO treatment (Fig. 3), irrespective of S and R morphotypes and the corresponding MIC values (Table 2). Overall, these findings suggest that RFB is very effective against intracellular clinical isolates and highlights the lack of direct correlation between MICs determined *in vitro* and the intracellular activity of RFB.

Reduced intra- and extracellular cording by RFB treatment. An important phenotypic difference between S and R morphotypes is that R morphotypes display increased bacterial aggregation. R bacilli remain attached during replication, forming compact colonies containing structures that resemble cords on agar and in broth medium (8, 12, 14). Fig. 4A clearly shows that, upon infection with *M. abscessus* R expressing TdTomato, the total number of cords per field was significantly reduced in the presence of 50 μg/ml AMK or 12.5 μg/ml RFB compared to 50 μg/ml RIF or DMSO alone. Moreover, we observed intracellular cords that are capable of growing inside the macrophage as well as in the extracellular milieu, which were easily observable at 3 dpi (Fig. 4B). As illustrated in Fig. 4C, treatment with AMK or RFB strongly impacted both intra- and extracellular cords. While AMK treatment severely reduced the number of both intra- and extracellular cords, this effect was almost completely abrogated with RFB at 3 dpi. Together, these results indicate that RFB is highly effective in reducing *M. abscessus* cords, which are thought to affect the outcome of the infection.

RFB treatment enhances protection of zebrafish infected with *M. abscessus*. *In vivo* drug efficacy has previously been well described using the zebrafish model of infection (41, 44, 45). Initial experiments indicated that RFB concentrations of ≤100 μg/ml (final concentration in fish water) did not interfere with larval development and was well tolerated in embryos when treatment was applied for 4 days with daily drug renewal (Fig. 5A). Higher concentrations of RFB, however, were associated with rapid larval death. As such, only lower RFB doses (≤100 μg/ml) were used in subsequent studies. Red fluorescent TdTomato-expressing *M. abscessus* (R variant) was microinjected in the caudal vein of embryos at 30 h postfertilization (hpf). RFB was directly added at 1 dpi to the water containing the infected embryos, with RFB-supplemented water changed on a daily basis for 4 days. Embryo survival was moni-

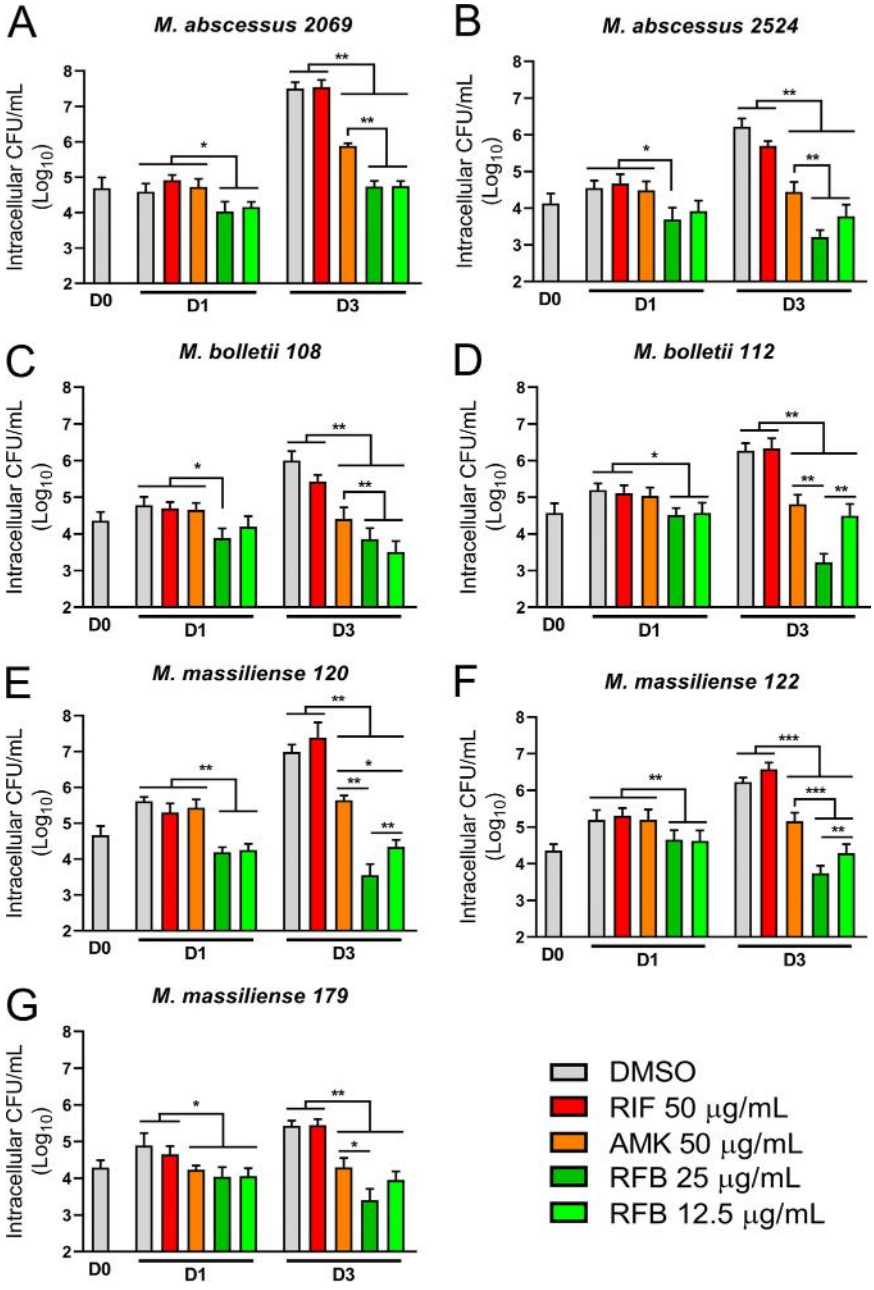

FIG 3 Intracellular activity of RFB on S and R clinical isolates. CFU counts of clinical isolates exposed to 25 and 12.5 μg/ml RFB. Macrophages were infected with *M. abscessus* (A and B), *M. bolletii* (C and D), or *M. massiliense* (E to G) clinical strains belonging to S or R morphotypes at an MOI of 2:1 for 3 h prior to treatment with 250 μg/ml AMK for 2 h to kill extracellular bacteria. Following extensive PBS washes, cells were exposed to 50 μg/ml RIF, 50 μg/ml AMK, or 25 or 12.5 μg/ml RFB. CFU were determined at 0, 1, and 3 days postinfection. Data are mean values $\pm$ SD for two independent experiments. Data were analyzed using the *t* test. *, $P \leq 0.05$; **, $P \leq 0.01$; ***, $P \leq 0.001$.

tored and recorded daily for 12 days. No decrease in the survival rate was observed in the presence of 5 μg/ml RFB; however, a significant dose-dependent increase in the survival of embryos exposed to 25 or 50 μg/ml RFB was observed compared to the untreated group (Fig. 5B). When exposed to 50 μg/ml RFB, the highest dose examined in this setting, nearly 80% of the treated embryos survived at 12 dpi, compared to 40% of the untreated group. This clearly indicates that RFB protects zebrafish from *M. abscessus* infection.

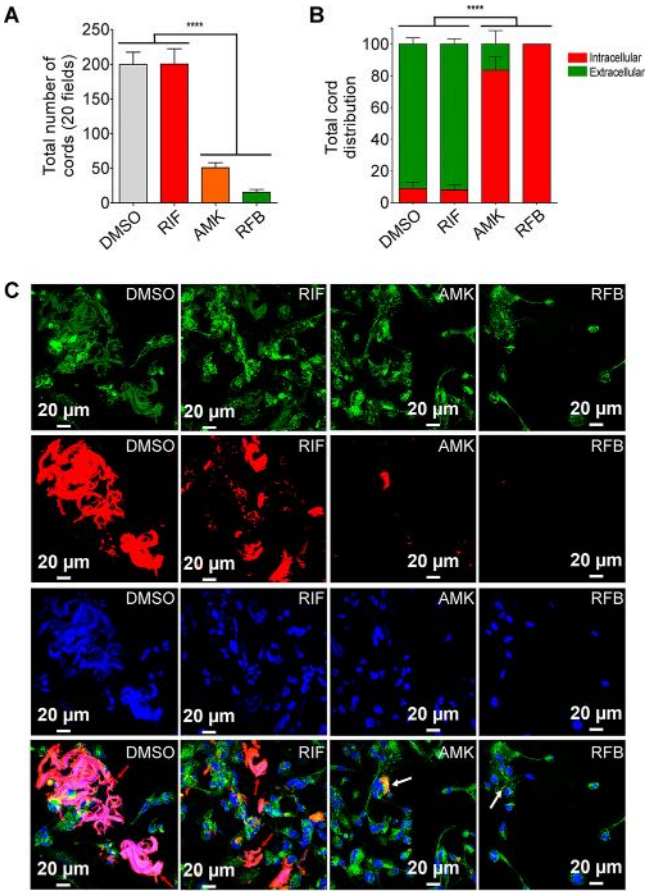

FIG 4 Activity of RFB on extracellular and intracellular cords. (A) Total number of cords displayed in 20 fields at 3 days after infection of macrophages with *M. abscessus* R variant. Data are mean values ± SD for three independent experiments performed in triplicate. Data were analyzed using one-tailed Mann-Whitney's *t* test. (B) Percentage of cords formed either extracellularly or intracellularly. The two categories were counted at 3 days postinfection in the absence of antibiotics or in the presence of 50 μg/ml RIF, 50 μg/ml AMK, or 12.5 μg/ml RFB. Extracellular or intracellular cords are highlighted using the indicated color codes. Values are means ± SD for two independent experiments performed each time in triplicate. (C) Four immunofluorescent fields were taken at 3 days postinfection showing the cords formed extracellularly or within macrophages infected with *M. abscessus* R variant expressing Tdtomato (red). Macrophages were infected for 3 days in the presence of DMSO, RIF (50 μg/ml), AMK (50 μg/ml), or RFB (12.5 μg/ml). The macrophage surface was stained using anti-CD63 antibodies (green). The nuclei were stained with DAPI (blue). White arrows indicate intracellular cords, while red arrows indicate extracellular cords. Scale bars represent 20 μm. Results represent the average of a total of 120 fields per condition. ****, $P \leq 0.0001$.

To test whether RFB exerts an effect on the bacterial burden in zebrafish, we quantified fluorescent pixel counts (FPC) (46). As expected, embryos treated with 50 μg/ml RFB had significantly decreased bacterial burdens at 2, 4, and 6 dpi compared to the untreated group (Fig. 5C). These results were corroborated by imaging whole embryos, which were characterized by the presence of large abscesses and cords in the brain when left untreated and which were observed much less frequently in the RFB-treated animals despite the presence of single bacilli or small aggregated bacteria (Fig. 5D).

RFB treatment reduces abscess formation by *M. abscessus* in zebrafish. Virulence of *M. abscessus* R variants in zebrafish is correlated with the presence of abscesses, particularly in the central nervous system (14, 46). To address whether the enhanced survival of RFB-treated fish is associated with decreased abscess formation, the percentages of abscesses and cords were determined by monitoring abscesses and cords in whole embryos, as reported previously (14, 46). Extracellular cords can be easily distinguished based on their serpentine-like shape and by their size, often greater

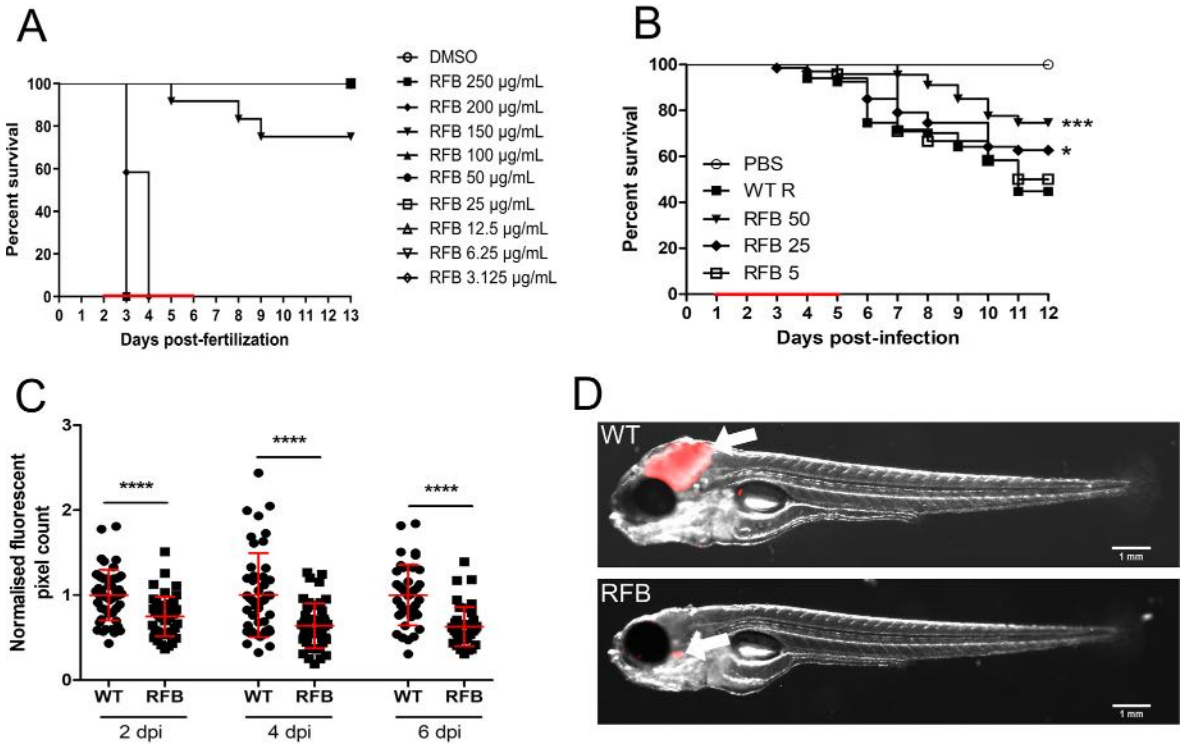

FIG 5 RFB displays high bactericidal activity against *M. abscessus* in an embryonic zebrafish infection model. (A) Groups of uninfected embryos were immersed in water containing increasing concentrations of RFB (ranging from 3.125 to 250 μg/ml) for 4 days. The red bar indicates the duration of treatment. The graph shows the survival of the RFB-treated and untreated (DMSO) embryos over a 12-day period. (B) Zebrafish embryos at 30 h post-fertilization were intravenously infected with approximately 250 to 300 CFU of *M. abscessus* CIP104536^T (R variant) expressing TdTomato ($n = 20$ to 25). A standard PBS injection control was included for each experiment. At 1 dpi, embryos were randomly split into equal groups of approximately 20 embryos per group, and various concentrations of RFB (5 to 50 μg/ml) were added to the water. DMSO was included as a positive control group. RFB was changed daily, after which, embryos were washed twice in fresh embryo water, maintained in embryo water, and monitored daily over a 12-day period. Each treatment group was compared against the untreated infected group with significant differences calculated using the log-rank (Mantel-Cox) statistical test for survival curves. Data shown are the merge of three independent experiments. (C) Bacterial burden was determined at 2, 4, and 6 days postinfection following treatment with either DMSO or 50 μg/ml RFB. Bacteria were quantified by fluorescent pixel count determination using ImageJ software, with each data point representing a single embryo. Error bars represent standard deviations. Statistical significance was determined using Student's *t* test. The plots represent a pool of 2 independent experiments containing approximately 20 to 25 embryos per group. (D) Representative embryos from the untreated group (WT) (top) and from the treated group with 50 μg/ml RFB at 6 days postinfection. White arrowheads show TdTomato-expressing bacteria. Scale bars represent 1 mm. *, $P \leq 0.05$; ***, $P \leq 0.001$; ****, $P \leq 0.0001$.

compared to the size of the surrounding macrophages and neutrophils. Exposure of infected embryos to 50 μg/ml RFB was accompanied by a significant decrease in the proportion of embryos with cords (Fig. 6A) at 4 dpi and the number of embryos with abscesses (Fig. 6B) at 4 and 6 dpi. This decrease in the physiopathological signs of RFB-treated larvae correlates also with the FPC analysis and whole-embryo imaging (Fig. 6C and D). Overall, these results demonstrate that RFB reduces the pathophysiology of *M. abscessus* infection in zebrafish larvae and protects them from bacterial killing.

DISCUSSION

Treatment success of infections caused by *M. abscessus* is unacceptably low even upon prolonged, multidrug chemotherapy with a significant risk of severe toxic side effects. Although RIF is used as a first-line drug against *M. tuberculosis*, it has no activity against *M. abscessus*. While ADP ribosyltransferases can utilize both RIF and RFB as substrates (47), a lower catalytic efficiency with RFB may explain its greater potency against *M. abscessus*. Our study supports and extends previous investigations highlighting the potential of RFB against *M. abscessus in vitro* against a wide panel of *M. abscessus* complex clinical isolates (31, 32, 48, 49). We found, however, that our MIC values were higher than those observed in previous investigations (31, 32). In our study,

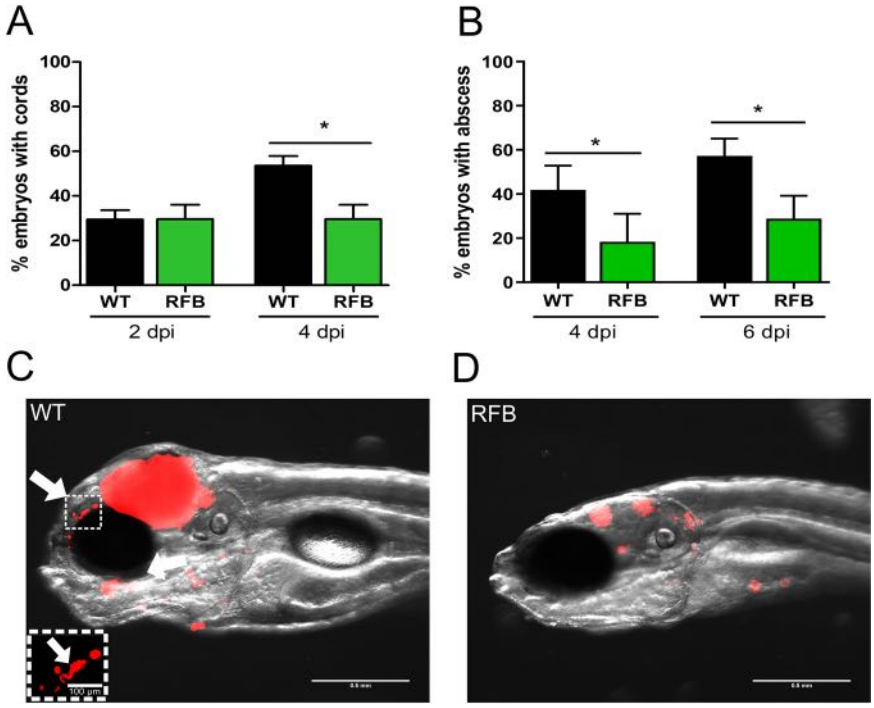

FIG 6 RFB reduces the pathophysiological traits of *M. abscessus* infection in zebrafish embryos. (A) Proportion of embryos with cords at 2 and 4 days postinfection in infected embryos that were either untreated or treated with 50 μg/ml RFB (250 to 300 CFU, $n = 30$). Data were analyzed using an unpaired Student's *t* test. Data shown are the mean of three independent experiments ± SD. (B) Total percentage of embryos with abscesses at 4 and 6 dpi in infected embryos that were either untreated or treated with 50 μg/ml RFB (250 to 300 CFU, $n = 30$). Data were analyzed using an unpaired Student's *t* test. Data shown are the mean of three independent experiments ± SD. (C and D) Representative zebrafish images of untreated (WT) embryos and those treated with 50 μg/ml RFB at 6 dpi. Scale bar represents 0.5 mm. White arrows indicate extracellular cords. The white box highlights a large extracellular cord based on the size and morphology, with the scale bar representing 100 μm. Red overlay represents *M. abscessus* expressing TdTomato. *, $P \leq 0.05$.

following the Clinical and Laboratory Standard Institute (CLSI) guidelines, MIC were determined in CaMHB, while Aziz et al. showed that MIC values were 2- to 3-fold higher in CaMHB compared to Middlebrook 7H9 (31), clearly implicating an effect of medium on RFB susceptibility testing. In line with these results, we noticed important variations in the MIC values depending on the culture medium used for RFB susceptibility assessments. It is also noteworthy that the growth curve of the untreated S strain is different from that of the R strain, which is very likely linked to the highly aggregative surface properties typifying the R strain, which in contrast to the S strain, produces very clumpy and corded cultures in broth medium (10, 46, 50). As a consequence, colonies on agar plates very likely emerge from aggregated bacteria rather than individual bacilli, explaining why the CFU counts were significantly lower in both cultures. Thus, the CFU counts of the R strain do not accurately reflect the absolute number of living bacilli in the culture. We also selected RFB-resistant mutants and identified mutations in *rpoB*, which is known as the primary target of rifampin in *M. tuberculosis* (51). Interestingly, the mutations identified are part of the rifampin-resistance-determining region (RRDR), an 81-bp central segment corresponding to codons 426 to 452 in *M. tuberculosis* that harbors the vast majority of *rpoB* mutations associated with resistance to RIF (51). It is noteworthy that S452L corresponds to one of the most frequently mutated coding regions in the *rpoB* gene in *M. tuberculosis* (S450L replacement) (51). Together, these results suggest that RpoB is very likely the target of RFB in *M. abscessus*.

Among the various studies reporting the activity of RFB against *M. abscessus in vitro*, very few discriminated the activity of RFB against the S or R morphotypes. Here, we found that the type strain CIP104536^T S was reproducibly more resistant to RFB than its

R counterpart. Supporting these results, deletion of *mmpL4b* in the S genetic background, resulting in an R morphotype lacking GPL (13, 37), increased susceptibility to RFB. Conversely, functional complementation of the *mmpL4b* mutant, restoring the S morphotype and GPL production (13, 37), partially rescued the higher MIC. This highlights the influence of the outermost GPL layer on susceptibility to RFB. Previously, the activity of other inhibitors was shown to be dependent on the presence or absence of GPL in *M. abscessus* (17, 18). A logical explanation is that the GPL layer protects the bacilli from the penetration of drugs. The absence of GPL may enhance the permeability of the cell wall and accumulation of the drug inside the bacteria. However, one cannot exclude the possibility that MmpL4b, like other MmpL transporters, can act as an efflux pump (52–54) and may participate in the extrusion of RFB in *M. abscessus* S, resulting in higher MIC. The implication of efflux pumps in resistance to RFB has been investigated, whereby the overexpression of MAB_1409c (a homologue of the *M. tuberculosis* Rv1258c) resulted in increased resistance to RFB in the R variant of *M. abscessus*. This effect was not observed in the S strain overexpressing MAB_1409c, presumably because of the already elevated MIC of the parental S strain toward RFB. However, while the increased susceptibility of the R strain compared to the S strain was true with respect to the type strain, this was not observed for all clinical strains tested. The heterogeneity of the clinical strains in response to RFB treatment cannot be simply explained by the presence or absence of GPL but may also include additional determinants of resistance to RFB (48), such as differences in the expression level of Arr_{Mab} or the expression of Rox monooxygenases, known to inactivate RIF in other bacterial species as proposed earlier (55). This, however, requires further investigation in follow-up studies.

One unanticipated finding from this study relies on the fact that, although S and R variants respond differently to RFB treatment *in vitro*, this was not the case against the intracellularly residing *M. abscessus*. We found that, using a macrophage model of infection, the isogenic S and R type strains responded equally well to treatment with 12.5 μg/ml RFB, largely exceeding the results obtained with AMK, a drug displaying weak intracellular activity (56). These observations are reminiscent of other studies indicating that various naphthalenic ansamycins, including RIF, differ profoundly in their capacity to kill extracellular *Staphylococcus aureus*, although there were few differences observed between them in promoting human macrophages to kill phagocytosed bacteria (57). There is no simple explanation for why *M. abscessus* S is as efficiently killed as *M. abscessus* R inside the cells. A plausible explanation may be that the stress response inside macrophages alters the composition/architecture of the cell wall of *M. abscessus*, thereby affecting the GPL layer and/or permeability of the S variant. It has been shown that the GPL layer significantly influences the hydrophobic surface properties (58), potentially impacting the adhesion and the uptake of the bacilli. Furthermore, electron microscopy observations revealed that the electron translucent zone (ETZ) that fills the entire space between the phagosome and the bacterial surface relies on GPL production in the S variant (11). Alternatively, RFB may directly induce the antimycobacterial activity of the macrophage, which in turn, translates into a rapid killing of the phagocytosed bacteria, regardless of their morphotype. Overall, these results suggest that the MIC values of RFB are not indicative of the intraphagocytic killing of *M. abscessus* and highlight the importance of testing the efficacy of drugs in a macrophage infection model.

Cords and abscesses are pathophysiological markers of *M. abscessus* infection, as revealed using the zebrafish model of infection (44). In particular, extracellular cords, due to their size, prevent the bacilli from being phagocytosed by macrophages and neutrophils, representing an important mechanism of immune evasion (14, 46). We demonstrate here that treatment of infected macrophages was associated with reduced intra- and extracellular cording of the R variant. It is very likely that RFB prevents cording, as a consequence of the inhibition of bacterial replication/killing. Cords are a hallmark of virulence of the R variant of *M. abscessus*, as emphasized by a deletion mutant of *MAB_4780*, encoding a dehydratase, displaying a pronounced defect in

cording and a highly attenuated phenotype in macrophages (59). Importantly, we observed also a significant decrease in the number of embryos with cords following RFB treatment in infected zebrafish. It is worth highlighting that in the presence of RFB, there is no change in the number of embryos with cords between 2 and 4 dpi, suggesting that while RFB does not degrade or modify the bacterial cord structure, it likely prevents the formation of additional cords. Moreover, the effect of RFB on cord reduction is particularly interesting, as it may prevent the subsequent formation of abscesses (14), considered a marker of the severity of the disease. Consistent with this hypothesis, a marked decrease in abscess formation was observed in RFB-treated zebrafish embryos. Overall, this work supports the practicality of zebrafish as a preclinical model to evaluate in real time the bactericidal efficacy of RFB against *M. abscessus* infection in the sole context of innate immunity.

In summary, although there is a clear lack of bactericidal activity of drugs against *M. abscessus* (60), these findings support the high level of activity of RFB against *M. abscessus in vivo* and *in vitro*. Our results further emphasize the efficacy of RFB against both extracellular and intracellular forms of *M. abscessus*, both coexisting in infected patients, as well as a protective effect in an animal model of *M. abscessus* infection. In addition, we provided further evidence that S and R variants are differentially susceptible to RFB, likely due to the GPL layer; however, the MIC values are not predictive of intracellular drug efficacy.

Together with the fact that RFB is an FDA-approved drug that is already used to treat tuberculosis (61) and *M. avium* infections (62) with favorable pharmacological properties (63), our data strengthen the view that RFB should be considered a repurposing drug candidate for the treatment of *M. abscessus* infections. Importantly, recent work has shown that RFB is synergistic in combination with other antimicrobials, such as clarithromycin, imipenem, and tigecycline, and significantly improves the activity of imipenem-tedizolid drug combinations (32, 42, 49, 64). Future studies are required to test whether these RFB combinations are effective against *M. abscessus* pulmonary infections.

MATERIALS AND METHODS

Mycobacterial strains and growth conditions. *M. abscessus* CIP104536^T, *M. bolletii* CIP108541^T, and *M. massiliense* CIP108297^T reference strains and clinical isolates from CF and non-CF patients were reported previously (65, 66). Strains were routinely grown and maintained at 30°C in Middlebrook 7H9 broth (BD Difco) supplemented with 0.05% Tween 80 (Sigma-Aldrich) and 10% oleic acid, albumin, dextrose, and catalase (OADC enrichment; BD Difco) (7H9$^{T/OADC}$) or on Middlebrook 7H10 agar (BD Difco) containing 10% OADC enrichment (7H10^{OADC}) and in the presence of antibiotics when required. For drug susceptibility testing, bacteria were grown in cation-adjusted Mueller-Hinton broth (CaMHB; Sigma-Aldrich). RFB was purchased from two independent commercial sources (AdooQ Bioscience and Selleckchem) and dissolved in DMSO.

Drug susceptibility testing. The MICs were determined according to the CLSI guidelines (67). The broth microdilution method was used in CaMHB with an inoculum of 5×10^6 CFU/ml in the exponential growth phase. The bacterial suspension was seeded in 100-μl volumes in all of the wells of a 96-well plate, except for the first column, to which 198 μl of the bacterial suspension was added. In the first column, 2 μl of drug at its highest concentration was added to the first well containing 198 μl of bacterial suspension. Then, 2-fold serial dilutions were carried out, and the plates were incubated for 3 to 5 days at 30°C. MICs were recorded by visual inspection. Assays were completed in triplicate in three independent experiments.

Growth inhibition kinetics. To monitor the growth inhibition of *M. abscessus* CIP104536^T S and R, 96-well plates were set up as for MIC determination, and serial dilutions of the bacterial suspensions exposed to increasing concentrations of RFB were plated on LB agar plates after 0, 24, 48, and 72 h. CFU were counted after 4 days of incubation at 30°C. Results from each drug concentration are representative of at least 2 independent experiments.

Cytotoxicity assay. THP-1 cells were differentiated with phorbol myristate acetate (PMA) for 48 h and exposed to decreasing concentrations of either RFB or RIF (starting at 200 μg/ml) for an additional 72 h at 37°C with 5% CO_2. Following incubation, 10% (vol/vol) resazurin dye was added to each well and left to incubate for 4 h at 37°C and 5% CO_2. Data were acquired using a fluorescent plate reader (excitation, 540 nm; emission, 590 nm). DMSO was included as a negative control, while SDS was included as a positive control.

Intracellular killing assay. Human THP-1 monocytes were grown in RPMI medium supplemented with 10% fetal bovine serum (Sigma-Aldrich) (RPMI^{FBS}) and incubated at 37°C in the presence of 5% CO_2. Cells were differentiated into macrophages in the presence of 20 ng/ml PMA in 24-well flat-bottom tissue culture microplates (1×10^5 cells/well) and incubated for 48 h at 37°C with 5% CO_2. Infection with clinical

isolates or *M. abscessus* harboring pTEC27 fluorescent TdTomato was carried out at 37°C in the presence of 5% CO_2 for 3 h at a multiplicity of resistance (MOI) of 2:1. After extensive washing with 1× phosphate-buffered saline (PBS), cells were incubated with RPMI^{FBS} containing 250 μg/ml amikacin for 2 h and washed again with PBS prior to the addition of 500 μl RPMI^{FBS} containing DMSO (negative control), 500 μl RPMI^{FBS} containing 50 μg/ml of RIF or AMK, or 12.5 μg/ml of RFB. Macrophages were washed with PBS and lysed with 100 μl of 1% Triton X-100 at required time points. Serial dilutions of macrophage lysates were plated onto LB agar plates, and colonies were counted to determine intracellular CFU.

Microscopy-based infectivity assays. Monocytes were differentiated into macrophages (THP-1) in the presence of PMA and were grown on coverslips in 24-well plates at a density of 10^5 cells/ml for 48 h at 37°C with 5% CO_2 prior to infection with Tdtomato expressing *M. abscessus* for 3 h at an MOI of 2:1. After washing and AMK treatment to remove the extracellular bacilli, macrophages were exposed to DMSO (negative control), 50 μg/ml RIF or AMK, or 12.5 μg/ml RFB and fixed at 0, 1, and 3 days postinfection with 4% paraformaldehyde in PBS for 20 min. Cells were then permeabilized using 0.2% Triton X-100 for 20 min, blocked with 2% BSA in PBS supplemented with 0.2% Triton X-100 for 20 min, incubated with anti-CD63 antibodies (Becton, Dickinson; dilution, 1:1,000) for 1 h and with an Alexa Fluor 488-conjugated anti-mouse secondary antibody (Molecular Probes, Invitrogen). After 5 min of incubation with DAPI (dilution, 1:1,000), cells were mounted onto microscope slides using Immu-mount (Calbiochem) and examined with an epifluorescence microscope using a 63× lens objective. The average proportion of macrophages containing <5, 5 to 10, or >10 bacilli were quantified using Zeiss AxioVision software. Images were acquired by focusing on combined signals (CD63 in green and red fluorescent *M. abscessus*) and captured on a Zeiss Axio Imager confocal microscope equipped with a 63× oil objective and processed using Zeiss AxioVision software. Quantification and scoring of the numbers of bacilli present within macrophages were performed using ImageJ. Equal parameters for the capture and scoring of images were consistently applied to all samples. For each condition, approximately 1,000 infected macrophages were analyzed. The presence of the intra- or extracellular cords within or among the macrophages infected with the R morphotype strain were treated in the presence of DMSO, RIF, RFB, or AMK at the concentrations previously described, counted, and imaged using confocal microscopy.

Assessment of RFB efficacy in infected zebrafish. Experiments in zebrafish were conducted according to the Comité d'Ethique pour l'Expérimentation Animale de la Région Languedoc Roussillon under the reference number CEEALR36-1145. Experiments were performed using the *golden* mutant (68). Embryos were obtained and maintained as described (14). Embryo age is expressed as hours postfertilization (hpf). Red fluorescent *M. abscessus* CIP104536^T (R) expressing TdTomato was prepared and microinjected in the caudal vein (2 to 3 nl containing ≈100 bacteria/nl) in 30 hpf embryos previously dechorionated and anesthetized with tricaine, as described earlier (46). The bacterial inoculum was checked *a posteriori* by injection of 2 nl in sterile phosphate-buffered saline with Tween (PBST) and plating on 7H10^{OADC}. Infected embryos were transferred into 24-well plates (2 embryos/well) and incubated at 28.5°C to monitor kinetics of infection and embryo survival. Survival curves were determined by counting dead larvae daily for up to 12 days, with the experiment concluded when uninfected embryos started to die. RFB treatment of infected embryos and uninfected embryos commenced at 24 hours postinfection (hpi) for 4 days. The drug-containing solution was renewed daily. Bacterial loads in live embryos were determined by anesthetizing embryos in tricaine as previously described (44), mounting on 3% (wt/vol) methylcellulose solution, and taking fluorescent images using a Zeiss Axio Zoom.V16 coupled with an Axiocam 503 mono (Zeiss). Fluorescence pixel count (FPC) measurements were determined using the "analyze particles" function in ImageJ (46). Bacterial cords were identified based on the size and shape of fluorescent bacteria within the live zebrafish embryo, vastly exceeding the surrounding size and shape of neighboring cells. All experiments were completed at least three times independently.

Overexpression of *MAB_1409c* in *M. abscessus*. Overexpression was achieved by PCR amplification of *MAB_1409c* (*tap*) in fusion with an HA tag using genomic DNA and the forward primer (5′-gagaCAA TTGCCATGTCCACTCCGACGGCGGATTC-3′; MfeI) and reverse primer (5′-gagaGTTAACCTAAGCGTAATCTG GAACATCGTATGGGTACCGAGTTGGTTCCTTGTCGGGCT-3′; HpaI). The amplified product was digested with MfeI/HpaI and ligated into the MfeI/HpaI-restricted pMV306 integrative vector to generate pMV306-*MAB_1409c*-HA, where *MAB_1409c-HA* is under the control of the *hsp60* promoter. The construct was sequenced and electroporated into *M. abscessus* S and R.

Selection of resistant *M. abscessus* mutants and target identification. Exponentially growing *M. abscessus* CIP104536^T R cultures were plated on LB agar containing either 25 or 50 μg/ml RFB. After 1 week of incubation at 37°C, two individual colonies from each RFB concentration were selected, grown in CaMHB, individually assessed for MIC determination, and scored for resistance to RFB. Identification of SNPs in the resistant strains was completed by PCR amplification using *rpoB_f* 5′-TCAGTGGGGCTGGTT AG-3′ and *rpoB_r* 5′-AAAACATCGCAGATGCGC-3′ to produce a 3,541-bp amplicon for full coverage sequencing of the *rpoB* gene.

Western blotting. Bacteria were harvested, resuspended in PBS, and disrupted by bead-beating with 1-mm-diameter glass beads. The protein concentration in the lysates was determined, and equal amounts of proteins (100 μg) were subjected to SDS-PAGE. Proteins were transferred to a nitrocellulose membrane. For detection of Tap-HA and KasA (loading control), the membranes were incubated for 1 h with either the rat anti-HA or rat anti-KasA antibodies (dilution, 1:2,000), washed, and subsequently incubated with goat anti-rat antibodies conjugated to HRP (Abcam; dilution, 1:5,000). The signal was revealed using the ChemiDoc MP system (Bio-Rad).

Statistical analyses. Statistical analyses were performed on Prism 5.0 (GraphPad) and detailed for each figure legend. *, $P \leq 0.05$, **, $P \leq 0.01$, ***, $P \leq 0.001$, ****, $P \leq 0.0001$.

SUPPLEMENTAL MATERIAL

Supplemental material is available online only.

SUPPLEMENTAL FILE 1, PDF file, 0.8 MB.

ACKNOWLEDGMENTS

M.D.J. received a postdoctoral fellowship granted by Labex EpiGenMed, an "Investissements d'Avenir" program (ANR-10-LABX-12-01). This study was supported by the Association Gregory Lemarchal and Vaincre la Mucoviscidose (RIF20180502320) to L.K.

We have no conflict of interest to declare.

REFERENCES

1. Johansen MD, Herrmann J-L, Kremer L. 2020. Non-tuberculous mycobacteria and the rise of *Mycobacterium abscessus*. Nat Rev Microbiol 18:392–407. https://doi.org/10.1038/s41579-020-0331-1.
2. Cowman S, van Ingen J, Griffith DE, Loebinger MR. 2019. Non-tuberculous mycobacterial pulmonary disease. Eur Respir J 54:1900250. https://doi.org/10.1183/13993003.00250-2019.
3. Jönsson BE, Gilljam M, Lindblad A, Ridell M, Wold AE, Welinder-Olsson C. 2007. Molecular epidemiology of *Mycobacterium abscessus*, with focus on cystic fibrosis. J Clin Microbiol 45:1497–1504. https://doi.org/10.1128/JCM.02592-06.
4. Esther CR, Esserman DA, Gilligan P, Kerr A, Noone PG. 2010. Chronic *Mycobacterium abscessus* infection and lung function decline in cystic fibrosis. J Cyst Fibros 9:117–123. https://doi.org/10.1016/j.jcf.2009.12.001.
5. Catherinot E, Roux A-L, Macheras E, Hubert D, Matmar M, Dannhoffer L, Chinet T, Morand P, Poyart C, Heym B, Rottman M, Gaillard J-L, Herrmann J-L. 2009. Acute respiratory failure involving an R variant of *Mycobacterium abscessus*. J Clin Microbiol 47:271–274. https://doi.org/10.1128/JCM.01478-08.
6. Adekambi T, Sassi M, van Ingen J, Drancourt M. 2017. Reinstating *Mycobacterium massiliense* and *Mycobacterium bolletii* as species of the *Mycobacterium abscessus* complex. Int J Syst Evol Microbiol 67:2726–2730. https://doi.org/10.1099/ijsem.0.002011.
7. Koh W-J, Jeon K, Lee NY, Kim B-J, Kook Y-H, Lee S-H, Park YK, Kim CK, Shin SJ, Huitt GA, Daley CL, Kwon OJ. 2011. Clinical significance of differentiation of *Mycobacterium massiliense* from *Mycobacterium abscessus*. Am J Respir Crit Care Med 183:405–410. https://doi.org/10.1164/rccm.201003-0395OC.
8. Howard ST, Rhoades E, Recht J, Pang X, Alsup A, Kolter R, Lyons CR, Byrd TF. 2006. Spontaneous reversion of *Mycobacterium abscessus* from a smooth to a rough morphotype is associated with reduced expression of glycopeptidolipid and reacquisition of an invasive phenotype. Microbiology) 152:1581–1590. https://doi.org/10.1099/mic.0.28625-0.
9. Gutiérrez AV, Viljoen A, Ghigo E, Herrmann J-L, Kremer L. 2018. Glycopeptidolipids, a double-edged sword of the *Mycobacterium abscessus* complex. Front Microbiol 9:1145. https://doi.org/10.3389/fmicb.2018.01145.
10. Roux A-L, Viljoen A, Bah A, Simeone R, Bernut A, Laencina L, Deramaudt T, Rottman M, Gaillard J-L, Majlessi L, Brosch R, Girard-Misguich F, Vergne I, de Chastellier C, Kremer L, Herrmann J-L. 2016. The distinct fate of smooth and rough *Mycobacterium abscessus* variants inside macrophages. Open Biol 6:160185. https://doi.org/10.1098/rsob.160185.
11. Bernut A, Viljoen A, Dupont C, Sapriel G, Blaise M, Bouchier C, Brosch R, de Chastellier C, Herrmann J-L, Kremer L. 2016. Insights into the smooth-to-rough transitioning in *Mycobacterium bolletii* unravels a functional Tyr residue conserved in all mycobacterial MmpL family members. Mol Microbiol 99:866–883. https://doi.org/10.1111/mmi.13283.
12. Sánchez-Chardi A, Olivares F, Byrd TF, Julián E, Brambilla C, Luquin M. 2011. Demonstration of cord formation by rough *Mycobacterium abscessus* variants: implications for the clinical microbiology laboratory. J Clin Microbiol 49:2293–2295. https://doi.org/10.1128/JCM.02322-10.
13. Nessar R, Reyrat J-M, Davidson LB, Byrd TF. 2011. Deletion of the *mmpL4b* gene in the *Mycobacterium abscessus* glycopeptidolipid biosynthetic pathway results in loss of surface colonization capability, but enhanced ability to replicate in human macrophages and stimulate their innate immune response. Microbiology) 157:1187–1195. https://doi.org/10.1099/mic.0.046557-0.
14. Bernut A, Herrmann J-L, Kissa K, Dubremetz J-F, Gaillard J-L, Lutfalla G, Kremer L. 2014. *Mycobacterium abscessus* cording prevents phagocytosis and promotes abscess formation. Proc Natl Acad Sci U S A 111:E943–952. https://doi.org/10.1073/pnas.1321390111.
15. Park IK, Hsu AP, Tettelin H, Shallom SJ, Drake SK, Ding L, Wu U-I, Adamo N, Prevots DR, Olivier KN, Holland SM, Sampaio EP, Zelazny AM. 2015. Clonal diversification and changes in lipid traits and colony morphology in *Mycobacterium abscessus* clinical isolates. J Clin Microbiol 53:3438–3447. https://doi.org/10.1128/JCM.02015-15.
16. Pawlik A, Garnier G, Orgeur M, Tong P, Lohan A, Le Chevalier F, Sapriel G, Roux A-L, Conlon K, Honoré N, Dillies M-A, Ma L, Bouchier C, Coppée J-Y, Gaillard J-L, Gordon SV, Loftus B, Brosch R, Herrmann JL. 2013. Identification and characterization of the genetic changes responsible for the characteristic smooth-to-rough morphotype alterations of clinically persistent *Mycobacterium abscessus*. Mol Microbiol 90:612–629. https://doi.org/10.1111/mmi.12387.
17. Madani A, Ridenour JN, Martin BP, Paudel RR, Abdul Basir A, Le Moigne V, Herrmann J-L, Audebert S, Camoin L, Kremer L, Spilling CD, Canaan S, Cavalier J-F. 2019. Cyclipostins and Cyclophostin analogues as multitarget inhibitors that impair growth of *Mycobacterium abscessus*. ACS Infect Dis 5:1597–1608. https://doi.org/10.1021/acsinfecdis.9b00172.
18. Lavollay M, Dubée V, Heym B, Herrmann J-L, Gaillard J-L, Gutmann L, Arthur M, Mainardi J-L. 2014. *In vitro* activity of cefoxitin and imipenem against *Mycobacterium abscessus* complex. Clin Microbiol Infect 20:O297–O300. https://doi.org/10.1111/1469-0691.12405.
19. Nessar R, Cambau E, Reyrat JM, Murray A, Gicquel B. 2012. *Mycobacterium abscessus*: a new antibiotic nightmare. J Antimicrob Chemother 67:810–818. https://doi.org/10.1093/jac/dkr578.
20. van Ingen J, Boeree MJ, van Soolingen D, Mouton JW. 2012. Resistance mechanisms and drug susceptibility testing of nontuberculous mycobacteria. Drug Resist Updat 15:149–161. https://doi.org/10.1016/j.drup.2012.04.001.
21. Brown-Elliott BA, Nash KA, Wallace RJ. 2012. Antimicrobial susceptibility testing, drug resistance mechanisms, and therapy of infections with nontuberculous mycobacteria. Clin Microbiol Rev 25:545–582. https://doi.org/10.1128/CMR.05030-11.
22. Lopeman R, Harrison J, Desai M, Cox J. 2019. *Mycobacterium abscessus*: environmental bacterium turned clinical nightmare. Microorganisms 7:90. https://doi.org/10.3390/microorganisms7030090.
23. Luthra S, Rominski A, Sander P. 2018. The role of antibiotic-target-modifying and antibiotic-modifying enzymes in *Mycobacterium abscessus* drug resistance. Front Microbiol 9:2179. https://doi.org/10.3389/fmicb.2018.02179.
24. Wu M-L, Aziz DB, Dartois V, Dick T. 2018. NTM drug discovery: status, gaps and the way forward. Drug Discov Today 23:1502–1519. https://doi.org/10.1016/j.drudis.2018.04.001.
25. Griffith DE, Aksamit T, Brown-Elliott BA, Catanzaro A, Daley C, Gordin F, Holland SM, Horsburgh R, Huitt G, Iademarco MF, Iseman M, Olivier K, Ruoss S, von Reyn CF, Wallace RJ, Winthrop K, ATS Mycobacterial Diseases Subcommittee, American Thoracic Society, Infectious Disease Society of America. 2007. An official ATS/IDSA statement: diagnosis, treatment, and prevention of nontuberculous mycobacterial diseases. Am J

Respir Crit Care Med 175:367–416. https://doi.org/10.1164/rccm.200604-571ST.
26. Floto RA, Olivier KN, Saiman L, Daley CL, Herrmann J-L, Nick JA, Noone PG, Bilton D, Corris P, Gibson RL, Hempstead SE, Koetz K, Sabadosa KA, Sermet-Gaudelus I, Smyth AR, van Ingen J, Wallace RJ, Winthrop KL, Marshall BC, Haworth CS. 2016. US Cystic Fibrosis Foundation and European Cystic Fibrosis Society consensus recommendations for the management of non-tuberculous mycobacteria in individuals with cystic fibrosis: executive summary. Thorax 71:88–90. https://doi.org/10.1136/thoraxjnl-2015-207983.
27. Daley CL, Iaccarino JM, Lange C, Cambau E, Wallace RJ, Andrejak C, Böttger EC, Brozek J, Griffith DE, Guglielmetti L, Huitt GA, Knight SL, Leitman P, Marras TK, Olivier KN, Santin M, Stout JE, Tortoli E, van Ingen J, Wagner D, Winthrop KL. 2020. Treatment of nontuberculous mycobacterial pulmonary disease: an official ATS/ERS/ESCMID/IDSA clinical practice guideline. Eur Respir J 56:2000535. https://doi.org/10.1183/13993003.00535-2020.
28. Wallace RJ, Dukart G, Brown-Elliott BA, Griffith DE, Scerpella EG, Marshall B. 2014. Clinical experience in 52 patients with tigecycline-containing regimens for salvage treatment of *Mycobacterium abscessus* and *Mycobacterium chelonae* infections. J Antimicrob Chemother 69:1945–1953. https://doi.org/10.1093/jac/dku062.
29. Roux A-L, Catherinot E, Soismier N, Heym B, Bellis G, Lemonnier L, Chiron R, Fauroux B, Le Bourgeois M, Munck A, Pin I, Sermet I, Gutierrez C, Véziris N, Jarlier V, Cambau E, Herrmann J-L, Guillemot D, Gaillard J-L, OMA Group. 2015. Comparing *Mycobacterium massiliense* and *Mycobacterium abscessus* lung infections in cystic fibrosis patients. J Cyst Fibros 14:63–69. https://doi.org/10.1016/j.jcf.2014.07.004.
30. Daniel-Wayman S, Abate G, Barber DL, Bermudez LE, Coler RN, Cynamon MH, Daley CL, Davidson RM, Dick T, Floto RA, Henkle E, Holland SM, Jackson M, Lee RE, Nuermberger EL, Olivier KN, Ordway DJ, Prevots DR, Sacchettini JC, Salfinger M, Sassetti CM, Sizemore CF, Winthrop KL, Zelazny AM. 2019. Advancing translational science for pulmonary nontuberculous mycobacterial infections. A road map for research. Am J Respir Crit Care Med 199:947–951. https://doi.org/10.1164/rccm.201807-1273PP.
31. Aziz DB, Low JL, Wu M-L, Gengenbacher M, Teo JWP, Dartois V, Dick T. 2017. Rifabutin is active against *Mycobacterium abscessus* complex. Antimicrob Agents Chemother 61:e00155-17. https://doi.org/10.1128/AAC.00155-17.
32. Pryjma M, Burian J, Thompson CJ. 2018. Rifabutin acts in synergy and is bactericidal with frontline *Mycobacterium abscessus* antibiotics clarithromycin and tigecycline, suggesting a potent treatment combination. Antimicrob Agents Chemother 62:e00283-18. https://doi.org/10.1128/AAC.00283-18.
33. Rominski A, Roditscheff A, Selchow P, Böttger EC, Sander P. 2017. Intrinsic rifamycin resistance of *Mycobacterium abscessus* is mediated by ADP-ribosyltransferase MAB_0591. J Antimicrob Chemother 72:376–384. https://doi.org/10.1093/jac/dkw466.
34. Dick T, Shin SJ, Koh W-J, Dartois V, Gengenbacher M. 2019. Rifabutin is active against *Mycobacterium abscessus* in mice. Antimicrob Agents Chemother 64:e01943-19. https://doi.org/10.1128/AAC.01943-19.
35. Lefebvre A-L, Dubée V, Cortes M, Dorchêne D, Arthur M, Mainardi J-L. 2016. Bactericidal and intracellular activity of β-lactams against *Mycobacterium abscessus*. J Antimicrob Chemother 71:1556–1563. https://doi.org/10.1093/jac/dkw022.
36. Story-Roller E, Maggioncalda EC, Lamichhane G. 2019. Select β-lactam combinations exhibit synergy against *Mycobacterium abscessus in vitro*. Antimicrob Agents Chemother 63:e00614-19. https://doi.org/10.1128/AAC.02613-18.
37. Medjahed H, Reyrat J-M. 2009. Construction of *Mycobacterium abscessus* defined glycopeptidolipid mutants: comparison of genetic tools. Appl Environ Microbiol 75:1331–1338. https://doi.org/10.1128/AEM.01914-08.
38. Roux A-L, Ray A, Pawlik A, Medjahed H, Etienne G, Rottman M, Catherinot E, Coppée J-Y, Chaoui K, Monsarrat B, Toubert A, Daffé M, Puzo G, Gaillard J-L, Brosch R, Dulphy N, Nigou J, Herrmann J-L. 2011. Overexpression of proinflammatory TLR-2-signalling lipoproteins in hypervirulent mycobacterial variants. Cell Microbiol 13:692–704. https://doi.org/10.1111/j.1462-5822.2010.01565.x.
39. Ripoll F, Pasek S, Schenowitz C, Dossat C, Barbe V, Rottman M, Macheras E, Heym B, Herrmann J-L, Daffé M, Brosch R, Risler J-L, Gaillard J-L. 2009. Non mycobacterial virulence genes in the genome of the emerging pathogen *Mycobacterium abscessus*. PLoS One 4:e5660. https://doi.org/10.1371/journal.pone.0005660.
40. Balganesh M, Dinesh N, Sharma S, Kuruppath S, Nair AV, Sharma U. 2012. Efflux pumps of *Mycobacterium tuberculosis* play a significant role in antituberculosis activity of potential drug candidates. Antimicrob Agents Chemother 56:2643–2651. https://doi.org/10.1128/AAC.06003-11.
41. Dupont C, Viljoen A, Thomas S, Roquet-Banères F, Herrmann J-L, Pethe K, Kremer L. 2017. Bedaquiline inhibits the ATP synthase in *Mycobacterium abscessus* and is effective in infected zebrafish. Antimicrob Agents Chemother 61:e01225-17. https://doi.org/10.1128/AAC.01225-17.
42. Cheng A, Tsai Y-T, Chang S-Y, Sun H-Y, Wu U-I, Sheng W-H, Chen Y-C, Chang S-C. 2019. *In vitro* synergism of rifabutin with clarithromycin, imipenem, and tigecycline against the *Mycobacterium abscessus* complex. Antimicrob Agents Chemother 63:e02234-18. https://doi.org/10.1128/AAC.02234-18.
43. Luna-Herrera J, Reddy MV, Gangadharam PRJ. 1995. *In vitro* and intracellular activity of rifabutin on drug-susceptible and multiple drug-resistant (MDR) tubercle bacilli. J Antimicrob Chemother 36:355–363. https://doi.org/10.1093/jac/36.2.355.
44. Bernut A, Le Moigne V, Lesne T, Lutfalla G, Herrmann J-L, Kremer L. 2014. *In vivo* assessment of drug efficacy against *Mycobacterium abscessus* using the embryonic zebrafish test system. Antimicrob Agents Chemother 58:4054–4063. https://doi.org/10.1128/AAC.00142-14.
45. Dubée V, Bernut A, Cortes M, Lesne T, Dorchene D, Lefebvre A-L, Hugonnet J-E, Gutmann L, Mainardi J-L, Herrmann J-L, Gaillard J-L, Kremer L, Arthur M. 2015. β-Lactamase inhibition by avibactam in *Mycobacterium abscessus*. J Antimicrob Chemother 70:1051–1058. https://doi.org/10.1093/jac/dku510.
46. Bernut A, Dupont C, Sahuquet A, Herrmann J-L, Lutfalla G, Kremer L. 2015. Deciphering and imaging pathogenesis and cording of *Mycobacterium abscessus* in zebrafish embryos. J Vis Exp 103:e53130. https://doi.org/10.3791/53130.
47. Baysarowich J, Koteva K, Hughes DW, Ejim L, Griffiths E, Zhang K, Junop M, Wright GD. 2008. Rifamycin antibiotic resistance by ADP-ribosylation: structure and diversity of Arr. Proc Natl Acad Sci U S A 105:4886–4891. https://doi.org/10.1073/pnas.0711939105.
48. Ganapathy US, Dartois V, Dick T. 2019. Repositioning rifamycins for *Mycobacterium abscessus* lung disease. Expert Opin Drug Discov 14:867–878. https://doi.org/10.1080/17460441.2019.1629414.
49. Le Run E, Arthur M, Mainardi J-L. 2018. *In vitro* and intracellular activity of imipenem combined with rifabutin and avibactam against *Mycobacterium abscessus*. Antimicrob Agents Chemother 62:e00623-18. https://doi.org/10.1128/AAC.00623-18.
50. Brambilla C, Llorens-Fons M, Julián E, Noguera-Ortega E, Tomàs-Martínez C, Pérez-Trujillo M, Byrd TF, Alcaide F, Luquin M. 2016. Mycobacteria clumping increase their capacity to damage macrophages. Front Microbiol 7:1562. https://doi.org/10.3389/fmicb.2016.01562.
51. Jagielski T, Bakuła Z, Brzostek A, Minias A, Stachowiak R, Kalita J, Napiórkowska A, Augustynowicz-Kopeć E, Żaczek A, Vasiliauskiene E, Bielecki J, Dziadek J. 2018. Characterization of mutations conferring resistance to rifampin in *Mycobacterium tuberculosis* clinical strains. Antimicrob Agents Chemother 62:e01093-18. https://doi.org/10.1128/AAC.01093-18.
52. Richard M, Gutiérrez AV, Viljoen AJ, Ghigo E, Blaise M, Kremer L. 2018. Mechanistic and structural insights into the unique TetR-dependent regulation of a drug efflux pump in *Mycobacterium abscessus*. Front Microbiol 9:649. https://doi.org/10.3389/fmicb.2018.00649.
53. Richard M, Gutiérrez AV, Viljoen A, Rodriguez-Rincon D, Roquet-Baneres F, Blaise M, Everall I, Parkhill J, Floto RA, Kremer L. 2018. Mutations in the MAB_2299c TetR regulator confer cross-resistance to clofazimine and bedaquiline in *Mycobacterium abscessus*. Antimicrob Agents Chemother 63:e01316-18. https://doi.org/10.1128/AAC.01316-18.
54. Gutiérrez AV, Richard M, Roquet-Banères F, Viljoen A, Kremer L. 2019. The TetR-family transcription factor MAB_2299c regulates the expression of two distinct MmpS-MmpL efflux pumps involved in cross-resistance to clofazimine and bedaquiline in *Mycobacterium abscessus*. Antimicrob Agents Chemother 63:e01000-19. https://doi.org/10.1128/AAC.01000-19.
55. Koteva K, Cox G, Kelso JK, Surette MD, Zubyk HL, Ejim L, Stogios P, Savchenko A, Sørensen D, Wright GD. 2018. Rox, a rifamycin resistance enzyme with an unprecedented mechanism of action. Cell Chem Biol 25:403–412.e5. https://doi.org/10.1016/j.chembiol.2018.01.009.
56. Lefebvre A-L, Le Moigne V, Bernut A, Veckerlé C, Compain F, Herrmann J-L, Kremer L, Arthur M, Mainardi J-L. 2017. Inhibition of the β-lactamase BlaMab by avibactam improves the *in vitro* and *in vivo* efficacy of

imipenem against *Mycobacterium abscessus*. Antimicrob Agents Chemother 61:e02440-16. https://doi.org/10.1128/AAC.02440-16.
57. Marshall VP, Cialdella JI, Ohlmann GM, Gray GD. 1983. MIC values do not predict the intraphagocytic killing of *Staphylococcus aureus* by naphthalenic ansamycins. J Antibiot (Tokyo) 36:1549–1560. https://doi.org/10.7164/antibiotics.36.1549.
58. Viljoen A, Viela F, Kremer L, Dufrêne YF. 2020. Fast chemical force microscopy demonstrates that glycopeptidolipids define nanodomains of varying hydrophobicity on mycobacteria. Nanoscale Horiz 5:944–953. https://doi.org/10.1039/c9nh00736a.
59. Halloum I, Carrère-Kremer S, Blaise M, Viljoen A, Bernut A, Le Moigne V, Vilchèze C, Guérardel Y, Lutfalla G, Herrmann J-L, Jacobs WR, Kremer L. 2016. Deletion of a dehydratase important for intracellular growth and cording renders rough *Mycobacterium abscessus* avirulent. Proc Natl Acad Sci U S A 113:E4228–E4237. https://doi.org/10.1073/pnas.1605477113.
60. Maurer FP, Bruderer VL, Ritter C, Castelberg C, Bloemberg GV, Böttger EC. 2014. Lack of antimicrobial bactericidal activity in *Mycobacterium abscessus*. Antimicrob Agents Chemother 58:3828–3836. https://doi.org/10.1128/AAC.02448-14.
61. Lee H, Ahn S, Hwang NY, Jeon K, Kwon OJ, Huh HJ, Lee NY, Koh W-J. 2017. Treatment outcomes of rifabutin-containing regimens for rifabutin-sensitive multidrug-resistant pulmonary tuberculosis. Int J Infect Dis 65:135–141. https://doi.org/10.1016/j.ijid.2017.10.013.
62. Griffith DE. 2018. Treatment of *Mycobacterium avium* complex (MAC). Semin Respir Crit Care Med 39:351–361. https://doi.org/10.1055/s-0038-1660472.
63. Blaschke TF, Skinner MH. 1996. The clinical pharmacokinetics of rifabutin. Clin Infect Dis 22(Suppl 1):S15–S21. discussion S21-22. https://doi.org/10.1093/clinids/22.Supplement_1.S15.
64. Le Run E, Arthur M, Mainardi J-L. 2019. *In vitro* and intracellular activity of imipenem combined with tedizolid, rifabutin, and avibactam against *Mycobacterium abscessus*. Antimicrob Agents Chemother 63:e01915-18. https://doi.org/10.1128/AAC.01915-18.
65. Singh S, Bouzinbi N, Chaturvedi V, Godreuil S, Kremer L. 2014. *In vitro* evaluation of a new drug combination against clinical isolates belonging to the *Mycobacterium abscessus* complex. Clin Microbiol Infect 20:O1124–O1127. https://doi.org/10.1111/1469-0691.12780.
66. Halloum I, Viljoen A, Khanna V, Craig D, Bouchier C, Brosch R, Coxon G, Kremer L. 2017. Resistance to thiacetazone derivatives active against *Mycobacterium abscessus* involves mutations in the MmpL5 transcriptional repressor MAB_4384. Antimicrob Agents Chemother 61:e02509-16. https://doi.org/10.1128/AAC.02509-16.
67. Woods GL, Brown-Elliott BA, Conville PS, Desmond EP, Hall GS, Lin G, Pfyffer GE, Ridderhof JC, Siddiqi SH, Wallace RJ. 2011. Susceptibility testing of mycobacteria, nocardiae and other aerobic actinomycetes: approved standard, 2nd ed. M24-A2. Clinical and Laboratory Standards Institute, Wayne, PA.
68. Lamason RL, Mohideen M-APK, Mest JR, Wong AC, Norton HL, Aros MC, Jurynec MJ, Mao X, Humphreville VR, Humbert JE, Sinha S, Moore JL, Jagadeeswaran P, Zhao W, Ning G, Makalowska I, McKeigue PM, O'donnell D, Kittles R, Parra EJ, Mangini NJ, Grunwald DJ, Shriver MD, Canfield VA, Cheng KC. 2005. SLC24A5, a putative cation exchanger, affects pigmentation in zebrafish and humans. Science 310:1782–1786. https://doi.org/10.1126/science.1116238.

Table S1. RFB susceptibility profile of the *M. abscessus* 104536^T S and R strains in different broth media at 30 °C. Results are representative of 3 independent experiments.

	MIC (μg/mL)	
Medium	**CIP104536 (S)**	**CIP104536 (R)**
CaMHB	100	12.5
7H9	25	6.25
7H9 + OADC	50	50
Sauton	25	25

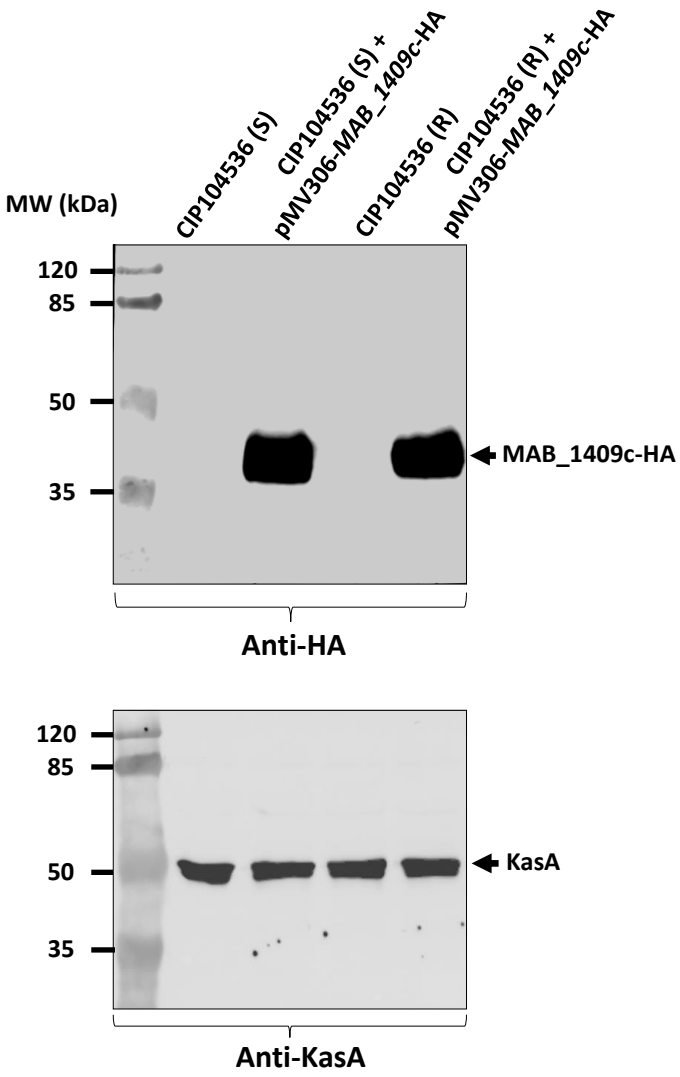

Figure S1. Overexpression of MAB_1409c-HA in *M. abscessus*. The *MAB_1409c* gene was fused to HA and expressed under the control of *hsp60* promotor. Western blot analysis of MAB_1409c overexpression in the CIP104536 S and R variants using anti-HA antibodies (upper panel). The KasA protein (probed with anti-KasA antibodies) was used as a loading control (lower panel).

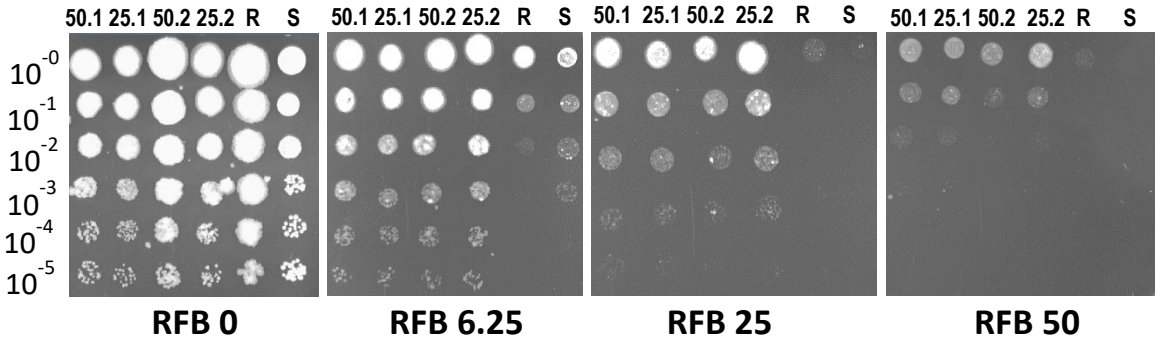

Figure S2. Drug susceptibility phenotypes of *M. abscessus* to RFB. Four microliter of 10-fold serially diluted bacterial suspension of exponentially growing cultures of S and R wild-type strains and resistant strains (50.1, 25.1, 50.2 and 25.2) derived from the R variant were spotted on Middlebrook 7H10 plates supplemented with OADC enrichment in the absence or presence of RFB (6.25 to 50 µg/mL). Plates were incubated at 37°C for 4 days.

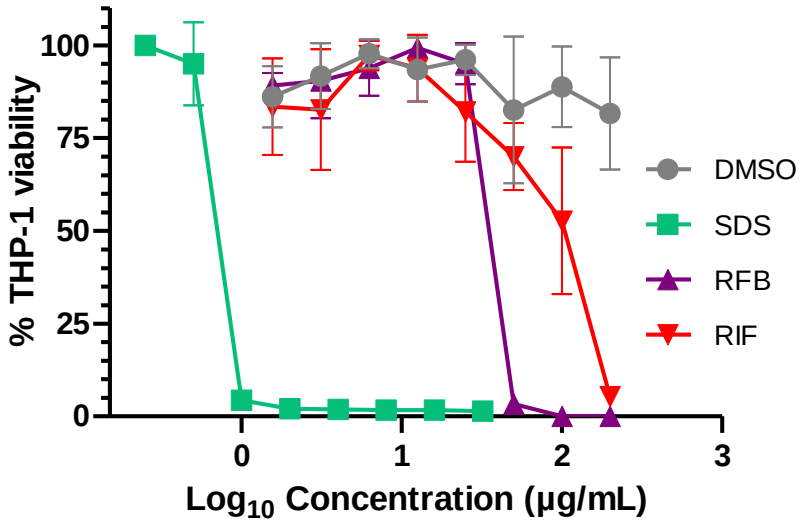

Figure S3. Cytotoxicity assay of rifabutin (RFB) and Rifampicin (RIF) on THP-1 differentiated macrophages. Cells were differentiated with PMA for 48 hrs and exposed to increasing concentration of either RFB or RIF (starting at 200 µg/mL) for an additional 72 hrs at 37°C with 5% CO_2. SDS was used as a positive control and DMSO as negative control. Results are representative of 3 independent experiments done in duplicate. CC_{50} SDS is 0.6 g/mL, CC_{50} RFB is 33. 6 µg/mL and CC_{50} RIF is 82.6 µg/mL.

DISCUSSION

L'émergence de pathogènes opportunistes tel que *M. abscessus* pose un réel problème de santé publique au niveau mondial. Cette bactérie est connue pour être l'espèce mycobactérienne la plus résistante aux antibiotiques. Le traitement actuel s'échelonne sur au moins 12 mois et associe trois antibiotiques durant sa phase initiale : un aminoglycoside (amikacine), un macrolide (clarithromycine ou azithromycine) et une β-lactamine (imipénème ou céfoxitine). Toutefois, dans un grand nombre de cas, ce traitement peut être inopérant du fait de la présence de mécanismes de résistance (innés ou acquis) mis en place par cette bactérie. Ces échecs thérapeutiques peuvent conduire à des rechutes qui nécessiteront une phase de prolongation du traitement, incluant une oxazolidinone (linézolide), une glycylcycline (tigécycline) et/ou une phénazine (clofazimine) (Daley et al. 2020). Par ailleurs, il n'existe pas une bonne corrélation entre les CMI déterminées *in vitro* et l'efficacité des traitements *in vivo*, rendant les prédictions thérapeutiques peu fiables. C'est dans ce contexte que ce travail a été réalisé, afin de proposer de nouvelles perspectives pour améliorer les traitements actuels en se concentrant sur deux axes de recherche majeurs : la découverte de nouvelles molécules actives contre *M. abscessus* et le repositionnement d'antibiotiques déjà utilisés en clinique pour le traitement d'autres infections bactériennes.

Axe I. Découverte de nouvelles molécules efficaces contre *M. abscessus*.

Durant ces dernières décennies, la découverte de nouvelles classes d'antibiotiques vis-à-vis des infections mycobactériennes, telle que la tuberculose, a été profondément ralentie. Ainsi, la découverte de nouvelles entités chimiques, capables d'inhiber de nouvelles voies métaboliques essentielles et/ou activités enzymatiques, est indispensable pour contourner l'émergence grandissante des souches multi-résistantes aux antibiotiques. Dans cette optique, l'inhibition du transport des acides mycoliques semble être une cible thérapeutique de choix car le transporteur MmpL3 est essentiel chez *M. tuberculosis* et *M. smegmatis* (Viljoen et al. 2017; Li et al. 2018). En effet, notre équipe est à l'origine de la découverte de trois familles chimiques distinctes capables d'inhiber le transport des acides mycoliques en ciblant MmpL3 : les dérivés du pipéridinol PIPD1 (Dupont et al. 2016; de Ruyck et al. 2020) ; les dérivés des indoles 2-carboxamides (Kozikowski et al. 2017) ainsi que certains dérivés des benzimidazoles qui ont fait l'objet de ce travail de thèse. MmpL3 étant le seul membre de la famille des MmpL qui soit essentiel chez *M. smegmatis* et chez *M. tuberculosis* (Degiacomi et al. 2017; Grzegorzewicz et al. 2012; Viljoen et al. 2017), il n'est pas surprenant que ces trois classes d'inhibiteurs soient

également très actifs contre *M. tuberculosis*. D'ailleurs, il a récemment été démontré que PIPD1 inhibe l'activité flippase de MmpL3 et agit de manière très efficaces sur les souches MDR et XDR de *M. tuberculosis* (Dupont et al. 2019). Ainsi, les résultats issus de nos travaux confirment l'intérêt d'inhiber la voie de transport des acides mycoliques dans une stratégie thérapeutique destinée à contrer les infections à *M. abscessus*, et probablement vis-à-vis d'autres NTM. Nous avons, en effet, démontré l'efficacité des dérivés du benzimidazole, notamment du composé phare EJMCh6, contre *M. abscessus* et décrit leur mode d'action en générant des mutants résistants spontanés portant des mutations dans le gène *mmpL3*. Ces composés inhibent également le transport des TMM chez *M. tuberculosis*, ce qui a été confirmé par marquage radioactif des acides mycoliques et permis d'observer l'accumulation de TMM tandis que les quantités de TDM et d'acides mycoliques liés à l'arabinogalactane diminuent fortement (Korycka-Machała et al. 2019). Mais MmpL3 pourrait ne pas être la seule cible de ces composés. En effet, chez *M. tuberculosis*, le THPP (Tetrahydropyrazolo[1,5-a]Pyrimidine-3-Carboxamide) a tout d'abord été décrit comme un inhibiteur de MmpL3 (Remuiñán et al. 2013) mais les mêmes auteurs ont, dans un second temps, montré que cette molécule inhibait en réalité l'enzyme EchA6, une enzyme clé du système FasII de la voie de biosynthèse des acides mycoliques (Cox et al. 2016). Ainsi, des mutations dans *mmpL3* peuvent, dans certains cas, masquer la véritable cible de certains inhibiteurs. Une autre étude montre que des dérivés tri-substitués du benzimidazole, structuralement différents des molécules que nous avons testées, peuvent cibler la protéine FtsZ impliquée dans la division et croissance de *M. tuberculosis* (Park et al. 2014).

Dans la plupart de ces études, incluant les nôtres, nous avons déterminé la cible en générant des mutants spontanés résistants montrant que l'activité de ces composés reste dépendante de certaines modifications génétiques dans *mmpL3* (Kozikowski et al. 2017; Dupont et al. 2016; Raynaud et al. 2020). Cependant, un autre système de résistance (induisant des résistances de faible niveau) peut impliquer d'autres membres de la famille des MmpL. Selon une étude récente, des mutations dans des régulateurs transcriptionnels s'accompagnent de la surexpression de la pompe à efflux MmpL5/MmpS5 (responsable de la résistance à la bédaquiline et à la clofazimine) (Richard et al. 2019) et permettent d'extruder certains inhibiteurs amphiphiles de MmpL3 chez *M. tuberculosis* (Li et al. 2020). Des études ultérieures nous permettront de vérifier si, chez *M. abscessus*, l'orthologue de MmpL5 est également impliqué dans des mécanismes de résistance secondaires vis-à-vis de EJMCh6.

Nous avons montré que ces inhibiteurs de MmpL3 sont efficaces *in vivo* dans un modèle zebrafish, et s'accompagnaient d'une réduction de la charge bactérienne et d'une augmentation de la survie des embryons infectés par *M. abscessus* sans pour autant présenter une activité cytotoxique vis-à-vis de cellules de mammifères. Ces résultats doivent être à présent étayés dans un modèle pré-clinique murin, tel que le modèle C3HeB/FeJ (Kramnik) développé pour tester l'efficacité de la BDQ (voir Axe II). Notons que les dérivés des indole-2-carboxamides utilisés dans notre étude ont par ailleurs été testé précédemment dans un modèle Balb/c contre *M. tuberculosis* sans présenter de toxicité particulière et associés à une forte réduction de la charge bactérienne (Stec et al. 2016). Plus récemment, l'activité d'indole-2-carboxamides présentant des structures différentes de nos composés, a été testé dans un modèle de souris SCID infecté par *M. abscessus*. Dans ce modèle de souris immunodéprimées, l'effet des composés est comparable à celui de l'amikacine (utilisée en contrôle) 12 jours après infection (Pandya et al. 2019). Par ailleurs, des études pré-cliniques ont été menées sur deux indolecarboxamides, NITD-304 et NITD-349, testées dans plusieurs espèces animales dont le rat et présentant des paramètres pharmacocinétiques favorables et une faible toxicité. Les résultats dans un modèle murin Balb/c infecté par *M. tuberculosis* montrent une forte activité de ces molécules 60 jours d'infection (Rao et al. 2013).

Dans une récente étude pré-clinique, *Cao et al.* ont montré sur un modèle cellulaire dérivé de cellules immunitaires infectées par *M. tuberculosis*, prélevées sur des patients sains et diabétiques, qu'un traitement par des indole-2-carboxamides (ceux issus de (Stec et al. 2016)) permettait de diminuer la charge bactérienne intracellulaire. Les auteurs proposent que le traitement par ces molécules permettait d'accroître la réponse immunitaire initialement déclenchée par l'infection (Cao et al. 2020).

Une molécule est actuellement en phase clinique, SQ109 et une première étude en phase initiale chez des patients atteints de tuberculose a été réalisée. Les auteurs ont montré que SQ109 administrée seule n'était pas très efficace mais une fois administrée en association avec la rifampicine, l'effet observé était supérieur à celui de la rifampicine seule (Heinrich et al. 2014). Une deuxième étude plus récente et plus importante (randomisée contrôlée), a été réalisée en Afrique dans laquelle les auteurs ont testé une combinaison avec de hautes doses de rifampicine associée à de la moxifloxacine et SQ109. Ils ont conclu que les résultats étaient encourageants mais nécessitaient d'être répétés. Toutefois ils ont soulevé un problème, le fait que SQ109 est métabolisé par les cytochromes CYP2D6 et CYP2C19, alors que CYP2C19 est connu pour être

induit par la rifampicine. Ils ont observé qu'en utilisant de hautes doses de SQ109, cette métabolisation semblait pouvoir être outrepassée (Boeree et al. 2017).

Le mode d'action des inhibiteurs directs de MmpL3 semble être lié à l'inhibition de l'activité flippase, ce qui a été démontrée pour des molécules telles que PIPD1, BM212 ou encore AU1235. Toutefois, *Xu et al.* ont montré qu'un autre composé actuellement en phase clinique dans le traitement de la tuberculose, SQ109, n'inhiberait pas directement l'activité flippase de MmpL3 (Xu et al. 2017; Dupont et al. 2019). Cependant, SQ109 a pu être mis en évidence au sein de la structure cristallographique de MmpL3 de *M. smegmatis* (B. Zhang et al. 2019) indiquant une interaction directe entre SQ109 et MmpL3. D'autres hypothèses reposent sur le fait que certains inhibiteurs se fixeraient dans le canal utilisé par les protons, bloquant ainsi la force protomotrice et donc l'apport d'énergétique nécessaire au transport du TMM à travers la membrane plasmique (Sethiya et al. 2020). Nos études *in silico* et de docking réalisées grâce à un modèle prédictif de la structure de MmpL3 de *M. abscessus* basé sur les coordonnées cristallographiques de la structure de MmpL3 de *M. smegmatis*, suggèrent que les dérivés du benzimidazole pourraient se loger dans la même cavité que celle décrite pour accommoder SQ109, AU1235 ou ICA38 (B. Zhang et al. 2019). Toutefois, des études cristallographiques et/ou de CryoEM seront nécessaires pour démontrer sans ambiguïté la présence d'un site de liaison des benzimidazoles dans MmpL3 de *M. abscessus.* L'accès à ces données structurales permettra également de guider les chimistes pour la synthèse d'une nouvelle génération d'inhibiteurs de MmpL3 présentant des activités et propriétés physicochimiques améliorées.

Une autre perspective intéressante émanant de nos travaux, consiste à d'étudier la relation entre les inhibiteurs de MmpL3 avec d'autres antibiotiques déjà utilisés en clinique. *Li et al.* ont identifié plusieurs synergies entre des inhibiteurs de MmpL3 et d'autres antibiotiques vis-à-vis contre *M. tuberculosis in vitro* (Li et al. 2017). Au cours de ce travail, nous avons également identifié des synergies entre les indole-2-carboxamides et des β-lactamines (imipénème et céfoxitine) *in vitro* ainsi que dans un modèle d'infection macrophagique (Raynaud et al. 2020). Ces résultats pourraient conférer un réel avantage à ces molécules pour être incluses au traitement des infections à *M. abscessus.*

Si le transport des acides mycoliques semble être un site de vulnérabilité chez *M. abscessus*, il n'en est pas de même la biosynthèse des acides mycoliques. L'INH, par exemple, est totalement inactif chez *M. abscessus*, vraisemblablement car il ne peut pas être activé efficacement par la catalase-péroxidase KatG de *M. abscessus* (Richard et al. 2019). Cependant,

une piste prometteuse à exploiter consisterait à tester des inhibiteurs directs de l'enoyl ACP réductase InhA, qui ne nécessitent pas une activation métabolique au préalable par KatG. De tels inhibiteurs ont été développés chez *M. tuberculosis* pour contrer les mécanismes de résistance à l'INH causées par des mutations dans KatG (Rožman et al. 2017). Nos données récentes au laboratoire ont montré que le triclosan (un inhibiteur direct d'InhA) est très efficace vis-à-vis de *M. abscessus* (CMI = 3.1 µg/mL ; données non publiées), indiquant qu'il est possible d'inhiber efficacement la voie de biosynthèse des mycolates chez *M. abscessus*.

Par ailleurs, outre les acides mycoliques, d'autres composants essentiels de la paroi de *M. abscessus* pourraient représenter des cibles de choix pour le développement de nouvelles approches thérapeutiques. Nous avons identifié et démontré l'activité de nouveaux composés hétérocycliques qui inhibent l'UDP-Gal mutase (UGM) de *M. tuberculosis*, une enzyme essentielle qui isomérise l'UDM-Gal*p* en UDP-Gal*f*, lequel représente l'unité de base pour la synthèse du galactane de l'AG (voir article de Maaliki et al. 2020 en Annexe I). Nous envisageons d'évaluer l'activité de ces inhibiteurs vis-à-vis de l'UGM de *M. abscessus* afin déterminer si elle représente une cible valide d'un point de vue thérapeutique.

Axe II. Repositionnement d'antibiotiques contre *M. abscessus*.

Une alternative permettant d'améliorer l'efficacité des traitements repose sur le repositionnement d'antibiotiques. Cette pratique consiste à tester contre *M. abscessus* l'efficacité de molécules utilisées dans le traitement des infections causées par d'autres pathogènes ou d'autres maladies. Ces molécules, déjà validées chez l'homme d'un point de vue toxicologique et pharmacologique pour un autre traitement pourront dès lors être directement incluses dans le traitement des infections à *M. abscessus*. Ce processus est de plus en plus courant car en quelques années, deux antibiotiques repositionnés ont rejoint l'arsenal thérapeutique pour lutter contre les infections à *M. abscessus* : la clofazimine (CFZ) et la tigécycline (TGC).

La CFZ est une phénazine utilisée dans le traitement de la lèpre *(Mungroo et al. 2020)* et plus récemment dans le traitement de la tuberculose MDR (Xu et al. 2012). Elle représente une alternative intéressante dans le traitement des infections persistantes aux MNT (Martiniano et al. 2017) et des infections à *M. abscessus* en particulier et est officiellement recommandée pour ce traitement (Daley et al. 2020). *Richard et al.* ont montré que des mutations situées dans un

gène codant pour un répresseur transcriptionnel de type TetR (MAB_2299c) entraînent la surexpression de la pompe à efflux MAB_2300/MAB_2301, apparentée au système de type MmpL5/MmpS5, ce qui permettrait d'extruder la CFZ hors de la bactérie (Richard et al. 2019). Ce mécanisme n'implique, toutefois, qu'un faible niveau de résistance.

La TGC est utilisée dans le traitement d'infections à diverses bactéries à $Gram^+$ ou $Gram^-$ (Petersen et al. 1999). Rapidement testée contre les MNT *in vitro* (Wallace et al. 2002), elle ne fût incluse en clinique que dans les années 2010 dans le traitement contre *M. abscessus* (Cherif et al. 2011). Les tétracyclines ont été pendant très longtemps délaissées dans le traitement des infections à *M. abscessus* du fait de leur faible activité. Ce n'est que très récemment qu'un mécanisme de résistance innée impliquant l'enzyme MAB_TetX n'a été décrit (Rudra et al. 2018). Contrairement aux tétracyclines, la TGC (une glycylcycline) est nettement moins affectée par ce mécanisme du fait de leurs différences structurales, ce qui la rend particulièrement active contre *M. abscessus* (Kwon et al. 2019). Sa stabilité a par ailleurs été démontrée dans un modèle synthétique reposant sur un système de fibres creuses (« Hollow fiber system model ») (Ferro et al. 2016). Ce « Hollow fiber system » consiste en un modèle pharmacocinétique qui imite le plasma humain et permet de définir des profils de concentration en fonction du temps des molécules testées. La bactérie, placée dans un compartiment extérieur, est séparée du compartiment intérieur par des fibres creuses semi-perméable, permettant les échanges de petites molécules mais dont les pores sont trop petits pour les bactéries (Cavaleri and Manolis 2015).

Plus récemment, la BDQ, a été utilisée dans le traitement des formes MDR de tuberculose (Lounis et al. 2006) et proposée comme candidate au repositionnement contre *M. abscessus*. Elle est très efficace contre les espèces du complexe *M. abscessus in vitro* (Brown-Elliott and Wallace 2019) et montre une très bonne activité dans le modèle zebrafish (Dupont et al. 2017). Cependant, son efficacité dans les modèles murins reste partagée. Si *Lerat et al.* ont montré qu'elle avait un effet modéré dans un modèle murin Nude (Lerat et al. 2014), *Obregon-Henao et al.* ont relaté une bonne activité dans un modèle murin GKO (Obregón-Henao et al. 2015). Dans notre étude, nous avons montré que la BDQ présente une meilleure activité que l'amikacine dans un modèle murin immunocompétent C3HeB/FeJ (Kramnik) (Le Moigne et al. 2020). Chez *M. tuberculosis*, son utilisation reste limitée aux souches MDR car une utilisation trop fréquente ou une mauvaise observance entraîneraient une émergence rapide de souches résistantes à la BDQ (Veziris et al. 2017). Plusieurs mécanismes de résistances ont été identifiés chez *M. tuberculosis* :

des mutations ont été identifiées dans le gène *atpE* codant pour la cible (Andries et al. 2005), des mutations dans le gène *Rv0678* codant un régulateur transcriptionnel de la pompe à efflux MmpL5/MmpS5 (Hartkoorn et al. 2014) ainsi que des mutations dans le gène *pepQ* dont le mécanisme de résistance n'a pas encore été décrit (Nguyen et al. 2018; Nimmo et al. 2020; Almeida et al. 2016). Chez *M. abscessus*, le système de pompe à efflux MAB_2300/MAB_2301 a été décrit dans la résistance croisée à la CFZ et à la BDQ (Richard et al. 2019). *Dupont et al.* ont montré que l'introduction de mutations (D29V et A64P) dans *atpE* chez *M. abscessus* entraînait une résistance très élevée à la BDQ (Dupont et al. 2017).

Durant ma thèse, j'ai également généré chez *M. abscessus* un mutant *ΔpepQ* (*MAB_2838c*) en utilisant la technique du recombineering (remplacement du gène cible par une cassette de résistance à la zéocine après un double évènement de recombinaison homologue) ainsi qu'une souche surexprimant *pepQ.* Aucun phénotype spécifique concernant la sensibilité aux antibiotiques, notamment la BDQ, n'a été observé dans ces souches. Des vérifications par RT-PCR ont montré que le gène *MAB_2838c* était en opéron avec le gène *MAB_2837c* codant pour un facteur d'élongation P (*elonP)* présentant, lui, une transcription altérée (par qRT-PCR) dans le mutant *ΔpepQ* (données non publiées). Pour pouvoir émettre des hypothèses concernant l'implication de *pepQ* dans l'éventuelle résistance à la BDQ, nous envisageons de réaliser un double mutant *ΔpepQΔelonP* ainsi qu'un mutant *ΔelonP* (si ce gène n'est pas essentiel) afin de comparer leurs différences phénotypiques et de pouvoir associer chaque différence à un gène ou l'autre.

Mais, si la BDQ cible l'ATP synthase bactérienne, les travaux récents de *Luo et al.* suggèrent qu'elle est également capable d'inhiber les ATP synthases de levure et humaine (Luo et al. 2020). Ces résultats pourraient avoir des conséquences importantes au niveau clinique car l'inhibition de la production d'ATP cellulaire pourrait s'avérer dangereuse chez certains patients à risque, notamment ceux présentant des antécédents cardiaques. Différentes interactions ont été évaluées entre la BDQ et d'autres antibiotiques au cours de notre travail mais aucune ne montre des synergies très claires (Le Moigne et al. 2020), confirmant les résultats de *Lindman et al.* qui suggèrent que l'effet de la BDQ empêcherait l'effet bactéricide des β-lactamines (Lindman and Dick 2019). Toutefois, nous avons identifié une molécule capable de potentialiser l'effet de la BDQ. Il s'agit du vérapamil, employé dans le traitement de maladies cardiaques comme inhibiteur de canaux calciques, et utilisé ici pour sa fonction d'inhibiteur de pompe à efflux (Viljoen et al. 2019).

Les rifamycines sont une classe d'antibiotiques très largement utilisées en première intention contre *M. tuberculosis*. Cependant, chez *M. abscessus*, un mécanisme de résistance innée impliquant l'ADP-ribosyltransférase Arr_{mab} rend inopérantes la plupart des molécules appartenant à cette classe d'antibiotique (Rominski et al. 2017b). Des mutations au niveau du gène codant pour la cible, *rpoB,* engendrent également un fort niveau de résistance aux rifamycines chez *M. tuberculosis* (Telenti et al. 1993) ainsi que chez *M. abscessus* comme nous l'avons démontré dans notre étude (Johansen et al. 2020). Une molécule analogue des rifamycines, la rifabutine (RFB), semble être inactivée plus lentement par Arr_{mab}, lui conférant une bonne activité *in vitro* contre *M. abscessus* et également dans un modèle d'infection macrophagique ainsi que dans le zebrafish (Dinah Binte Aziz et al. 2017; Johansen et al. 2020). Si la CMI *in vitro* du variant S est plus élevée que celle du variant R, nous avons toutefois observé que les deux variants étaient, de façon similaire, très sensibles à l'action de la RFB dans le macrophage, renforçant l'idée d'une mauvaise corrélation entre CMI et activité *in vivo*. La proposition du repositionnement de la RFB est récente puisque *Crabol et al.* proposaient déjà une utilisation de cette dernière contre les MNT mais mettaient en avant un manque de données cliniques concernant ce type d'infections (Crabol et al. 2016). En 2019, *Ganapathy et al.* proposent un repositionnement de la RFB contre les infections pulmonaires causées par *M. abscessus* (Ganapathy et al. 2019). Concernant les modèles pré-cliniques, il a été montré que la RFB présente une efficacité comparable à celle de la clarithromycine (CLR) dans un modèle murin NOD-SCID infecté par *M. abscessus* (Dick et al. 2020). Un autre avantage de cette molécule réside dans ses relations synergiques avec d'autres antibiotiques utilisés pour les traitements des infections à *M. abscessus*, tels que la CLR, la TGC ou encore l'IPM (Pryjma et al.2018b; Cheng et al. 2019). Un autre avantage de la RFB a été avancé par *Aziz et al.*, cette dernière permettrait de réduire l'expression de WhiB7, un régulateur transcriptionnel impliqué dans l'induction de l'expression d'Erm41 par les macrolides (Aziz et al. 2020). Contrer ce mécanisme de résistance permettrait d'accélérer les traitements car les souches ne nécessiteraient plus d'être séquencées pour en déterminer la sous-espèce et le sérovar. Malgré tous ces aspects positifs, l'utilisation en clinique de la RFB doit être poursuivie chez l'homme afin de juger de son efficacité thérapeutique. Par ailleurs, d'autres études seront nécessaires pour déterminer les éventuelles synergies ou antagonismes avec les antibiotiques déjà utilisés dans les traitements usuels.

Une autre alternative très prometteuse est la phagothérapie, cette pratique datant du début du siècle dernier, très utilisée dans les pays d'Europe de l'Est tels que la Géorgie, consiste à utiliser des bactériophages lytiques capables de lyser rapidement les bactéries mais également

très espèce spécifique. Dans les pays occidentaux, leur utilisation a été interdite du fait d'un manque de réglementations. Cependant, l'accroissement des phénomènes de résistance aux antibiotiques motivent à l'heure actuelle des études sur la phagothérapie même si les autorités sanitaires ne sont toujours pas favorables à l'utilisation à grande échelle de cette approche, autorisant pour l'instant uniquement des études à titre compassionnel (Azimi et al. 2019). *Dedrick et al.* ont démontré les bienfaits d'un traitement d'une patiente atteinte de mucoviscidose ayant contracté une infection persistante à *M. massiliense,* multi résistante aux antibiotiques, avec un cocktail de trois bactériophages préalablement sélectionnés pour leur capacité lytique contre cette souche. La combinaison antibiotiques et bactériophages a permis de réduire considérablement la charge bactérienne et d'augmenter l'état de santé général de la patiente (Dedrick et al. 2019). A ce titre, nous avons démontré dans l'équipe que la combinaison de ces mêmes phages avec la RFB s'accompagne d'un effet notoire sur la réduction de la charge bactérienne par rapport aux bactéries traitées uniquement avec les phages ou uniquement avec la RFB (données non publiées). Ainsi, sous réserve que ces études puissent être reproduites et étendues avec d'autres couples phages/*M. abscessus*, ces résultats suggèrent que la RFB puisse également représenter un élément central d'une nouvelle approche thérapeutique combinant antibiothérapie et phagothérapie.

Pour conclure, les infections à *M. abscessus* restent pour le clinicien extrêmement compliquées à traiter. Devant le choix très restreint des antibiotiques mis à disposition, il apparait nécessaire d'améliorer les traitements actuels (Meir and Barkan 2020). L'ensemble de ce travail de thèse nous permet de mettre en avant de nouvelles molécules, cibles et combinaisons thérapeutiques qui nécessitent d'être validées dans des essais pré-cliniques et/ou cliniques (Figure 22). L'ensemble de ces résultats propose des perspectives encourageantes pour l'amélioration du traitement des infections pulmonaires à *M. abscessus.*

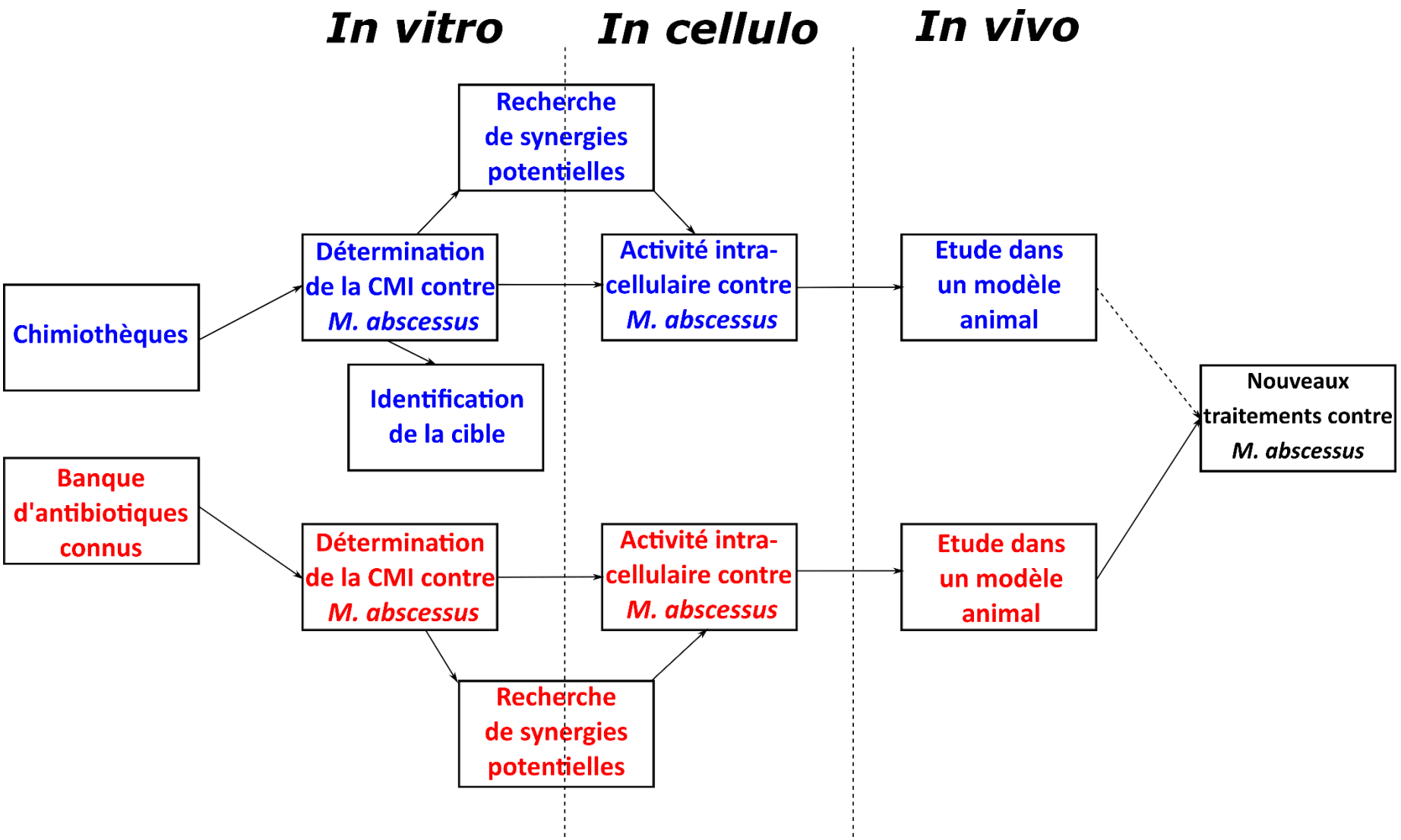

Figure 22.Représentation des différentes étapes de la recherche de nouveaux traitements contre *M. abscessus*.

En bleu, la recherche de nouvelles molécules et de nouvelles cibles contre *M. abscessus*. En rouge, le repositionnement d'antibiotiques contre *M. abscessus*

REFERENCES

Abrahams, Katherine A., and Gurdyal S. Besra. 2018. “Mycobacterial Cell Wall Biosynthesis: A Multifaceted Antibiotic Target.” *Parasitology* 145 (2): 116–33. https://doi.org/10.1017/S0031182016002377.

Adekambi, Toidi, Mohamed Sassi, Jakko Van Ingen, and Michel Drancourt. 2017. “Reinstating Mycobacterium Massiliense and Mycobacterium Bolletii as Species of the Mycobacterium Abscessus Complex.” *International Journal of Systematic and Evolutionary Microbiology* 67 (8): 2726–30. https://doi.org/10.1099/ijsem.0.002011.

Alderwick, Luke J., Jame Harrison, Georgina S. Lloyd, and Helen L Birch. 2015. “The Mycobacterial Cell Wall—Peptidoglycan and Arabinogalactan Luke.” *Cold Spring Harb Perspect Med*. https://doi.org/10.1351/pac197125010135.

Almeida, Deepak, Thomas Ioerger, Sandeep Tyagi, Si Yang Li, Khisimuzi Mdluli, Koen Andries, Jacques Grosset, Jim Sacchettini, and Eric Nuermberger. 2016. “Mutations in PepQ Confer Low-Level Resistance to Bedaquiline and Clofazimine in Mycobacterium Tuberculosis.” *Antimicrobial Agents and Chemotherapy* 60 (8): 4590–99. https://doi.org/10.1128/AAC.00753-16.

Alsayed, Shahinda S.R., Shichun Lun, Giuseppe Luna, Chau Chun Beh, Alan D. Payne, Neil Foster, William R. Bishai, and Hendra Gunosewoyo. 2020. “Design, Synthesis, and Biological Evaluation of Novel Arylcarboxamide Derivatives as Anti-Tubercular Agents.” *RSC Advances* 10 (13): 7523–40. https://doi.org/10.1039/c9ra10663d.

Andries, Koen, Peter Verhasselt, Jerome Guillemont, Hinrich W.H. Göhlmann, Jean Marc Neefs, Hans Winkler, Jef Van Gestel, et al. 2005. “A Diarylquinoline Drug Active on the ATP Synthase of Mycobacterium Tuberculosis.” *Science* 307 (5707): 223–27. https://doi.org/10.1126/science.1106753.

Azimi, Taher, Mehrdad Mosadegh, Mohammad Javad Nasiri, Sahar Sabour, Samira Karimaei, and Ahmad Nasser. 2019. “Phage Therapy as a Renewed Therapeutic Approach to Mycobacterial Infections: A Comprehensive Review.” *Infection and Drug Resistance*. https://doi.org/10.2147/IDR.S218638.

Aziz, Dinah B., Jeanette W.P. Teo, Véronique Dartois, and Thomas Dick. 2018. “Teicoplanin - Tigecycline Combination Shows Synergy against Mycobacterium Abscessus.” *Frontiers in Microbiology* 9 (MAY): 1–8. https://doi.org/10.3389/fmicb.2018.00932.

Aziz, Dinah Binte, Mei Lin Go, and Thomas Dick. 2020. “Rifabutin Suppresses Inducible Clarithromycin Resistance in Mycobacterium Abscessus by Blocking Induction of WhiB7 and Erm41.” *Antibiotics* 9 (2). https://doi.org/10.3390/antibiotics9020072.

Aziz, Dinah Binte, Jian Liang Low, Mu-Lu Wu, Martin Gengenbacher, Jeanette W. P. Teo, Véronique Dartois, and Thomas Dick. 2017. “Rifabutin Is Active against Mycobacterium Abscessus Complex.” *Antimicrobial Agents and Chemotherapy* 61 (6).

Banaschewski, Brandon, Deepshikha Verma, Lian J. Pennings, Matthew Zimmerman, Qihua Ye, Jake Gadawa, Veronique Dartois, et al. 2019. “Clofazimine Inhalation Suspension for the Aerosol Treatment of Pulmonary Nontuberculous Mycobacterial Infections.” *Journal of Cystic Fibrosis* 18 (5): 714–20. https://doi.org/10.1016/j.jcf.2019.05.013.

Banerjee, Asesh, Eugenie Dubnau, Annaik Quemard, V Balasubramanian, Kyung Sun Um, Theresa Wilson, Des Collins, Geoffrey De Lisle, and William R. Jacobs. 1994. “InhA, a Gene

Encoding a Target for Isoniazid and Ethionamide in Mycobacterium Tuberculosis." *Science* 263 (5144): 227–30. https://doi.org/10.1126/science.8284673.

Banerjee, Asesh, Michele Sugantino, James C. Sacchettini, and William R. Jacobs. 1998. "The MabA Gene from the InhA Operon of Mycobacterium Tuberculosis Encodes a 3-Ketoacyl Reductase That Fails to Confer Isoniazid Resistance." *Microbiology* 144 (10): 2697–2704. https://doi.org/10.1099/00221287-144-10-2697.

Bax, Hannelore I., Corné P. de Vogel, Johan W. Mouton, and Jurriaan E.M. de Steenwinkel. 2019. "Omadacycline as a Promising New Agent for the Treatment of Infections with Mycobacterium Abscessus." *The Journal of Antimicrobial Chemotherapy* 74 (10): 2930–33. https://doi.org/10.1093/jac/dkz267.

Bechara, Chadi, Edouard MacHeras, Beate Heym, Adele Pages, and Nicole Auffret. 2010. "Mycobacterium Abscessus Skin Infection after Tattooing: First Case Report and Review of the Literature." *Dermatology* 221 (1): 1–4. https://doi.org/10.1159/000313974.

Becker, Katja, Klara Haldimann, Petra Selchow, Lukas M. Reinau, Michael Dal Molin, and Peter Sander. 2017. "Lipoprotein Glycosylation by Protein-O-Mannosyltransferase (MAB_1122c) Contributes to Low Cell Envelope Permeability and Antibiotic Resistance of Mycobacterium Abscessus." *Frontiers in Microbiology* 8 (NOV): 1–12. https://doi.org/10.3389/fmicb.2017.02123.

Belardinelli, Juan Manuel, Gérald Larrouy-Maumus, Victoria Jones, Luiz Pedro Sorio De Carvalho, Michael R. McNeil, and Mary Jackson. 2014. "Biosynthesis and Translocation of Unsulfated Acyltrehaloses in Mycobacterium Tuberculosis." *Journal of Biological Chemistry* 289 (40): 27952–65. https://doi.org/10.1074/jbc.M114.581199.

Belardinelli, Juan Manuel, Amira Yazidi, Liang Yang, Lucien Fabre, Wei Li, Benoit Jacques, Shiva Kumar Angala, et al. 2016. "Structure-Function Profile of MmpL3, the Essential Mycolic Acid Transporter from Mycobacterium Tuberculosis." *ACS Infectious Diseases* 2 (10): 702–13. https://doi.org/10.1021/acsinfecdis.6b00095.

Benwill, Jeana L., and Richard J. Wallace. 2014. "Mycobacterium Abscessus: Challenges in Diagnosis and Treatment." *Current Opinion in Infectious Diseases* 27 (6): 506–10. https://doi.org/10.1097/QCO.0000000000000104.

Bernut, A., J.-L. Herrmann, K. Kissa, J.-F. Dubremetz, J.-L. Gaillard, G. Lutfalla, and L. Kremer. 2014. "Mycobacterium Abscessus Cording Prevents Phagocytosis and Promotes Abscess Formation." *Proceedings of the National Academy of Sciences* 111 (10): E943–52. https://doi.org/10.1073/pnas.1321390111.

Bernut, Audrey, Christian Dupont, Nikolay V. Ogryzko, Aymeric Neyret, Jean Louis Herrmann, R. Andres Floto, Stephen A. Renshaw, and Laurent Kremer. 2019. "CFTR Protects against Mycobacterium Abscessus Infection by Fine-Tuning Host Oxidative Defenses." *Cell Reports* 26 (7): 1828-1840.e4. https://doi.org/10.1016/j.celrep.2019.01.071.

Bernut, Audrey, Jean-louis Herrmann, Diane Ordway, and Laurent Kremer. 2017. "The Diverse Cellular and Animal Models to Decipher the Physiopathological Traits of Mycobacterium Abscessus Infection." *Frontiers in Cellular and Infection Microbiology* 7 (April): 1–8. https://doi.org/10.3389/fcimb.2017.00100.

Bernut, Audrey, Jean Louis Herrmann, Karima Kissa, Jean François Dubremetz, Jean Louis Gaillard, Georges Lutfalla, and Laurent Kremer. 2014. "Mycobacterium Abscessus Cording

Prevents Phagocytosis and Promotes Abscess Formation." *Proceedings of the National Academy of Sciences of the United States of America* 111 (10). https://doi.org/10.1073/pnas.1321390111.

Bernut, Audrey, Vincent Le Moigne, Tiffany Lesne, Georges Lutfalla, Jean Louis Herrmann, and Laurent Kremer. 2014. "In Vivo Assessment of Drug Efficacy against Mycobacterium Abscessus Using the Embryonic Zebrafish Test System." *Antimicrobial Agents and Chemotherapy* 58 (7): 4054–63. https://doi.org/10.1128/AAC.00142-14.

Bernut, Audrey, Albertus Viljoen, Christian Dupont, Guillaume Sapriel, Mickaël Blaise, Christiane Bouchier, Roland Brosch, Chantal de Chastellier, Jean Louis Herrmann, and Laurent Kremer. 2016. "Insights into the Smooth-to-Rough Transitioning in Mycobacterium Bolletii Unravels a Functional Tyr Residue Conserved in All Mycobacterial MmpL Family Members." *Molecular Microbiology* 99 (5): 866–83. https://doi.org/10.1111/mmi.13283.

Beveridge, Terry J. 1999. "Structures of Gram-Negative Cell Walls and Their Derived Membrane Vesicles." *Journal of Bacteriology* 181 (16): 4725–33. https://doi.org/10.1128/jb.181.16.4725-4733.1999.

Bhatt, Apoorva, Laurent Kremer, Annie Z. Dai, James C. Sacchettini, and William R. Jacobs. 2005. "Conditional Depletion of KasA, a Key Enzyme of Mycolic Acid Biosynthesis, Leads to Mycobacterial Cell Lysis." *Journal of Bacteriology* 187 (22): 7596–7606. https://doi.org/10.1128/JB.187.22.7596-7606.2005.

Blair, Jessica M.A., Mark A. Webber, Alison J. Baylay, David O. Ogbolu, and Laura J.V. Piddock. 2015. "Molecular Mechanisms of Antibiotic Resistance." *Nature Reviews Microbiology* 13 (1): 42–51. https://doi.org/10.1038/nrmicro3380.

Bloch, K., and D. Vance. 1977. "Control Mechanisms in the Synthesis of Saturated Fatty Acids." *Annual Review of Biochemistry* 46: 263–98. https://doi.org/10.1146/annurev.bi.46.070177.001403.

Boeree, Martin J., Norbert Heinrich, Rob Aarnoutse, Andreas H. Diacon, Rodney Dawson, Sunita Rehal, Gibson S. Kibiki, et al. 2017. "High-Dose Rifampicin, Moxifloxacin, and SQ109 for Treating Tuberculosis: A Multi-Arm, Multi-Stage Randomised Controlled Trial." *The Lancet Infectious Diseases* 17 (1): 39–49. https://doi.org/10.1016/S1473-3099(16)30274-2.

Bohlin, Jon, Vegard Eldholm, John H.O. Pettersson, Ola Brynildsrud, and Lars Snipen. 2017. "The Nucleotide Composition of Microbial Genomes Indicates Differential Patterns of Selection on Core and Accessory Genomes." *BMC Genomics* 18 (1): 1–11. https://doi.org/10.1186/s12864-017-3543-7.

Brown-Elliott, Barbara A., Sruthi Vasireddy, Ravikiran Vasireddy, Elena Iakhiaeva, Susan T. Howard, Kevin Nash, Nicholas Parodi, et al. 2015. "Utility of Sequencing the Erm(41) Gene in Isolates of Mycobacterium Abscessus Subsp. Abscessus with Low and Intermediate Clarithromycin MICs." *Journal of Clinical Microbiology* 53 (4): 1211–15. https://doi.org/10.1128/JCM.02950-14.

Brown-Elliott, Barbara A., and Richard J. Wallace. 2019. "In Vitro Susceptibility Testing of Bedaquiline against Mycobacterium Abscessus Complex." *Antimicrobial Agents and Chemotherapy* 63 (2): 1–8. https://doi.org/10.1128/AAC.01919-18.

Brown, Alistair K., Apoorva Bhatt, Albel Singh, Elesh Saparia, Alex F. Evans, and Gurdyal S. Besra. 2007. "Identification of the Dehydratase Component of the Mycobacterial Mycolic Acid-

Synthesizing Fatty Acid Synthase-II Complex." *Microbiology* 153 (12): 4166–73. https://doi.org/10.1099/mic.0.2007/012419-0.

Cabañas, María Jesús; Vázquez, David; 1978. "Inhibition of Ribosomal Translocation by Aminoglycoside Antibiotics." *Biochemical and Biophysical Research Communications* 83 (3): 991–97.

Camacho, Luis R., Patricia Constant, Catherine Raynaud, Marie Antoinette Lanéelle, James A. Triccas, Brigitte Gicquel, Mamadou Daffé, and Christophe Guilhot. 2001. "Analysis of the Phthiocerol Dimycocerosate Locus of Mycobacterium Tuberculosis. Evidence That This Lipid Is Involved in the Cell Wall Permeability Barrier." *Journal of Biological Chemistry* 276 (23): 19845–54. https://doi.org/10.1074/jbc.M100662200.

Campbell, Elizabeth A., Nataliya Korzheva, Arkady Mustaev, Katsuhiko Murakami, Satish Nair, Alex Goldfarb, and Seth A. Darst. 2001. "Structural Mechanism for Rifampicin Inhibition of Bacterial RNA Polymerase." *Cell* 104 (6): 901–12. https://doi.org/10.1016/S0092-8674(01)00286-0.

Cao, Ruoqiong, Hicret Islamoglu, Garrett Teskey, Karo Gyurjian, Rachel Abrahem, Oluseye K. Onajole, Shichun Lun, et al. 2020. "The Preclinical Candidate Indole-2-Carboxamide Improves Immune Responses to Mycobacterium Tuberculosis Infection in Healthy Subjects and Individuals with Type 2 Diabetes." *International Microbiology* 23 (2): 161–70. https://doi.org/10.1007/s10123-019-00086-0.

Carel, Clément, Kanjana Nukdee, Sylvain Cantaloube, Mélanie Bonne, Cheikh T. Diagne, Françoise Laval, Mamadou Daffé, and Didier Zerbib. 2014. "Mycobacterium Tuberculosis Proteins Involved in Mycolic Acid Synthesis and Transport Localize Dynamically to the Old Growing Pole and Septum." *PLoS ONE* 9 (5). https://doi.org/10.1371/journal.pone.0097148.

Carvalho, Natalia F.G. de, Fernando Pavan, Daisy N. Sato, Clarice Q.F. Leite, Robert D. Arbeit, and Erica Chimara. 2018. "Genetic Correlates of Clarithromycin Susceptibility among Isolates of the Mycobacterium Abscessus Group and the Potential Clinical Applicability of a PCR-Based Analysis of Erm(41)." *Journal of Antimicrobial Chemotherapy* 73 (4): 862–66. https://doi.org/10.1093/jac/dkx476.

Catherinot, Emilie, Anne Laure Roux, Edouard Macheras, Dominique Hubert, Moussa Matmar, Luc Dannhoffer, Thierry Chinet, et al. 2009. "Acute Respiratory Failure Involving an R Variant of Mycobacterium Abscessus." *Journal of Clinical Microbiology* 47 (1): 271–74. https://doi.org/10.1128/JCM.01478-08.

Cavaleri, Marco, and Efthymios Manolis. 2015. "Hollow Fiber System Model for Tuberculosis: The European Medicines Agency Experience." *Clinical Infectious Diseases* 61 (Suppl 1): S1–4. https://doi.org/10.1093/cid/civ484.

Caverly, Lindsay J., Silvia M. Caceres, Cori Fratelli, Carrie Happoldt, Kelley M. Kidwell, Kenneth C. Malcolm, Jerry A. Nick, and David P. Nichols. 2015. "Mycobacterium Abscessus Morphotype Comparison in a Murine Model." *PLoS ONE* 10 (2): 1–18. https://doi.org/10.1371/journal.pone.0117657.

Chalut, Christian, Laure Botella, Célia De Sousa-D'Auria, Christine Houssin, and Christophe Guilhot. 2006. "The Nonredundant Roles of Two 4'-Phosphopantetheinyl Transferases in Vital Processes of Mycobacteria." *Proceedings of the National Academy of Sciences of the United States of America* 103 (22): 8511–16. https://doi.org/10.1073/pnas.0511129103.

Chen, Chao, Susana Gardete, Robert Sander Jansen, Annanya Shetty, Thomas Dick, Kyu Y. Rhee, and Véronique Dartoisa. 2018. “Verapamil Targets Membrane Energetics in Mycobacterium Tuberculosis.” *Antimicrobial Agents and Chemotherapy* 62 (5). https://doi.org/10.1128/AAC.02107-17.

Chen, Xi, Yan Jin, Kara Melissa T. Torres, Bo Li, Fenglin Zhuo, Xiaolan Ding, Lin Cai, Jianzhong Zhang, and Cheng Zhou. 2019. “Mycobacterium Abscessus Cutaneous Infection Secondary to Botulinum Toxin Injection: A Report of 2 Cases.” *JAAD Case Reports* 5 (11): 982–84. https://doi.org/10.1016/j.jdcr.2019.09.017.

Cheng, Aristine, Yi Tzu Tsai, Shu Yuan Chang, Hsin Yun Sun, Un In Wu, Wang Huei Sheng, Yee Chun Chen, and Shan Chwen Chang. 2019a. “In Vitro Synergism of Rifabutin with Clarithromycin, Imipenem, and Tigecycline against the Mycobacterium Abscessus Complex.” *Antimicrobial Agents and Chemotherapy* 63 (4). https://doi.org/10.1128/AAC.02234-18.

———. 2019b. “In Vitro Synergism of Rifabutin with Clarithromycin, Imipenem, and Tigecycline against the Mycobacterium Abscessus Complex.” *Antimicrobial Agents and Chemotherapy* 63 (4): AAC.02234-18. https://doi.org/10.1128/AAC.02234-18.

Cherif, E., L. Ben Hassine, S. Azzabi, Z. Kaouech, and N. Khalfallah. 2011. “Infection Pulmonaire à Mycobacterium Abscessus Chez Une Patiente Diabétique Traitée Par l’association Tigécycline- Amikacine-Céfoxitime.” *Medecine et Maladies Infectieuses* 41 (8): 440–41. https://doi.org/10.1016/j.medmal.2011.03.004.

Chim, Nicholas, Rodrigo Torres, Yuqi Liu, Joe Capri, Gaëlle Batot, Julian P. Whitelegge, and Celia W. Goulding. 2015. “The Structure and Interactions of Periplasmic Domains of Crucial MmpL Membrane Proteins from Mycobacterium Tuberculosis.” *Chemistry and Biology* 22 (8): 1098–1107. https://doi.org/10.1016/j.chembiol.2015.07.013.

Cho, Hongbaek, Tsuyoshi Uehara, and Thomas G. Bernhardt. 2014. “Beta-Lactam Antibiotics Induce a Lethal Malfunctioning of the Bacterial Cell Wall Synthesis Machinery.” *Cell* 159 (6): 1300–1311. https://doi.org/10.1016/j.cell.2014.11.017.

Choi, Go Eun, Ki Nam Min, Choul Jae Won, Kyeongman Jeon, Sung Jae Shin, and Won Jung Koh. 2012. “Activities of Moxifloxacin in Combination with Macrolides against Clinical Isolates of Mycobacterium Abscessus and Mycobacterium Massiliense.” *Antimicrobial Agents and Chemotherapy* 56 (7): 3549–55. https://doi.org/10.1128/AAC.00685-12.

Choi, Keum Hwa, Laurent Kremer, Gurdyal S. Besra, and Charles O. Rock. 2000. “Identification and Substrate Specificity of β-Ketoacyl (Acyl Carrier Protein) Synthase III (MtFabH) from Mycobacterium Tuberculosis.” *Journal of Biological Chemistry* 275 (36): 28201–7. https://doi.org/10.1074/jbc.M003241200.

Clary, Gillian, Smitha J. Sasindran, Nathan Nesbitt, Laurel Mason, Sara Cole, Abul Azad, Karen McCoy, Larry S. Schlesinger, and Luanne Hall-Stoodley. 2018. “Mycobacterium Abscessus Smooth and Rough Morphotypes Form Antimicrobial-Tolerant Biofilm Phenotypes but Are Killed by Acetic Acid.” *Antimicrobial Agents and Chemotherapy* 62 (3): 1–17. https://doi.org/10.1128/AAC.01782-17.

Colin, Andrew A., and Tarig Ali-Dinar. 2010. “Aerosolized Amikacin and Oral Clarithromycin to Eradicate Mycobacterium Abscessus in a Patient with Cystic Fibrosis: An 8-Year Follow-Up.” *Pediatric Pulmonology* 45 (6): 626–27. https://doi.org/10.1002/ppul.21222.

Combrink, Keith D., Andrea Ramirez Ramos, Stephanie Spring, Sebastian Schmidl, Kira Elizondo, Petronilo Morin, Bryant De Jesus, and Florian P. Maurer. 2019. “Rifamycin Derivatives Active against Pathogenic Rapidly-Growing Mycobacteria.” *Bioorganic and Medicinal Chemistry Letters* 29 (16): 2112–15. https://doi.org/10.1016/j.bmcl.2019.07.001.

Compain, Fabrice, Daria Soroka, Beate Heym, Jean Louis Gaillard, Jean Louis Herrmann, Delphine Dorchène, Michel Arthur, and Vincent Dubée. 2018. “In Vitro Activity of Tedizolid against the Mycobacterium Abscessus Complex.” *Diagnostic Microbiology and Infectious Disease* 90 (3): 186–89. https://doi.org/10.1016/j.diagmicrobio.2017.11.001.

Converse, Scott E., Joseph D. Mougous, Michael D. Leavell, Julie A. Leary, Carolyn R. Bertozzi, and Jeffery S. Cox. 2003. “MmpL8 Is Required for Sulfolipid-1 Biosynthesis and Mycobacterium Tuberculosis Virulence.” *Proceedings of the National Academy of Sciences of the United States of America* 100 (10): 6121–26. https://doi.org/10.1073/pnas.1030024100.

Cox, Jeffery S., Bing Chess, Michael McNeil, and William R. Jacobs. 1999. “Complex Lipid Determines Tissue-Specific Replication of Mycobacterium Tuberculosis in Mice.” *Nature* 402 (6757): 79–83. https://doi.org/10.1038/47042.

Cox, Jonathan A. G., Katherine A. Abrahams, Stephen Bethell, Klaus Fütterer, Nicholas C. Cammack, Ulrich Kruse, Albel Singh, et al. 2016. “THPP Target Assignment Reveals EchA6 as an Essential Fatty Acid Shuttle in Mycobacteria.” *Nature Microbiology* 1 (2): 15006. https://doi.org/10.1038/nmicrobiol.2015.6.

Crabol, Yoann, Emilie Catherinot, Nicolas Veziris, Vincent Jullien, and Olivier Lortholary. 2016. “Rifabutin: Where Do We Stand in 2016?” *Journal of Antimicrobial Chemotherapy* 71 (7): 1759–71. https://doi.org/10.1093/jac/dkw024.

Cremades, Rosa, Ana Santos, Juan Carlos Rodríguez, Eduardo Garcia-Pachón, Montserrat Ruiz, and Gloria Royo. 2009. “Mycobacterium Abscessus from Respiratory Isolates: Activities of Drug Combinations.” *Journal of Infection and Chemotherapy* 15 (1): 46–48. https://doi.org/10.1007/s10156-008-0651-y.

Daffé, Mamadou, and Hedia Marrakchi. 2019. “Unraveling the Structure of the Mycobacterial Envelope.” *Microbiology Spectrum* 7 (4). https://doi.org/10.1128/microbiolspec.gpp3-0027-2018.

Dal Molin, Michael, Myriam Gut, Anna Rominski, Klara Haldimann, Katja Becker, and Peter Sander. 2018. “Molecular Mechanisms of Intrinsic Streptomycin Resistance in Mycobacterium Abscessus.” *Antimicrobial Agents and Chemotherapy* 62 (1): 1–11. https://doi.org/10.1128/AAC.01427-17.

Dal Molin, Michael, Petra Selchow, Daniel Schäfle, Andreas Tschumi, Thomas Ryckmans, Stephan Laage-Witt, and Peter Sander. 2019. “Identification of Novel Scaffolds Targeting Mycobacterium Tuberculosis.” *Journal of Molecular Medicine* 97 (11): 1601–13. https://doi.org/10.1007/s00109-019-01840-7.

Daley, Charles L, Jonathan M Iaccarino, Christoph Lange, Emmanuelle Cambau, Richard J Wallace, Claire Andrejak, Erik C Böttger, et al. 2020. “Treatment of Nontuberculous Mycobacterial Pulmonary Disease: An Official ATS/ERS/ESCMID/IDSA Clinical Practice Guideline.” *The European Respiratory Journal* 56 (1). https://doi.org/10.1183/13993003.00535-2020.

Dedrick, Rebekah M., Carlos A. Guerrero-Bustamante, Rebecca A. Garlena, Daniel A. Russell, Katrina Ford, Kathryn Harris, Kimberly C. Gilmour, et al. 2019. “Engineered Bacteriophages for Treatment of a Patient with a Disseminated Drug-Resistant Mycobacterium Abscessus.” *Nature Medicine* 25 (5): 730–33. https://doi.org/10.1038/s41591-019-0437-z.

Degiacomi, Giulia, Andrej Benjak, Jan Madacki, Francesca Boldrin, Roberta Provvedi, Giorgio Palù, Jana Kordulakova, Stewart T. Cole, and Riccardo Manganelli. 2017. “Essentiality of MmpL3 and Impact of Its Silencing on Mycobacterium Tuberculosis Gene Expression.” *Scientific Reports* 7 (February): 1–8. https://doi.org/10.1038/srep43495.

Dick, Thomas, Sung Jae Shin, Won Jung Koh, Véronique Dartois, and Martin Gengenbacher. 2020. “Rifabutin Is Active against Mycobacterium Abscessus in Mice.” *Antimicrobial Agents and Chemotherapy* 64 (2): 2019–21. https://doi.org/10.1128/AAC.01943-19.

Domenech, Pilar, Reed Michael B., and Barry III Clifton E. 2005. “Contribution of the Mycobacterium Tuberculosis MmpL Protein Family to Virulence and Drug Resistance.” *Infection and Immunity* 73 (6): 2–3. https://doi.org/10.1128/IAI.73.6.3492.

Dover, Lynn G., Anuradha Alahari, Paul Gratraud, Jessica M. Gomes, Veemal Bhowruth, Robert C. Reynolds, Gurdyal S. Besra, and Laurent Kremer. 2007. “EthA, a Common Activator of Thiocarbamide-Containing Drugs Acting on Different Mycobacterial Targets.” *Antimicrobial Agents and Chemotherapy* 51 (3): 1055–63. https://doi.org/10.1128/AAC.01063-06.

Drlica, Karl, and Muhammad Malik. 2005. “Fluoroquinolones: Action and Resistance.” *Current Topics in Medicinal Chemistry* 3 (3): 249–82. https://doi.org/10.2174/1568026033452537.

Dubee, V., D. Dorchene, A. Bernut, J.-L. Herrmann, J.-L. Mainardi, J.-E. Hugonnet, A.-L. Lefebvre, et al. 2015. “β-Lactamase Inhibition by Avibactam in Mycobacterium Abscessus.” *Journal of Antimicrobial Chemotherapy*, no. June: 1051–58. https://doi.org/10.1093/jac/dku510.

Dubée, Vincent, Audrey Bernut, Mélanie Cortes, Tiffany Lesne, Delphine Dorchene, Anne Laure Lefebvre, Jean Emmanuel Hugonnet, et al. 2015. “β-Lactamase Inhibition by Avibactam in Mycobacterium Abscessus.” *Journal of Antimicrobial Chemotherapy* 70 (4): 1051–58. https://doi.org/10.1093/jac/dku510.

Dubois, Violaine, Alexandre Pawlik, Anouchka Bories, Vincent Le Moigne, Odile Sismeiro, Rachel Legendre, Hugo Varet, et al. 2019. “Mycobacterium Abscessus Virulence Traits Unraveled by Transcriptomic Profiling in Amoeba and Macrophages.” *Plos Pathogens*, 1–24. https://doi.org/10.1101/529057.

Dubois, Violaine, Albertus Viljoen, Laura Laencina, Vincent Le Moigne, Audrey Bernut, Faustine Dubar, Mickaël Blaise, et al. 2018. “MmpL8MAB Controls Mycobacterium Abscessus Virulence and Production of a Previously Unknown Glycolipid Family.” *Proceedings of the National Academy of Sciences of the United States of America* 115 (43): E10147–56. https://doi.org/10.1073/pnas.1812984115.

Dupont, Christian, Yushu Chen, Zhujun Xu, Françoise Roquet-Banères, Mickaël Blaise, Anne Kathrin Witt, Faustine Dubar, et al. 2019. “A Piperidinol-Containing Molecule Is Active against Mycobacterium Tuberculosis by Inhibiting the Mycolic Acid Flippase Activity of MmpL3.” *Journal of Biological Chemistry* 294 (46): 17512–23. https://doi.org/10.1074/jbc.RA119.010135.

Dupont, Christian, Albertus Viljoen, Audrey Bernut, Faustine Dubar, Alexandre Pawlik, and Christiane Bouchier. 2016. “A New Piperidinol Derivative Targeting Mycolic Acid Transport

in Mycobacterium Abscessus" 101 (June): 515–29. https://doi.org/10.1111/mmi.13406.

Dupont, Christian, Albertus Viljoen, Sangeeta Thomas, Françoise Roquet-Banères, Jean Louis Herrmann, Kevin Pethe, and Laurent Kremer. 2017. "Bedaquiline Inhibits the ATP Synthase in Mycobacterium Abscessus and Is Effective in Infected Zebrafish." *Antimicrobial Agents and Chemotherapy* 61 (11): 1–15. https://doi.org/10.1128/AAC.01225-17.

Fay, Allison, Nadine Czudnochowski, Jeremy M Rock, Jeffrey R Johnson, Nevan J Krogan, Oren Rosenberg, and Michael S Glickman. 2019. "Two Accessory Proteins Govern MmpL3 Mycolic Acid Transport in Mycobacteria." *MBio*, no. May: 1–17.

Ferro, Beatriz E., Shashikant Srivastava, Devyani Deshpande, Jotam G. Pasipanodya, Dick Van Soolingen, Johan W. Mouton, Jakko Van Ingen, and Tawanda Gumbo. 2016. "Tigecycline Is Highly Efficacious against Mycobacterium Abscessus Pulmonary Disease." *Antimicrobial Agents and Chemotherapy* 60 (5): 2895–2900. https://doi.org/10.1128/AAC.03112-15.

Foerstner, Konrad U., Christian von Mering, Sean D. Hooper, and Peer Bork. 2005. "Environments Shape the Nucleotide Composition of Genomes." *EMBO Reports* 6 (12): 1208–13. https://doi.org/10.1038/sj.embor.7400538.

Franz, Nicholas D., Juan Manuel Belardinelli, Michael A. Kaminski, Louis C. Dunn, Vinicius Calado Nogueira de Moura, Michael A. Blaha, Dan D. Truong, Wei Li, Mary Jackson, and E. Jeffrey North. 2017. "Design, Synthesis and Evaluation of Indole-2-Carboxamides with Pan Anti-Mycobacterial Activity." *Bioorganic and Medicinal Chemistry* 25 (14): 3746–55. https://doi.org/10.1016/j.bmc.2017.05.015.

Ganapathy, Uday S., Véronique Dartois, and Thomas Dick. 2019. "Repositioning Rifamycins for Mycobacterium Abscessus Lung Disease." *Expert Opinion on Drug Discovery* 14 (9): 867–78. https://doi.org/10.1080/17460441.2019.1629414.

Gavalda, Sabine, Fabienne Bardou, Françoise Laval, Cécile Bon, Wladimir Malaga, Christian Chalut, Christophe Guilhot, Lionel Mourey, Mamadou Daffé, and Annaïk Quémard. 2014. "The Polyketide Synthase Pks13 Catalyzes a Novel Mechanism of Lipid Transfer in Mycobacteria." *Chemistry and Biology* 21 (12): 1660–69. https://doi.org/10.1016/j.chembiol.2014.10.011.

Gavalda, Sabine, Mathieu Léger, Benoît van der Rest, Alexandre Stella, Fabienne Bardou, Henri Montrozier, Christian Chalut, et al. 2009. "The Pks13/FadD32 Crosstalk for the Biosynthesis of Mycolic Acids in Mycobacterium Tuberculosis." *Journal of Biological Chemistry* 284 (29): 19255–64. https://doi.org/10.1074/jbc.M109.006940.

Genilloud, Olga. 2017. "Actinomycetes: Still a Source of Novel Antibiotics." *Natural Product Reports* 34 (10): 1203–32. https://doi.org/10.1039/c7np00026j.

Gobis, Katarzyna, Henryk Foks, Marcin Serocki, Ewa Augustynowicz-Kopeć, and Agnieszka Napiórkowska. 2014. "Synthesis and Evaluation of in Vitro Antimycobacterial Activity of Novel 1H-Benzo[d]Imidazole Derivatives and Analogues." *European Journal of Medicinal Chemistry* 89: 13–20. https://doi.org/10.1016/j.ejmech.2014.10.031.

Gobis, Katarzyna, Henryk Foks, Karolina Suchan, Ewa Augustynowicz-Kopeć, Agnieszka Napiórkowska, and Krzysztof Bojanowski. 2015. "Novel 2-(2-Phenalkyl)-1H-Benzo[d]Imidazoles as Antitubercular Agents. Synthesis, Biological Evaluation and Structure-Activity Relationship." *Bioorganic and Medicinal Chemistry* 23 (9): 2112–20. https://doi.org/10.1016/j.bmc.2015.03.008.

Graham, James, Christina E. Wong, Joshua Day, Elizabeth McFaddin, Urs Ochsner, Teresa Hoang, Casey L. Young, et al. 2018. “Discovery of Benzothiazole Amides as Potent Antimycobacterial Agents.” *Bioorganic and Medicinal Chemistry Letters* 28 (19): 3177–81. https://doi.org/10.1016/j.bmcl.2018.08.026.

Griffith, David E, William M Girard, and Richard J Wallace. 1993. “Clinical Features of Pulmonary Disease Caused by Rapidly Growing Mycobacteria An Analysis of 154 Patients.” *American Review of Respiratory Disease* 147: 1271–78.

Grzegorzewicz, Anna E., Ha Pham, Vijay A.K.B. Gundi, Michael S. Scherman, Elton J. North, Tamara Hess, Victoria Jones, et al. 2012. “Inhibition of Mycolic Acid Transport across the Mycobacterium Tuberculosis Plasma Membrane.” *Nature Chemical Biology* 8 (4): 334–41. https://doi.org/10.1038/nchembio.794.

Guillemin, Isabelle, Vincent Jarlier, and Emmanuelle Cambau. 1998. “Correlation between Quinolone Susceptibility Patterns and Sequences in the A and B Subunits of DNA Gyrase in Mycobacteria.” *Antimicrobial Agents and Chemotherapy* 42 (8): 2084–88. https://doi.org/10.1128/aac.42.8.2084.

Gupta, Shashank, Keira A Cohen, Kathryn Winglee, Mamoudou Maiga, Bassirou Diarra, and William R. Bishai. 2014. “Efflux Inhibition with Verapamil Potentiates Bedaquiline in Mycobacterium Tuberculosis.” *Antimicrobial Agents and Chemotherapy* 58 (1): 574–76. https://doi.org/10.1128/AAC.01462-13.

Gupta, Shashank, Seep Tyagi, and William R. Bishai. 2015. “Verapamil Increases the Bactericidal Activity of Bedaquiline against Mycobacterium Tuberculosis in a Mouse Model.” *Antimicrobial Agents and Chemotherapy* 59 (1): 673–76. https://doi.org/10.1128/AAC.04019-14.

Gutiérrez, Ana Victoria, Matthias Richard, Françoise Roquet-Banères, Albertus Viljoen, and Laurent Kremer. 2019. “The TetR Family Transcription Factor MAB_2299c Regulates the Expression of Two Distinct MmpS-MmpL Efflux Pumps Involved in Cross-Resistance to Clofazimine and Bedaquiline in Mycobacterium Abscessus.” *Antimicrobial Agents and Chemotherapy* 63 (10): 1–16. https://doi.org/10.1128/AAC.01000-19.

Gutiérrez, Ana Victoria, Albertus Viljoen, Eric Ghigo, Jean-Louis Herrmann, and Laurent Kremer. 2018. “Glycopeptidolipids, a Double-Edged Sword of the Mycobacterium Abscessus Complex.” *Frontiers in Microbiology* 9 (JUN): 1–8. https://doi.org/10.3389/fmicb.2018.01145.

H., Zheng, Williams J.T., Coulson G.B., Haiderer E.R., and Abramovitch R.B. 2018. “HC2091 Kills Mycobacterium Tuberculosis by Targeting the MmpL3 Mycolic Acid Transporter.” *Antimicrobial Agents and Chemotherapy* 62 (7). http://www.embase.com/search/results?subaction=viewrecord&from=export&id=L622692178%0Ahttp://dx.doi.org/10.1128/AAC.02459-17.

Halloum, Iman, Albertus Viljoen, Varun Khanna, Derek Craig, Christiane Bouchier, Roland Brosch, Geoffrey Coxon, and Laurent Kremer. 2017. “Resistance to Thiacetazone Derivatives Active against Mycobacterium Abscessus Involves Mutations in the MmpL5 Transcriptional Repressor MAB_4384.” *Antimicrobial Agents and Chemotherapy* 61 (4): 1–14.

Hannah, Claire E, Bradley A Ford, Jina Chung, Dilek Ince, and Karolyn A Wanat. 2020. “Characteristics of Nontuberculous Mycobacterial Infections at a Midwestern Tertiary

Hospital: A Retrospective Study of 365 Patients." *Open Forum Infectious Diseases* 7 (6): 1–9. https://doi.org/10.1093/ofid/ofaa173.

Hartkoorn, Ruben C., Swapna Uplekar, and Stewart T. Cole. 2014. "Cross-Resistance between Clofazimine and Bedaquiline through Upregulation of Mmpl5 in Mycobacterium Tuberculosis." *Antimicrobial Agents and Chemotherapy* 58 (5): 2979–81. https://doi.org/10.1128/AAC.00037-14.

Hashemian, Seyed Mohammad Reza, Tayebeh Farhadi, and Mojdeh Ganjparvar. 2018. "Linezolid: A Review of Its Properties, Function, and Use in Critical Care." *Drug Design, Development and Therapy* 12: 1759–67. https://doi.org/10.2147/DDDT.S164515.

Heinrich, Norbert, Rodney Dawson, Jeannine Bois, Kim Narunsky, Gary Horwith, Andrew J Phipps, Carol A Nacy, et al. 2014. "Early Phase Evaluation of SQ109 Alone and in Combination with Rifampicin in Pulmonary TB Patients." *Journal of Antimicrobial Chemotherapy* 70 (5): 1558–66. https://doi.org/10.1093/jac/dku553.

Holdiness, Mack R. 1989. "Clinical Pharmacokinetics of Clofazimine. A Review." *Clinical Pharmacokinetics* 16 (8): 74–85. https://doi.org/10.1111/j.2042-7158.1996.tb03973.x.

Howard, Susan T., and Thomas F. Byrd. 2000. "The Rapidly Growing Mycobacteria: Saprophytes and Parasites." *Microbes and Infection* 2 (15): 1845–53. https://doi.org/10.1016/S1286-4579(00)01338-1.

Huang, Chien Wen, Jiann Hwa Chen, Shiau Ting Hu, Wei Chang Huang, Yen Chung Lee, Chen Cheng Huang, and Gwan Han Shen. 2013. "Synergistic Activities of Tigecycline with Clarithromycin or Amikacin against Rapidly Growing Mycobacteria in Taiwan." *International Journal of Antimicrobial Agents* 41 (3): 218–23. https://doi.org/10.1016/j.ijantimicag.2012.10.021.

Ingen, Jakko Van, Sarah E. Totten, Niels K. Helstrom, Leonid B. Heifets, Martin J. Boeree, and Charles L. Daley. 2012. "In Vitro Synergy between Clofazimine and Amikacin in Treatment of Nontuberculous Mycobacterial Disease." *Antimicrobial Agents and Chemotherapy* 56 (12): 6324–27. https://doi.org/10.1128/AAC.01505-12.

Johansen, Matt D, Wassim Daher, Françoise Roquet-banères, and Clément Raynaud. 2020. "Rifabutin Is Bactericidal against Intracellular and Extracellular Forms of Mycobacterium Abscessus." *Antimicrobial Agents and Chemotherapy*, no. August. https://doi.org/10.1128/AAC.00363-20.

Johansen, Matt D, and Laurent Kremer. 2020a. "CFTR Depletion Confers Hypersusceptibility to Mycobacterium Fortuitum in a Zebrafish Model" 10 (July): 1–14. https://doi.org/10.3389/fcimb.2020.00357.

———. 2020b. "Large Extracellular Cord Formation in a Zebrafish Model of Mycobacterium Kansasii Infection." *The Journal of Infectious Diseases*, no. Xx Xxxx: 1–5. https://doi.org/10.1093/infdis/jiaa187.

Jonsson, Bodil E, Marita Gilljam, Anders Lindblad, Malin Ridell, Agnes E Wold, and Christina Welinder-olsson. 2007. "Molecular Epidemiology of Mycobacterium Abscessus , with Focus on Cystic Fibrosis ." *Journal of Clinical Microbiology* 45 (5): 1497–1504. https://doi.org/10.1128/JCM.02592-06.

Kaushik, Amit, Nicole C. Ammerman, Olumide Martins, Nicole M. Parrish, and Eric L. Nuermberger. 2019. "In Vitro Activity of New Tetracycline Analogs Omadacycline and

Eravacycline against Drug-Resistant Clinical Isolates of Mycobacterium Abscessus." *Antimicrobial Agents and Chemotherapy* 63 (6): 2–6. https://doi.org/10.1128/AAC.00470-19.

Kaushik, Amit, Chhavi Gupta, Stefanie Fisher, Elizabeth Story-Roller, Christos Galanis, Nicole Parrish, and Gyanu Lamichhane. 2017. "Combinations of Avibactam and Carbapenems Exhibit Enhanced Potencies against Drug-Resistant Mycobacterium Abscessus." *Future Microbiology* 12 (6): 473–80. https://doi.org/10.2217/fmb-2016-0234.

Kaushik, Amit, Nayani Makkar, Pooja Pandey, Nicole Parrish, Urvashi Singh, and Gyanu Lamichhane. 2015. "Carbapenems and Rifampin Exhibit Synergy against Mycobacterium Tuberculosis and Mycobacterium Abscessus." *Antimicrobial Agents and Chemotherapy* 59 (10): 6561–67. https://doi.org/10.1128/AAC.01158-15.

Kim, Kyoung Hoon, Doo Ri An, Jinsu Song, Ji Young Yoon, Hyoun Sook Kim, Hye Jin Yoon, Ha Na Im, et al. 2012. "Mycobacterium Tuberculosis Eis Protein Initiates Suppression of Host Immune Responses by Acetylation of DUSP16/MKP-7." *Proceedings of the National Academy of Sciences of the United States of America* 109 (20): 7729–34. https://doi.org/10.1073/pnas.1120251109.

Kim, Su-Young, Byung Woo Jhun, Seong Mi Moon, Sun Hye Shin, Kyeongman Jeon, O Jung Kwon, In Young Yoo, et al. 2018. "Mutations in GyrA and GyrB in Moxifloxacin-Resistant Mycobacterium Avium Complex and Mycobacterium Abscessus Complex Clinical Isolates." *Antimicrobial Agents and Chemotherapy* 62 (9): 1–5.

Koh, Won Jung, Jun Haeng Lee, Yong Soo Kwon, Kyung Soo Lee, Gee Young Suh, Man Pyo Chung, Hojoong Kim, and O. Jung Kwon. 2007. "Prevalence of Gastroesophageal Reflux Disease in Patients with Nontuberculous Mycobacterial Lung Disease." *Chest* 131 (6): 1825–30. https://doi.org/10.1378/chest.06-2280.

Korycka-Machała, Małgorzata, Albertus Viljoen, Jakub Pawełczyk, Paulina Borówka, Boz˙ena Dziadek, Katarzyna Gobis, Anna Brzostek, et al. 2019. "1H-Benzo[d]Imidazole Derivatives Affect MmpL3 in Mycobacterium Tuberculosis." *Antimicrobial Agents and Chemotherapy* 63 (10): 1–13.

Koteva, Kalinka, Georgina Cox, Jayne K. Kelso, Matthew D. Surette, Haley L. Zubyk, Linda Ejim, Peter Stogios, Alexei Savchenko, Dan Sørensen, and Gerard D. Wright. 2018. "Rox, a Rifamycin Resistance Enzyme with an Unprecedented Mechanism of Action." *Cell Chemical Biology* 25 (4): 403-412.e5. https://doi.org/10.1016/j.chembiol.2018.01.009.

Kozikowski, Alan P., Oluseye K. Onajole, Jozef Stec, Christian Dupont, Albertus Viljoen, Matthias Richard, Tridib Chaira, et al. 2017. "Targeting Mycolic Acid Transport by Indole-2-Carboxamides for the Treatment of Mycobacterium Abscessus Infections." *Journal of Medicinal Chemistry* 60 (13): 5876–88. https://doi.org/10.1021/acs.jmedchem.7b00582.

Kremer, Laurent, K. Madhavan Nampoothiri, Sarah Lesjean, Lynn G. Dover, Steven Graham, Joanna Betts, Patrick J. Brennan, David E. Minnikin, Camille Locht, and Gurdyal S. Besra. 2001. "Biochemical Characterization of Acyl Carrier Protein (AcpM) and Malonyl-CoA:AcpM Transacylase (MtFabD), Two Major Components of Mycobacterium Tuberculosis Fatty Acid Synthase II." *Journal of Biological Chemistry* 276 (30): 27967–74. https://doi.org/10.1074/jbc.M103687200.

Kundu, Subhashri, Goran Biukovic, Gerhard Grüber, and Thomas Dick. 2016. "Bedaquiline Targets the ε Subunit of Mycobacterial F-ATP Synthase." *Antimicrobial Agents and*

Chemotherapy 60 (11): 6977–79. https://doi.org/10.1128/AAC.01291-16.

Kurth, Daniel G., Gabriela M. Gago, Augustina de la Iglesia, Bernardo Bazet Lyonnet, Tin Wang Lin, Héctor R. Morbidoni, Shiuo Chuan Tsai, and Hugo Gramajo. 2009. "ACCase 6 Is the Essential Acetyl-CoA Carboxylase Involved in Fatty Acid and Mycolic Acid Biosynthesis in Mycobacteria." *Microbiology* 155 (8): 2664–75. https://doi.org/10.1099/mic.0.027714-0.

Kwon, Yong Soo, Adrah Levin, Shannon H. Kasperbauer, Gwen A. Huitt, and Charles L. Daley. 2019. "Efficacy and Safety of Tigecycline for Mycobacterium Abscessus Disease." *Respiratory Medicine* 158: 89–91. https://doi.org/10.1016/j.rmed.2019.10.006.

Laencina, Laura, Violaine Dubois, Vincent Le Moigne, Albertus Viljoen, Laleh Majlessi, Justin Pritchard, Audrey Bernut, et al. 2018. "Identification of Genes Required for Mycobacterium Abscessus Growth in Vivo with a Prominent Role of the ESX-4 Locus." *Proceedings of the National Academy of Sciences of the United States of America* 115 (5): E1002–11. https://doi.org/10.1073/pnas.1713195115.

Lamichhane, Gyanu, Sandeep Tyagi, and William R Bishai. 2005. "Designer Arrays for De Ned Mutant Analysis To Detect Genes Essential for Survival Of." *Society* 73 (4): 2533–40. https://doi.org/10.1128/IAI.73.4.2533.

Lavollay, Marie, Michel Arthur, Martine Fourgeaud, Lionel Dubost, Arul Marie, Nicolas Veziris, Didier Blanot, Laurent Gutmann, and Jean Luc Mainardi. 2008. "The Peptidoglycan of Stationary-Phase Mycobacterium Tuberculosis Predominantly Contains Cross-Links Generated by L,D-Transpeptidation." *Journal of Bacteriology* 190 (12): 4360–66. https://doi.org/10.1128/JB.00239-08.

Lavollay, Marie, Martine Fourgeaud, Jean Louis Herrmann, Lionel Dubost, Arul Marie, Laurent Gutmann, Michel Arthur, and Jean Luc Mainardi. 2011. "The Peptidoglycan of Mycobacterium Abscessus Is Predominantly Cross-Linked by L,D-Transpeptidases." *Journal of Bacteriology* 193 (3): 778–82. https://doi.org/10.1128/JB.00606-10.

Lea-Smith, David J., James S. Pyke, Dedreia Tull, Malcolm J. McConville, Ross L. Coppel, and Paul K. Crellin. 2007. "The Reductase That Catalyzes Mycolic Motif Synthesis Is Required for Efficient Attachment of Mycolic Acids to Arabinogalactan." *Journal of Biological Chemistry* 282 (15): 11000–8. https://doi.org/10.1074/jbc.M608686200.

Lee, Meng Rui, Wang Huei Sheng, Chien Ching Hung, Chong Jen Yu, Li Na Lee, and Po Ren Hsueh. 2015. "Mycobacterium Abscessus Complex Infections in Humans." *Emerging Infectious Diseases* 21 (9): 1638–46. https://doi.org/10.3201/eid2109.141634.

Lefebvre, Anne Laure, Vincent Dubée, Mélanie Cortes, Delphine Dorchêne, Michel Arthur, and Jean Luc Mainardi. 2016. "Bactericidal and Intracellular Activity of β-Lactams against Mycobacterium Abscessus." *Journal of Antimicrobial Chemotherapy* 71 (6): 1556–63. https://doi.org/10.1093/jac/dkw022.

Lefebvre, Anne Laure, Vincent Le Moigne, Audrey Bernut, Carole Veckerlé, Fabrice Compain, Jean Louis Herrmann, Laurent Kremer, Michel Arthur, and Jean Luc Mainardi. 2017. "Inhibition of the β-Lactamase BlaMab by Avibactam Improves the in Vitro and in Vivo Efficacy of Imipenem against Mycobacterium Abscessus." *Antimicrobial Agents and Chemotherapy* 61 (4): 1–7. https://doi.org/10.1128/AAC.02440-16.

Leitch, AE, and Helen Rodgers. 2013. "Cystic Fibrosis." *J R Coll Physicians Edinb* 43: 144–50. https://doi.org/10.4997/JRCPE.2013.212.

Lerat, Isabelle, Emmanuelle Cambau, Romain Roth Dit Bettoni, Jean Louis Gaillard, Vincent Jarlier, Chantal Truffot, and Nicolas Veziris. 2014. “In Vivo Evaluation of Antibiotic Activity against Mycobacterium Abscessus.” *Journal of Infectious Diseases* 209 (6): 905–12. https://doi.org/10.1093/infdis/jit614.

Li, Ming, Samuel Agyei Nyantakyi, Mei-Lin Go, and Thomas Dick. 2020. “Resistance against Membrane-Inserting MmpL3 Inhibitor through Upregulation of MmpL5 in M. Tuberculosis.” *Antimicrobial Agents and Chemotherapy*, no. March: 1–16. https://doi.org/10.1128/AAC.00483-20.

Li, Wei, Andrea Sanchez-Hidalgo, Victoria Jones, Calado Nogueira de Moura Vinicius, E. Jeffrey North, and Mary Jackson. 2017. “Synergistic Interactions of MmpL3 Inhibitors with Antitubercular Compounds In Vitro.” *Antimicrobial Agents and Chemotherapy* 61 (4): 1–6.

Li, Wei, Casey M. Stevens, Amitkumar N. Pandya, Zbigniew Darzynkiewicz, Pankaj Bhattarai, Weiwei Tong, Mercedes Gonzalez-Juarrero, E. Jeffrey North, Helen I. Zgurskaya, and Mary Jackson. 2019. “Direct Inhibition of MmpL3 by Novel Antitubercular Compounds.” *ACS Infectious Diseases* 5 (6): 1001–12. https://doi.org/10.1021/acsinfecdis.9b00048.

Li, Wei, Amira Yazidi, Amitkumar N. Pandya, Pooja Hegde, Weiwei Tong, Vinicius Calado Nogueira de Moura, E. Jeffrey North, Jurgen Sygusch, and Mary Jackson. 2018. “MmpL3 as a Target for the Treatment of Drug-Resistant Nontuberculous Mycobacterial Infections.” *Frontiers in Microbiology* 9 (JUL): 1–9. https://doi.org/10.3389/fmicb.2018.01547.

Lindman, Marissa, and Thomas Dick. 2019. “Bedaquiline Eliminates Bactericidal Activity of β-Lactams against Mycobacterium Abscessus.” *Antimicrobial Agents and Chemotherapy* 63 (8): 1–5. https://doi.org/10.1128/AAC.00827-19.

Liu, Weijia, Bing Li, Haiqing Chu, Zhemin Zhang, Liulin Luo, Wei Ma, Shiyi Yang, and Qi Guo. 2017. “Rapid Detection of Mutations in Erm(41) and Rrl Associated with Clarithromycin Resistance in Mycobacterium Abscessus Complex by Denaturing Gradient Gel Electrophoresis.” *Journal of Microbiological Methods* 143 (507): 87–93. https://doi.org/10.1016/j.mimet.2017.10.010.

Llorens-Fons, Marta, Míriam Pérez-Trujillo, Esther Julián, Cecilia Brambilla, Fernando Alcaide, Thomas F. Byrd, and Marina Luquin. 2017. “Trehalose Polyphleates, External Cell Wall Lipids in Mycobacterium Abscessus, Are Associated with the Formation of Clumps with Cording Morphology, Which Have Been Associated with Virulence.” *Frontiers in Microbiology* 8 (JUL): 1–15. https://doi.org/10.3389/fmicb.2017.01402.

Lopes-Pacheco, Miquéias. 2016. “CFTR Modulators: Shedding Light on Precision Medicine for Cystic Fibrosis.” *Frontiers in Pharmacology* 7 (SEP): 1–20. https://doi.org/10.3389/fphar.2016.00275.

Lounis, Nacer, Nicolas Veziris, Aurélie Chauffeur, Chantal Truffot-Pernot, Koen Andries, and Vincent Jarlier. 2006. “Combinations of R207910 with Drugs Used to Treat Multidrug-Resistant Tuberculosis Have the Potential to Shorten Treatment Duration.” *Antimicrobial Agents and Chemotherapy* 50 (11): 3543–47. https://doi.org/10.1128/AAC.00766-06.

Luo, Min, Wenchang Zhou, Hiral Patel, Anurag P. Srivastava, Jindrich Symersky, Michał M. Bonar, José D. Faraldo-Gómez, Maofu Liao, and David M. Mueller. 2020. “Bedaquiline Inhibits the Yeast and Human Mitochondrial ATP Synthases.” *Communications Biology* 3 (1): 1–10. https://doi.org/10.1038/s42003-020-01173-z.

Luthra, Sakshi, Anna Rominski, and Peter Sander. 2018. “The Role of Antibiotic-Target-Modifying and Antibiotic-Modifying Enzymes in Mycobacterium Abscessus Drug Resistance.” *Frontiers in Microbiology* 9 (SEP): 1–13. https://doi.org/10.3389/fmicb.2018.02179.

Maggioncalda, Emily C., Elizabeth Story-Roller, Julian Mylius, Peter Illei, Randall J. Basaraba, and Gyanu Lamichhane. 2020. “A Mouse Model of Pulmonary Mycobacteroides Abscessus Infection.” *Scientific Reports* 10 (1): 1–8. https://doi.org/10.1038/s41598-020-60452-1.

Mainardi, Jean Luc, Véronique Morel, Martine Fourgeaud, Julie Cremniter, Didier Blanot, Raymond Legrand, Claude Fréhel, Michel Arthur, Jean Van Heijenoort, and Laurent Gutmann. 2002. “Balance between Two Transpeptidation Mechanisms Determines the Expression of β-Lactam Resistance in Enterococcus Faecium.” *Journal of Biological Chemistry* 277 (39): 35801–7. https://doi.org/10.1074/jbc.M204319200.

Marrakchi, Hedia, Stéphanie Ducasse, Gilles Labesse, Henri Montrozier, Emmanuel Margeat, Laurent Emorine, Xavier Charpentier, Mamadou Daffé, and Annaïk Quémard. 2002. “MabA (FabG1), a Mycobacterium Tuberculosis Protein Involved in the Long-Chain Fatty Acid Elongation System FAS-II.” *Microbiology* 148 (4): 951–60. https://doi.org/10.1099/00221287-148-4-951.

Marrakchi, Hedia, Marie Antoinette Lanéelle, and Mamadou Daffé. 2014. “Mycolic Acids: Structures, Biosynthesis, and Beyond.” *Chemistry and Biology* 21 (1): 67–85. https://doi.org/10.1016/j.chembiol.2013.11.011.

Martiniano, Stacey L., Brandie D. Wagner, Adrah Levin, Jerry A. Nick, Scott D. Sagel, Charles L. Daley, and Stacey L. Martiniano. 2017. “Safety and Effectiveness of Clofazimine for Primary and Refractory Nontuberculous Mycobacterial Infection.” *Chest* 152 (4): 800–809. https://doi.org/10.1016/j.chest.2017.04.175.

Matrat, Stéphanie, Alexandra Aubry, Claudine Mayer, Vincent Jarlier, and Emmanuelle Cambau. 2008. “Mutagenesis in the A3α4 GyrA Helix and in the Toprim Domain of GyrB Refines the Contribution of Mycobacterium Tuberculosis DNA Gyrase to Intrinsic Resistance to Quinolones.” *Antimicrobial Agents and Chemotherapy* 52 (8): 2909–14. https://doi.org/10.1128/AAC.01380-07.

Maurer, Florian P., Vera L. Bruderer, Claudio Castelberg, Claudia Ritter, Dimitri Scherbakov, Guido V. Bloemberg, and Erik C. Böttger. 2014. “Aminoglycoside-Modifying Enzymes Determine the Innate Susceptibility to Aminoglycoside Antibiotics in Rapidly Growing Mycobacteria.” *Journal of Antimicrobial Chemotherapy* 70 (5): 1412–19. https://doi.org/10.1093/jac/dku550.

Maurer, Florian P., Vera L. Bruderer, Claudia Ritter, Claudio Castelberg, Guido V. Bloemberg, and Erik C. Böttger. 2014. “Lack of Antimicrobial Bactericidal Activity in Mycobacterium Abscessus.” *Antimicrobial Agents and Chemotherapy* 58 (7): 3828–36. https://doi.org/10.1128/AAC.02448-14.

Maxwell, I. H. 1968. “Studies of the Binding of Tetracycline to Ribosomes in Vitro.” *Molecular Pharmacology* 4 (1): 25–37.

Medjahed, Halima, Jean Louis Gaillard, and Jean Marc Reyrat. 2010. “Mycobacterium Abscessus: A New Player in the Mycobacterial Field.” *Trends in Microbiology* 18 (3): 117–23. https://doi.org/10.1016/j.tim.2009.12.007.

Meir, Michal, and Daniel Barkan. 2020. “Alternative and Experimental Therapies of Mycobacterium Abscessus Infections.” *International Journal of Molecular Sciences* 21 (18): 1–12. https://doi.org/10.3390/ijms21186793.

Mirnejad, Reza, Arezoo Asadi, Saeed Khoshnood, Habibollah Mirzaei, Mohsen Heidary, Lanfranco Fattorini, Arash Ghodousi, and Davood Darban-Sarokhalil. 2018. “Clofazimine: A Useful Antibiotic for Drug-Resistant Tuberculosis.” *Biomedicine and Pharmacotherapy* 105 (April): 1353–59. https://doi.org/10.1016/j.biopha.2018.06.023.

Miyasaka, Tomomitsu, Hiroyuki Kunishima, Mayumi Komatsu, Kiyoko Tamai, Kotaro Mitsutake, Keiji Kanemitsu, Yoshiharu Ohisa, Hideji Yanagisawa, and Mitsuo Kaku. 2007. “In Vitro Efficacy of Imipenem in Combination with Six Antimicrobial Agents against Mycobacterium Abscessus.” *International Journal of Antimicrobial Agents* 30 (3): 255–58. https://doi.org/10.1016/j.ijantimicag.2007.05.003.

Mocé-llivina, Laura, Francisco Lucena, Juan Jofre, and Laura Moce. 2004. “Double-Layer Plaque Assay for Quantification of Enteroviruses Double-Layer Plaque Assay for Quantification of Enteroviruses.” *Applied and Environmental Mcrobiology* 70 (May 2004): 2801–5. https://doi.org/10.1128/AEM.70.5.2801.

Moigne, Vincent Le, Clément Raynaud, Flavie Moreau, Christian Dupont, Jérôme Nigou, Olivier Neyrolles, Laurent Kremer, and Jean Louis Herrmann. 2020. “Efficacy of Bedaquiline, Alone or in Combination with Imipenem, against Mycobacterium Abscessus in C3HeB/FeJ Mice.” *Antimicrobial Agents and Chemotherapy* 64 (6): 1–6. https://doi.org/10.1128/AAC.00114-20.

Mougari, Faiza, Lorenzo Guglielmetti, Laurent Raskine, Isabelle Sermet-Gaudelus, Nicolas Veziris, and Emmanuelle Cambau. 2016. “Infections Caused by Mycobacterium Abscessus: Epidemiology, Diagnostic Tools and Treatment.” *Expert Review of Anti-Infective Therapy* 14 (12): 1139–54. https://doi.org/10.1080/14787210.2016.1238304.

Mukherjee, Devika, Mu Lu Wu, Jeanette W.P. Teo, and Thomas Dick. 2017. “Vancomycin and Clarithromycin Show Synergy against Mycobacterium Abscessus in Vitro.” *Antimicrobial Agents and Chemotherapy* 61 (12): 1–5. https://doi.org/10.1128/AAC.01298-17.

Mungroo, Mohammad Ridwane, Naveed Ahmed Khan, and Ruqaiyyah Siddiqui. 2020. “Mycobacterium Leprae: Pathogenesis, Diagnosis, and Treatment Options.” *Microbial Pathogenesis* 149 (September): 104475. https://doi.org/10.1016/j.micpath.2020.104475.

Nash, Kevin A, A. Barbara Brown-Elliott, and Richard J Wallace. 2009. “A Novel Gene, Erm(41), Confers Inducible Macrolide Resistance to Clinical Isolates of Mycobacterium Abscessus but Is Absent from Mycobacterium Chelonae.” *Antimicrobial Agents and Chemotherapy* 53 (4): 1367–76. https://doi.org/10.1128/AAC.01275-08.

Nessar, Rachid, Emmanuelle Cambau, Jean Marc Reyrat, Alan Murray, and Brigitte Gicquel. 2012. “Mycobacterium Abscessus: A New Antibiotic Nightmare.” *Journal of Antimicrobial Chemotherapy* 67 (4): 810–18. https://doi.org/10.1093/jac/dkr578.

Nguyen, Thi Van Anh, Richard M. Anthony, Anne Laure Bañuls, Dinh Hoa Vu, and Jan Willem C. Alffenaar. 2018. “Bedaquiline Resistance: Its Emergence, Mechanism, and Prevention.” *Clinical Infectious Diseases* 66 (10): 1625–30. https://doi.org/10.1093/cid/cix992.

Nikaido, Hiroshi. 2010. “Structure and Mechanism of RND-Type Multidrug Efflux Pumps.” *Advances in Enzymology and Related Areas of Molecular Biology* 77 1 (11): 1–60.

https://doi.org/10.1002/9780470920541.ch1.

Nimmo, Camus, James Millard, Lucy van Dorp, Kayleen Brien, Sashen Moodley, Allison Wolf, Alison D Grant, et al. 2020. “Population-Level Emergence of Bedaquiline and Clofazimine Resistance-Associated Variants among Patients with Drug-Resistant Tuberculosis in Southern Africa: A Phenotypic and Phylogenetic Analysis.” *The Lancet Microbe* 1 (4): e165–74. https://doi.org/10.1016/s2666-5247(20)30031-8.

Obregón-Henao, Andrés, Kimberly A. Arnett, Marcela Henao-Tamayo, Lisa Massoudi, Elizabeth Creissen, Koen Andries, Anne J. Lenaerts, and Diane J. Ordway. 2015. “Susceptibility of Mycobacterium Abscessus to Antimycobacterial Drugs in Preclinical Models.” *Antimicrobial Agents and Chemotherapy* 59 (11): 6904–12. https://doi.org/10.1128/AAC.00459-15.

Oh, Chun Taek, Cheol Moon, Ok Kyu Park, Seung Hae Kwon, and Jichan Jang. 2014. “Novel Drug Combination for Mycobacterium Abscessus Disease Therapy Identified in a Drosophila Infection Model.” *Journal of Antimicrobial Chemotherapy* 69 (6): 1599–1607. https://doi.org/10.1093/jac/dku024.

Oh, Tae Jin, Jaiyanth Daniel, Hwa Jung Kim, Tatiana D. Sirakova, and Pappachan E. Kolattukudy. 2006. “Identification and Characterization of Rv3281 as a Novel Subunit of a Biotin-Dependent Acyl-CoA Carboxylase in Mycobacterium Tuberculosis H37Rv.” *Journal of Biological Chemistry* 281 (7): 3899–3908. https://doi.org/10.1074/jbc.M511761200.

Pacheco, Sophia A., Fong Fu Hsu, Katelyn M. Powers, and Georgiana E. Purdy. 2013. “MmpL11 Protein Transports Mycolic Acid-Containing Lipids to the Mycobacterial Cell Wall and Contributes to Biofilm Formation in Mycobacterium Smegmatis.” *Journal of Biological Chemistry* 288 (33): 24213–22. https://doi.org/10.1074/jbc.M113.473371.

Pandya, Amit N., Pavan K. Prathipati, Pooja Hegde, Wei Li, Kyle F. Graham, Subhra Mandal, Kristen M. Drescher, et al. 2019. “Indole-2-Carboxamides Are Active against Mycobacterium Abscessus in a Mouse Model of Acute Infection.” *Antimicrobial Agents and Chemotherapy* 63 (3): 14–18. https://doi.org/10.1128/AAC.02245-18.

Parish, Tanya, Gretta Roberts, Francoise Laval, Merrill Schaeffer, Mamadou Daffé, and Ken Duncan. 2007. “Functional Complementation of the Essential Gene FabG1 of Mycobacterium Tuberculosis by Mycobacterium Smegmatis FabG but Not Escherichia Coli FabG.” *Journal of Bacteriology* 189 (10): 3721–28. https://doi.org/10.1128/JB.01740-06.

Park, Bora, Divya Awasthi, Soumya R. Chowdhury, Eduard H. Melief, Kunal Kumar, Susan E. Knudson, Richard A. Slayden, and Iwao Ojima. 2014. “Design, Synthesis and Evaluation of Novel 2,5,6-Trisubstituted Benzimidazoles Targeting FtsZ as Antitubercular Agents.” *Bioorganic and Medicinal Chemistry* 22 (9): 2602–12. https://doi.org/10.1016/j.bmc.2014.03.035.

Pawlik, Alexandre, Guillaume Garnier, Mickael Orgeur, Pin Tong, Amanda Lohan, Fabien Le Chevalier, Guillaume Sapriel, et al. 2013. “Identification and Characterization of the Genetic Changes Responsible for the Characteristic Smooth-to-Rough Morphotype Alterations of Clinically Persistent Mycobacterium Abscessus.” *Molecular Microbiology* 90 (3): 612–29. https://doi.org/10.1111/mmi.12387.

Petersen, P. J., N. V. Jacobus, W. J. Weiss, P. E. Sum, and R. T. Testa. 1999. “In Vitro and in Vivo Antibacterial Activities of a Novel Glycylcycline, the 9-t-Butylglycylamido Derivative of Minocycline (GAR-936).” *Antimicrobial Agents and Chemotherapy* 43 (4): 738–44.

https://doi.org/10.1128/aac.43.4.738.

Pier, Gerald B., Martha Grout, Tanweer S. Zaidi, and Joanna B. Goldberg. 1996. “How Mutant CFTR May Contribute to Pseudomonas Aeruginosa Infection in Cystic Fibrosis.” *American Journal of Respiratory and Critical Care Medicine* 154 (4_pt_2): S175–82. https://doi.org/10.1164/ajrccm/154.4_Pt_2.S175.

Pier, Gerald B, Martha Grout, Tanweer S Zaidi, John C Olsen, Larry G Johnson, James R Yankaskas, and Joanna B Goldberg. 1996. “Role of Mutant CFTR in Hypersusceptibility of Cystic Fibrosis Patients to Lung Infections.” *Science* 271 (January).

Poehlsgaard, Jacob, and Stephen Douthwaite. 2005. “The Bacterial Ribosome as a Target for Antibiotics.” *Nature Reviews Microbiology* 3 (11): 870–81. https://doi.org/10.1038/nrmicro1265.

Portevin, Damien, Célia De Sousa-D’Auria, Henri Montrozier, Christine Houssin, Alexandre Stella, Marie Antoinette Lanéelle, Fabienne Bardou, Christophe Guilhot, and Mamadou Daffé. 2005. “The Acyl-AMP Ligase FadD32 and AccD4-Containing Acyl-CoA Carboxylase Are Required for the Synthesis of Mycolic Acids and Essential for Mycobacterial Growth: Identification of the Carboxylation Product and Determination of the Acyl-CoA Carboxylase Componen.” *Journal of Biological Chemistry* 280 (10): 8862–74. https://doi.org/10.1074/jbc.M408578200.

Prammananan, Therdsak, Peter Sander, Barbara A. Brown, Klaus Frischkorn, Grace O. Onyi, Yansheng Zhang, Erik C. Böttger, and Richard J. Wallace, Jr. 1998. “ A Single 16S Ribosomal RNA Substitution Is Responsible for Resistance to Amikacin and Other 2-Deoxystreptamine Aminoglycosides in Mycobacterium Abscessus and Mycobacterium Chelonae .” *The Journal of Infectious Diseases* 177 (6): 1573–81. https://doi.org/10.1086/515328.

Preiss, Laura, Julian D. Langer, Özkan Yildiz, Luise Eckhardt-Strelau, Jérôme E.G. Guillemont, Anil Koul, and Thomas Meier. 2015. “Structure of the Mycobacterial ATP Synthase Fo Rotor Ring in Complex with the Anti-TB Drug Bedaquiline.” *Science Advances* 1 (4): 1–8. https://doi.org/10.1126/sciadv.1500106.

Pryjma, Mark, Ján Burian, and Charles J. Thompson. 2018. “Rifabutin Acts in Synergy and Is Bactericidal with Frontline Mycobacterium Abscessus Antibiotics Clarithromycin and Tigecycline, Suggesting a Potent Treatment Combination.” *Antimicrobial Agents and Chemotherapy* 62 (8): 1–27. https://doi.org/10.1128/AAC.00283-18.

Quémard, Annaik, James C. Sacchettini, Andréa Dessen, Catherine Vilcheze, Robert Bittman, William R. Jacobs, and John S. Blanchard. 1995. “Enzymatic Characterization of the Target for Isoniazid in Mycobacterium Tuberculosis.” *Biochemistry* 34 (26): 8235–41. https://doi.org/10.1021/bi00026a004.

Ramón-García, Santiago, Isabel Otal, Carlos Martín, Rafael Gómez-Lus, and José A. Aínsa. 2006. “Novel Streptomycin Resistance Gene from Mycobacterium Fortuitum.” *Antimicrobial Agents and Chemotherapy* 50 (11): 3920–22. https://doi.org/10.1128/AAC.00223-06.

Rao, Srinivasa P.S., Suresh B. Lakshminarayana, Ravinder R. Kondreddi, Maxime Herve, Luis R. Camacho, Pablo Bifani, Sarath K. Kalapala, et al. 2013. “Indolcarboxamide Is a Preclinical Candidate for Treating Multidrug-Resistant Tuberculosis.” *Science Translational Medicine* 5 (214). https://doi.org/10.1126/scitranslmed.3007355.

Raynaud, Clément, Wassim Daher, Matt D. Johansen, Françoise Roquet-Banères, Mickael Blaise,

Oluseye K. Onajole, Alan P. Kozikowski, et al. 2020. “Active Benzimidazole Derivatives Targeting the MmpL3 Transporter in Mycobacterium Abscessus.” *ACS Infectious Diseases*. https://doi.org/10.1021/acsinfecdis.9b00389.

Raynaud, Clément, Wassim Daher, Françoise Roquet-Banères, Matt D Johansen, Jozef Stec, Oluseye K Onajole, Diane Ordway, Alan P Kozikowski, and Laurent Kremer. 2020. “Synergistic Interactions of Indole-2-Carboxamides and β-Lactam Antibiotics against Mycobacterium Abscessus.” *Antimicrobial Agents and Chemotherapy* 64 (5): 1–8. https://doi.org/10.1128/AAC.02548-19.

Raynaud, Clément, and Laurent Kremer. 2020. “Un Nouvel Espoir Pour Traiter Les Infections Persistantes à Mycobacterium Abscessus ?” *Medecine Sciences : M/S* 36 (8–9): 691–94. https://doi.org/10.1051/medsci/2020138.

Remuiñán, Modesto J., Esther Pérez-Herrán, Joaquín Rullás, Carlos Alemparte, María Martínez-Hoyos, David J. Dow, Johnson Afari, et al. 2013. “Tetrahydropyrazolo[1,5-a]Pyrimidine-3-Carboxamide and N-Benzyl-6’,7’-Dihydrospiro[Piperidine-4,4’-Thieno[3,2-c]Pyran] Analogues with Bactericidal Efficacy against Mycobacterium Tuberculosis Targeting MmpL3.” *PLoS ONE* 8 (4). https://doi.org/10.1371/journal.pone.0060933.

Renna, Maurizio, Catherine Schaffner, Karen Brown, Shaobin Shang, Marcela Henao Tamayo, Krisztina Hegyi, Neil J Grimsey, et al. 2011. “Azithromycin Blocks Autophagy and May Predispose Cystic Fibrosis Patients to Mycobacterial Infection.” *Journal of Clinical Investigation* 121 (10): 3554–63. https://doi.org/10.1172/JCI46095DS1.

Richard, Matthias, Ana Victoria Gutiérrez, Albertus Viljoen, Daniela Rodriguez-Rincon, Françoise Roquet-Baneres, Mickael Blaise, Isobel Everall, Julian Parkhill, R. Andres Floto, and Laurent Kremer. 2019. “Mutations in the MAB_2299c TetR Regulator Confer Cross-Resistance to Clofazimine and Bedaquiline in Mycobacterium Abscessus.” *Antimicrobial Agents and Chemotherapy* 63 (1): 1–15. https://doi.org/10.1128/AAC.01316-18.

Rohde, Manfred. 2019. “The Gram-Positive Bacterial Cell Wall.” *Microbiology Spectrum*, 1–21. https://doi.org/10.1128/microbiolspec.GPP3-0044-2018.Correspondence.

Rominski, Anna, Anna Roditscheff, Petra Selchow, Erik C. Böttger, and Peter Sander. 2017. “Intrinsic Rifamycin Resistance of Mycobacterium Abscessus Is Mediated by ADP-Ribosyltransferase MAB_0591.” *Journal of Antimicrobial Chemotherapy* 72 (2): 376–84. https://doi.org/10.1093/jac/dkw466.

Rominski, Anna, Petra Selchow, Katja Becker, Juliane K. Brülle, Michael Dal Molin, and Peter Sander. 2017. “Elucidation of Mycobacterium Abscessus Aminoglycoside and Capreomycin Resistance by Targeted Deletion of Three Putative Resistance Genes.” *Journal of Antimicrobial Chemotherapy* 72 (8): 2191–2200. https://doi.org/10.1093/jac/dkx125.

Roux, Anne Laure, Aurélie Ray, Alexandre Pawlik, Halima Medjahed, Gilles Etienne, Martin Rottman, Emilie Catherinot, et al. 2011. “Overexpression of Proinflammatory TLR-2-Signalling Lipoproteins in Hypervirulent Mycobacterial Variants.” *Cellular Microbiology* 13 (5): 692–704. https://doi.org/10.1111/j.1462-5822.2010.01565.x.

Roux, Anne Laure, Albertus Viljoen, Aïcha Bah, Roxane Simeone, Audrey Bernut, Laura Laencina, Therese Deramaudt, et al. 2016. “The Distinct Fate of Smooth and Rough Mycobacterium Abscessus Variants inside Macrophages.” *Open Biology* 6 (11). https://doi.org/10.1098/rsob.160185.

Rožman, Kaja, Izidor Sosič, Raquel Fernandez, Robert J. Young, Alfonso Mendoza, Stanislav Gobec, and Lourdes Encinas. 2017. "A New 'Golden Age' for the Antitubercular Target InhA." *Drug Discovery Today* 22 (3): 492–502. https://doi.org/10.1016/j.drudis.2016.09.009.

Rudra, Paulami, Kelley Hurst-Hess, Pascal Lappierre, and Pallavi Ghosha. 2018. "High Levels of Intrinsic Tetracycline Resistance in Mycobacterium Abscessus Are Conferred by a Tetracycline-Modifying Monooxygenase." *Antimicrobial Agents and Chemotherapy* 62 (6): 1–14. https://doi.org/10.1128/AAC.00119-18.

Rudra, Paulami, Kelley R. Hurst-Hess, Katherine L Cotten, Andrea Partida-Miranda, and Pallavi Ghosh. 2020. "Mycobacterial HflX Is a Ribosome Splitting Factor That Mediates Antibiotic Resistance." *Proceedings of the National Academy of Sciences of the United States of America* 117 (1): 629–34. https://doi.org/10.1073/pnas.1906748117.

Run, Eva Le, Michel Arthur, and Jean-Luc Mainardi. 2019. "*In Vitro* and Intracellular Activity of Imipenem Combined with Tedizolid, Rifabutin, and Avibactam against *Mycobacterium Abscessus*." *Antimicrobial Agents and Chemotherapy*, no. February. https://doi.org/10.1128/AAC.01915-18.

Run, Eva Le, Heiner Atze, Michel Arthur, and Jean Luc Mainardi. 2020. "Impact of Relebactam-Mediated Inhibition of Mycobacterium Abscessus BlaMab β-Lactamase on the in Vitro and Intracellular Efficacy of Imipenem." *Journal of Antimicrobial Chemotherapy* 75 (2): 379–83. https://doi.org/10.1093/jac/dkz433.

Ruth, Mike M., Jasper J.N. Sangen, Lian J. Pennings, Jodie A. Schildkraut, Wouter Hoefsloot, Cecile Magis-Escurra, Heiman F.L. Wertheim, and Jakko Van Ingen. 2018. "Minocycline Has No Clear Role in the Treatment of Mycobacterium Abscessus Disease." *Antimicrobial Agents and Chemotherapy* 62 (10): 62–65. https://doi.org/10.1128/AAC.01208-18.

Ruyck, Jérôme de, Christian Dupont, Elodie Lamy, Vincent Le Moigne, Christophe Biot, Yann Guérardel, Jean Louis Herrmann, et al. 2020. "Structure-Based Design and Synthesis of Piperidinol-Containing Molecules as New Mycobacterium Abscessus Inhibitors." *ChemistryOpen* 9 (3): 351–65. https://doi.org/10.1002/open.202000042.

Sacco, Emmanuelle, Virginie Legendre, Françoise Laval, Didier Zerbib, Henri Montrozier, Nathalie Eynard, Christophe Guilhot, Mamadou Daffé, and Annaïk Quémard. 2007. "Rv3389C from Mycobacterium Tuberculosis, a Member of the (R)-Specific Hydratase/Dehydratase Family." *Biochimica et Biophysica Acta - Proteins and Proteomics* 1774 (2): 303–11. https://doi.org/10.1016/j.bbapap.2006.11.016.

Sethiya, Jigar P, Melanie A Sowards, Mary Jackson, and Elton Jeffrey North. 2020. "MmpL3 Inhibition: A New Approach to Treat Nontuberculous Mycobacterial Infections." *International Journal of Molecular Sciences*. https://doi.org/10.3390/ijms21176202.

Shah, Parth, Tejas M. Dhameliya, Rohit Bansal, Manesh Nautiyal, Damodara N. Kommi, Pradeep S. Jadhavar, Jonnalagadda Padma Sridevi, Perumal Yogeeswari, Dharmarajan Sriram, and Asit K. Chakraborti. 2014. "N-Arylalkylbenzo[d]Thiazole-2-Carboxamides as Anti-Mycobacterial Agents: Design, New Methods of Synthesis and Biological Evaluation." *MedChemComm* 5 (10): 1489–95. https://doi.org/10.1039/c4md00224e.

Shen, Gwan Han, Bo Da Wu, Shiau Ting Hu, Chen Fu Lin, Kun Ming Wu, and Jiann Hwa Chen. 2010. "High Efficacy of Clofazimine and Its Synergistic Effect with Amikacin against Rapidly Growing Mycobacteria." *International Journal of Antimicrobial Agents* 35 (4): 400–404.

https://doi.org/10.1016/j.ijantimicag.2009.12.008.

Singh, S., N. Bouzinbi, V. Chaturvedi, S. Godreuil, and L. Kremer. 2014. “In Vitro Evaluation of a New Drug Combination against Clinical Isolates Belonging to the Mycobacterium Abscessus Complex.” *Clinical Microbiology and Infection* 20 (12): O1124–27. https://doi.org/10.1111/1469-0691.12780.

Slayden, R. A., and Clifton E. Barry. 2002. “The Role of KasA and KasB in the Biosynthesis of Meromycolic Acids and Isoniazid Resistance in Mycobacterium Tuberculosis.” *Tuberculosis* 82 (4–5): 149–60. https://doi.org/10.1054/tube.2002.0333.

Soroka, Daria, Clément Ourghanlian, Fabrice Compain, Marion Fichini, Vincent Dubée, Jean Luc Mainardi, Jean Emmanuel Hugonnet, and Michel Arthur. 2017. “Inhibition of β-Lactamases of Mycobacteria by Avibactam and Clavulanate.” *Journal of Antimicrobial Chemotherapy* 72 (4): 1081–88. https://doi.org/10.1093/jac/dkw546.

Stec, Jozef, Oluseye K. Onajole, Shichun Lun, Haidan Guo, Benjamin Merenbloom, Giulio Vistoli, William R. Bishai, and Alan P. Kozikowski. 2016. “Indole-2-Carboxamide-Based MmpL3 Inhibitors Show Exceptional Antitubercular Activity in an Animal Model of Tuberculosis Infection.” *Journal of Medicinal Chemistry* 59 (13): 6232–47. https://doi.org/10.1021/acs.jmedchem.6b00415.

Talati, Naasha J., Nadine Rouphael, Krutika Kuppalli, and Carlos Franco-Paredes. 2008. “Spectrum of CNS Disease Caused by Rapidly Growing Mycobacteria.” *The Lancet Infectious Diseases* 8 (6): 390–98. https://doi.org/10.1016/S1473-3099(08)70127-0.

Telenti, Amalio, Douglas Lowrie, Lukas Matter, Paul Imbroden, Stewart Cole, Kurt Schopfer, Francine Marchesi, Joseph M Colston, and Thomas Bodmer. 1993. “Detection of Rifampicin-Resistance Mutations in Mycobacterium Tuberculosis.” *The Lancet* 341: 647–50.

Torraca, Vincenzo, Samrah Masud, Herman P. Spaink, and Annemarie H. Meijer. 2014. “Macrophage-Pathogen Interactions in Infectious Diseases: New Therapeutic Insights from the Zebrafish Host Model.” *DMM Disease Models and Mechanisms* 7 (7): 785–97. https://doi.org/10.1242/dmm.015594.

Tortoli, Enrico, Tarcisio Fedrizzi, Conor J. Meehan, Alberto Trovato, Antonella Grottola, Elisabetta Giacobazzi, Giulia Fregni Serpini, et al. 2017. “The New Phylogeny of the Genus Mycobacterium: The Old and the News.” *Infection, Genetics and Evolution* 56 (August): 19–25. https://doi.org/10.1016/j.meegid.2017.10.013.

Tortoli, Enrico, Thomas A. Kohl, Barbara A. Brown-Elliott, Alberto Trovato, Sylvia Cardoso Leão, Maria Jesus Garcia, Sruthi Vasireddy, et al. 2016. “Emended Description of Mycobacterium Abscessus Mycobacterium Abscessus Subsp. Abscessus and Mycobacterium Abscessus Subsp. Bolletii and Designation of Mycobacterium Abscessus Subsp. Massiliense Comb. Nov.” *International Journal of Systematic and Evolutionary Microbiology* 66 (11): 4471–79. https://doi.org/10.1099/ijsem.0.001376.

Trivedi, Omita A., Pooja Arora, Vijayalakshmi Sridharan, Rashmi Tickoo, Debasisa Mohanty, and Rajesh S. Gokhale. 2004. “Enzymic Activation and Transfer of Fatty Acids as Acyl-Adenylates in Mycobacteria.” *Nature* 428 (6981): 441–45. https://doi.org/10.1038/nature02384.

Ung, Kien Lam, Husam M.A.B. Alsarraf, Laurent Kremer, and Mickaël Blaise. 2020. “The Crystal

Structure of the Mycobacterial Trehalose Monomycolate Transport Factor A, TtfA, Reveals an Atypical Fold." *Proteins: Structure, Function and Bioinformatics* 88 (6): 809–15. https://doi.org/10.1002/prot.25863.

Ung, Kien Lam, Husam M.A.B. Alsarraf, Vincent Olieric, Laurent Kremer, and Mickaël Blaise. 2019. "Crystal Structure of the Aminoglycosides N-Acetyltransferase Eis2 from Mycobacterium Abscessus." *FEBS Journal* 286 (21): 4342–55. https://doi.org/10.1111/febs.14975.

Ung, Kien Lam, Laurent Kremer, and Mickaël Blaise. 2020. "Structural Analysis of the N-Acetyltransferase Eis1 from Mycobacterium Abscessus Reveals the Molecular Determinants of Its Incapacity to Modify Aminoglycosides." *Proteins: Structure, Function and Bioinformatics*. https://doi.org/10.1002/prot.25997.

Vaghaiwalla, Tanaz, Shevonne S. Satahoo, Rolla Zarifa, Marc Dauer, James S. Davis, Doreann Dearmas, Nicholas Namias, Louis R. Pizano, and Carl I. Schulman. 2014. "Mycobacterium Abscessus Infection in a Burn Intensive Care Unit Patient." *Surgical Infections* 15 (6): 847–49. https://doi.org/10.1089/sur.2014.052.

Varela, Cristian, Doris Rittmann, Albel Singh, Karin Krumbach, Kiranmai Bhatt, Lothar Eggeling, Gurdyal S. Besra, and Apoorva Bhatt. 2012. "MmpL Genes Are Associated with Mycolic Acid Metabolism in Mycobacteria and Corynebacteria." *Chemistry and Biology* 19 (4): 498–506. https://doi.org/10.1016/j.chembiol.2012.03.006.

Veziris, Nicolas, Christine Bernard, Lorenzo Guglielmetti, Damien Le Du, Dhiba Marigot-Outtandy, Marie Jaspard, Eric Caumes, et al. 2017. "Rapid Emergence of Mycobacterium Tuberculosis Bedaquiline Resistance: Lessons to Avoid Repeating Past Errors." *European Respiratory Journal* 49 (3). https://doi.org/10.1183/13993003.01719-2016.

Vilchèze, Catherine, and Laurent Kremer. 2017. "Acid-Fast Positive and Acid-Fast Negative Mycobacterium Tuberculosis: The Koch Paradox." *Microbiology Spectrum* 2 (3): 1–16. https://doi.org/10.1128/microbiolspec.

Vilchèze, Catherine, Hector R. Morbidoni, Torin R. Weisbrod, Hiroyuki Iwamoto, Mack Kuo, James C. Sacchettini, and William R. Jacobs. 2000. "Inactivation of the InhA-Encoded Fatty Acid Synthase II (FASII) Enoyl- Acyl Carrier Protein Reductase Induces Accumulation of the FASI End Products and Cell Lysis of Mycobacterium Smegmatis." *Journal of Bacteriology* 182 (14): 4059–67. https://doi.org/10.1128/JB.182.14.4059-4067.2000.

Viljoen, Albertus, Violaine Dubois, Fabienne Girard-Misguich, Mickaël Blaise, Jean Louis Herrmann, and Laurent Kremer. 2017. "The Diverse Family of MmpL Transporters in Mycobacteria: From Regulation to Antimicrobial Developments." *Molecular Microbiology* 104 (6): 889–904. https://doi.org/10.1111/mmi.13675.

Viljoen, Albertus, Jean-Louis Herrmann, Oluseye K. Onajole, Jozef Stec, Alan P. Kozikowski, and Laurent Kremer. 2017. "Controlling Extra- and Intramacrophagic Mycobacterium Abscessus by Targeting Mycolic Acid Transport." *Frontiers in Cellular and Infection Microbiology* 7 (September): 1–6. https://doi.org/10.3389/fcimb.2017.00388.

Viljoen, Albertus, Clément Raynaud, Matt D. Johansen, Françoise Roquet-Banères, Jean Louis Herrmann, Wassim Daher, and Laurent Kremer. 2019. "Verapamil Improves the Activity of Bedaquiline against Mycobacterium Abscessus in Vitro and in Macrophages." *Antimicrobial Agents and Chemotherapy* 63 (9): 1–6. https://doi.org/10.1128/AAC.00705-19.

Wallace, Richard J., Barbara A. Brown-Elliott, Christopher J. Crist, Linda Mann, and Rebecca W. Wilson. 2002. “Comparison of the in Vitro Activity of the Glycylcycline Tigecycline (Formerly GAR-936) with Those of Tetracycline, Minocycline, and Doxycycline against Isolates of Nontuberculous Mycobacteria.” *Antimicrobial Agents and Chemotherapy* 46 (10): 3164–67. https://doi.org/10.1128/AAC.46.10.3164-3167.2002.

Wee, Wei Yee, Avirup Dutta, and Siew Woh Choo. 2017. “Comparative Genome Analyses of Mycobacteria Give Better Insights into Their Evolution.” *PLoS ONE* 12 (3): 1–13. https://doi.org/10.1371/journal.pone.0172831.

Whang, Jake, Yong Woo Back, Kang In Lee, Nagatoshi Fujiwara, Seungwha Paik, Chul Hee Choi, Jeong Kyu Park, and Hwa Jung Kim. 2017. “Mycobacterium Abscessus Glycopeptidolipids Inhibit Macrophage Apoptosis and Bacterial Spreading by Targeting Mitochondrial Cyclophilin D.” *Cell Death & Disease* 8 (8): e3012. https://doi.org/10.1038/cddis.2017.420.

Williams, John T., Elizabeth R. Haiderer, Garry B. Coulson, Kayla N. Conner, Edmund Ellsworth, Chao Chen, Nadine Alvarez-Cabrera, et al. 2019. “Identification of New MMPL3 Inhibitors by Untargeted and Targeted Mutant Screens Defines MMPL3 Domains with Differential Resistance.” *Antimicrobial Agents and Chemotherapy* 63 (10). https://doi.org/10.1128/AAC.00547-19.

Wiseman, Ben, Xavi Carpena, Miguel Feliz, Lynda J. Donald, Miquel Pons, Ignacio Fita, and Peter C. Loewen. 2010. “Isonicotinic Acid Hydrazide Conversion to Isonicotinyl-NAD by Catalase-Peroxidases.” *Journal of Biological Chemistry* 285 (34): 26662–73. https://doi.org/10.1074/jbc.M110.139428.

Won-Jung Koh. 2016. “Nontuberculous Mycobacteria-Overview.” *Microbiology Spectrum*. https://doi.org/10.1136/thx.50.6.634.

Wu, Mingyan, Bing Li, Qi Guo, Liyun Xu, Yuzhen Zou, Yongjie Zhang, Mengling Zhan, et al. 2019. “Detection and Molecular Characterisation of Amikacin-Resistant Mycobacterium Abscessus Isolated from Patients with Pulmonary Disease.” *Journal of Global Antimicrobial Resistance* 19: 188–91. https://doi.org/10.1016/j.jgar.2019.05.016.

Xu, H. B., R. H. Jiang, and H. P. Xiao. 2012. “Clofazimine in the Treatment of Multidrug-Resistant Tuberculosis.” *Clinical Microbiology and Infection* 18 (11): 1104–10. https://doi.org/10.1111/j.1469-0691.2011.03716.x.

Xu, Zhujun, Vladimir A. Meshcheryakov, Giovanna Poce, and Shu Sin Chng. 2017. “MmpL3 Is the Flippase for Mycolic Acids in Mycobacteria.” *Proceedings of the National Academy of Sciences of the United States of America* 114 (30): 7993–98. https://doi.org/10.1073/pnas.1700062114.

Yamaguchi, Akihito, Ryosuke Nakashima, and Keisuke Sakurai. 2015. “Structural Basis of RND-Type Multidrug Exporters.” *Frontiers in Microbiology* 6 (APR): 1–19. https://doi.org/10.3389/fmicb.2015.00327.

Yang, Tianming, Wilfried Moreira, Samuel Agyei Nyantakyi, Huan Chen, Dinah binte Aziz, Mei Lin Go, and Thomas Dick. 2017. “Amphiphilic Indole Derivatives as Antimycobacterial Agents: Structure-Activity Relationships and Membrane Targeting Properties.” *Journal of Medicinal Chemistry* 60 (7): 2745–63. https://doi.org/10.1021/acs.jmedchem.6b01530.

Yano, Takahiro, Sacha Kassovska-Bratinova, J. Shin Teh, Jeffrey Winkler, Kevin Sullivan, Andre Isaacs, Norman M. Schechter, and Harvey Rubin. 2011. “Reduction of Clofazimine by

Mycobacterial Type 2 NADH: Quinone Oxidoreductase: A Pathway for the Generation of Bactericidal Levels of Reactive Oxygen Species." *Journal of Biological Chemistry* 286 (12): 10276–87. https://doi.org/10.1074/jbc.M110.200501.

Ye, Meiping, Liyun Xu, Yuzhen Zou, Bing Li, Qi Guo, Yongjie Zhang, Mengling Zhan, et al. 2019. "Molecular Analysis of Linezolid-Resistant Clinical Isolates of Mycobacterium Abscessus." *Antimicrobial Agents and Chemotherapy* 63 (2): 1–5. https://doi.org/10.1128/AAC.01842-18.

Ying, Lanqing, Hongkun Zhu, Shinichiro Shoji, and Kurt Fredrick. 2019. "Roles of Specific Aminoglycoside–Ribosome Interactions in the Inhibition of Translation." *Rna* 25 (2): 247–54. https://doi.org/10.1261/rna.068460.118.

Zhang, Bing, Jun Li, Xiaolin Yang, Lijie Wu, Jia Zhang, Yang Yang, Yao Zhao, et al. 2019. "Crystal Structures of Membrane Transporter MmpL3, an Anti-TB Drug Target." *Cell* 176 (3): 636-648.e13. https://doi.org/10.1016/j.cell.2019.01.003.

Zhang, Nannan, Jordi B. Torrelles, Michael R. McNeil, Vincent E. Escuyer, Kay Hooi Khoo, Patrick J. Brennan, and Delphi Chatterjee. 2003. "The Emb Proteins of Mycobacteria Direct Arabinosylation of Lipoarabinomannan and Arabinogalactan via an N-Terminal Recognition Region and a C-Terminal Synthetic Region." *Molecular Microbiology* 50 (1): 69–76. https://doi.org/10.1046/j.1365-2958.2003.03681.x.

Zhang, Zhijian, Jie Lu, Min Liu, Yufeng Wang, Yanlin Zhao, Yu Pang, and Yanlin Zhao. 2017. "In Vitro Activity of Clarithromycin in Combination with Other Antimicrobial Agents against Mycobacterium Abscessus and Mycobacterium Massiliense." *International Journal of Antimicrobial Agents* 49 (3): 383–86. https://doi.org/10.1016/j.ijantimicag.2016.12.003.

Zhang, Zhijian, Jie Lu, Yuanyuan Song, and Yu Pang. 2018. "In Vitro Activity between Linezolid and Other Antimicrobial Agents against Mycobacterium Abscessus Complex." *Diagnostic Microbiology and Infectious Disease* 90 (1): 31–34. https://doi.org/10.1016/j.diagmicrobio.2017.09.013.

Zimhony, Oren, Alon Schwarz, Maria Raitses-Gurevich, Yoav Peleg, Orly Dym, Shira Albeck, Yigal Burstein, and Zippora Shakked. 2015. "AcpM, the Meromycolate Extension Acyl Carrier Protein of Mycobacterium Tuberculosis, Is Activated by the 4'-Phosphopantetheinyl Transferase PptT, a Potential Target of the Multistep Mycolic Acid Biosynthesis." *Biochemistry* 54 (14): 2360–71. https://doi.org/10.1021/bi501444e.

Zimhony, Oren, Catherine Vilchèze, and William R. Jacobs. 2004. "Characterization of Mycobacterium Smegmatis Expressing the Mycobacterium Tuberculosis Fatty Acid Synthase I (Fas1) Gene." *Journal of Bacteriology* 186 (13): 4051–55. https://doi.org/10.1128/JB.186.13.4051-4055.2004.

Annexes

Article. Synthesis and evaluation of heterocycle structures as potential inhibitors of *Mycobacterium tuberculosis* UGM

Maaliki C, Fu J, Villaume S, Viljoen A, Raynaud C, Hammoud S, Thibonnet J, Kremer L, Vincent SP, Thiery E. Bioorg Med Chem. 2020 Jul 1;28(13):115579. doi: 10.1016/j.bmc.2020.115579. Epub 2020 Jun 2. PMID: 32546296.

Bioorganic & Medicinal Chemistry 28 (2020) 115579

Contents lists available at ScienceDirect

Bioorganic & Medicinal Chemistry

journal homepage: www.elsevier.com/locate/bmc

Synthesis and evaluation of heterocycle structures as potential inhibitors of *Mycobacterium tuberculosis* UGM

Carine Maaliki[a], Jian Fu[b], Sydney Villaume[b], Albertus Viljoen[c], Clément Raynaud[c], Sokaina Hammoud[a], Jérôme Thibonnet[a], Laurent Kremer[c,d], Stéphane P. Vincent[b], Emilie Thiery[a,*]

[a] Laboratoire Synthèse et Isolement de Molécules Bioactives (SIMBA, EA 7502), Université de Tours, Faculté de Pharmacie, Parc de Grandmont, 31 Avenue Monge, 37200 Tours, France
[b] Department of Chemistry, University of Namur, Rue de Bruxelles 61, 5000 Namur, Belgium
[c] Institut de Recherche en Infectiologie de Montpellier (IRIM), CNRS UMR 9004, Université de Montpellier, 34293 Montpellier, France
[d] INSERM, IRIM, 34293 Montpellier, France

ARTICLE INFO

Keywords:
Heterocycles
Mycobacterium tuberculosis
UDP-galactopyranose mutase
Inhibitor
Docking

ABSTRACT

In this study, we screen three heterocyclic structures as potential inhibitors of UDP-galactopyranose mutase (UGM), an enzyme involved in the biosynthesis of the cell wall of *Mycobacterium tuberculosis*. In order to understand the binding mode, docking simulations are performed on the best inhibitors. Their activity on *Mycobacterium tuberculosis* is also evaluated. This study made it possible to highlight an "oxazepino-indole" structure as a new inhibitor of UGM and of *M. tuberculosis* growth *in vitro*.

1. Introduction

Tuberculosis (TB) is the world's deadliest infectious disease, responsible for 1.8 million deaths every year. According to the WHO report "Antibacterial agents in clinical development" published in 2017, inadequate new treatment options exist for antibiotic-resistant TB.[1] The emergence of drug-resistant strains of *Mycobacterium tuberculosis (Mt)* decreases the efficacy of treatment, which requires a combination of at least three antibiotics as first-line therapy. In the case of multi- and extensively-drug-resistant (MDR-TB and XDR-TB) strains, complex, prolonged, costly and highly toxic multidrug second-line therapy is required and only 30–50% of patients are treated successfully. In more than 70 years, only two antibiotics for the treatment of drug-resistant TB reached the market, and seven are currently being evaluated in clinical trials.[1] The development of new strategies and new molecular scaffolds is, therefore, necessary to counter the increasing threat of antimicrobial resistance and to propose new therapeutic options for TB treatment.[2]

Mt has a complex lifestyle involving several developmental stages. Its success results from its remarkable capacity to survive within the infected host, where it can persist in a non-replicating state for several decades in granulomas. The survival strategies developed by *Mt* are essentially linked to the presence of an unusual cell wall, which consists of two major layers (Fig. 1). The highly impermeable outer layer is composed of mycolic acids consisting of 70–90 carbon-containing fatty acids. The inner layer consists of peptidoglycan. These two layers are covalently tethered *via* the connecting polysaccharide arabinogalactan (AG).[3] AG itself comprises three regions: i) a disaccharide 'linker' attached to the peptidoglycan, ii) the galactofuran [(→6)-β-D-Gal*f*-(1 → 5)- β-D-(Gal*f*)]n which is attached to the linker unit, and iii) a complex arabinan linked to the galactofuran and representing the site of attachment of mycolic acids. These are oriented perpendicular to the plane of the membrane, providing a barrier responsible for the natural resistance of *Mt* to many antibiotic classes, and contribute to the physiopathological aspects characterizing TB. In addition, within this lipid environment are intercalated several glycolipids with exotic structures, such as the phthiocerol dimycocerosate, phenolic glycolipids, trehalose dimycolate (TDM) or sulfolipids. The role of these lipids in signaling events, pathogenesis, immune response and even in coughing has been established.[4]

Therefore, the integrity of both the mycolic acid-arabinogalactan-peptidoglycan skeleton (mAGP) and the outer mycomembrane leaflet of extractable lipids hinges on the integrity of the arabinan moiety of AG. In addition to its crucial structural role, arabinan exhibits also specific immunomodulatory activities although these functions have mostly been connected to the arabinan part of lipoarabinomannan that shares

* Corresponding author.
E-mail address: emilie.thiery@univ-tours.fr (E. Thiery).

https://doi.org/10.1016/j.bmc.2020.115579
Received 27 March 2020; Received in revised form 26 May 2020; Accepted 29 May 2020
Available online 02 June 2020

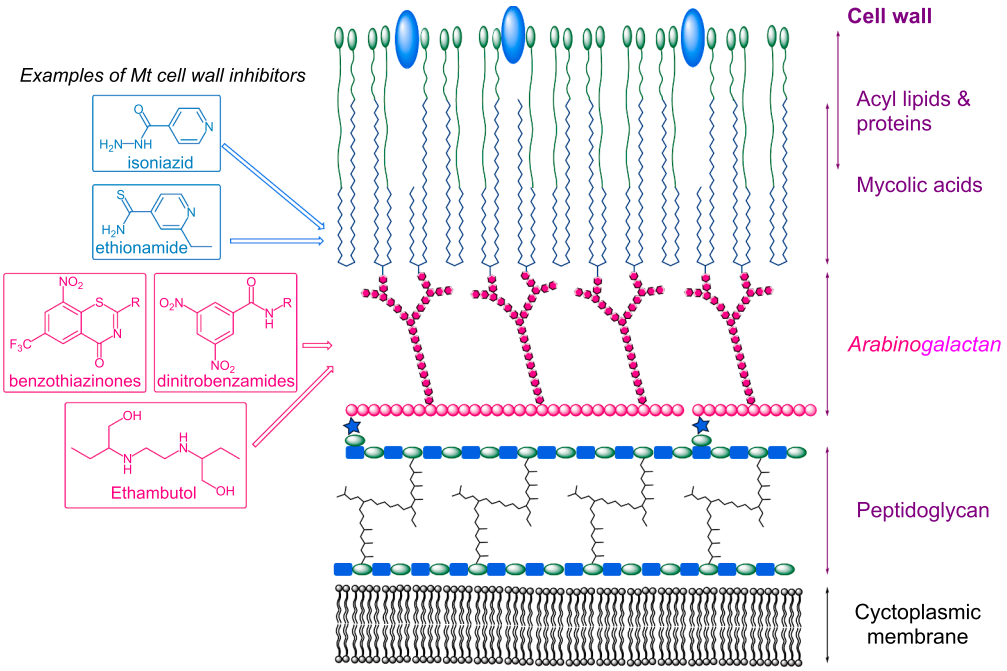

Fig. 1. Schematic structure of the *M. tuberculosis* cell envelope. Structures and sites of action of several anti-TB drugs targeting the cell wall are shown. Chemical entities inhibiting AG biosynthesis are in pink.

structural features with mAGP.[5]

During the past two decades, intensive efforts conducted to the discovery of new leads for TB drug development using either target-based or cell-based approaches and the molecular mechanisms of action of several anti-TB drugs were deciphered.[6] Several major anti-TB agents disrupt the biosynthesis of cell wall components. For instance, isoniazid and ethionamide are key inhibitors of mycolic acid biosynthesis, while ethambutol and the recently identified chemical classes the benzothiazinones and dinitrobenzamide derivatives inhibit biosynthesis of arabinan (Fig. 1).[7]

Several enzymes are involved in the biosynthesis of the galactan moiety of the cell wall but marketed antitubercular agents targeting this polysaccharide are currently lacking. One such enzyme is the UDP-galactopyranose (UDP-Gal*p*) mutase (UGM), which catalyzes the interconversion of UDP-galactopyranose (UDP-Gal*p*) into UDP-galactofuranose (UDP-Gal*f*) (Scheme 1), subsequently used by the Gal*f* transferases GlfT1 and GlfT2 to polymerize the galactofuran subunit of arabinogalactan.[8] Interestingly, UGM, which is absent in humans, is essential for the growth of mycobacteria, therefore representing a privileged and validated therapeutic target.[9]

Until recently, the search for UGM inhibitors has mainly focused on the preparation of substrate analogues.[10] However, screening studies have also shown that heterocyclic molecules can exhibit strong interactions with the catalytic site of the enzyme.[11] Recently, various heterocyclic compounds, including flavonoids,[12] acylhydrazones[13] and thiazol-2-amines[14] were shown to inhibit *Mt* UGM.

Herein, we present the screening of novel heterocyclic compounds for *Mt* UGM inhibition. We explored the relative levels of UGM inhibition by the three scaffolds represented in Fig. 2. Indeed, butenolides and indole derivatives are important pharmacophores that have not been explored for UGM inhibition yet. To evaluate the binding mode of

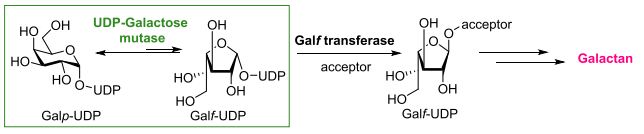

Scheme 1. Isomerization of UDP-Gal*p* by UGM and elaboration of galactan.

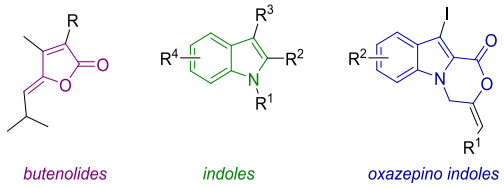

Fig. 2. Three heterocyclic structures studied for *Mt* UGM inhibition.

the best inhibitors, molecular docking experiments are described. The *in vitro* anti-bacterial activities of the best UGM inhibitors are also reported.

2. Results and discussion

2.1. Initial screening

Two distinct biochemical assays have been developed to evaluate the binding affinity of small molecules towards purified *Mt* UGM. An HPLC-based assay allows the monitoring of the conversion of the substrate, UDP-Gal*f*, into UDP-Gal*p* using *Mt* UGM in its active reduced form. Percentages of inhibition are usually described with this assay. The concentration of UDP-Gal*f* (25 μM) was chosen to be close to its K_m (23 μM for *Mt*UGM).[10]

A higher-throughput fluorescence polarization (FP) assay has also been developed and exploited on the non-reduced form of the enzyme.[15] The latter is based on the competition between the screened ligand(s) and a fluorescent probe and can be performed in multi-well plates.

Our methodology consisted first to screen chemical libraries by FP at inhibitor concentrations of 100 μM and 1 mM (only the values at 1 mM are displayed in Tables 1–3). When the percentage of inhibition was greater than 30% at 1 mM, the affinity of the inhibitors (K_d's) was determined using the FP assay.[16]

Being much more demanding, the HPLC assay was only used for the very best hits.

Butenolides and their derivatives represent a large family of natural products. Since the 1970's, many furan heterocycles have been isolated

Table 1
The *Mt* UGM inhibition data for the butenolide series.

Entry	Compound	*Mt* UGM Inhibition[a] [%]
1	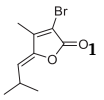 **1**	7.3
2	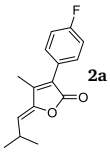 **2a**	9.0
3	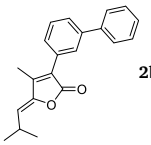 **2b**	19.2
4	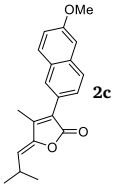 **2c**	7.4
5	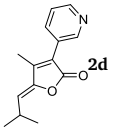 **2d**	3.0
6	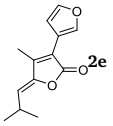 **2e**	5.2
7	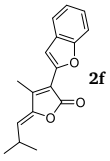 **2f**	0

[a] FP inhibition assay conditions: [inhibitor] = 1 mM, non-reduced enzyme, [*Mt* UGM] = 580 nM, [fluorescent probe] = 18 nM.

with a wide range of biological activities. As examples, xerulin and derivatives are inhibitors of cholesterol biosynthesis[17] while tetrenolin[18] and freelyngine[19] display antibiotic activities.

To generate a first representative set of butenolides **2a-f**, we developed a new stereoselective synthetic strategy of (*E*)-*α*-substituted *β*-methyl (*Z*)-γ-alkylidene butenolides (Scheme 2). As previously reported for *β*-iodopropenoic acid derivatives,[20] the first step is based on the cross-coupling-heterocyclization reaction sequence between terminal alkynes and (*E*)-2,3-dibromobutenoic acid in order to obtain *α*-bromo *β*-methyl (*Z*)-γ-isobutylidene furan-2-one **1** (Scheme 2). The presence of the bromide in the *α* position allows the modification of the furanone moiety *via* Suzuki coupling, providing access to a wide panel of *α*-substituted furan-2-one **2** (Scheme 2, Table 1).

The inhibition data for compounds **1** and **2a-f** are reported in Table 1. All butenolides were tested at 1 mM using the FP-based assay. However, none of them displayed a satisfactory inhibition level, encouraging us to explore two other targeted scaffolds.

We next examined the indole series of molecules. These heterocycles are present in many bioactive molecules, including antituberculous agents.[21] According to procedures previously described in the literature,[22] ethyl 3-iodo-1*H*-indole-2-carboxylates **5** were prepared from commercially available compounds **4** in the presence of *N*-iodosuccinimide (Scheme 3). The propargylation of compounds **4** and **5** led to

Table 2
The *Mt* UGM inhibition data for the indole series.

Entry	Compound	Inhibition *Mt* UGM [%][a]	K_d[b] [μM] *Mt* UGM
1	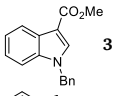 **3**	5.1	–
2	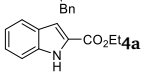 **4a**	2.0	–
3	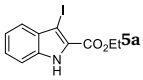 **5a**	11.5	–
4	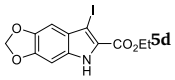 **5d**	23.1	–
5	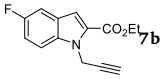 **7b**	0	–
6	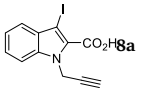 **8a**	7.4	–
7	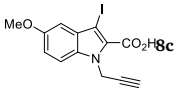 **8c**	15.0	–
8	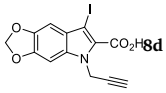 **8d**	46.2	220 ± 2

[a] FP inhibition assay conditions: [inhibitor] = 1 mM, non-reduced enzyme, [*Mt* UGM] = 580 nM, [fluorescent probe] = 18 nM [b] FP assay conditions: [inhibitors] = 0–1 mM, non-reduced enzyme, [*Mt* UGM] = 580 nM, [fluorescent probe] = 18 nM.

compounds **6** and **7**, respectively. Saponification of carboxylated indoles **7** yielded the corresponding acids **8**. Molecules **4a-d**, **6**, **7** and **8a-d** were selected for preliminary UGM inhibition assays because if a hit is discovered, they offer the possibility to be further derivatized for a structure activity relationship (SAR) study.

The UGM inhibitory activity of a selection of eight indoles was evaluated (Table 2). The tested compounds were very poor inhibitors (Entries 1–7), except product **8d** (Entry 8) which reduced the activity of *Mt* UGM to 46% (entry 8). However, **8d** showed low affinity for *Mt* UGM (K_d = 220 μM). As compared to the other molecules in this series, the presence of both the dioxolane ring and the free carboxylic acid on the indole scaffold appears important for UGM inhibition (Entries 3–4 and 6–8).

Finally, we prepared a series of tricyclic indoles based on synthetic protocols described in the literature (Scheme 4).[22] The iodocyclisation of indoles **8** in the presence of silver nitrate, diiodine and sodium carbonate in tetrahydrofuran led to the oxazinoindole compounds **9**. The functionalization of vinyl iodine by Sonogashira coupling made it possible to generate products **10.**

The inhibition data for compounds **9** and **10** are reported in Table 3. Compound **9a** displayed a poor inhibitory activity for *Mt* UGM (FP assay) for the enzyme (Entry 1). The functionalization of the indole cycle by a fluorine lead to a decrease in activity (Entry 2). The same effect is observed when a methyl or a phenyl is present on the vinylic pattern (Entries 3 and 4). In contrast, compounds **10** showed good inhibitory activities and affinities for *Mt* UGM (Entries 5–7). K_d values for molecules **10a**, **10c** and **10d** were found in the same range (58–66 μM). To make sure that these molecules are not false positive, we evaluated them by the HPLC assay. More significant inhibitory differences could be measured: molecule **10c** displayed a 95% inhibition level as compared to 73% for **10a** and 60% for **10d**. Such differences between these assays are not surprising as the FP assay is conducted with the non-reduced enzyme against a fluorescent probe whereas the HPLC uses the

Table 3
The *Mt* UGM inhibition data for the "oxazino-indole" series.

Entry	Compound	Inhibition *Mt* UGM [%]	K_d[b] [μM] *Mt* UGM
1	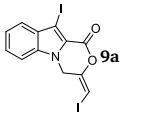 **9a**	61.6[a]	2000
2	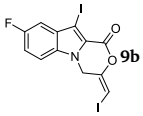 **9b**	19.1[a]	–
3	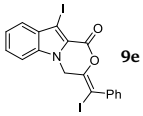 **9e**	22.8[a]	–
4	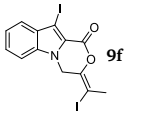 **9f**	14.9[a]	–
5	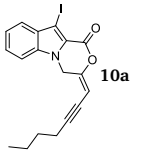 **10a**	72.9 ± 3.3[c]	66 ± 1.5
6	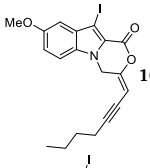 **10c**	95.5 ± 0.5[c]	61.3 ± 1.4
7	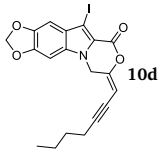 **10d**	60.2 ± 3.6[c]	58.3 ± 1.2

[a]Inhibition assay conditions: [inhibitor] = 1 mM, non-reduced enzyme, [*Mt* UGM] = 580 nM, [fluorescent probe] = 18 nM. [b] FP assay conditions: [inhibitors] = 0–1 mM, non-reduced enzyme, [*Mt* UGM] = 580 nM, [fluorescent probe] = 18 nM. [c] HPLC inhibition assay conditions: [inhibitor] = 0.5 mM, [*Mt* UGM] = 25 nM, [UDP-Gal*f*] = 25 μM.

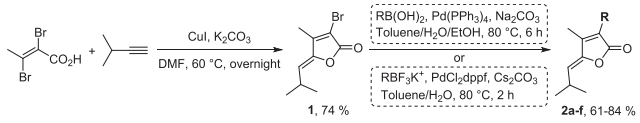

Scheme 2. Synthesis of *α*-substituted *β*-methyl γ-alkylidene butenolides.

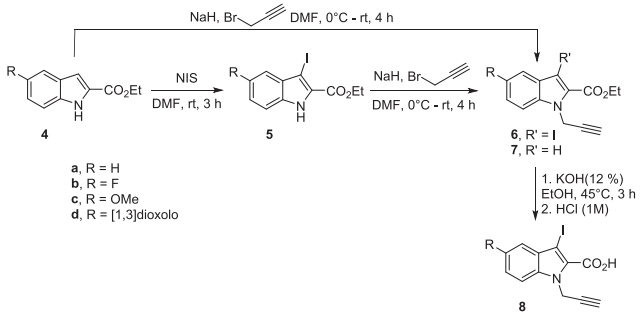

Scheme 3. Synthesis of indole derivatives.

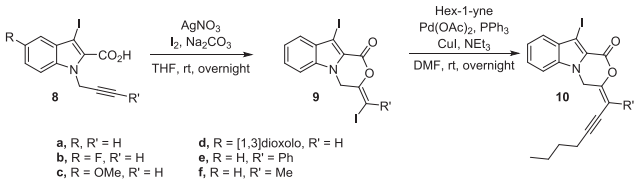

Scheme 4. Synthesis of tricyclic indole derivatives.

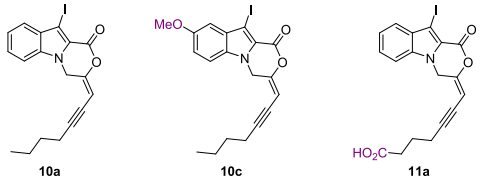

Fig. 3. Molecules subjected to docking simulations.

reduced UGM against the natural substrate UDP-Gal*f*.

2.2. Docking of "oxazepino indole" compounds with Mt UGM

To evaluate their binding modes, the best inhibitory candidates (**10a** and **10c**, Fig. 3) were subjected to docking simulations. All modelling calculations were performed by using *Mt* UGM crystal structures in its closed conformation (PDB code: 4RPG).[10] The UDP-galactose binding pocket of UGM consists of a galactose sub-pocket close to the FAD cofactor, a pyrophosphate sub-pocket where two arginine residues (Arg 292 and 180) can be found and a more hydrophobic uridine binding pocket.

For molecules **10a** and **10c**, only one binding mode could be observed: the tricyclic indole core strongly interacts with the residues of the uridine sub-pocket while the alkynyl chain lies within the pyrophosphate pocket without making noticeable contacts (Fig. 4 and Supplementary information). The methoxy group in **10c** does not significantly change the position of the molecule in the cavity as compared to **10a** and makes a contact with asparagine 284. In order to optimize interactions, the modelling was carried out with a tricyclic "oxazepino indole" bearing a carboxylic acid (molecule **11a**, Fig. 3). The binding mode remains the same as for **10a** and **10c** with characteristic contacts in the uridine pocket with residues Tyr366, Leu141, Thr162, Tyr161 and Tyr191. However, a clear interaction with Arg292 and the carboxylate could be observed. Such an attractive interaction could induce a better affinity for *Mt* UGM. We thus concentrated efforts on the synthesis of compound **11a**.

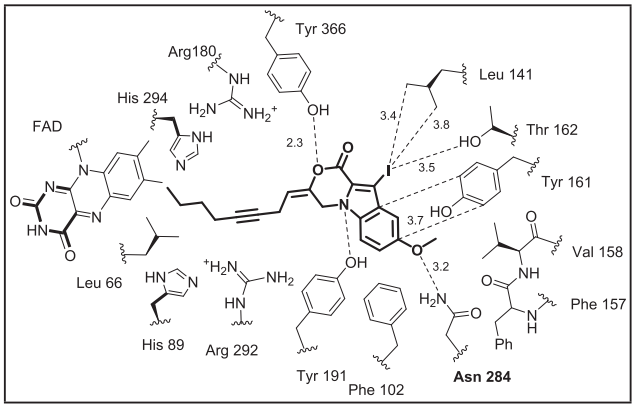

Fig. 4. Interaction map of **10c** with *Mt* UGM.

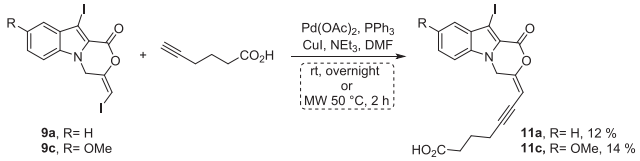

Scheme 5. Synthesis of compounds **11a** and **11c.**

Table 4
The *Mt* UGM inhibition data for the compounds **11a** and **11c.**

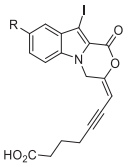

Entry	Compound	Inhibition[a] *Mt* UGM [%]	K_d[b] [μM] *Mt* UGM
1	**11a**, R = H	84.0	56.8 ± 1.2
2	**11c**, R = OMe	83.5	33.8 ± 1.2

[a] [inhibitor] = 1 mM, non-reduced enzyme, [*Mt* UGM] = 580 nM, [fluorescent probe] = 18 nM. [b] FP assay conditions: [inhibitors] = 0–1 mM, non-reduced enzyme, [*Mt* UGM] = 580 nM, [fluorescence probe] = 18 nM.

2.3. Synthesis and evaluation of new "oxazepino-indole" compounds

The promising results obtained with molecules **10** prompted us to explore further this design by incorporating a polar carboxylic acid to improve the water solubility and find evidence of hydrophobic/hydrophilic effects in the association of **10** with UGM. Compounds **11a** and **11c** were respectively prepared under Sonogashira conditions from iodoalkenes **9a** and **9c** (Scheme 5). The reaction was performed at room temperature or at 50 °C under microwave irradiation. Compounds **11** were partially degraded on silica gel, which explains the low yields.

The inhibition and FP assays (Table 4) indicated that both **11a** and **11c** display a good affinity for *Mt* UGM and a strong inhibitory activity. These levels of affinity are comparable to the best heterocyclic UGM inhibitors reported to date that have been found in the low micromolar range (Fig. 5).[10–13,15,23]

2.4. Antitubercular activity

The anti-tubercular activities of the best inhibitors of UGM (K_d < 70 μM) were then tested by determination of the minimal inhibitory concentration (MIC) against *M. tuberculosis* mc^{2}6230 (Table 5). All compounds have MICs below or equal to 50 μg/mL, thus highlighting their potent anti-mycobacterial activity. Compounds **10a** and **10d** share MIC values comparable to the best UGM inhibitors reported so far (Entries 1 and 3).[11,12,23]

3. Conclusion

This study revealed a new tricyclic structure with good affinity for *Mt* UGM and potent antitubercular activity and opens the door for subsequent SAR studies to generate derivatives with increased activity against drug susceptible and drug-resistant *Mt* strains.

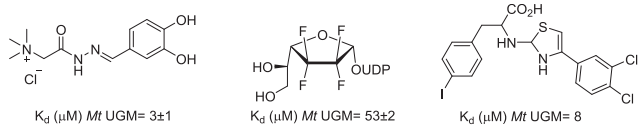

Fig. 5. Example of the best inhibitors of *Mt* UGM.[10e,13,15]

Table 5
MIC values of *Mt* UGM inhibitors.

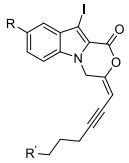

Entry	Compound	MIC[a] [μg/mL]
1	**10a**, R = H, R'= H	6.2
2	**10c**, R = OMe, R'= H	50
3	**10d**, R = [1,3]dioxolo, R'= H	3.1
4	**11a**, R = H, R'= CO_2H	50
5	**11c**, R = OMe, R'= CO_2H	50

[a] The concentrations tested varied over a discrete 2-fold range: 1.5, 3.1, 6.2, 12.5, 25, 50, 100 μg/ml. MIC determinations were performed in duplicate on three independent occasions, with zero variation between experiments for the five compounds tested.

4. Experimental section

4.1. Chemistry

4.1.1. General methods

All reactions were carried out under argon atmosphere in dried glassware. Tetrahydrofuran was dried and freshly distilled from sodium and benzophenone. Dry DMF and catalysts were purchased from Sigma-Aldrich®. ^{1}H NMR spectra were recorded on a Bruker® Avance 300 (300 MHz) NMR spectrometer, using $CDCl_3$ as solvent. Data, reported using $CHCl_3$ (δ_H = 7.26 ppm) as internal reference, were as follows (in order): chemical shift (δ in ppm relative to $CHCl_3$), multiplicity (s, d, t, q, quint, m, br for singlet, doublet, triplet, quartet, quintuplet, multiplet, broad) and coupling constants (*J* in Hz). ^{13}C NMR was recorded at 75 MHz on the same instrument, using the $CDCl_3$ solvent peak at (δ_C = 77.16 ppm) as reference. ^{19}F NMR was recorded at 282 MHz on the same instrument. HRMS was obtained with a LCMS-IT-TOF mass spectrometer under conditions of ESI. IR spectra were recorded on a Perkin-Elmer Spectrum One spectrophotometer. Melting points were uncorrected.

4.1.2. Preparation of butenolides compounds.

A sealed tube was loaded with (*E*)-2,3-dibromobut-2-enoic acid (3 g, 12.3 mmol, 1 equiv.) and potassium carbonate (3.4 g, 24.6 mmol, 2 equiv.) in DMF (30 mL). The mixture is degassed with argon for 10 min. 3-Methylbut-1-yne (6 mL, 61.5 mmol, 5 equiv.) and copper iodide (2.3 g, 12.3 mmol, 1 equiv.) were added. The tube was filled with argon and sealed. The solution was stirred at 60 °C overnight, then hydrolyzed with aqueous saturated solution of NH_4Cl (100 mL) and filtered on Celite®. The filtrate was extracted with AcOEt (300 mL). The organic phase was washed with aqueous saturated solution of NH_4Cl (50 mL × 3), saturated solution of NaCl (50 mL), dried over anhydrous $MgSO_4$, filtered and solvents were evaporated under vacuum. The residue was purified by recrystallization in CH_2Cl_2 to afford the expected compound.

(*Z*)-3-Bromo-4-methyl-5-(2-methylpropylidene)furan-2(5*H*)-one (1): $C_9H_{11}BrO_2$, MW = 231.09 g/mol, yield = 74%, white solid, mp = 93–95 °C. **IR** (ATR) ν (cm^{-1}) = 2964, 2868, 1760, 1674, 1222, 995, 963, 870. **^{1}H NMR** (300 MHz, $CDCl_3$) δ (ppm) = 5.27 (d, *J* = 9.7 Hz, 1H), 3.00 (dsept, *J* = 9.7 Hz, 6.8 Hz, 1H), 2.12 (s, 3H), 1.10 (d, *J* = 6.8 Hz, 6H). **^{13}C NMR** (75 MHz, $CDCl_3$) δ (ppm) = 165.2 (C=O), 151.3 (C), 147.6 (C), 121.2 (CH), 110.1 (C), 26.2 (CH), 22.6 ($2CH_3$), 11.7 (CH_3). **HRMS** (ESI) calcd. for $C_9H_{12}{}^{81}BrO_2$ $[M + H]^+$: 233.00002; found: 232.99946.

General procedure for Suzuki coupling, conditions A: In a Schlenk tube under argon, boronic acid (1.3 mmol, 1.2 equiv.), sodium

carbonate (1 M in H_2O, 1.3 mL, 1 mmol, 1.2 equiv.) and tetrakis(triphenylphosphine)palladium(0) (100 mg, 0.087 mmol, 10 mol%) were added to a solution of (*Z*)-3-bromo-4-methyl-5-(2-methylpropylidene) furan-2(5*H*)-one (**1**) (250 mg, 1.08 mmol, 1 equiv.) in toluene and ethanol (6:4, 10 mL/6 mL). The resulting mixture was stirred for 8 h at 80 °C, cooled at room temperature and filtered on Celite®. The solvents were removed from the filtrate under the vacuum and water (10 mL) was added to the resulting residue. The aqueous phase was extracted with diethyl ether (3 × 20 mL). The combined organic phases were washed with brine (25 mL), dried over anhydrous $MgSO_4$, filtered and solvents were evaporated under vacuum. The residue was purified by column chromatography on silica gel with petroleum ether/EtOAc as eluent to afford expected compound.

(*Z*)-3-(4-Fluorophenyl)-4-methyl-5-(2-methylpropylidene) furan-2(5*H*)-one (2a): $C_{15}H_{15}FO_2$, MW = 246.28 g/mol, yield = 67%, white solid, mp = 87–89 °C. **IR** (ATR) ν (cm^{-1}) = 2967, 2870, 1743, 1663, 1590, 1508, 1224, 979, 837. **^{1}H NMR** (300 MHz, $CDCl_3$) δ (ppm) = 7.52 (dd, *J* = 8.8 Hz, 5.4 Hz, 2H), 7.14 (t, *J* = 8.8 Hz, 2H), 5.26 (d, *J* = 9.6 Hz, 1H), 3.08 (dsept, *J* = 9.6 Hz, 6.7 Hz, 1H), 2.22 (s, 3H), 1.13 (d, *J* = 6.7 Hz, 6H). **^{19}F NMR** (282 MHz, $CDCl_3$) δ (ppm) = − 112.0. **^{13}C NMR** (75 MHz, $CDCl_3$) δ (ppm) = 169.2 (C═O), 162.8 (d, *J* = 248 Hz, C-F), 148.3 (C), 146.9 (C), 131.0 (d, *J* = 8 Hz, 2CH), 126.2 (d, *J* = 3 Hz, C), 125.6 (C), 120.2 (CH), 115.8 (d, *J* = 22 Hz, 2CH), 26.4 (CH), 22.8 ($2CH_3$), 11.1 (CH_3). **HRMS** (ESI) calcd. for $C_{15}H_{16}FO_2$ $[M + H]^+$: 247.11288; found: 247.11222.

(*Z*)-3-([1,1′-Biphenyl]-4-yl)-4-methyl-5-(2 methylpropylidene) furan-2(5*H*)-one (2b): $C_{21}H_{20}O_2$, MW = 304.39 g/mol, yield = 66%, white paste. **IR** (ATR) ν (cm^{-1}) = 2963, 1760, 1598, 1583, 1572, 1479, 1452, 1383, 1265, 1172, 921, 805, 755, 735, 698. **^{1}H NMR** (300 MHz, $CDCl_3$) δ (ppm) = 7.74–7.72 (m, 1H), 7.62–7.58 (m, 3H), 7.55–7.51 (m, 2H), 7.49–7.43 (m, 2H), 7.36 (m, 1H), 5.27 (d, *J* = 9.6 Hz, 1H), 3.11 (dsept, *J* = 9.6 Hz, 6.8 Hz, 1H), 2.27 (s, 3H), 1.14 (d, *J* = 6.7 Hz, 6H). **^{13}C NMR** (75 MHz, $CDCl_3$) δ (ppm) = 169.2 (C═O), 148.4 (C), 147.3 (C), 141.7 (C), 140.8 (C), 131.5 (C), 126.3 (C), 129.1(CH), 129.0 (2CH), 128.0 (CH), 127.9 (CH), 127.7 (CH), 127.5 (CH), 127.4 (2CH), 120.1 (CH), 26.4 (CH), 22.9 ($2CH_3$), 11.2 (CH_3). **HRMS** (ESI) calcd. for $C_{21}H_{21}O_2$ $[M + H]^+$: 305.15361; found: 305.15286.

(*Z*)-3-(6-Methoxynaphthalen-2-yl)-4-methyl-5-(2-methylpropylidene)furan-2(5*H*)-one (2c): $C_{20}H_{20}O_3$, MW = 308.38 g/mol, yield = 61%, white solid, mp = 144–146 °C. **IR** (ATR) ν (cm^{-1}) = 2964, 1749, 1664, 1628, 1595, 1483, 1217, 988, 880, 809 **^{1}H NMR** (300 MHz, $CDCl_3$) δ (ppm) = 7.96 (d, *J* = 1.4 Hz, 1H), 7.79 (dd, *J* = 8.6 Hz, 3.5 Hz, 2H), 7.61 (dd, *J* = 8.7 Hz, 1.8 Hz, 1H), 7.19–7.13 (m, 2H), 5.26 (d, *J* = 9.6 Hz, 1H), 3.94 (s, 3H), 3.12 (dsept, *J* = 9.6 Hz, 6.8 Hz, 1H), 2.29 (s, 3H), 1.14 (d, *J* = 6.8 Hz, 6H). **^{13}C NMR** (75 MHz, $CDCl_3$) δ (ppm) = 169.5 (C═O), 158.5 (C), 148.5 (C), 146.5 (C), 134.4 (C), 130.1 (CH), 128.7 (C, CH), 127.1 (CH), 126.8 (CH), 126.6 (C), 125.4 (C), 119.6 (CH), 119.4 (CH), 105.7 (CH), 55.5 (CH_3), 26.4 (CH), 22.9 ($2CH_3$), 11.2 (CH_3). **HRMS** (ESI) calcd. for $C_{20}H_{21}O_3$ $[M + H]^+$: 309.14907; found: 309.14832.

(*Z*)-4-Methyl-5-(2-methylpropylidene)-3-(pyridin-4-yl)furan-2(5*H*)-one (2d): $C_{14}H_{15}NO_2$, MW = 229.28 g/mol, yield = 84%, yellow oil. **IR** (ATR) ν (cm^{-1}) = 3054, 2961, 2869, 1754, 1664, 1577, 1437, 1297, 1192, 1119, 1032, 972, 878, 694. **^{1}H NMR** (300 MHz, $CDCl_3$) δ (ppm) = 8.74 (d, *J* = 1.5 Hz, 1H), 8.62 (dd, *J* = 4.9 Hz, 1.4 Hz, 1H), 8.03 (dt, *J* = 8.0 Hz, 1.9 Hz, 1H), 7.45 (ddd, *J* = 8.0 Hz, 4.9 Hz, 0.6 Hz, 1H), 5.35 (d, *J* = 9.6 Hz, 1H), 3.09 (dsept, *J* = 9.6 Hz, 6.8 Hz, 1H), 2.29 (s, 3H), 1.14 (d, *J* = 6.7 Hz, 6H). **^{13}C NMR** (75 MHz, $CDCl_3$) δ (ppm) = 168.7 (C), 149.5 (CH), 149.4 (CH), 148.4 (C), 148.2 (C), 136.6 (CH), 126.5 (C), 123.6 (CH), 123.5 (C), 121.3 (CH), 26.5 (CH), 22.7 ($2CH_3$), 11.2 (CH_3). **HRMS** (ESI) calcd. for $C_{14}H_{16}NO_2$ $[M + H]^+$: 230.11756; found: 230.11699.

(*Z*)-4-Methyl-5-(2-methylpropylidene)-[3,3′-bifuran]-2(5*H*)-one (2e): $C_{13}H_{14}O_3$, MW = 218.25 g/mol, yield = 64%, white solid, mp = 64–66 °C. **IR** (ATR) ν (cm^{-1}) = 3155, 3134, 2958, 2870, 1756, 1669, 1545, 1467, 1304, 1205, 1157, 1021, 964, 931; 830, 800, 740, 644, 601. **^{1}H NMR** (300 MHz, $CDCl_3$) δ (ppm) = 8.07 (bs, 1H), 7.50 (t, *J* = 1.8 Hz, 1H), 6.82 (dd, *J* = 1.8 Hz, 0.8 Hz, 1H), 5.21 (d, *J* = 9.6 Hz, 1H), 3.06 (dsept, *J* = 9.6 Hz, 6.7 Hz, 1H), 2.24 (s, 3H), 1.11 (d, *J* = 6.7 Hz, 6H). **^{13}C NMR** (75 MHz, $CDCl_3$) δ (ppm) = 168.8 (C), 148.6 (C), 143.8 (C), 143.4 (CH), 142.9 (CH), 119.4 (CH), 119.1 (C), 115.8 (C), 108.9 (CH), 26.4 (CH), 22.9 ($2CH_3$), 11.1 (CH_3). **HRMS** (ESI) calcd. for $C_{13}H_{15}O_3$ $[M + H]^+$: 219.10212; found: 219.10100.

(*Z*)-3-(Benzofuran-2-yl)-4-methyl-5-(2-methylpropylidene) furan-2(5*H*)-one (2f): $C_{17}H_{16}O_3$, MW = 268.31 g/mol, yield = 62%, white solid, mp = 87–89 °C. **IR** (ATR) ν (cm^{-1}) = 2961, 2928, 2865, 1750, 1669, 1443, 1297, 1216, 1123, 1037, 995, 925, 824, 751, 659. **^{1}H NMR** (300 MHz, $CDCl_3$) δ (ppm) = 7.63 (dd, *J* = 7.4 Hz, 1.0 Hz, 1H), 7.56 (s, 1H), 7.50 (dd, *J* = 7.4 Hz, 0.8 Hz, 1H), 7.33 (td, *J* = 7.3 Hz, 1.4 Hz, 1H), 7.25 (td, *J* = 7.4 Hz, 1.2 Hz, 1H), 5.36 (d, *J* = 9.7 Hz, 1H), 3.09 (dsept, *J* = 9.6 Hz, 6.7 Hz, 1H), 2.55 (s, 3H), 1.14 (d, *J* = 6.7 Hz, 6H). **^{13}C NMR** (75 MHz, $CDCl_3$) δ (ppm) = 167.3 (C═O), 155.0 (C), 148.7 (C), 148.6 (C), 145.2 (C), 128.2 (C), 125.5 (CH), 123.4 (CH), 122.0 (CH), 121.3 (CH), 116.7 (C), 111.2 (CH), 108.4 (CH), 26.6 (CH), 22.8 ($2CH_3$), 11.4 (CH_3). **HRMS** (ESI) calcd. for $C_{17}H_{17}O_3$ $[M + H]^+$: 269.11722; found: 269.11698.

*4.1.3. Preparation of new oxazinoindoles **11a** and **11c***

Aryl iodide (260 mg, 0.6 mmol), alkyne (0.9 mmol), triphenylphosphine (15 mg, 10% mol), CuI (11 mg, 10% mol), and triethylamine (120 µl, 0.9 mmol) were combined with DMF (4.0 mL) in schlenk sealing tube. The resulting reaction mixture was stirred under argon for overnight at room temperature or for 2 h on MW at 50 °C. The solvent was removed from the reaction mixture under the vacuum and the resulting crude product was purified by flash chromatography on silica gel (petroleum ether/AcOEt = 100:0 to 50:50).

(*E*)-7-(10-Iodo-8-methoxy-1-oxo-1*H*-[1,4]oxazino[4,3-*a*]indol-3(4*H*)-ylidene)hept-5-ynoic acid (11a): $C_{19}H_{16}INO_5$, MW = 465.24 g/mol, yield = 12%, yellow solid, mp = 177–179 °C. **IR** (ATR) ν (cm^{-1}) = 3050, 2891, 1744, 1696, 1645, 1508, 1412, 1378, 1308, 1227, 1194, 1076, 922, 737. **^{1}H NMR** (300 MHz, $CDCl_3$) δ (ppm) = 7.62 (d, *J* = 8.2 Hz, 1H), 7.50 (dd, *J* = 6.8 Hz, 1.0 Hz, 1H), 7.42 (d, *J* = 8.4 Hz, 1H), 7.31 (dd, *J* = 6.8 Hz, 1.0 Hz, 1H), 5.65 (m, 1H), 5.15 (d, *J* = 0.8 Hz, 2H), 2.59–2.51 (m, 4H), 1.95 (quint, *J* = 6.9 Hz, 2H). **^{13}C NMR** (75 MHz, $CDCl_3$) δ (ppm) = 177.4 (C), 154.3 (C), 151.4 (C), 136.9 (C), 131.3 (C), 130.0 (CH), 124.3 (CH), 122.9 (CH), 121.0 (C), 110.6 (CH), 97.1 (C), 96.0 (CH), 74.3 (C), 69.4 (C), 40.8 (CH_2), 32.7 (CH_2), 23.6 (CH_2), 19.2 (CH_2). **HRMS** (ESI) calcd. For $C_{18}H_{15}INO_4$ $[M + H]^+$: 436.0046, found 436.0034.

(*E*)-7-(10-Iodo-1-oxo-1*H*-[1,4]oxazino[4,3-*a*]indol-3(4*H*)-ylidene)hept-5-ynoic acid (11c): $C_{18}H_{14}INO_4$, MW = 435.00 g/mol, yield = 14%, yellow solid, mp = 157–159 °C. **IR** (ATR) ν (cm^{-1}) = 3066, 2929, 1741, 1705, 1638, 1510, 1433, 1313, 1281, 1236, 1195, 1080, 953, 917, 834, 809, 739. **^{1}H NMR** (300 MHz, $CDCl_3$) δ (ppm) = 7.30 (d, *J* = 9.1 Hz, 1H), 7.12 (dd, *J* = 9.1 Hz, 2.4 Hz, 1H), 6.89 (d, *J* = 2.3 Hz, 1H), 5.67–5.64 (m, 1H), 5.11 (d, *J* = 1.0 Hz, 2H), 3.90 (s, 3H), 2.59–2.51 (m, 4H), 1.95 (quint, *J* = 7.0 Hz, 2H). **^{13}C NMR** (75 MHz, $CDCl_3$) δ (ppm) = 177.3 (C), 156.4 (C), 154.2 (C), 151.5 (C), 132.2 (C), 131.8 (C), 120.9 (CH), 120.4 (CH), 111.7 (CH), 103.2 (CH), 97.0 (C), 95.8 (CH), 74.4 (C), 68.2 (C), 55.9 (CH_3), 40.9 (CH_2), 32.6 (CH_2), 23.6 (CH_2), 19.2 (CH_2). **HRMS** (ESI) calcd. For $C_{18}H_{15}INO_4$ $[M + H]^+$: 436.00403, found: 436.0034.

4.2. Docking

Molecular docking studies were carried out using GOLD v 5.3.[24] GOLD is based on a genetic algorithm and allows to perform docking of flexible ligands inside proteins with partial flexibility in the

neighborhood of the active site. The crystal structure used as macromolecular receptor was *Mt* UGM in closed form with the substrate bound (PDB code: 4RPG). Prior to docking calculation, water molecules and the bound substrate UDP-Gal*p* were removed from the crystal structure. The inhibitors docked conformations were obtained using the score function ChemPLP.[25] Examination of the structures of the complex were carried out using PyMOL software.

4.3. Mt UGM inhibitory activity

UGM preparation: A vector construct (pET-29b) containing the gene encoding for UGM from *Mt* was provided by Prof. Laura L. Kiessling. The overexpression and UGM purification followed our previously published procedure.[12]

HPLC assay: Inhibition of UGM was performed following the procedure already described by Liu et al.[26] as well as by our group.[27] All assays were performed at room temperature using a phosphate buffer (NaH_2PO_4 100 mM, pH 7.4), and fresh solutions of sodium dithionite which provide reductive conditions. The activity of the enzyme (in the presence and in the absence of an inhibitor) is evaluated by measuring the conversion of UDP-α-Gal*f* into UDP-α-Gal*p*. The enzyme (60 nM *Mt* UGM) in phosphate buffer was first pre-incubated for 5 min, then reduced with sodium dithionite (final concentration 12.5 mM) and incubated for specific time at room temperature, in absence and presence of inhibitor. The substrate UDP-α-Gal*f* (final concentration 25 μM) was added and allowed the reaction to proceed at five different times. The reaction was stopped by quenching the samples with liquid N_2. The conversion of UDP-α-Gal*f* into UDP-α-Gal*p* was monitored by HPLC (Waters 600 E with a C_{18} Atlantis T3 column, 5 μM 4.6 × 250 mm, elution with 50 mM triethylamine acetic acid pH 6.8, 0.5% CH_3CN; UV detection at 262 nm and flow rate 1 mL/min).

FP assay. The assay described by Kiessling *et al.* was strictly followed, including the synthesis of the fluorescent probe (UDP-fluorescein).[16] To determine the binding affinity of UDP-fluorescein towards *Mt* UGM, serial dilutions of dialyzed UGM (final concentration: 1×10^{-5} to 10 μM) were incubated with 18 nM of the fluorescent probe in 50 mM sodium phosphate buffer, pH 7.0 at room temperature. Final volumes were 30 μl in 384 well black microtiter plates and the measurements were realized in triplicate. Fluorescence polarization was analyzed using DTX880 Multimode Detector Beckman-Coulter device ($\lambda_{excitation}$ = 485 nm, $\lambda_{emission}$ = 535 nm).

4.4. In vitro anti-tubercular activity

Antitubercular evaluations were performed against the avirulent, pantothenate-auxotrophic *Mt* mc^26230 strain[28] cultured in 7H9 (Middlebrook) broth supplemented with oleic-albumin-dextrose-catalase enrichment (OADC) and 109 μM pantothenic acid (complete 7H9 medium) at 37 °C without agitation. MIC determination was done using the broth dilution method. Briefly, a log-phase (OD_{600} ~ 1) culture was diluted to an OD_{600} = 0.05 in complete 7H9 medium and deposited in all the wells of a 96 well microtiter plate (for the first row 200 μl/well, for all other rows 100 μl/well). The tested compounds were then directly added (2 μl per well of a 10 mg/ml stock solution) to the first row wells. Serial 2-fold dilutions were then done starting from the first row. As a measure to minimize evaporation of media, plates were wrapped in plastic. They were then placed in a 37 °C incubator and observed after 7 days. Control wells included a control for the vehicle that compounds were dissolved in (DMSO), in which bacterial growth was not inhibited (as for untreated wells) and wells containing a drug with known antitubercular activity (INH), in which bacterial growth was inhibited at ~30 ng/ml in line with the reported MIC of this drug.[29] The MIC was defined as the lowest concentration of compound at which no visible bacterial growth (change in turbidity) was observed.

Declaration of Competing Interest

The authors declare that they have no known competing financial interests or personal relationships that could have appeared to influence the work reported in this paper.

Acknowledgments

This study was supported by the Fondation pour la Recherche Médicale (grant DEQ20150331719 to L.K.), the Association Gregory Lemarchal and Vaincre la Mucoviscidose (grant RIF20180502320 to C.R.) The University of Namur (PhD grant to SV) and China Scholarship Council (PhD grant to JF). We acknowledge the French Ministry for Research and Innovation for the financial support and Dr. Frédéric Montigny (Analysis Department, Tours University) for HRMS.

Appendix A. Supplementary data

Supplementary data to this article can be found online at https://doi.org/10.1016/j.bmc.2020.115579.

References

1. "Antibacterial agents in clinical development. An analysis of the antibacterial clinical development pipeline, including tuberculosis", September 2017, World Health Organization.
2. Koul A, Arnoult E, Lounis N, Guillemont J, Andries K. *Nature.* 2011;469:483–490.
3. Brennan PJ. *Tuberculosis (Edinb).* 2003;83:91–97.
4. (a) Karakousis PC, Bishai WR, Dorman SE. *Cell Microbiol.* 2004;6:105–116
   (b) Ruhl CR, Pasko BL, Khan HS, et al. *Cell.* 2020;181:1–13.
5. (a) Guerardel Y, Maes E, Elass E, et al. *J Biol Chem.* 2002;277:30635–30648
   (b) Vignal C, Guérardel Y, Kremer L, et al. *J Immunol.* 2003;171:2014–2023
   (c) Briken V, Porcelli SA, Besra GS, Kremer L. *Mol Microbiol.* 2004;53:391–403
   (d) Birch HL, Alderwick LJ, Appelmelk BJ, et al. *Proc Natl Acad Sci USA.* 2010;107:2634–2639.
6. (a) Brennan PJ, Crick DC. *Curr Top Med Chem.* 2007;7:475–488
   (b) Nzila A, Ma Z, Chibale K. *Future Med Chem.* 2011;3:1413–1426.
7. (a) Makarov V, Manina G, Mikusova K, et al. *Science.* 2009;324:801–804
   (b) Christophe T, Jackson M, Jeon HK, et al. *PLoS Pathog.* 2009;5:e1000645.
8. (a) Kremer L, Dover LG, Morehouse C, et al. *J Biol Chem.* 2001;276:26430–26440
   (b) Richards MR, Lowary TL. *ChemBioChem.* 2009;10:1920–1938
   (c) Eppe G, El Bkasiny S, Vincent SP. Galactofuranose biosynthesis: discovery, mechanisms and therapeutic relevance. In: Jimenés-Barbeo J, Cañada FJ, Martin-Santamaria S, eds. *Carbohydrates in Drug Design and Discovery.* RSC; 2015:209–241.
9. (a) Sanders DAR, Staines AG, McMahon SA, McNeil MR, Whitfield C, Naismith JH. *Nat Struct Biol.* 2001;8:858–863
   (b) Konyariková Z, Savková K, Kozmo S, Mikušová K. *Antibiotics.* 2020;9:20.
10. (a) van Straaten KE, Kuttiyatveetil JRA, Sevrain CM, et al. *J Am Chem Soc.* 2015;137:1230–1244
    (b) Errey JC, Mann MC, Fairhurst SA, et al. *Org Biomol Chem.* 2009;7:1009–1016
    (c) Yuan Y, Bleile DW, Wen X, et al. *J Am Chem Soc.* 2008;130:3157–3168
    (d) El Bkassiny S, N'Go I, Sevrain CM, Tikad A, Vincent SP. *Org Lett.* 2014;16:2462–2465
    (e) N'Go I, Golten S, Ana Ardá J, et al. *Chem Eur J.* 2014;20:106–112
    (f) Dumitrescu L, Eppe G, Tikad A, et al. *Chem Eur J.* 2014;20:15208–15215
    (g) Caravano A, Vincent SP. *Eur J Org Chem.* 2009:1771–1780
    (h) Dhatwalia R, Singh H, Solano LM, et al. *J Am Chem Soc.* 2012;134:18132–18138.
11. Kincaid VA, London N, Wangkanont K, et al. *ACS Chem Biol.* 2015;10:2209–2218 and cited references.
12. Villaume SA, Fu J, N'Go I, et al. *Chem Eur J.* 2017:10423–10429.
13. Fu J, Fu H, Dieu M, et al. *Chem Commun.* 2017;53:10632–10635.
14. Kiessling LL, Winton VJ, Justen AM. *US Pat Appl Publ.* 2017 US 20170258805 A1 20170914.
15. Dykhuizen EC, May JF, Tongpenyai A, Kiessling LL. *J Am Chem Soc.* 2008;130:6706–6707.
16. Carlson EE, May JF, Kiessling LL. *Chem Biol.* 2006;13:825–837.
17. Kuhnt D, Anke T, Besl H, et al. *J Antibiot.* 1990;43:1413–1420.
18. (a) Miao S, Andersen RJ. *J Org Chem.* 1991;56:6275–6280
    (b) Kotora M, Negishi E. *Synthesis.* 1997:121–128

(c) Gallo GG, Coronelli C, Vigevani A, Lancini GC. *Tetrahedron.* 1969;25:5677–5680.
19. (a) Liu F, Negishi E. *J Org Chem.* 1997;62:8591–8594
(b) Von der Ohe F, Brückner R. *Tetrahedron Lett.* 1998;39:1909–1910.
20. Inack-Ngi S, Rahmani R, Commeiras L, et al. *Adv Synth Catal.* 2009;351:779–788.
21. Thanikachalam PV, Maurya RK, Garg V, Monga V. *Eur J Med Chem.* 2019;180:562–612.
22. Hammoud S, Anselmi E, Cherry K, Kizirian J-C, Thibonnet J. *Eur J Org Chem.* 2018:6314–6327.
23. Winton VJ, Aldrich C, Kiessling LL. *ACS Infect Dis.* 2016;2:538–543.
24. Verdonk ML, Cole JC, Hartshorn MJ, Murray CW, Taylor RD. *Prot Struct Func Bioinform.* 2003;52:609–623.
25. Liebeschuetz J, Cole J, Korb O. *J Comput Aided Mol Des.* 2012;26:737–748.
26. Itoh K, Huang Z, Liu H-W. *Org Lett.* 2007;9:879–882.
27. (a) Eppe G, Peltier P, Daniellou R, Nugier-Chauvin C, Ferrières V, Vincent SP. *Bioorg Med Chem Lett.* 2009;19:814–816
(b) Ansiaux C, N'Go I, Vincent SP. *Chem Eur J.* 2012;18:14860–14866.
28. Sambandamurthy VK, Derrick SC, Tsungda Hsu B, et al. *Vaccine.* 2006;24:6309–6320.
29. Kremer L, Douglas JD, Baulard AR, et al. *J Biol Chem.* 2000;275:16857–16864.

Synthesis and evaluation of heterocycle structures as potential inhibitors of *Mycobacterium tuberculosis* UGM

Carine Maaliki[a], Jian Fu[b], Sydney Villaume[b], Albertus Viljoen[c], Clément Raynaud[c], Sokaina Hammoud[a], Jérôme Thibonnet[a], Laurent Kremer[c,d], Stéphane P. Vincent[b], Emilie Thiery[a,*]

[a] *Laboratoire Synthèse et Isolement de Molécules Bioactives (SIMBA, EA 7502), Université de Tours, Faculté de Pharmacie, Parc de Grandmont, 31 Avenue Monge, 37200 Tours, France*

[b] *Department of Chemistry, University of Namur, Rue de Bruxelles 61, 5000 Namur, Belgium*

[c] *Institut de Recherche en Infectiologie de Montpellier (IRIM), CNRS UMR 9004, Université de Montpellier, 34293 Montpellier, France*

[d] *INSERM, IRIM, 34293 Montpellier France*

Supplementary Material

Table of Contents

* Corresponding author. e-mail: emilie.thiery@univ-tours.fr

1. The ^{1}HNMR and ^{13}CNMR spectra

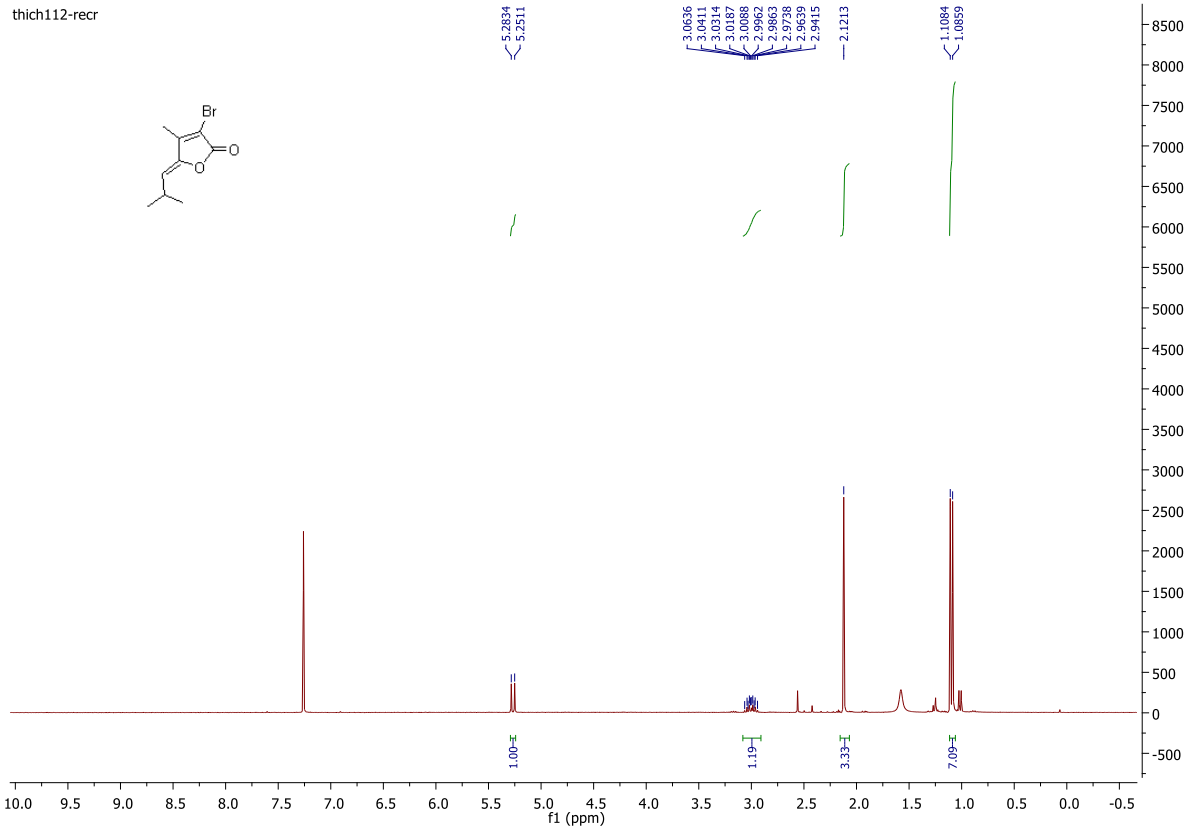

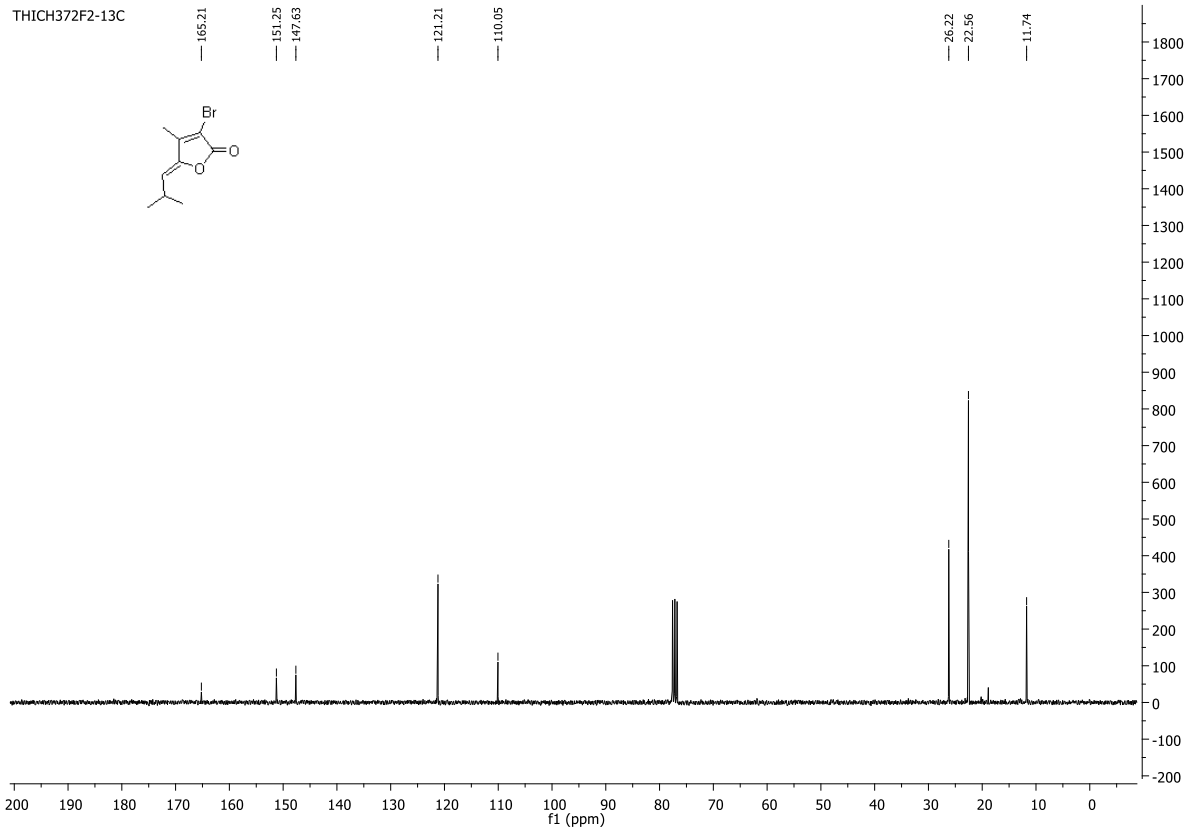

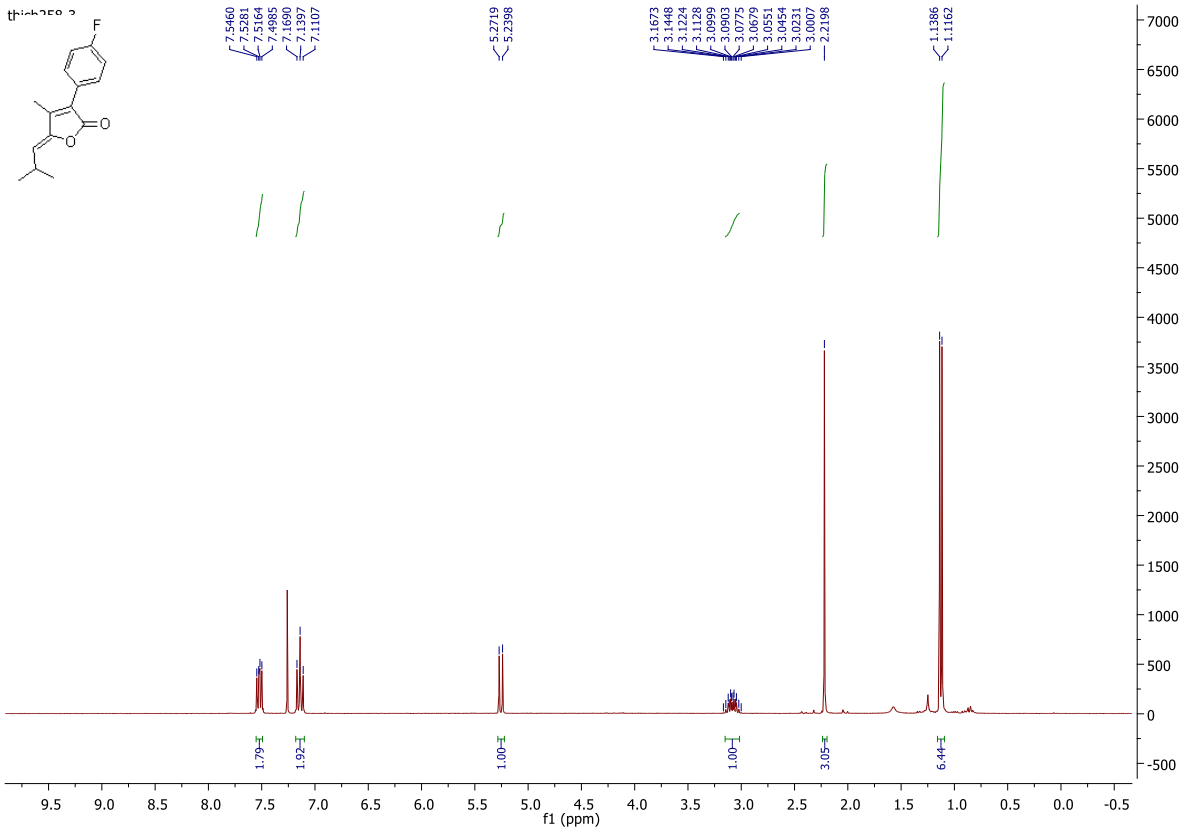
7.5460
7.5281
7.5164
7.4985
7.1690
7.1397
7.1107
5.2719
5.2398
3.1673
3.1448
3.1224
3.1128
3.0999
3.0903
3.0775
3.0679
3.0551
3.0454
3.0231
3.0007
2.2198
1.1386
1.1162
1.79
1.92
1.00
1.00
3.05
6.44
f1 (ppm)

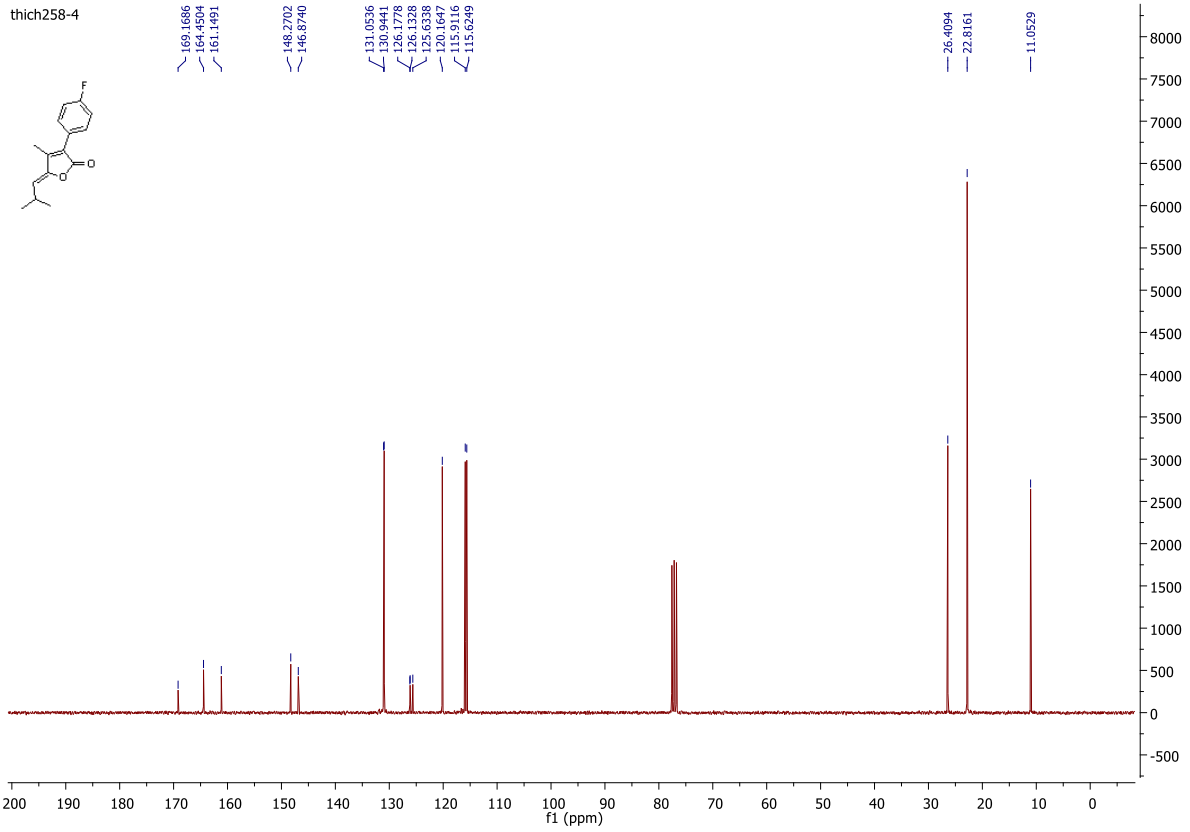
thich258-4
169.1686
164.4504
161.1491
148.2702
146.8740
131.0536
130.9441
126.1778
126.1328
125.6338
120.1647
115.9116
115.6249
26.4094
22.8161
11.0529
f1 (ppm)

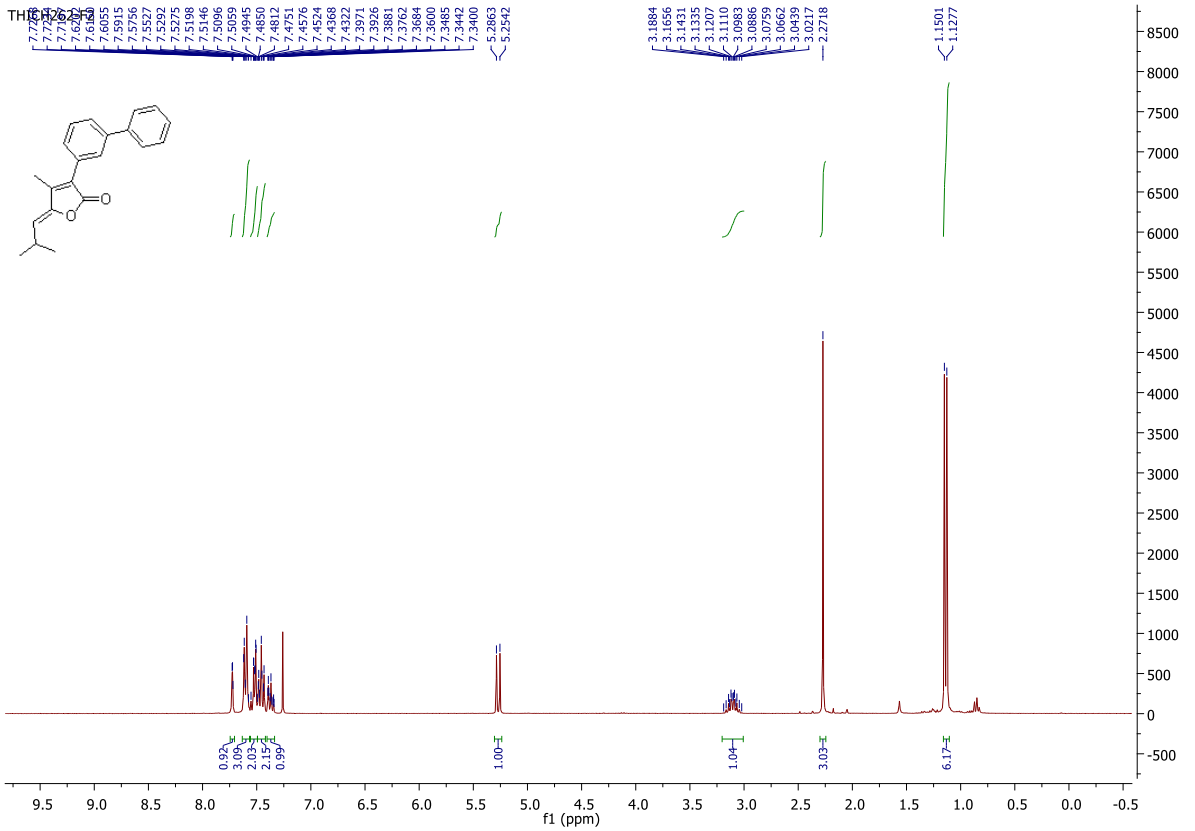
f1 (ppm)

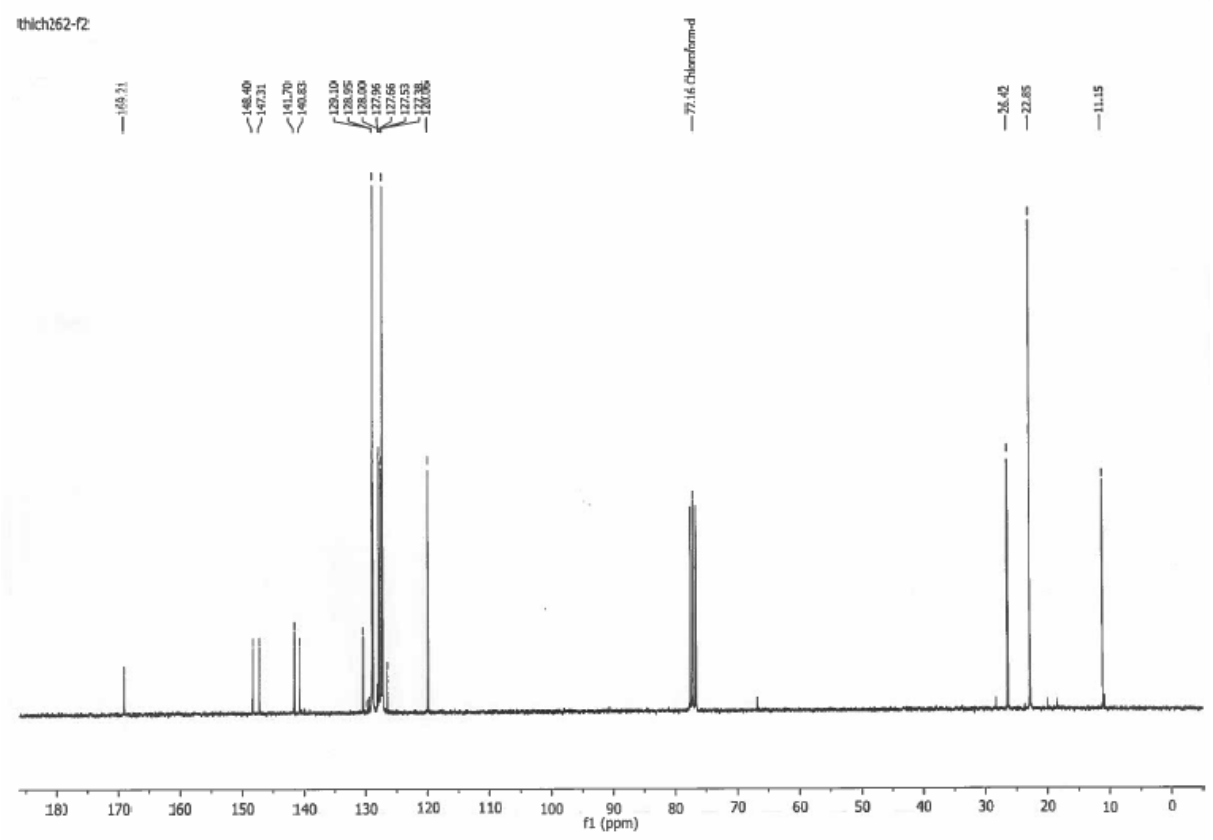
thich262-f2
f1 (ppm)

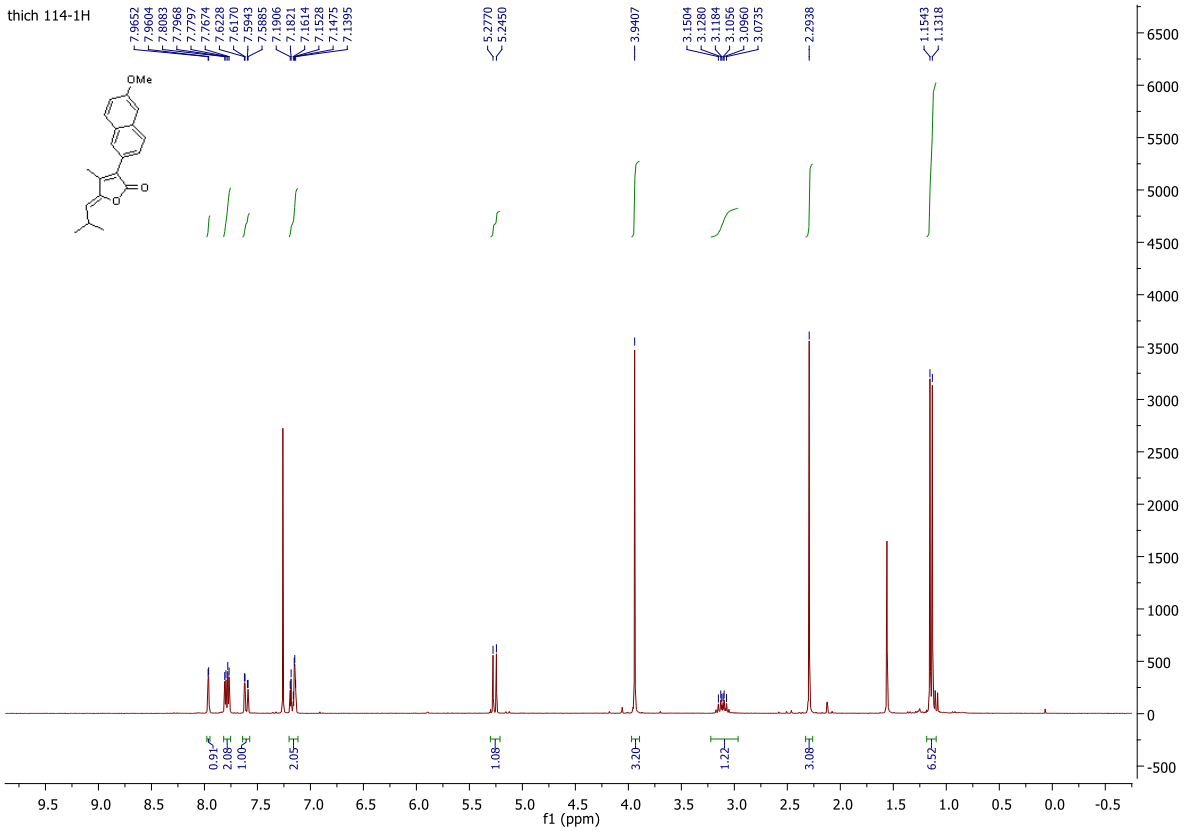
thich 114-1H
7.9652
7.9604
7.8083
7.7968
7.7797
7.7674
7.6228
7.6170
7.5943
7.5885
7.1906
7.1821
7.1614
7.1528
7.1475
7.1395
5.2770
5.2450
3.9407
3.1504
3.1280
3.1184
3.1056
3.0960
3.0735
2.2938
1.1543
1.1318
OMe
O
O
0.91
2.08
1.00
2.05
1.08
3.20
1.22
3.08
6.52
f1 (ppm)

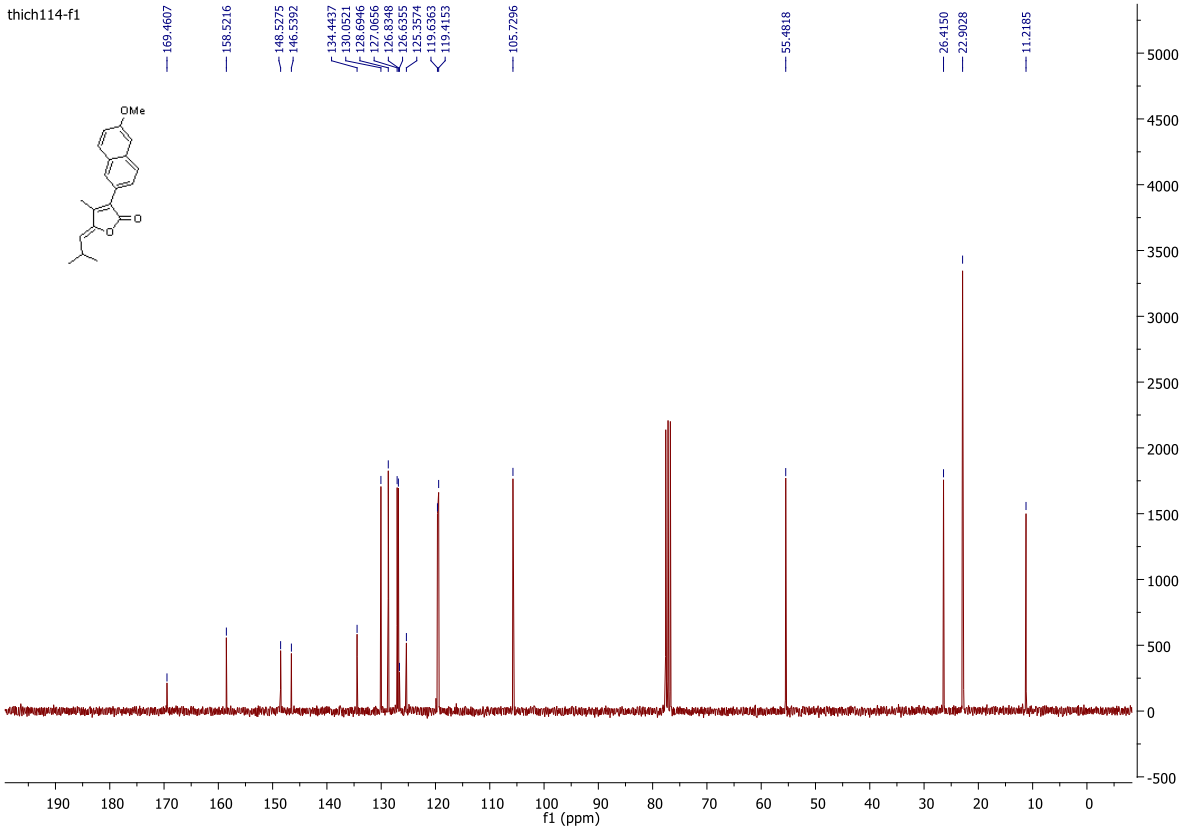
thich114-f1
169.4607
158.5216
148.5275
146.5392
134.4437
130.0521
128.6946
127.0656
126.8348
126.6355
125.3574
119.6363
119.4153
105.7296
55.4818
26.4150
22.9028
11.2185
OMe
O
O
f1 (ppm)

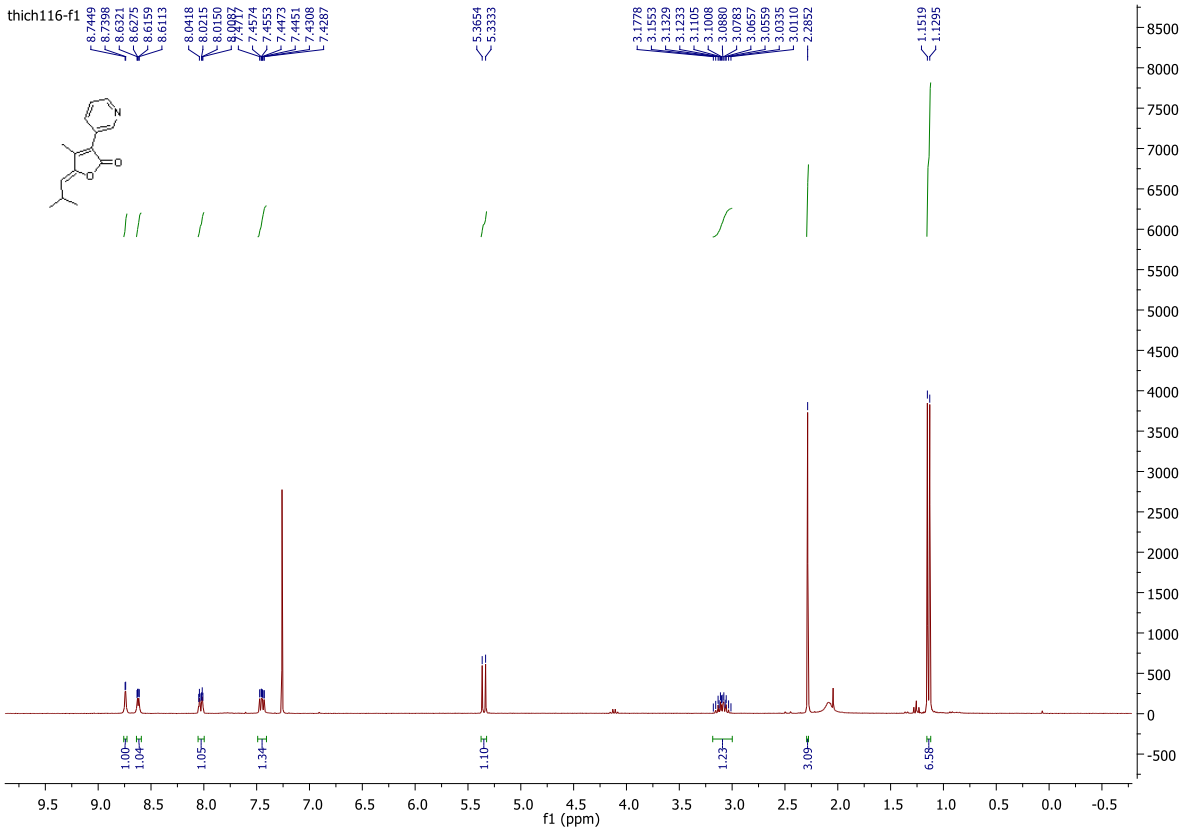
thich116-f1
8.7449
8.7398
8.6321
8.6275
8.6159
8.6113
8.0418
8.0215
8.0150
7.4574
7.4553
7.4473
7.4451
7.4308
7.4287
5.3654
5.3333
3.1778
3.1553
3.1329
3.1233
3.1105
3.1008
3.0880
3.0783
3.0657
3.0559
3.0335
3.0110
2.2852
1.1519
1.1295
1.00
1.04
1.05
1.34
1.10
1.23
3.09
6.58
f1 (ppm)

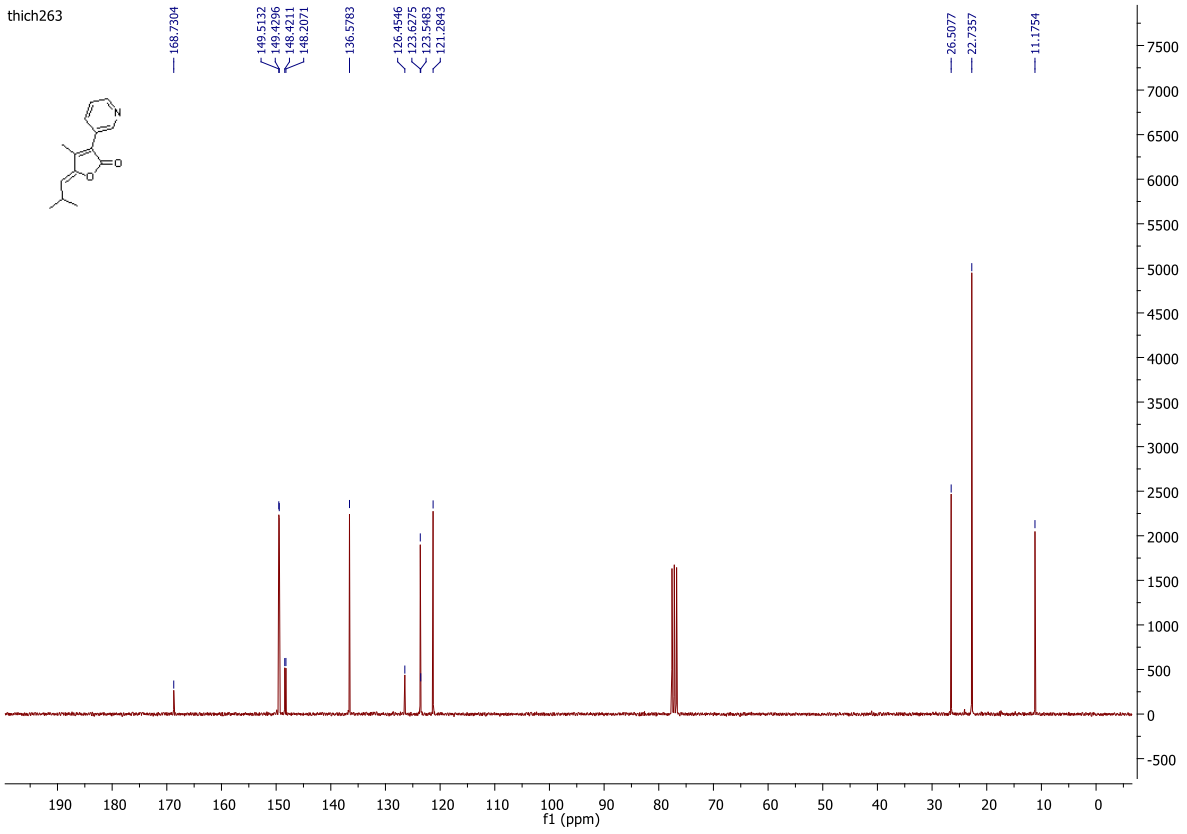
thich263
168.7304
149.5132
149.4296
148.4211
148.2071
136.5783
126.4546
123.6275
123.5483
121.2843
26.5077
22.7357
11.1754
f1 (ppm)

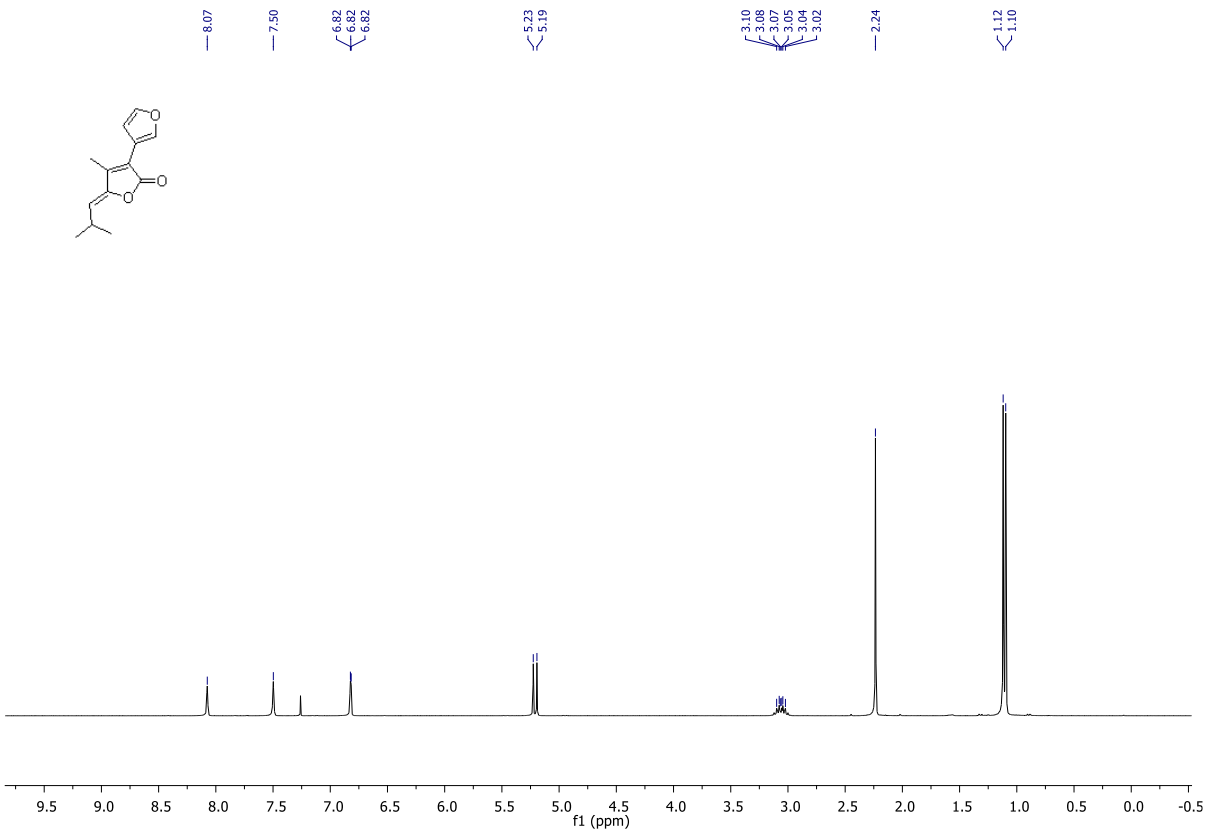
8.07
7.50
6.82
6.82
6.82
5.23
5.19
3.10
3.08
3.07
3.05
3.04
3.02
2.24
1.12
1.10
f1 (ppm)

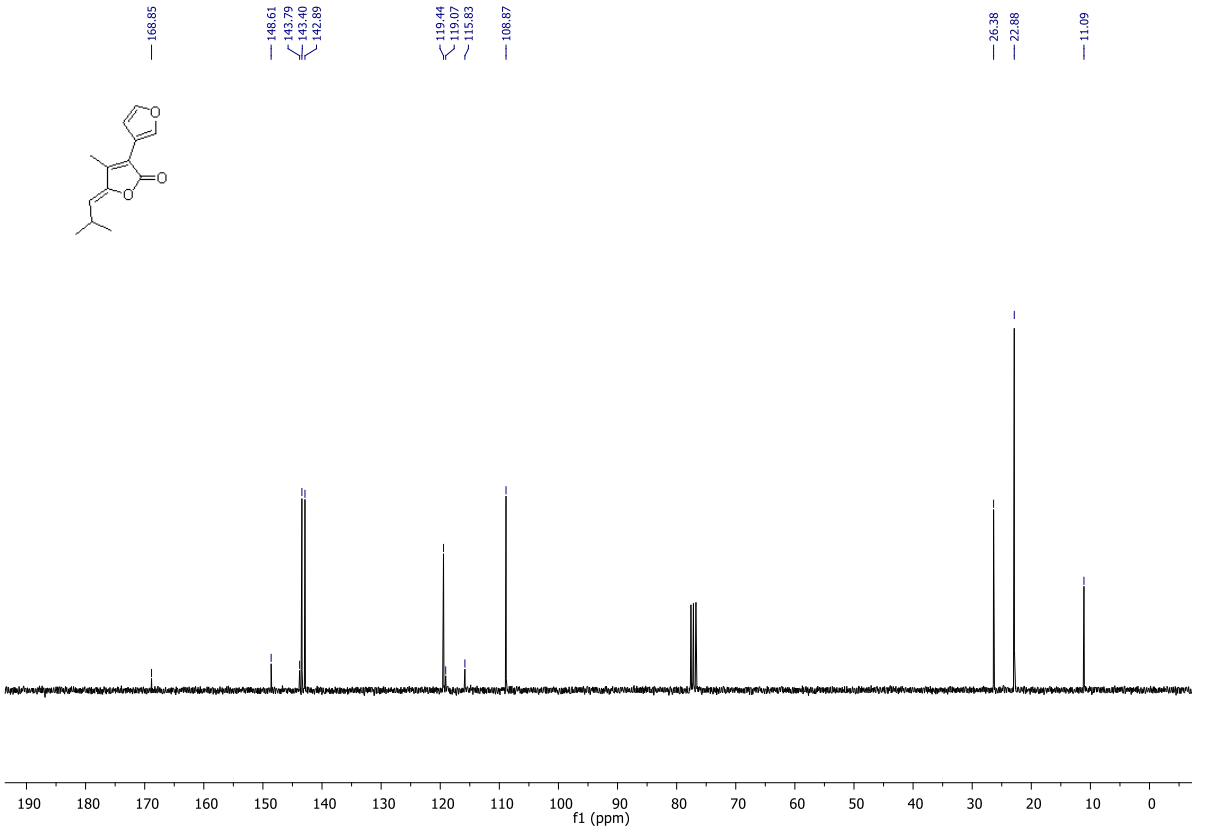
168.85
148.61
143.79
143.40
142.89
119.44
119.07
115.83
108.87
26.38
22.88
11.09
f1 (ppm)

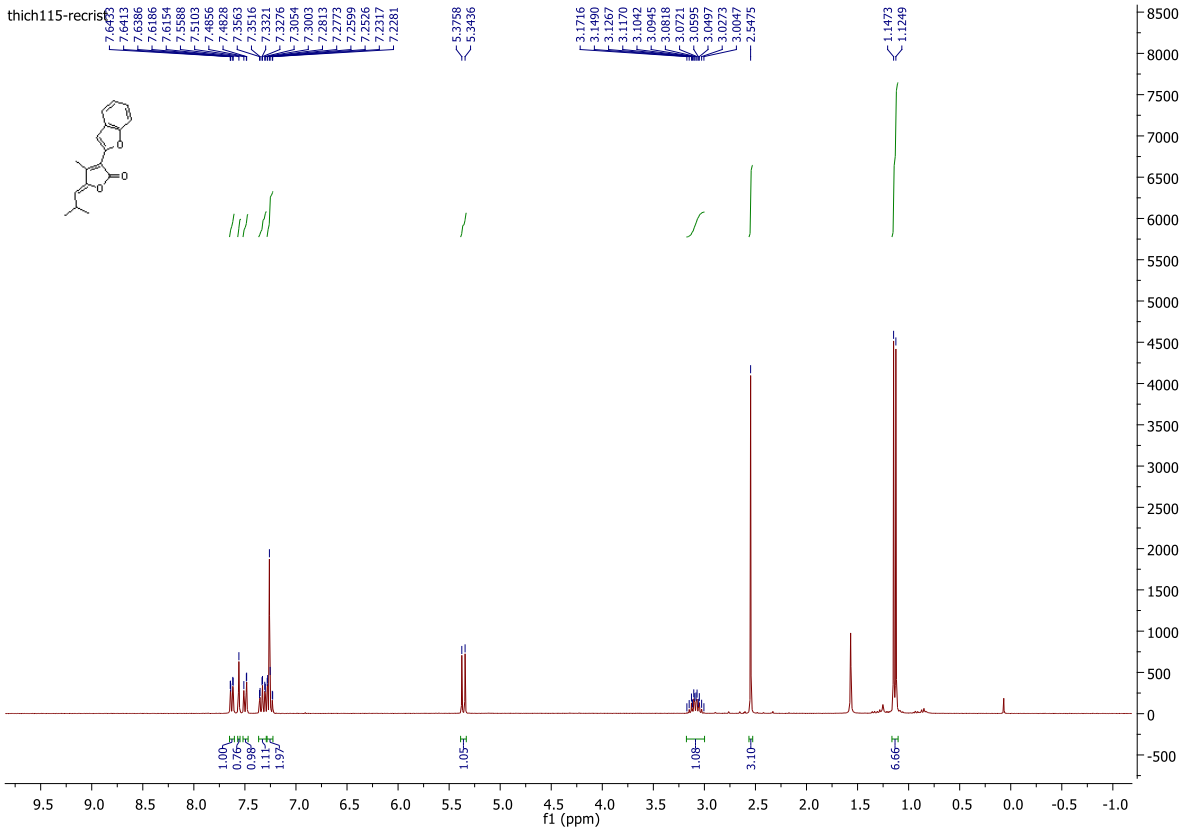
thich115-recris
7.6433
7.6413
7.6386
7.6186
7.6154
7.5588
7.5103
7.4856
7.4828
7.3563
7.3516
7.3321
7.3276
7.3054
7.3003
7.2813
7.2773
7.2599
7.2526
7.2317
7.2281
5.3758
5.3436
3.1716
3.1490
3.1267
3.1170
3.1042
3.0945
3.0818
3.0721
3.0595
3.0497
3.0273
3.0047
2.5475
1.1473
1.1249
1.00
0.76
0.98
1.11
1.97
1.05
1.08
3.10
6.66
f1 (ppm)

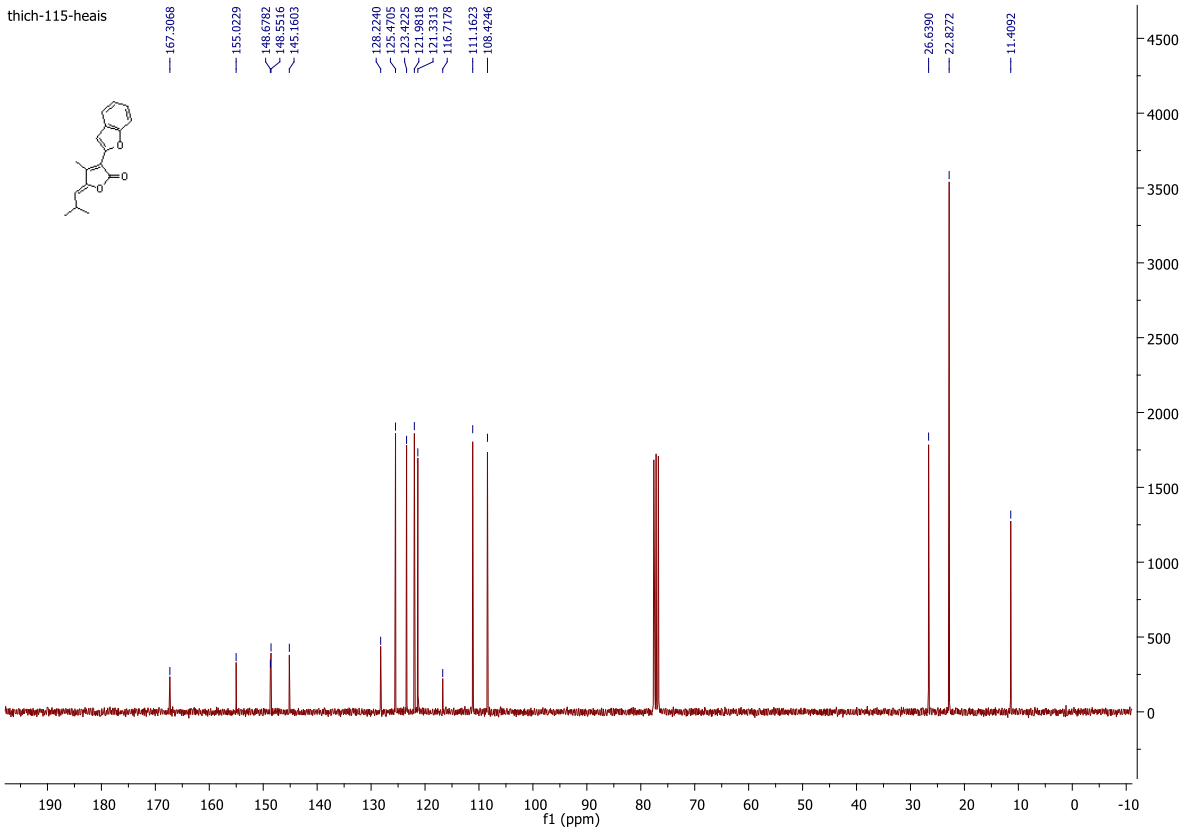
thich-115-heais
167.3068
155.0229
148.6782
148.5516
145.1603
128.2240
125.4705
123.4225
121.9818
121.3313
116.7178
111.1623
108.4246
26.6390
22.8272
11.4092
f1 (ppm)

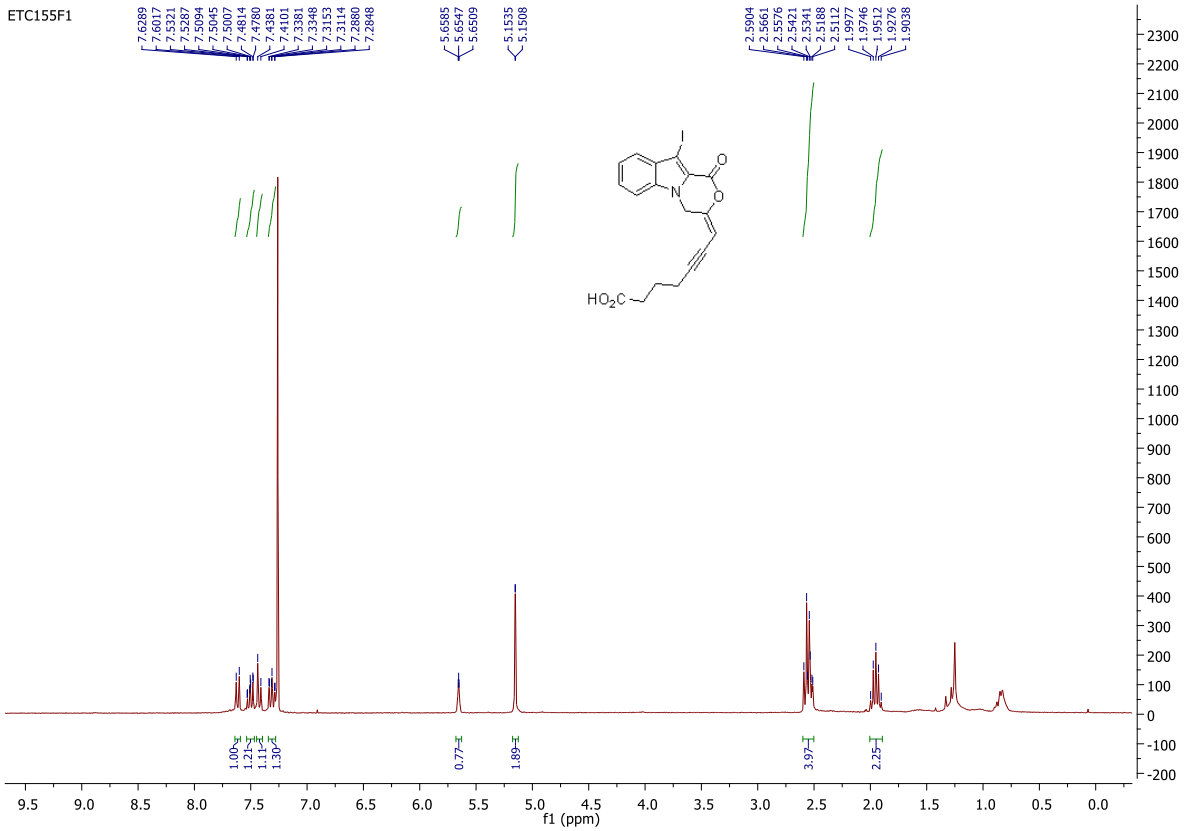
ETC155F1
7.6289
7.6017
7.5321
7.5287
7.5094
7.5045
7.5007
7.4814
7.4780
7.4381
7.4101
7.3381
7.3348
7.3153
7.3114
7.2880
7.2848
5.6585
5.6547
5.6509
5.1535
5.1508
2.5904
2.5661
2.5576
2.5421
2.5341
2.5188
2.5112
1.9977
1.9746
1.9512
1.9276
1.9038
1.00
1.21
1.11
1.30
0.77
1.89
3.97
2.25
f1 (ppm)

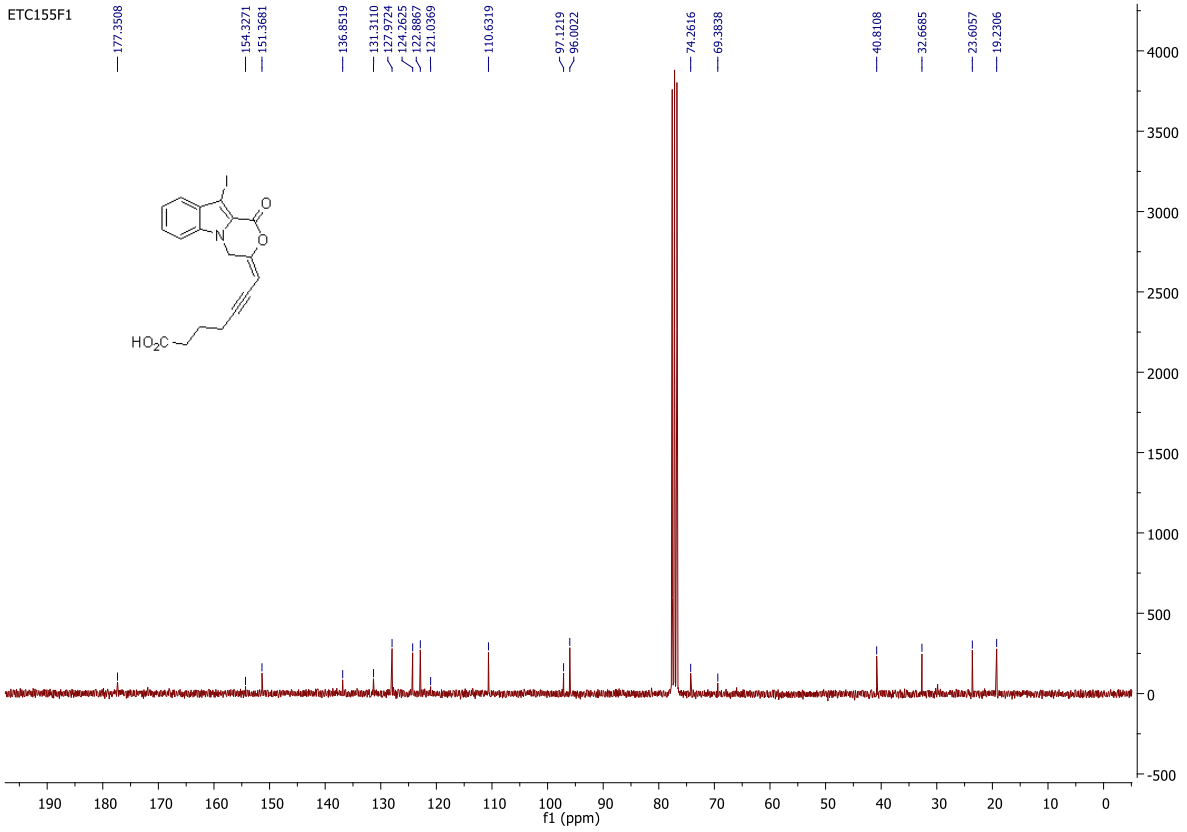
ETC155F1
177.3508
154.3271
151.3681
136.8519
131.3110
127.9724
124.2625
122.8867
121.0369
110.6319
97.1219
96.0022
74.2616
69.3838
40.8108
32.6685
23.6057
19.2306
f1 (ppm)

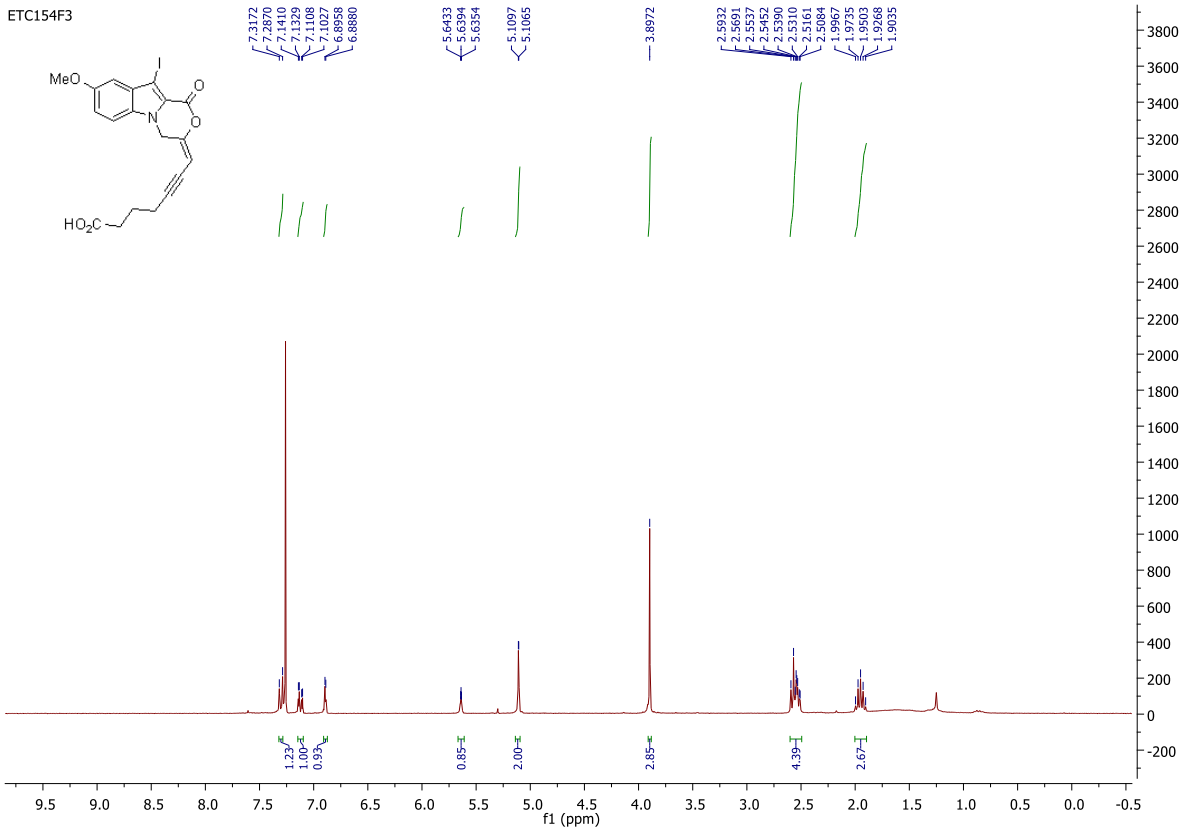
ETC154F3
7.3172
7.2870
7.1410
7.1329
7.1108
7.1027
6.8958
6.8880
5.6433
5.6394
5.6354
5.1097
5.1065
3.8972
2.5932
2.5691
2.5537
2.5452
2.5390
2.5310
2.5161
2.5084
1.9967
1.9735
1.9503
1.9268
1.9035
MeO
I
O
N
O
HO2C
1.23
1.00
0.93
0.85
2.00
2.85
4.39
2.67
f1 (ppm)

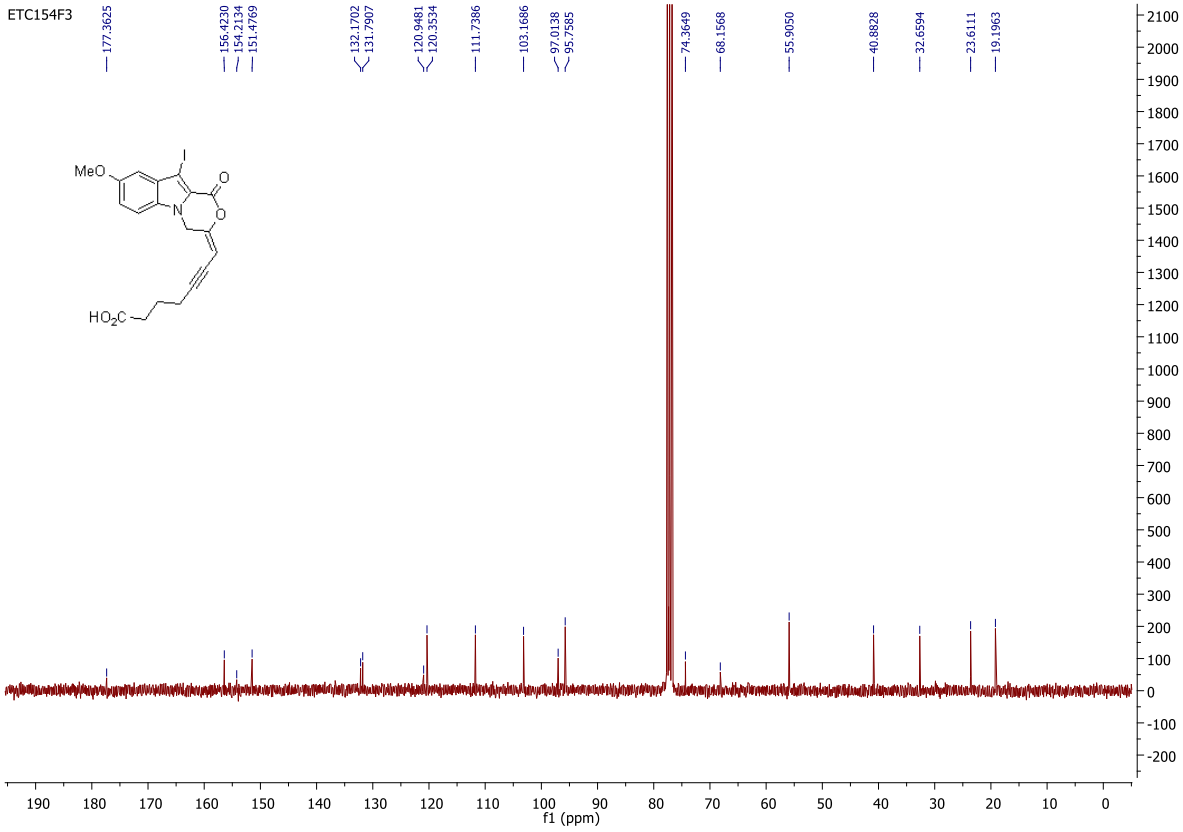
ETC154F3
177.3625
156.4230
154.2134
151.4769
132.1702
131.7907
120.9481
120.3534
111.7386
103.1686
97.0138
95.7585
74.3649
68.1568
55.9050
40.8828
32.6594
23.6111
19.1963
MeO
I
O
N
O
HO2C
f1 (ppm)

2. Docking poses for molecules 10a, 10b and 11a

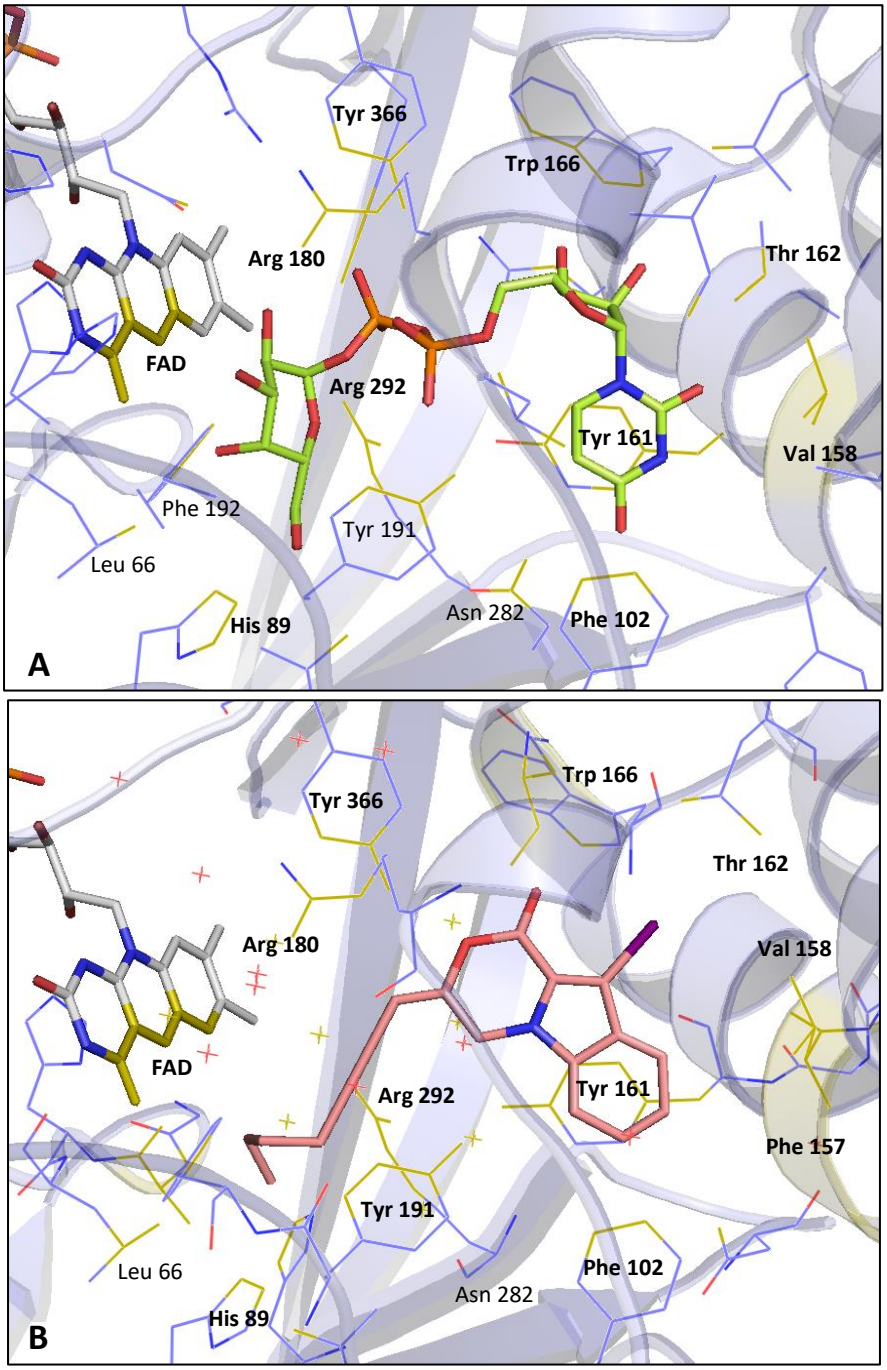

Figure SI-1 : Crystallized UDP Gal*p* (**A**) and docked **10a** (**B**) in *Mt* UGM closed form (yellow atoms are at a distance <4 Å).

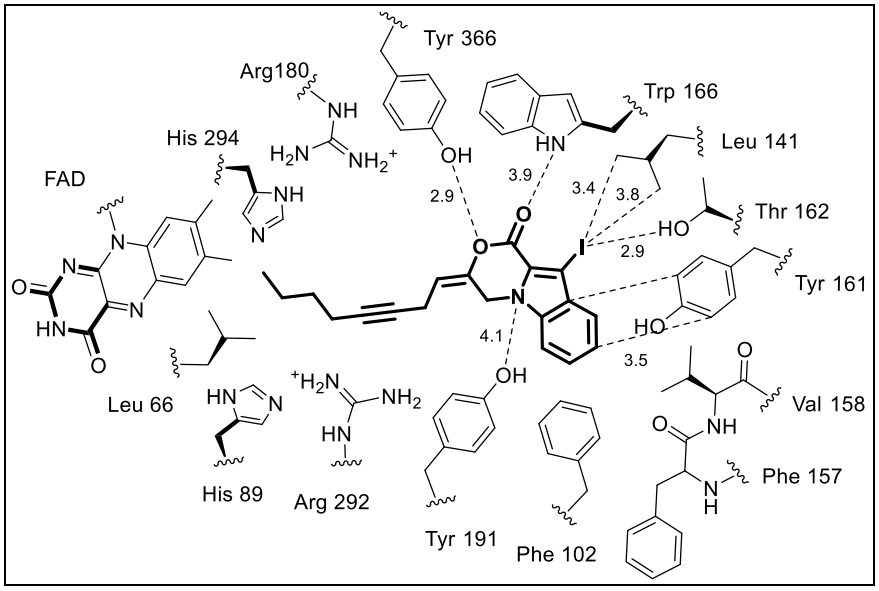

Figure SI-2: Interactions of **10a** with *Mt* UGM.

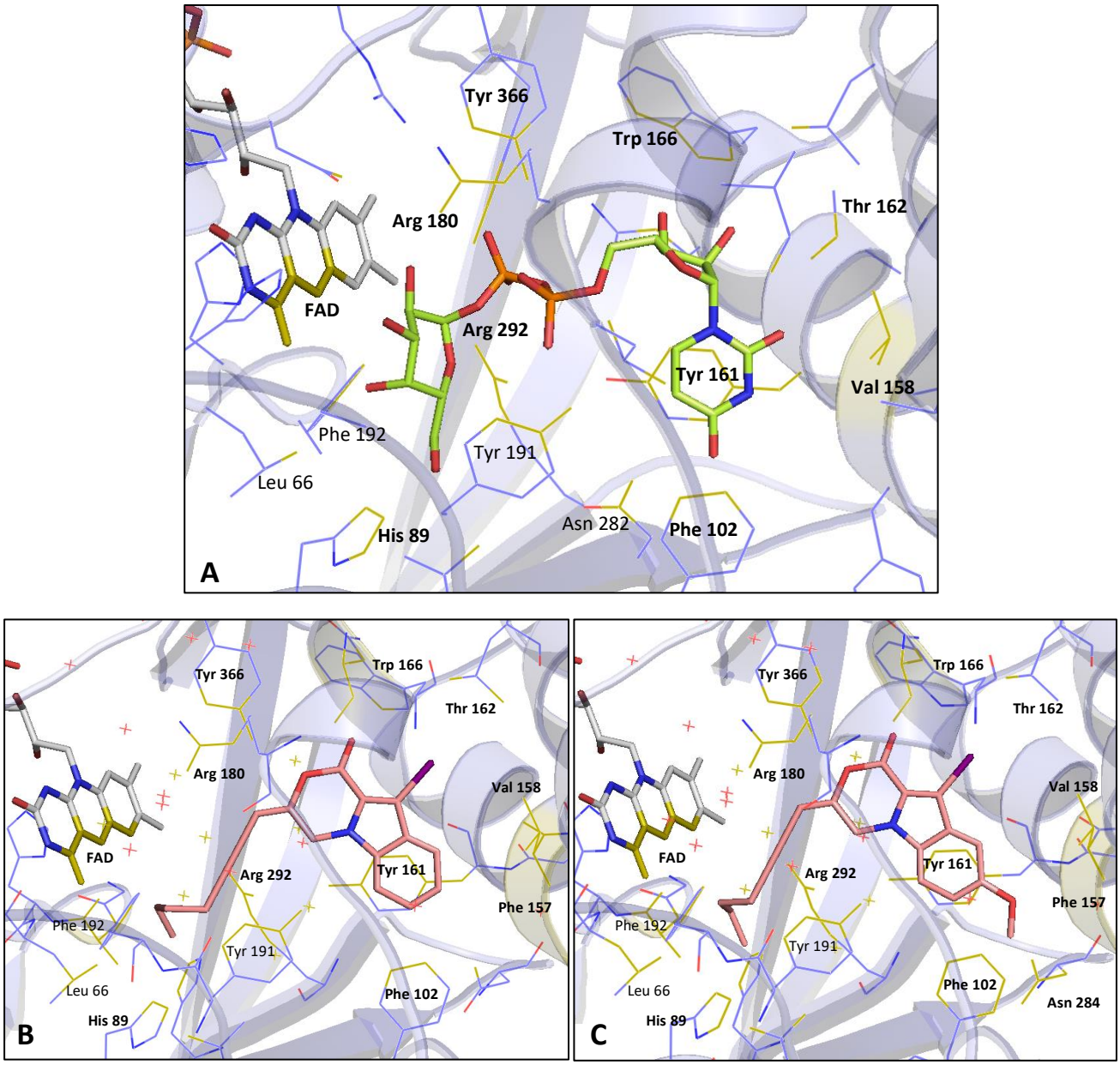

Figure SI-3 : Crystallized UDP Gal*p* (**A**), docked **10a** (**B**) and docked **10c** (**C**) in *Mt* UGM closed form (yellow atoms are at a distance <4 Å).

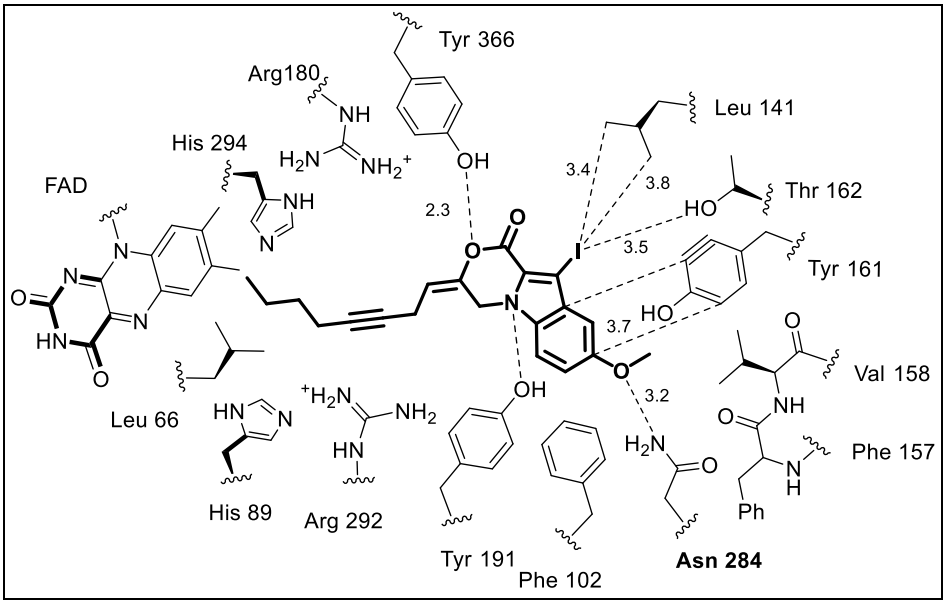

Figure SI-4: Interactions of **10c** with *Mt* UGM.

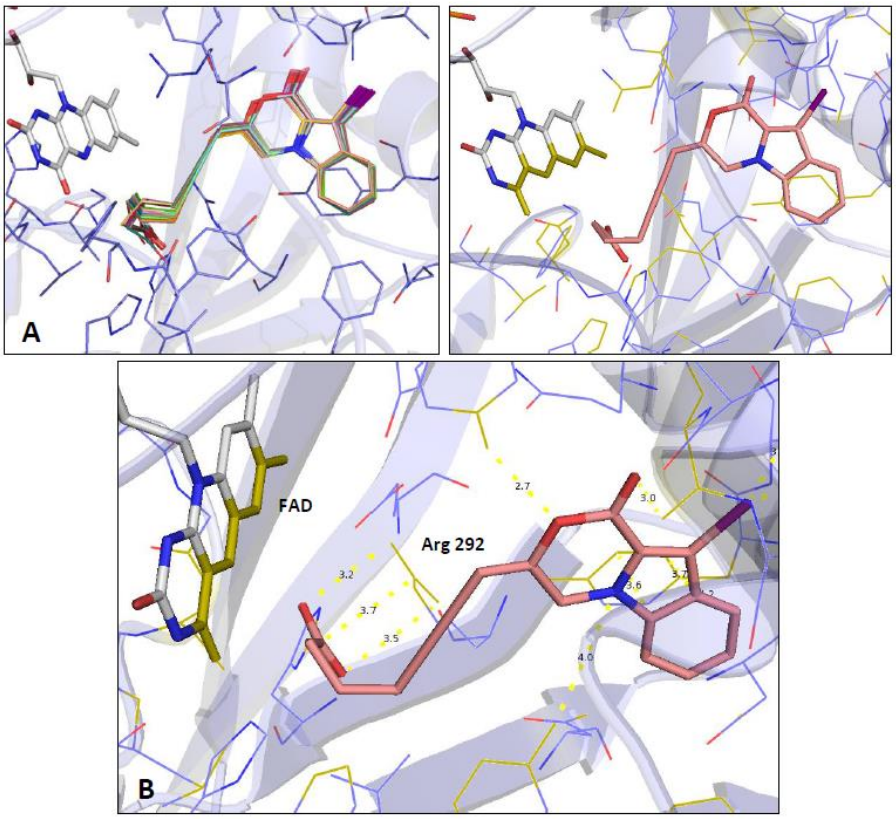

Figure SI-5 – A) Binding mode of molecule **11a** (50 best solutions superimposed) B) Zoom on the carboxylic acid interactions (Measured distances between COOH and Arg 292 are indicated).

3. Inhibition data

Fluorescence polarization plots
K_d determination for compound 10a,10c, 10d, 11a and 11c against *Mt* UGM.

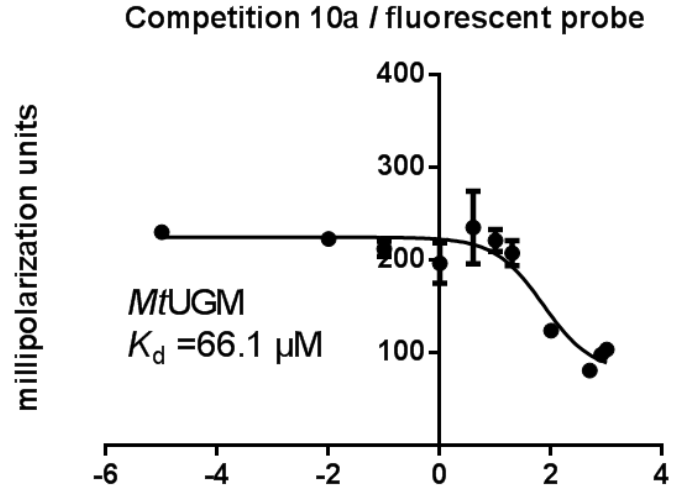

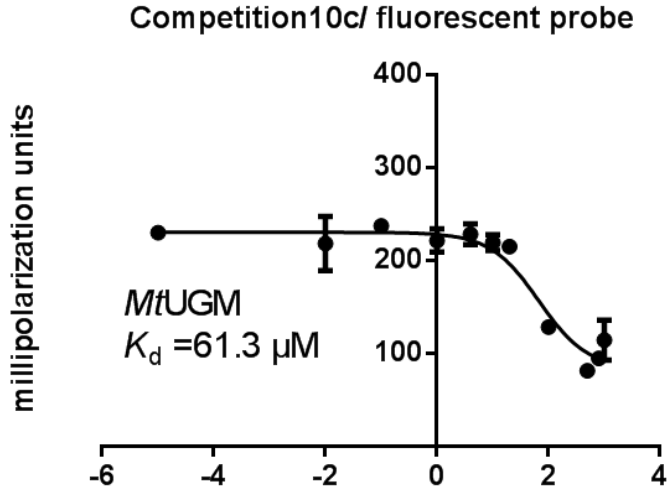

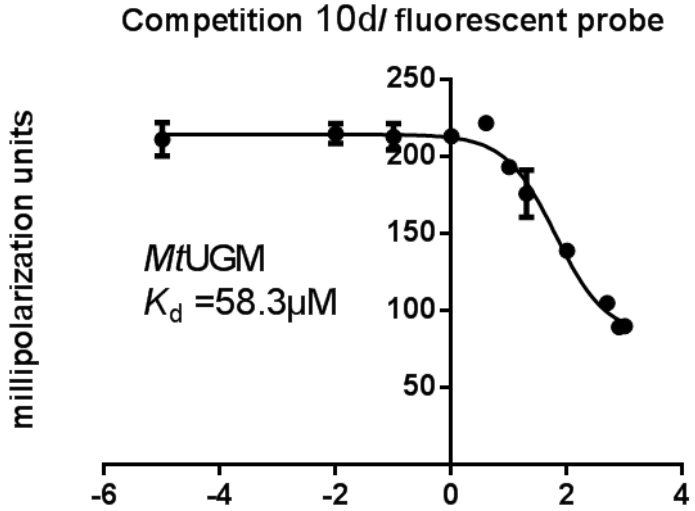

Competition 11a / fluorescent probe

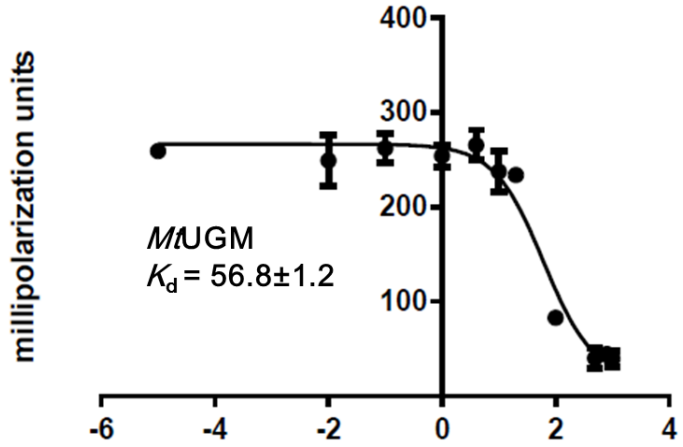

Competition 11c / fluorescent probe

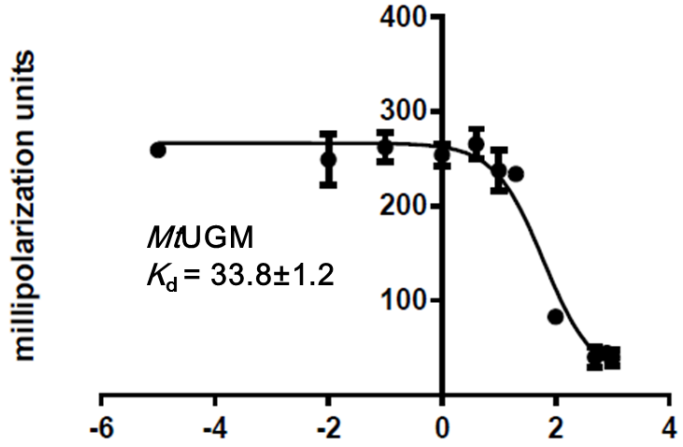

HPLC inhibition assay plots and tables

10a

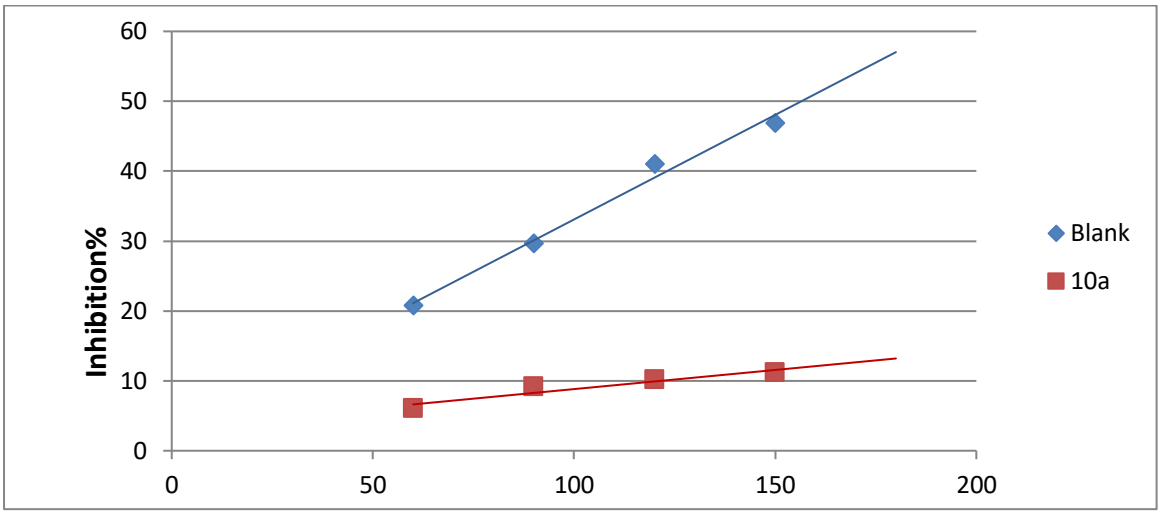

Time/seconds	Blank	**10a**	Inhibition%	Average%
60	20.76	6.00	71.10	
90	29.66	9.10	69.32	72.98
120	41.02	10.16	75.23	
150	46.90	11.12	76.29	
180			Error	±3.32

10c

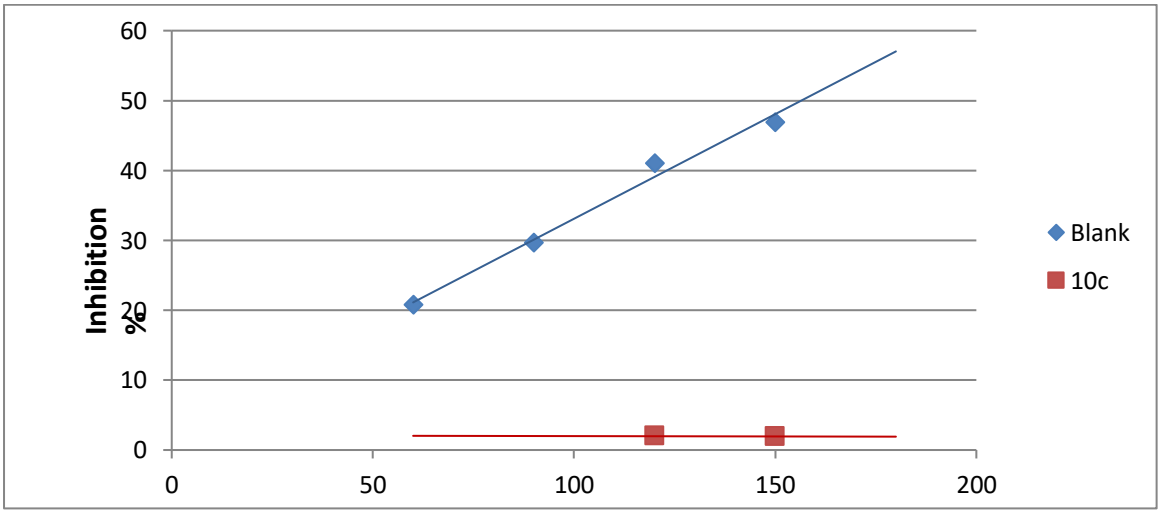

Time/seconds	Blank	**10c**	Inhibition%	Average%
60	20.76			
90	29.66			95.53
120	41.02	1.97	95.20	
150	46.90	1.94	95.86	
180				
			Error	±0.47

10d

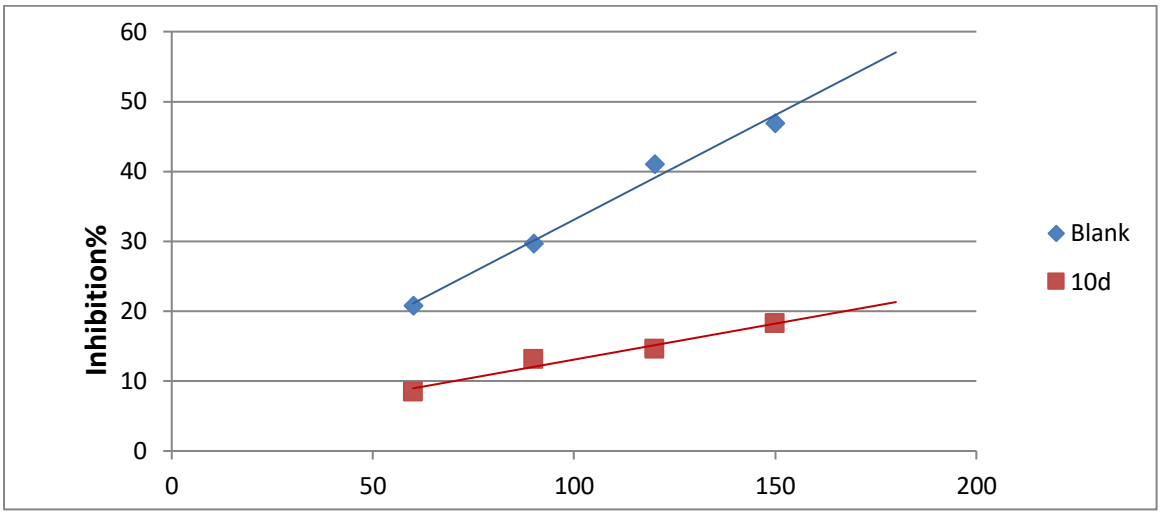

Time/seconds	Blank	**10d**	Inhibition%	Average%
60	20.76	8.43	59.39	
90	29.66	13.11	55.80	
120	41.02	14.59	64.43	60.19
150	46.9	18.23	61.13	
180				
			Error	±3.60

Mycobacterium abscessus est une mycobactérie non-tuberculeuse responsable d'infections chroniques sévères, notamment chez les patients atteints de mucoviscidose. Cette bactérie est naturellement résistante à la plupart des antibiotiques, rendant les traitements très compliqués et aboutissant souvent à des impasses thérapeutiques. Ainsi, la découverte de nouvelles molécules et de traitements plus efficaces pour lutter contre les infections à *M. abscessus* s'avère nécessaire. Dans ce contexte, ce travail a porté sur la recherche de nouvelles entités chimiques ainsi que sur de nouvelles combinaisons thérapeutiques actives contre *M. abscessus.* Une première approche a consisté à caractériser des dérivés du benzimidazole qui se sont révélés être très efficaces *in vitro*, *in cellulo* et *in vivo*. La détermination du mode d'action de ces composés a montré leur capacité à cibler la protéine membranaire MmpL3, impliquée dans le transport des acides mycoliques. Une seconde approche a consisté à étudier le repositionnement de molécules déjà utilisées en clinique, en nous focalisant notamment sur la bédaquiline. Nos résultats ont démontré l'efficacité de la bédaquiline contre *M. abscessus* dans un nouveau modèle d'infection murin. Par ailleurs, nous avons démontré que la rifabutine, une autre molécule candidate au repositionnement, présente une bonne activité contre les formes intracellulaires et extracellulaires de *M. abscessus*. Enfin, dans l'optique d'identifier de nouvelles combinaisons thérapeutiques optimisées, permettant de réduire les doses utilisées avec un effet supérieur à celui observé en utilisant les molécules prises séparément, nous avons mis en évidence une synergie entre des inhibiteurs de MmpL3 et des β-lactamines (imipénème et céfoxitine). D'autres composés sans effets anti-microbiens peuvent également potentialiser l'effet d'un antibiotique comme nous l'avons observé avec le vérapamil qui permet d'améliorer l'activité de la bédaquiline *in vitro* et dans le macrophage infecté. En résumé, l'ensemble de ces résultats ouvrent de nouvelles perspectives d'applications thérapeutiques des infections pulmonaires à *M. abscessus*.

Mycobacterium abscessus is a non-tuberculous mycobacterium responsible for severe and chronic infections, especially in cystic fibrosis patients. This bacterium is naturally resistant to most commonly used antibiotics, rendering treatments very challenging and often leading to therapeutic failure. Therefore, there is an urgent need for the discovery of new chemical entities and effective therapies to fight against *M. abscessus*. In this context, this study aimed at identifying new compounds and therapeutic combinations active against *M. abscessus.* A first approach consisted in characterizing new benzimidazole derivatives displaying high activity *in vitro, in cellulo* and *in vivo* against *M. abscessus*. MmpL3, the mycolic acid transporter, was identified as the primary target of these compounds. A second approach focused on the repurposing of existing antibiotics, as highlighted by the efficacy of bedaquiline in a new murine model of persistent infection. Furthermore, we demonstrated that rifabutin, another repurposed drug candidate, is active against both the intracellular and extracellular forms of *M. abscessus*. A third axis of this work was dedicated to identify possible synergistic drug combinations, allowing to use lower drug concentrations required to achieve the same or greater effect than with drugs used separately. To this end, we showed the synergistic effects between MmpL3 inhibitors and β-lactams (imipenem and cefoxitin). Other molecules, lacking anti-microbial activity, can also be used to potentiate the activity of antibiotics, as demonstrated with verapamil, which enhances the efficacy of bedaquiline *in vitro* and in macrophages. Collectively, these results open the door to new therapeutic perspectives against *M. abscessus* pulmonary diseases.